

https://dspace.org/

Exploration of the synthesis of imidazo[1,2-a]pyridin-3-amine derivatives with heteroatom linkers as potential HIV-1 reverse transcriptase inhibitors

Mkhize, J. Sandile

2023
https://hdl.handle.net/10539/35664

Downloaded from a DSpace repository. https://dspace.org/



WITS
UNIVERSITY



Exploration of the synthesis of imidazo[1,2-*a*]pyridin-3-amine derivatives with heteroatom linkers as potential HIV-1 reverse transcriptase inhibitors

SANDILE J MKHIZE

Supervised by: Prof Moira L. Bode
Co-supervised by: Prof Amanda L. Rousseau and Dr Jenny-lee Panayides

A dissertation submitted to the Faculty of Science, University of Witwatersrand, Johannesburg, in fulfilment of the requirements for the degree of Master of Science

Submitted November 2022

Declaration

I, Sandile Mkhize, hereby declare that this work, never been submitted to any university and for any degree purposes before, is my own work and is hereby submitted to the University of Witwatersrand for the fulfilment of the Master of Science degree requirements. This dissertation was supervised by Prof Moira Bode and co-supervised by Prof Amanda Rousseau and Dr Jenny-lee Panayides.



……

November 2022

Dedication

This work is dedicated to my younger brother, Linda.

You were more than just a sibling, but a companion with a warm shoulder to fall on. Your ambitious and curious mind will never be forgotten…so long little brother.

Acknowledgements

I would like to extend my warmest gratitude first and foremost to my supervisor, Prof Moira Bode. Prof, I could not find words to thank you enough. Coming from a clinical/therapeutic sciences background was always going to be a challenge for me to adapt the various techniques and methods applied in synthetic chemistry. Yet you carried my hand, inspired me and encouraged me to keep going. Your particular attention to detail and research ethic has left a spark of curiosity in me. Thank you to my co-supervisors, Prof Amanda Rousseau and Dr Jenny-lee Panayides. Prof Rousseau, thank you for your suggestions and input into my project. You were always there when challenges and obstacles struck me. The short meetings we had on the status of my project were refreshing and informative in many ways than you can imagine. Dr Jenny-lee thank you for all your support and for allowing this project to be a reality. Thank you for giving me a platform to grow and pursue my ambitions of being a scientist.

A big thank you to CSIR for the generous financial support towards this project and myself. May you not grow weary and continue to lend a helping hand to others.

To the zealots of the organic research group for all the fun, fellowship, and the spirit of camaraderie that you guys had. I will forever be grateful for the opportunity to have had my journey intertwined with all of you. To Bianca Davids, the chit chats we had about chemistry and life in general were valuable. Thank you for all the crazy laughter we had and for always being there when I needed assistance. To Khonzisizwe Somnandi, Kabelo Zimba, Kabelo Bramley and Mudzuli Maphupha it was a great pleasure meeting you guys. Dissecting weekend soccer matches on a Monday morning with Kabelo Bramley was epic. We would argue about minute issues yet end up laughing about it. I will always cherish those moments.

Lebogang Tefu, thank you for all the support you gave me, your endless smile and encouragement. You were an amazing friend. Kamogelo Butsi, your laughter was contagious, and your beaming energy was more contagious. Thank you for having such an open and warm heart. Nompumelelo Mathebula, you took my hand the very first day I came to the lab. You taught me everything about the chemistry lab which I was not familiar with. You introduced me to each and every person in the lab and guided me on how to use the instruments. You were truly an amazing person, and I will always be grateful for all your guidance and helping hand. Josephine Maboya, I can never thank you enough for your help with mass spectrometer. Aneesa Gani, you made the lab environment easy to love with your warm heart and gentle laughter. Alexandra Plakas, you would run up the stairs from the NMR

and throw yourself in my lab to catch a breather and would always say “I’m not as fit as I look.” Thank you for your positive energy and for sharing your columns. Matthew Maree, for all your unwavering assistance with mass spectrometer. Dr Songezo Ntsimango, for constantly organizing our gathering at the PIGS club so we can connect, laugh, and remind ourselves that we are still a bunch of young students after all. Dr Zimuwandeyi, for your unwavering assistance with the NMR and your general input towards my project. You truly are inspirational.

To the rest of the organic research group, Nafisa, Cecilia, Edward, Bongi, Fatema, Priscilla, Dr Thabo Peme and Ntombi, thank you for being part of my second family.

A big thank you to Matthew Bracken and Prof Manuel Fernandes for their assistance with X-ray crystal structure analysis.

Finally, I would like to thank my family and friends for support and encouraging me to pursue this journey. To my sister, Busi, thank you for your endless support. To my little sister, Zama, you are an amazing shining star. Thank you for painting a smile on my face.

Contents

CHAPTER 1: INTRODUCTION.....1

1.1 An overview of the history of the HI Virus.....1
1.2 Social and health impact of HIV/AIDS.....2
1.3 Complementary factors contributing to HIV/AIDS.....3
1.4 Fundamental challenges in HIV/AIDS prevention.....5
1.5 HIV drug resistance.....6
1.6 The life cycle of the HI virus.....8
1.7 HIV-1 Reverse Transcriptase (RT).....10
1.8 Potential drug binding sites on Reverse Transcriptase.....11
1.9 RTIs as potential drug inhibitors of reverse transcriptase.....12
1.10 NNRTIs and their mode of action against RT.....13
1.11 Latest NNRTIs.....15
1.12 Imidazopyridines as structural fragments in the design and synthesis of novel NNRTIs.....20
1.12.1 Synthesis of imidazo[1,2-*a*]pyridines.....21
1.12.2 Pharmaceutically active imidazo[1,2-*a*]pyridines and drug candidates..30
1.13 Study aims and objectives.....36

CHAPTER 2: RESULTS AND DISCUSSION.....40

2.1 Molecular modelling studies.....41
2.2 Synthesis of imidazo[1,2-*a*]pyridine compounds.....49
-UNEXPECTED TWIST.....58
-UNEXPECTED TWIST.....62
2.3 Conclusion.....93
2.4. Future work.....96

CHAPTER 3: EXPERIMENTAL PROCEDURES.....97

3.1 General experimental procedures.....97
3.2 6-Bromo-2-chloroimidazo[1,2-*a*]pyridine 29.....98
3.3 Synthesis of rigid Imidazo[1,2-*a*]pyridines.....99
3.4 Synthesis of position-2 unsubstituted imidazo[1,2-*a*]pyridine analogues..104
3.5 Synthesis of imidazo[1,2-*a*]pyridin-2-carboxylate derivatives.....108
3.6 6-Bromo-*N*-(2-chlorophenyl)-3-(cyclohexylamino)imidazo[1,2-*a*]pyridine-2-carboxamide 53.....111
3.7 Synthesis of 3-(cyclohexylamino)imidazo[1,2-*a*]pyridin-2-yl-methanol analogues.....112
3.8. Preparation of 3-cyclohexylaminoimidazo[1,2-*a*]pyridine-2-carbaldehyde 115
3.9. Oxidative ring-opening of imidazopyridine alcohols.....116

3.10 6-Bromo-2(bromomethyl)-*N*-cyclohexylimidazo[1,2-*a*]pyridin-amine 58 120
3.11 Reductive amination 121
3.11.2 6-Bromo-2-(((2-chlorophenyl)amino)methyl)-*N*-cyclohexylimidazo[1,2-*a*] pyridin-3-amine 59a.....122
MOLECULAR MODELING STUDIES 123
4.1 Docking analysis 123
4.2 Protein preparation.....123
4.3 Ligand preparation 123
4.4 Docking method validation.....123
4.5 Ligand minimization.....123
4.6 Selection of compounds for synthesis 124
REFERENCES.....125
APPENDIX 1: ^{1}H NMR AND ^{13}C NMR SPECTRAL DATA FOR A SELECT NUMBER OF COMPOUNDS 135

List of figures

Figure	Page number
Figure 1	9
Figure 2	11
Figure 3	12
Figure 4	14
Figure 5	14
Figure 6	16
Figure 7	17
Figure 8	18
Figure 9	19
Figure 10	20
Figure 11	26
Figure 12	30
Figure 13	31
Figure 14	32
Figure 15	33
Figure 16	33
Figure 17	34
Figure 18	34
Figure 19	41
Figure 20	42
Figure 21	47
Figure 22	48
Figure 23	51
Figure 24	53
Figure 25	65
Figure 26	69
Figure 27	81
Figure 28	82
Figure 29	83
Figure 30	84
Figure 31	96

List of tables

Table 1	43
Table 2	44
Table 3	46
Table 4	61
Table 5	68

List of abbreviations

AcOH	Acetic acid
AIDS	acquired immunodeficiency syndrome
$AlCl_3$	Aluminium chloride
Ar	Aryl
AUC	Area Under the Curve
C-2	Carbon number 2
$CDCl_3$	Deuterated chloroform
CD4	Cluster of differentiation
cDNA	Complementary DNA
$CHCl_3$	Chloroform
DAPY	Diarypyrimidine
DCM	Dichloromethane
DEPT-135	Distortionless enhancement by polarization transfer
DLV	Delavirdine
DMAP	4-Dimethylaminopyridine
DNA	Deoxyribonucleic acid
d_6-DMSO	Deuterated dimethyl sulfoxide
DMSO	Dimethyl sulfoxide
DRV	Doravirine
dsDNA	Double stranded DNA
EFV	Efavirenz
eq	Equivalents
Et_3N	Triethylamine
Et_2O	Diethyl ether
EtOAC	Ethyl Acetate
EtOH	Ethanol
ETV	Etravirine
GBB-3CR	Groebke-Blackburn-Bienaymé three component reaction
HAART	Highly active antiretroviral therapy
$HClO_4$	Perchloric acid
Hex/EtOAC	Hexane/Ethyl acetate

HIV	Human immunodeficiency virus
HPLC	High Pressure Liquid Chromatography
HSQC	Hetero single nuclear quantum coupling
HTLV	Human T-cell leukemia virus
IBX	Iodobenzoic acid
IPA	Isopropyl Alcohol
IR	Infra-red
KO^tBu	Potassium *tert*-butoxide
LAH	Lithium aluminium hydride
MeOH	Methanol
MeOD	Deuterated methanol
$MgSO_4$	Magnesium sulfate
MS 4Å	Molecular sieves 4 angstroms
$NaBH_3CN$	Sodium cyanoborohydride
NAH	Sodium Hydride
$NaHCO_3$	Sodium bicarbonate
Na_2SO_4	Sodium sulfate
NMR	Nuclear Magnetic Resonance Spectroscopy
NVP	Nevirapine
^{31}P	Phosphorus isotope-31
P-3CR	Passerini three component reaction
PBr_3	Phosphorus tribromide
$Pd_2(dba)_3$	Palladium dibenzylacetone
RMSD	Relative Mean Standard Deviation
RPV	Rilpivirine
r.t	room temperature
RT	Reverse transcriptase
S_N2	Substitution nucleophilic-2
THF	Tetrahydrofuran
TLC	Thin layer chromatography
TsCl	Tosyl chloride
U-4CR	Ugi four component reaction

Chapter 1: Introduction

The human immunodeficiency virus (HIV) is a virus that attacks host cells of the human immune system, which is the body's defence system against foreign perceived threats and illnesses, thus resulting in acquired immune deficiency syndrome (AIDS)[1]. To date, close to 38 million people globally are said to be living with HIV/AIDS and close to 35 million more are said to have died from HIV/AIDS since the first reported case of the epidemic[2]. Sub-Saharan population accounts for less than 15% of the world population, yet more than 70% of global HIV infections are reported to be in Sub-Saharan Africa[3]. Countries with the most prevalent burden of the disease include South Africa, Ethiopia, Mozambique, Zambia, Kenya, Zimbabwe, Uganda, Nigeria, Malawi and Tanzania; combined, these countries account for nearly 80% of global HIV cases[4]. South Africa is said to have a staggering 7.8 million citizens living with the HI virus, making it the country with the highest HIV cases globally[5]. Currently with no cure and no vaccine for the virus, the country is facing devastating socio-economic effects with far-reaching implications on population growth and sustainability. It is thus imperative that an intervention is sourced to combat the HIV/AIDS epidemic in order to ensure economic and social stability in the country.

1.1 An overview of the history of the HI Virus

The origins and discovery of HIV had for a long time been a subject of debate within the scientific community. There is now significant evidence as to when, where and how the HI virus began to cause illness among human beings[1]. HIV was first isolated in 1983 by Luc Antoine Montagnier at the Pasteur Institute in France[5] from a lymph node biopsy and was subsequently named "Lymphadenopathy-Associated-Virus" (LAV) as there was not enough research at the time to distinguish whether there was a direct link between HIV and AIDS[6]. Montagnier's findings were published in the *Science* journal on 20 May 1983. Meanwhile, at the Laboratory for Tumor Cell Biology (LTCB) of the National Cancer Institute (NCI), United States of America, a research team led by Robert Gallo reported similar findings to that of Montagnier's group in the same issue of the *Science* journal and presented the first evidence that the virus was indeed a major cause of AIDS. Subsequently, Gallo named the virus "Human T-Lymphotropic Virus type III" (HTLV III). For many years researchers argued as to which of the two research groups was to be credited for first isolating the virus[7]. In 1986, an agreement was reached to do away with the names Lymphadenopathy-Associated-Virus and Human T-Lymphotropic Virus type III in favour of a more descriptive

term *Human Immunodeficiency Virus* (HIV) and both scientists were credited for their discovery of the virus[7].

The HI virus, specifically HIV-1, is believed to have its origins from chimpanzees in the central African region near the Congo basin. A virus known as Simian Immunodeficiency Virus (SIV) with similar traits to HIV was detected in monkeys and apes[8]. Research found that HIV-1 showed similar traits to a strain of SIV commonly found in chimpanzees and that HIV-2 showed similar traits to an SIV strain commonly prevalent in sooty mangabeys[9]. Further research concluded the connection between the SIV in chimpanzees and the HIV in humans and that at some point the SI virus had crossed species from chimpanzees to humans[10,11]. Researchers concluded on the now acceptable theory of chimps being hunted and possibly eaten or their blood coming into contact with humans in the process of hunting them down. The SI virus would then adapt to the new human host environment and would mutate into an HI virus[9]. This theory is further supported by the fact that the HI virus consists of four main strains (M, N, O and P) each with a variable genome make-up. The SIV passed from chimps to humans would have had to adapt to different human host environments resulting in various strains. This explains the existence of more than one HIV-1 strain[9].

The most common HIV strain is the group M strain, which is responsible for the vast majority of global HIV infections[12]. HIV-2, which unlike its counterpart, HIV-1, is far less common and in addition is less infectious, is believed to originate from sooty mangabey monkeys rather than chimpanzees. It has a very low infection rate and is mainly localized in countries in the west of Africa like Nigeria, Mauritania, Mali and Sierra Leone[11].

1.2 Social and health impact of HIV/AIDS

HIV is well known to have physical, mental, psychological, and socio-economic impact on individuals and communities affected by the scourge[13]. Women and young people are said to be the most affected with children bearing the biggest brunt when one or both parents are infected. Often, infected adults are parents or are responsible for the care of children. Over the course of the past decade, a great deal of information has been acquired with regards to the implications of adult HIV and the impact it has in the workplace and within the family structure, particularly on children. One of the well-studied implications of adult HIV on children is vertical transmission. Although significant advances have been made in understanding and preventing vertical transmissions through prophylaxis, a great number of

children exposed to HIV are from low and middle-income countries (LMICs), wherein HIV management programmes such as prevention of mother-to-child-transmission (PMTCT) remain limited and significant interventions are needed. Facilities with adequate antenatal care resources, improved funding and capacitation of healthcare programmes are often required to remedy the situation. This intervention, however, would not prevent child exposure to HIV. Evidence suggests that biological exposure alone can have severe implications as these children will be born into households impacted by HIV leading to further health, psychological and social risks[14].

It is worth noting that most children reside in households with families, broadly speaking, and their upbringing is shaped and defined by the context of their surroundings[14]. Children rely on adults for their developmental needs, for protection, care and for their wellbeing. HIV infection can impact the family supportive structure when an adult is affected, potentially leading to developmental strain and hardships on the child as they grow. The risk is amplified for poor and underdeveloped communities. Research has provided significant information detailing that community and family resources play a crucial role in protecting children against the impact and extent of exposure and vulnerability to the effects of HIV. Parents, in general, as part of their HIV management would shield their children from the adverse social and psychological effects of the virus. Thus, access to treatment, social support, state of the community, employment, good nutrition, and good quality of health have been shown to provide support to affected adults thus ensuring that children grow up in an environment where they are protected from ameliorating adverse effects of the virus[14].

The stigma generally attached to HIV/AIDS often results in discrimination of those infected by the virus. This negatively impacts prevention and care efforts as it perpetuates silence, denialism, and non-disclosure of HIV status[15]. It further entrenches stigmatization of individuals living with the virus and those at potentially high risk of infection. Stigma can also be a result of internalization by those living with the virus as a result of negative perceptions about themselves. This often has devastating psychological consequences, poor management of the illness and may ultimately lead to depression, apathy, and despair[15].

1.3 Complementary factors contributing to HIV/AIDS

There are various complementary factors that contribute towards the spread of HIV/AIDS. These can be regional-based factors, ethnic or prevalent across an entire continent. Poverty,

for example, is one of the contributing factors and it is prevalent in Sub-Saharan Africa as well as some parts of Asia and South America. The United Nations Office for the Coordination of Humanitarian Affairs (OCHA) says that around 600 million people or roughly eight percent of the world population lives below the poverty line. This it defines as any person who survives on US $2 or less a day[16].

This figure, however, was around 1.8 billion people in 1990. Significant progress has indeed been made, notes OCHA. The UN office also believes that it is possible to eradicate poverty but to do this; the major causes of poverty must be borne in mind. These factors also happen to contribute towards the spread of HIV/AIDS. These include inequality and marginalization, conflict, poor nutrition, lack of healthcare infrastructure which impacts mothers and children the most, lack of clean water, sanitation and hygiene, unpredictable weather patterns, poor or no education, lack of government support, lack of investments and job opportunities which ultimately impact livelihoods and lack of social and welfare programmes[16].

Inequality, for example, is often loosely used to describe systemic barriers that prevent certain individuals from being represented in a community. For communities to end poverty, all voices need to be considered during decision-making processes particularly on issues that directly affect individuals within the community. Issues such as gender inequality and gender-based violence (GBV), caste system, marginalization based on religious affiliation, race or gender and tribal affiliation need to be addressed holistically by direct engagement with the affected individuals or group of people. These issues are both economic and social inequalities that ultimately result in marginalization in access to resources required to live a stable and productive life[16].

Conflict is considered one of the main pillars contributing towards poverty. The trail of destruction on infrastructure, people displacement and unavailability of clean running water and sanitation often disrupts provision of healthcare and social services. This results in increase in illnesses, malnutrition, and developmental challenges particularly in children[16]. During conflict, for example, many farmers disinvest, and farming output diminishes. This threatens food security and can lead to hunger and poverty. Although the two terms might be synonymous, the United Nations considers hunger to be the cause and maintainer of poverty. For example, a person who lacks food will also lack strength, courage, and the ability to work. As a result their immune system will also be weakened from poor nutrition, and this will leave them vulnerable to illness and diseases and eventually prevent them from

performing basic tasks. This is a debilitating problem in pregnant and lactating mothers. It is said that the first 1000 days of a child's life, often referred to as "from the womb to the world" period, are the most crucial to ensuring the child's future health and their escape from poverty. However, should the mother lack proper nutrition during pregnancy that can have a knock-on effect on the unborn child leading to wasting and stunted growth. Stunted growth and other congenital disorders as a result of malnutrition can have serious impact on the life of a child as well as throughout their development until adulthood. Studies have found that the majority of adults who had stunted growth earn on average 22% less than adults who did not suffer from stunted growth. This is particularly pervasive in countries such as Ethiopia[16].

1.4 Fundamental challenges in HIV/AIDS prevention

There are various challenges that contribute towards prevention of HIV/AIDS. In particular, political commitment and the reluctance to address issues of sexuality and reproduction rank high among those. Government has a big role to play in preventing the spread of HIV/AIDS by ending social, racial, economic and gender inequalities, doing away with non-progressive and self-limiting laws, regulations and policies, stigmatization, and collateral forms of discrimination, particularly those based on the HIV status of a person, and any other violations of human rights that seek to perpetuate the spread of HIV/AIDS[17]. On June 8, 2021, the United Nations General Assembly adopted the political declaration entitled "Political declaration on HIV and AIDS: Ending inequalities and getting on track to end AIDS BY 2030". The declaration committed governments and heads of state across the globe to urgently take steps within the next 5 years through a globally coordinated HIV/AIDS response based on global solidarity and shared responsibilities, to fully commit to the implementation of the declaration.

Access to HIV treatment and destigmatization remain a big challenge in HIV prevention. However, the last decade has seen improvement in improving the quality of life of those who tested positive. This has been achieved through the availability of generic drugs which are much more cost effective as well as government funding and international donor funding. Investments in science research as well as data gathering, and patient monitoring has seen a dramatic improvement in HIV management. Extensive HIV programmes involving HIV education through social campaigns, sexual and reproductive education, as well as the availability of specialist healthcare professionals in the field of HIV management has had a positive impact in slowing down the disease progression.

1.5 HIV drug resistance

During the past decade, the world has witnessed an unprecedented availability and access to life-saving highly active antiretroviral therapy (HAART) which has saved millions of lives of people living with HIV/AIDS. The WHO estimates that at the end of 2020, 27.5 million people had received ART globally, out of an estimated 37.7 million people that are said to be living with HIV/AIDS. Accordingly, an increase in HIV medicine uptake has seen an emergence of drug resistance due to viral mutations as the virus tries to evade suppression and elimination. This has been steadily increasing in recent years[18].

HIV drug resistance occurs as a result of the virus mutating one or more of its protein side chains within the drug binding site in an attempt to evade the inhibitor. This affects the ability of the drug to perform its functions. All HIV drugs, notwithstanding the newer antiretroviral classes, are at risk of becoming partially or fully inactive as a result of drug resistance emanating from viral mutations. If not managed properly, HIV drug resistance can jeopardize the efficacy of ART and can result in uncontrollable HIV infection rates as well as HIV-associated mortality and morbidity.

The World Health regulatory body suggests that routine monitoring and surveillance of HIV drug resistance can provide countries with evidence that can be utilized to optimize population and individual-based treatment outcomes. This body's 2021 report on HIV drug resistance shows significant progress in the development of strategic action plans to reduce, monitor, and respond speedily and accordingly to HIV drug resistance emergence and implementation of country specific surveys in low-and middle-income countries. The WHO also noted the steadily increasing number of individuals and infants that are HIV drug resistant even before commencement of ART. In mothers and infants this is mainly as a result of pre-exposure to HIV medicines i.e., antiretroviral medicines given to prevent mother-to-child transmission of HIV. The WHO recommends pre-screening of HIV drug resistance in the adult population prior to commencement or reinitiating of ART and in treatment naïve infants initiating ART in order to select optimal first line regimens[18].

Studies by the WHO also noted that up to 10% of adults commencing ART are most likely to have drug resistance against an NNRTI drug class. It also noted that the prevalence of HIV drug resistance was highest among children under 18 months of age and those that have recently been diagnosed with HIV. Based on studies conducted in 10 countries between

2012-2020, almost half of infants newly diagnosed with HIV were found to have NNRTI drug resistance even before commencement of treatment. The WHO has thus recommended the fast-tracking of transitioning to integrase inhibitor dolutegravir-based treatments.

Some people who are regarded as being at high risk of exposure to HIV are often offered prophylaxis to reduce chances of acquiring the virus. In the latest treatment guidelines, the WHO recommends oral pre-exposure prophylaxis (PrEP) as an additional preventative measure against contracting the virus. This has proven to be effective in preventing infection by the HI virus. However, among individuals contracting the virus despite the use of PrEP, HIV drug resistance becomes a serious problem. This could reduce options available for treatment. The WHO recommends continuous monitoring of HIV drug resistance as well as implementation of nationally representative surveys to monitor HIV drug resistance among individuals commencing ART, reinitiating ART and among those who were on PrEP and subsequently got infected.

Minimizing HIV drug resistance falls within the ambit of the broader global response to antimicrobial drug resistance and requires a coordinated multisectoral approach by different spheres of government and society. For example, in countries such as South Africa, where HIV/AIDS is prevalent, some individuals are known to flush their expired HIV medication down the drain. This poses a serious threat as municipal water treatment facilities do not have means of extracting and removing medicines in wastewater. The result is the recirculation of medicines back into household tap drinking water and the emergence and risk of HIV drug resistance becomes more prevalent.

The WHO's Global plan of action program on HIV drug resistance 2017-2021, aligned with the Global action plan on antimicrobial drug resistance and the HIV drug resistance strategy 2021 update prescribe key actions that countries should adopt to minimize, survey, and respond appropriately to HIV drug resistance and to safeguard the on-going measures to achieve global targets of HIV control by 2030. These actions include prevention and control, which is the implementation of impact-based measures for a speedy response to HIV drug resistance, including emphasis on transitioning to dolutegravir-based antiretroviral regimens and systems to ensure uninterrupted drug supplies. Pharmacovigilance and obtaining accurate figures on HIV drug resistance and service delivery centred on HIV care while continuously monitoring routine viral load and HIV drug resistance testing and monitoring. The WHO also encourages countries to be innovative and invest in their own individual research that will

have a positive impact on public health and will help minimize HIV drug resistance. It encourages countries to bolster their laboratory capacity to expand viral load testing and continuously monitor HIV drug resistance[18].

1.6 The life cycle of the HI virus

Reference to HIV for the purpose of this study shall be confined to the HIV-1 type. HIV is transmitted from one human to another by direct contact with the blood, body fluids such as semen, breast milk and vaginal fluids of an infected person. It can also be transmitted through sexual intercourse (vaginal or anal sex) with an infected person, sharing of needles or other sharp objects as well as mother-to-child transmission during pregnancy, birth or breastfeeding[3]. Once inside the body of the host, the virus uses two of its proteins for attachment. The docking glycoprotein (gp120) and the transmembrane glycoprotein (gp140). The docking glycoprotein (gp120) attaches to the T-cell surface CD4 receptor protein via high-affinity binding[19]. This is subsequently followed by binding of gp120 to a host cell co-receptor, CCR5 or CXCR4[5]. Preference to either of the co-receptors depends on the type of HIV strain as well as the cell type being infected by the virus. This binding initiates conformational changes in the gp120 folding pattern and allows gp140 to anchor into the host cell membrane, resulting in fusion of the viral envelope across the host cell membrane (**Figure 1**). This ultimately allows the viral contents, nucleic acids and enzymes, to enter the host cell cytoplasm[5].

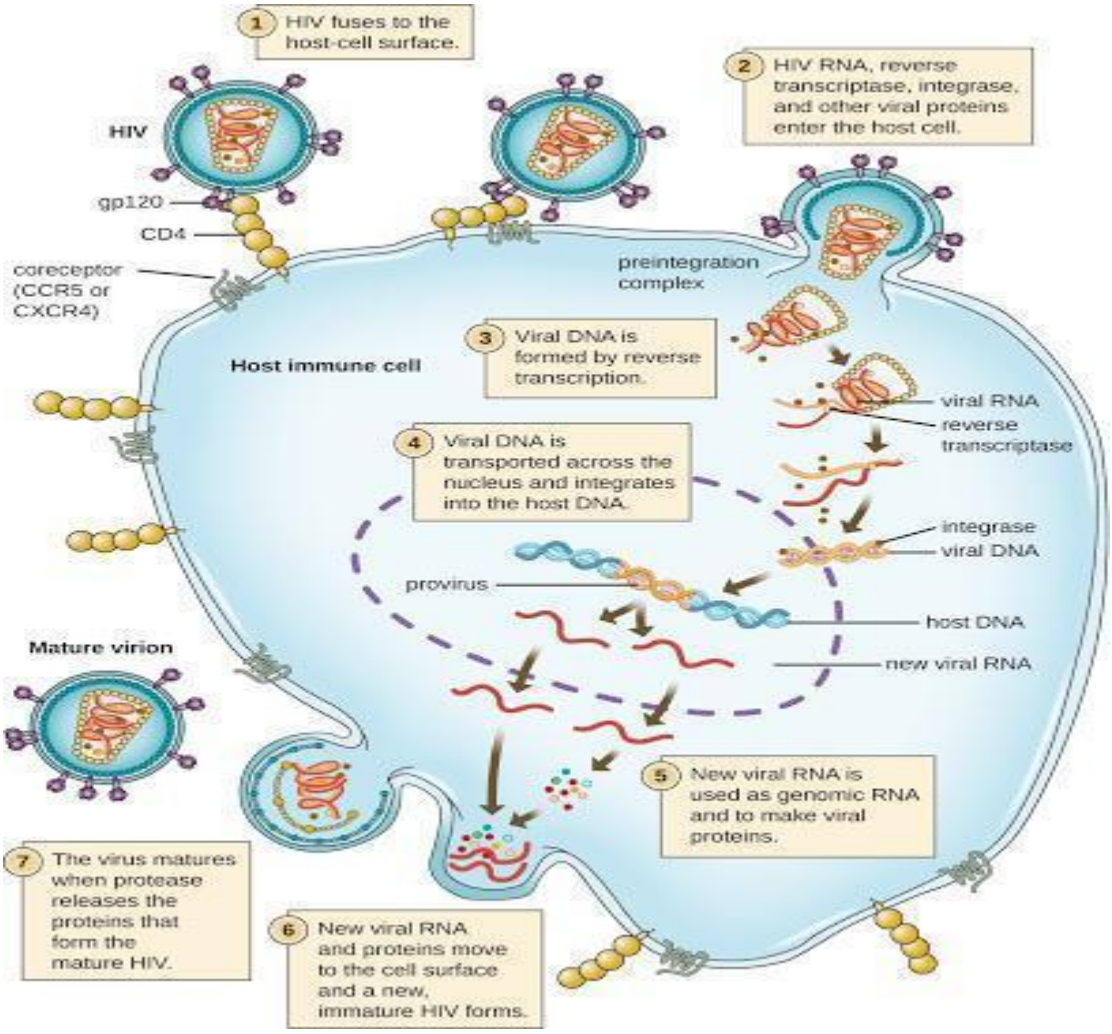


Figure 1: **Life cycle of the HI virus. Adapted from brotherhoodinc.org**

Although this process is considered a primary entry of the virus into the host cell and most particularly the T-cells, a number of other distinct interactions influence binding of the HI virus to host cells. These include the promotion and facilitation of adhesion by a β-galactoside-binding protein, Galectin-1[20], the capture and mediation of transmission of the HI virus by Syndecan-3 and DC-SIGN, both dendritic cell-specific attachment receptors for HIV-1[21] and the virus's interaction with ICAM-3. The binding of the virus to DC-SIGN on dendritic cells and macrophages is as significant as the binding to the CD4 receptors on T-cells in that it facilitates and enhances co-infection of the CD4+ T-cells by dendritic cells as infection by other viruses such as Hepatitis C[22].

Once in the host cytoplasm, host enzymes slice open the viral capsid exposing the viral contents, viral RNA and viral enzymes. A complementary DNA (cDNA) strand of the viral RNA is then transcribed retrospectively by the viral enzyme, Reverse Transcriptase (RT) (**Figure 1**), resulting in a DNA/RNA complex reminiscent of most retroviruses. A double

stranded DNA (dsDNA) is furthermore synthesised by the same enzyme using the complementary single strand template that has been created. This double stranded viral DNA then migrates chemotactically into the host cell nucleus and integrates with the host's chromosomes under influence by the viral enzyme integrase. This host/viral DNA network, known as the provirus, begins to transcribe viral genomic RNA and mRNA using host enzymes. Viral mRNA then leaves the nucleus and begins synthesis of viral proteins on neighbouring ribosomes. These viral proteins are then functionalized by the viral enzyme protease and assembled by the host enzymes into new virus particles on the surface of the host cell membrane. Budding of these particles out of the cell promulgates maturation of the proteins which subsequently become infectious virions[23].

1.7 HIV-1 Reverse Transcriptase (RT)

Reverse Transcriptase is a DNA- and RNA-dependent DNA polymerase enzyme which was discovered in many retroviruses, including HIV. It catalyses the conversion of RNA templates into DNA complementary strands[24]. The discovery of RT has revolutionized molecular biology resulting in paradigm shifts in some of the methodologies used in the study of nucleic acids, protein informatics, cloning and gene expression.

HIV RT is one of the most extensively studied reverse transcriptases in the context of better analysing the biology of this devastating virus, as well as enabling rational design of RT inhibitor drugs to control and contain the spread of HIV infections[25]. Reverse Transcriptase is fundamental for HIV replication as the viral genome on its own is highly susceptible to degradation by intracellular RNases. As such, upon entering the host cell RT rapidly synthesises a much more nuclease-resistant double-stranded DNA copy of the viral RNA template which later integrates to form the proviral DNA copy[26,27].

Reverse Transcriptase consists of three enzyme active sites: (1) RNA–dependent DNA polymerase which synthesises single strand DNA from single strand RNA, (2) DNA-dependent DNA polymerase which completes the double stranded DNA synthesis and (3) RNase-H which chemoselectively degenerates the RNA strand in the RNA/DNA hybrid[25]. Furthermore, HIV RT is a heterodimer composed of two polypeptide chains, a 66 kDa subunit (p66) and a 51 kDa subunit (p51). The p66 domain is responsible for almost all catalytic functions of HIV RT, meanwhile p51 only serves to support p66[26].

Unlike most cellular polymerases, HIV RT lacks proof-reading capabilities meaning that the HIV genome is prone to high error rates during its own DNA synthesis. As a result, mutations

due to uncorrected RT activity are very common in the HIV genome, appearing at rates of almost 1 in 3000 nucleotides incorporated[24]. By comparison, the average rate of mutation of a human cellular genome is roughly 1 in 10^7 base pairs[27]. This high error rate provides the HI virus a selective advantage for survival within the host environment. It is for this reason that inhibitors of reverse transcriptase activity remain a pivotal target for HIV drug discovery[26].

1.8 Potential drug binding sites on Reverse Transcriptase

HIV-1 Reverse Transcriptase is a heterodimer consisting of two domains, p66 and p51 (**Figure 2**). The p66 subunit houses all catalytic activity of the enzyme and as such contains both nucleoside reverse transcriptase inhibitor (NRTI) as well as non-nucleoside reverse transcriptase inhibitor (NNRTI) binding sites[28]. In addition, the p66 subunit also consists of other binding sites on polymerase as well as the ribonuclease H (RNase H) domain. Both of these domains play a pivotal role in the assembly of a double stranded DNA from a single stranded viral RNA[26]. Any of these sites can be exploited for drug synthesis of potential inhibitors.

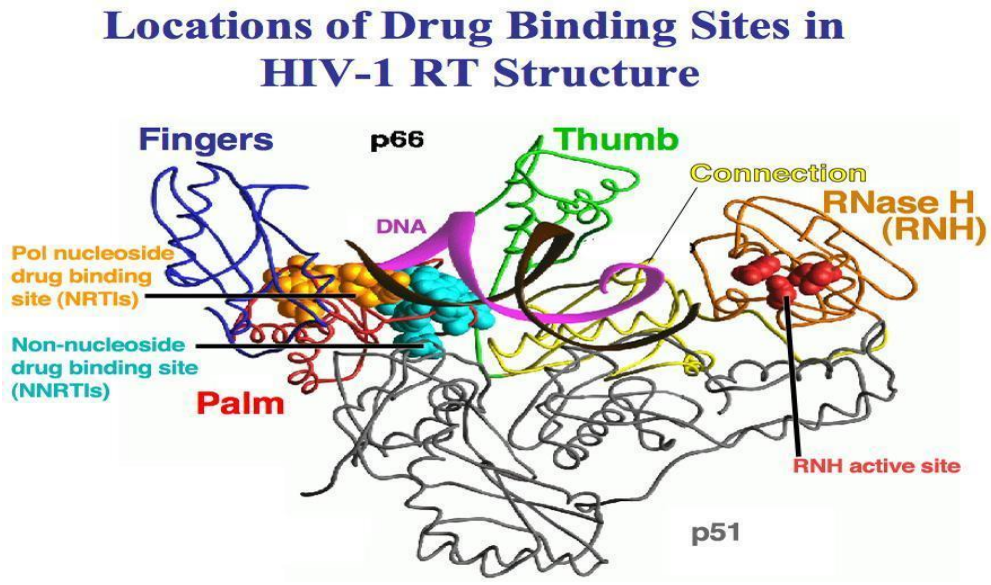


Figure 2: A broad overview of HIV reverse transcriptase protein. Indicated in the depiction are various potential drug binding sites. Nucleoside reverse transcriptase inhibitors (NRTIs) bind directly at the polymerase active site whereas non-nucleoside reverse transcriptase (NNRTIs) bind outside the enzyme catalytic site in a hydrophobic cleft just 10Å away from polymerase. Various domains of the p66 subunit are indicated[29].

1.9 RTIs as potential drug inhibitors of reverse transcriptase

Reverse transcriptase inhibitors have remained the cornerstone of antiretroviral therapy since their discovery[30]. Currently there are two classes of clinically relevant RT inhibitors, nucleoside/nucleotide reverse transcriptase inhibitors (NRTIs) and non-nucleoside reverse transcriptase inhibitors (NNRTIs)[31]. Zidovudine or AZT, a non-nucleoside/nucleotide reverse transcriptase inhibitor (NRTI) was the first commercial drug approved by the FDA for treatment and management of HIV/AIDS in 1987 and ever since then, several NRTIs with structural resemblance to AZT have been synthesised and commercialized for the treatment of HIV/AIDS[32] (**Figure 3**).

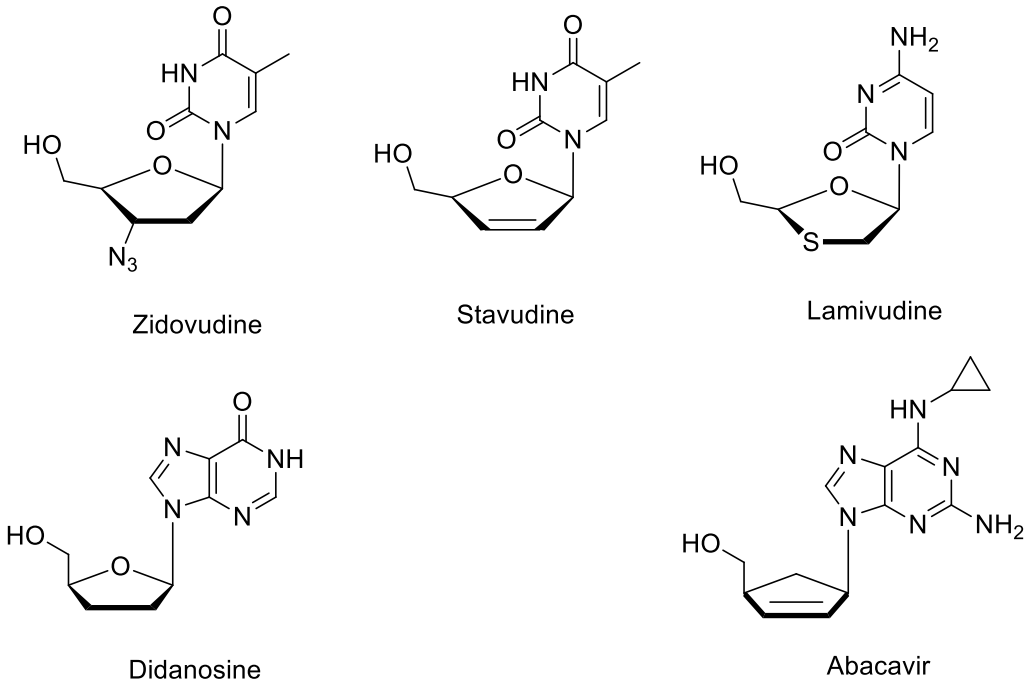


Figure 3: Nucleoside reverse transcriptase inhibitors (NRTIs)

NRTIs are by nature, prodrugs. They undergo intracellular phosphorylation into the active triphosphate form which is then able to inhibit viral replication by competing with naturally occurring purine and pyrimidine nucleotides, thus preventing further incorporation of these nucleotides by RT, thereby terminating viral DNA replication[32]. NNRTIs on the other hand act by binding at the hydrophobic cleft of the palm domain of p66, a site located separately from the enzyme catalytic site often targeted by NRTIs[33]. Essentially, NNRTIs are allosteric inhibitors of RT. Their binding results in conformational changes in the protein structure, ultimately reducing the ability of nucleotides to bind to the enzyme active site thus blocking cDNA elongation[34].

Although both classes of RT inhibitors have remained in use for HIV treatment for a very long time, both have shown significant limitations against the virus in recent years. The main threats affecting their use include emergence of drug resistant mutants, drug toxicity and intolerance of the medication, the requirements for routine daily administration and the ever-rising cost of the medication[32]. In spite of these challenges, RTIs remain effective against HIV due to their ability to cause impaired viral fitness. Nonetheless, synthesis and development of novel RTIs with improved effectiveness against resistant viral strains remains a focal point for most HIV research groups around the globe.

1.10 NNRTIs and their mode of action against RT

NNRTIs (**Figure 4)** work by binding to a highly hydrophobic pocket on the p66 domain of HIV-1 RT known as the NNRTI binding pocket[35,36]. The site is located away from the RT polymerase active site, effectively rendering it an allosteric site. In the absence of an inhibitor the site is not known to exist but rather, binding of the inhibitor causes the side chains of amino acids Tyr181 and Tyr188 to flip from a 'down' to an 'up' conformation thus creating the NNRTIs binding site[37]. Furthermore, NNRTI binding forces the Thumb to adopt an open and extended conformation, which resulted in the hypothesis that NNRTIs induce 'molecular arthritis' whereby movement of the domains lining up the enzyme catalytic site are inhibited, thus rendering the enzyme ineffective[38]. As opposed to NRTIs, NNRTIs are not prodrugs and as such do not require cellular activation or phosphorylation to induce their activity.

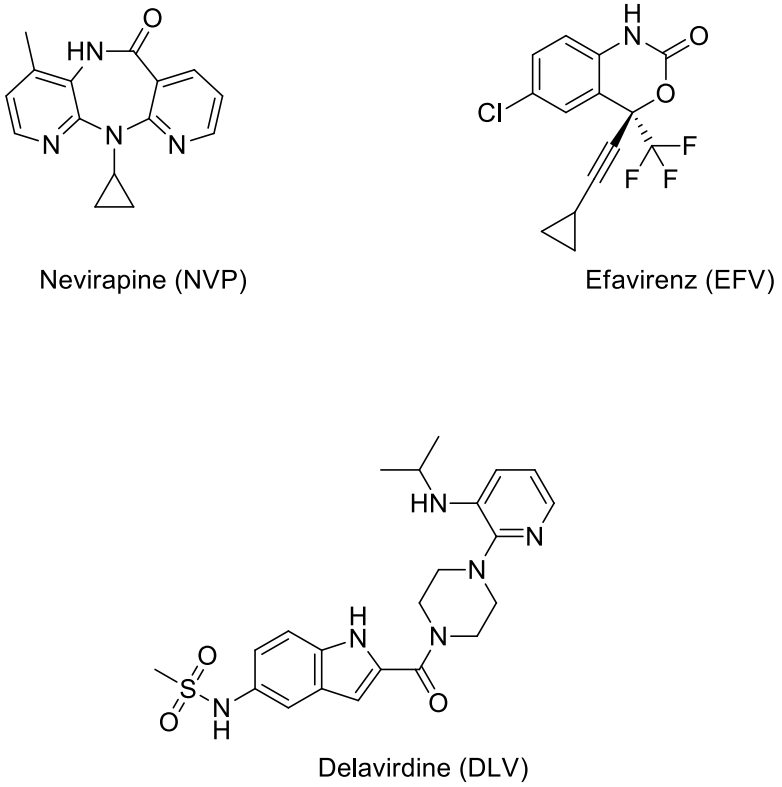


Figure 4: Non-nucleoside reverse transcriptase inhibitors (NNRTIs)

Molecular modeling and docking studies together with x-ray crystallography have revealed significant data on the interaction of NNRTIs with RT via non-competitive binding at the allosteric site. In addition, studies show that NNRTIs assume a butterfly-like conformation upon their binding[37,39] (**Figure 5**).

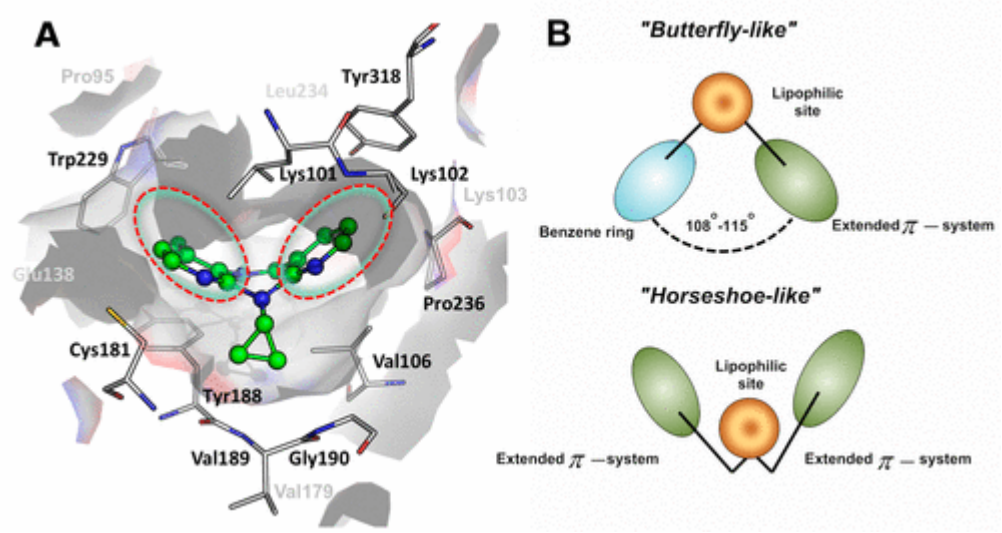


Figure 5: Illustration of the butterfly-like conformation often adopted by NNRTIs at RT binding site. *Adapted from ResearchGate, image by Peng Zhan*

Data from modeling studies by Himmel *et al*. also shows that anchoring of NNRTI binding at the binding site is achieved by: (i) pi-pi induced forces between the NNRTI phenyl substituents and the amino acid side chains of Tyr181, Tyr188, W229 and Tyr318 residues in the RT hydrophobic pocket; (ii) ionic interaction, significantly important for Lys101, Glu138 and Lys103 side chains; (iii) weak van der Waals forces with Y318, V106 , Y181, L100, G190, V179, W229, and L234 residues; and (iv) strong hydrogen bond interactions between the ligand and the peptide chain of RT[37]. As a result of their large size, first-generation class of inhibitors such as delavirdine, are said to expand towards the alternating loops consisting of the P236 residues while preserving significant pi interactions with the highly mutative Y181 and Y188 residues and hydrogen bonding interactions with K103 residue[31]. The main challenges with regards to newer NNRTIs would be to address the many mutations conferred by RT while minimizing severe adverse effects often experienced by patients on NNRTIs, and at the same time extending the duration of action of the drug.

1.11 Latest NNRTIs

Docking of the inhibitor at the NNRTI binding pocket is believed to reduce the degree of free motion of RT subdomains, consequently forcing the enzyme to remain in an open conformation allowing the DNA/RNA substrate or ssDNA to glide through with limited processing by polymerase[37]. The exact explanation as to how polymerase activity is affected by this binding is still not clear. However, several explanations have been drawn up: (1) NNRTI binding leads to displacement of W229 from the NNRTI binding pocket which effectively reduces the polymerase primer grip to a conformation that compromises its processing capability of the nucleic substrate, and (2) NNRTI binding cripples the geometrical conformation of the "YMDD" active site chain which houses D185 and D186 residues which are thought to affect catalysis by polymerase. The second generation NNRTIs (**Figure 6**) are designed to exploit this binding due to torsional flexibility in their structural make up.

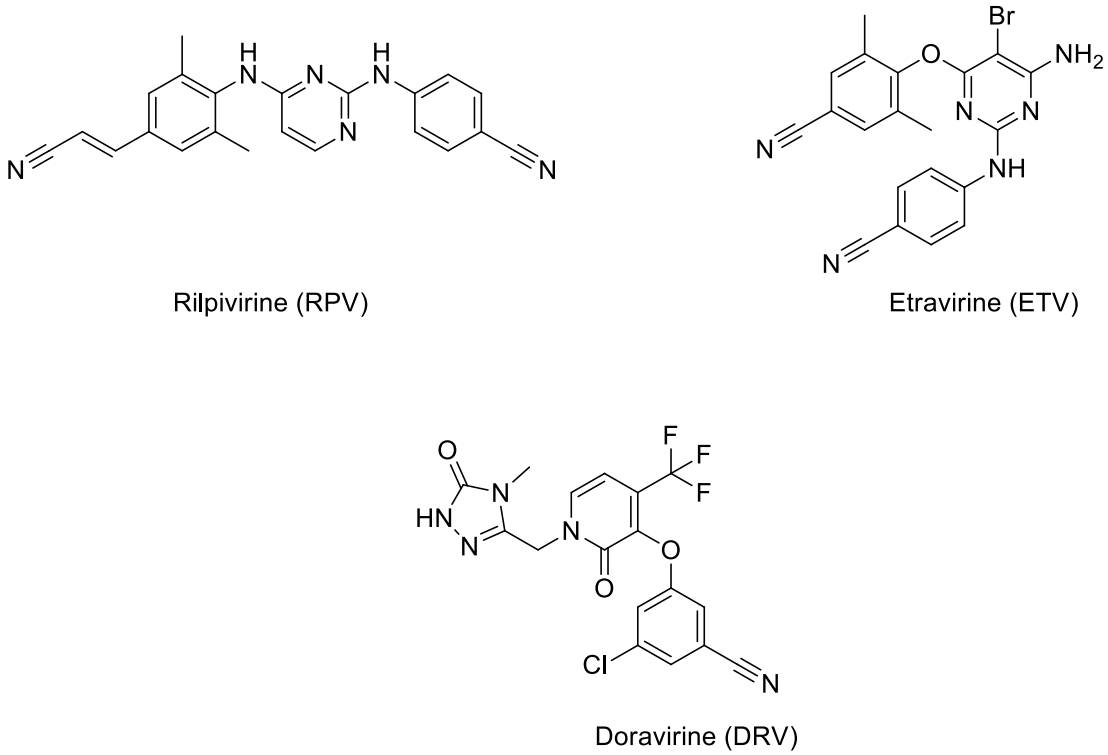


Figure 6: Newer NNRTIs rilpivirine (RPV), etravirine (ETV), and doravirine (DRV).

Although the second generation NNRTIs (RPV and ETV), from the diarylpyrimidine (DAPY) class, show improved tolerance against resistant mutations than the first generation NNRTIs (NVP, DLV and EFV), they still show poor pharmacokinetic profiles and suffer from cross-drug resistance with some chronic medications[40]. More recently, pyridinone derivatives have shown significant potency against RT and its resistance-associated variants[41]. This class resulted from structural modifications of the DAPY NNRTIs and has seen a commercial breakthrough in the FDA approval of doravirine. **Figure 7** shows an example of three NNRTIs currently in clinical trial stages that have shown significant improvements in activity against RT.

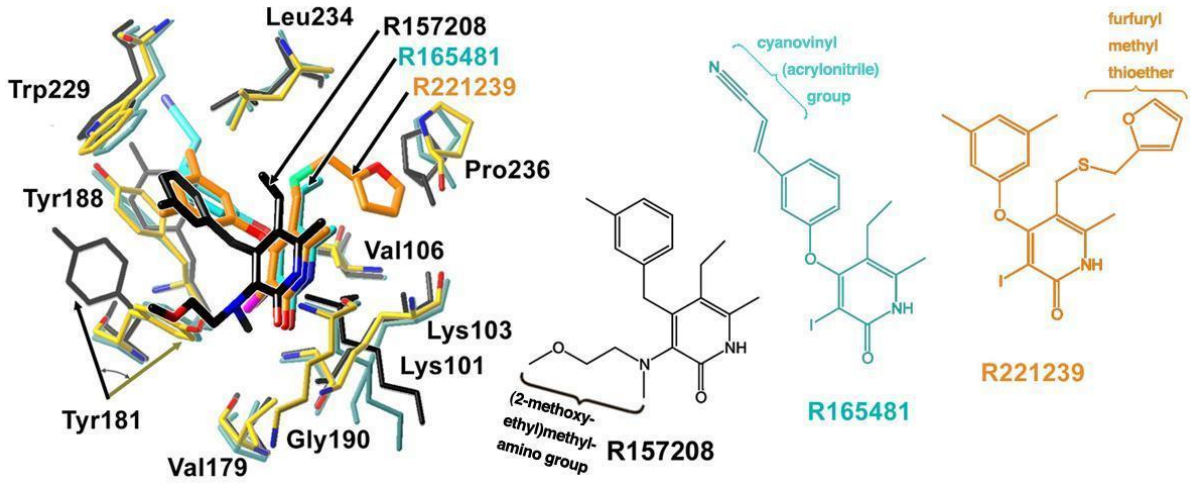


Figure 7: A superposition of three pyridinones at the RT binding site to study their binding modes[37]. The carbons for R157208 are shown in black, for R165481 are shown in cyan and for R221239 are shown in orange. Binding of R157208 causes Tyr181 side chain to rotate upward towards Trp229 due to extension of the (2-methoxyethyl) methylamino group. This observation is, however, absent upon binding of the other two pyridinone derivatives with an iodo substituent at the same position as the (2-methoxyethyl) methylamino group. In addition, the two iodo substituted derivatives (R165481 and R221239) exploit the lipophilic tunnel composed of highly hydrophobic amino acid side chains, which in turn is created as a result of Tyr181 maintaining its downward position.

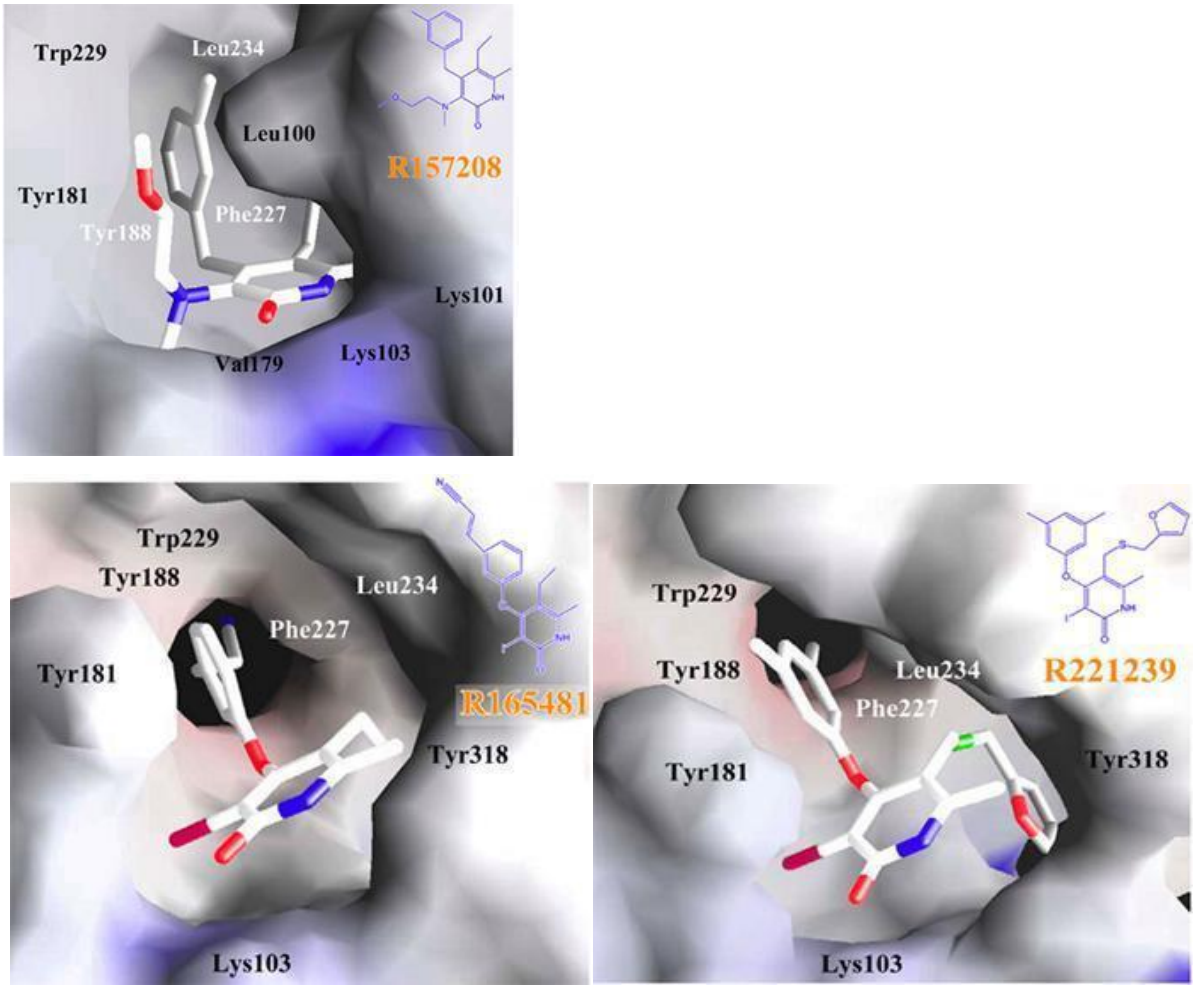


Figure 8: Modelling illustration of the pyridinone inhibitors at the surfaces of NNRTI binding site. Notice the clearly visible tunnel in each image which R165481, shown above, is said to exploit using the cyanovinyl substituent[37].

Figure 8 shows more detail regarding the binding of these pyridinones. Important to note is that when the ligand R157208 is bound, the amino acid side chain of Y181 flips to an upward position to accommodate the methylamine group of the inhibitor, resulting in various interactions between R157208 and Y181[37]. Several NNRTIs are dependent on stacking interactions with Y181 and as a result are highly susceptible to tolerance in drug-resistant strains where Y181 is mutated to a different amino acid such as Cys. In the example above R165481 and R221239 do not exhibit much interaction with Tyr 181 such that the side chain maintains its downward position. Thus, R165481 and R221239 have been shown to be effective against Y181/Cys mutations.

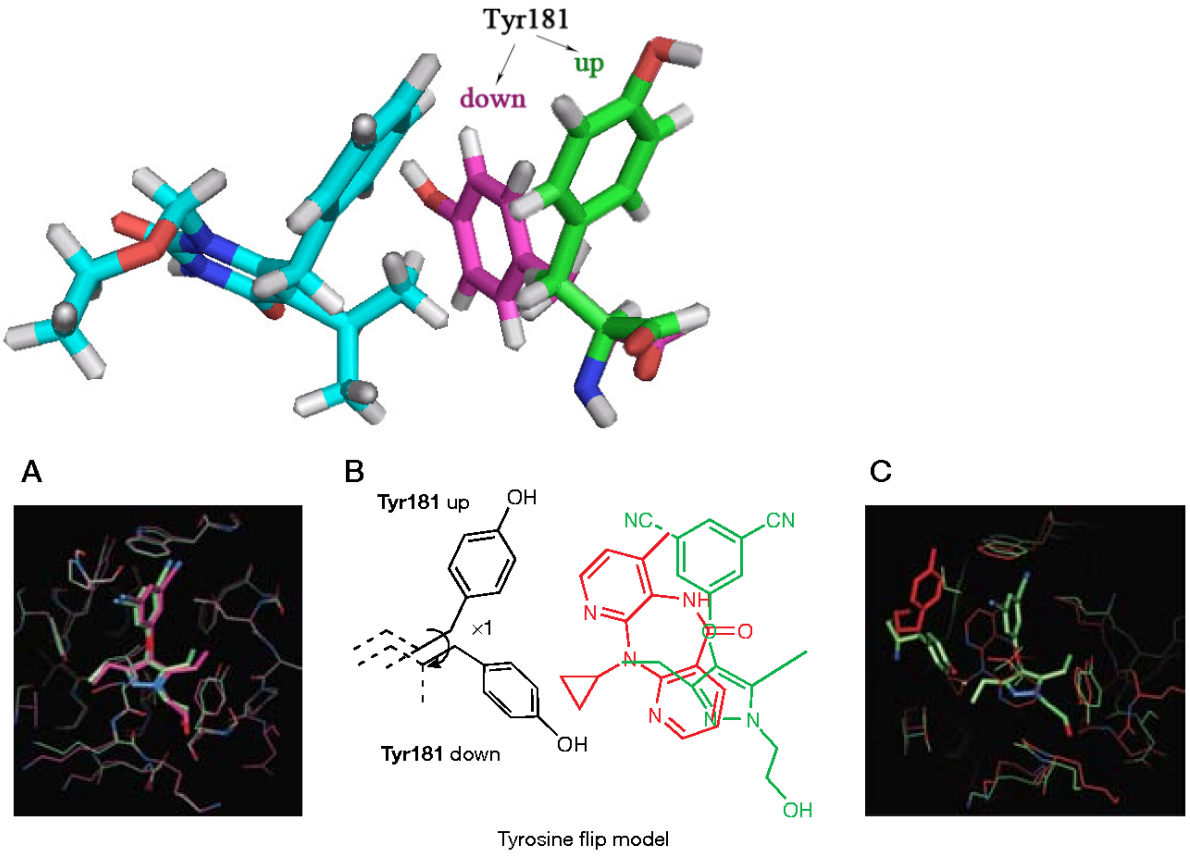


Figure 9: **A**) Conformational structures of an inhibitor bound to HIV-1 RT wild-type (pink) and mutant K103N (green), **B&C**). The 'tyrosine flip' model. Comparison of HIV-1 WT RT inhibitor-bound (green, Tyr 181 'down') and HIV-1 WT RT inhibitor-bound (red, Tyr 181 'up'). *Adapted from semanticscholar.org*

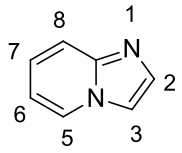
The cyanovinyl functional group of R165481 is said to significantly improve the inhibition of several drug-resistant mutant strains of RT by its interaction with a lipophilic tunnel which is composed of amino acid side chains L228, Y188, V108, F227, and the highly conserved W229 on its surface. The said cyanovinyl group is a significant moiety of the drug rilpivirine (**Figure 6**), allowing the drug extensive and strategic flexibility within the NNRTI binding pocket and thus the ability to geometrically accommodate various drug resistant mutations. Nonetheless, R165481 is said to be susceptible to drug-resistant strains where Y188 or Phen227 are mutated.

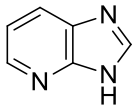
Of the three inhibitors outlined above, R221239 is said to be the most effective of the trio. Its effectiveness is proposed to be as a result of the presence of the furfuryl methyl thioether group connected to the central core by a flexible heteroatom bridge. The flexible heteroatom linker is believed to exert an influence in helping R221239 to respond flexibly to various

mutations by adopting strategic conformations without displacement from the binding site. As a result, both R221239 and R165481 are now said to utilise strategic flexibility in various ways in order to accommodate for the reduction of significant ligand to protein interactions when one or more mutations are encountered at the binding pocket. This study aims to exploit and expand on the flexibility of a heteroatom linker of an RT inhibitor based on imidazopyridine as the backbone.

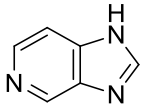
1.12 Imidazopyridines as structural fragments in the design and synthesis of novel NNRTIs

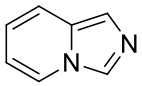
Imidazopyridines are important structural components of several biologically active compounds. The two-membered ring fused heterocyclic structure resembles those of indole and azaindole, two of the most common heterocycles known for their important biological properties. Imidazopyridines consist of four known isomers (**Figure 10**): imidazo[1,2-*a*]pyridine **i**, imidazo[4,5-*b*]pyridine **ii**, imidazo[4,5-*c*]pyridine **iii**, and imidazo[1,5-*a*]pyridine **iv**[42]. This study focuses on the synthesis and application of imidazo[1,2-*a*]pyridine





(i) Imidazo[1,2-*a*]pyridine **(ii)** 1*H*-imidazo[4,5-*b*]pyridine





(iii) 1*H*-imidazo[4,5-*c*]pyridine **(iv)** Imidazo[1,5-*a*]pyridine

Figure 10: Structural isomers of imidazopyridine

Imidazopyridine scaffolds have shown remarkable biological properties in recent years finding application as anti-inflammatory agents, antiviral, anticancer, antifungal, antibacterial, antiprotozoal, antiapoptotic, analgesic, antipyretic, anxioselective and hypnoselective agents[43]. Previous studies have demonstrated the binding mode of NNRTIs at the allosteric site of RT which shows a butterfly-like structural binding[44]. It is this structural binding mode that this study aims to exploit using flexible imidazo[1,2-*a*]pyridine derivatives with heteroatom linkers as RT inhibitors. This torsional flexibility is envisaged to accommodate enzymatic mutations by enabling the inhibitor to adopt different conformations.

1.12.1 Synthesis of imidazo[1,2-*a*]pyridines

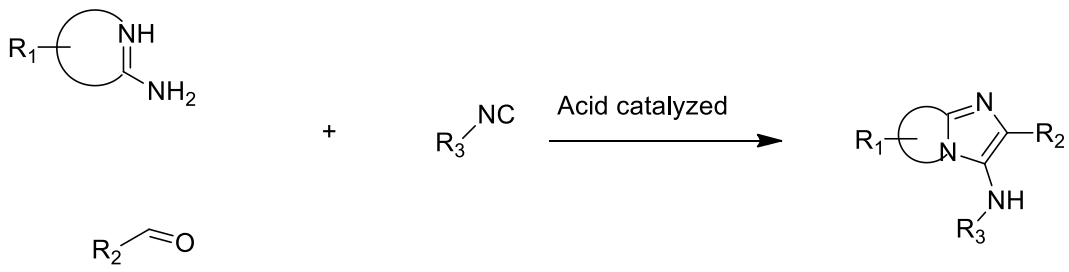
The growing interest in properties and applications of imidazo[1,2-*a*]pyridines has seen a continuous effort towards fast-tracking the development of new synthetic techniques for synthesis of derivatives with structural diversity potential at the 2- and 3-positions of the moiety[43]. Various approaches have been adopted in an effort to develop new synthetic strategies for the diversification of the imidazo[1,2-*a*]pyridine structural backbone. These approaches are categorized and, in some instances, subcategorized into condensation reactions, oxidative coupling, one-pot multicomponent reactions, hydroamination reactions, amino-oxygenation reactions, tandem reactions *etc*[45].

1.12.1.1 Multicomponent reactions of 2-aminopyridine, aldehyde and isocyanide

This is a rapid and atom efficient method of accessing imidazo[1,2-*a*]pyridines with a potential for structural diversification in three distinct zones[46]. The Groebke-Blackburn-Bienaymé- multicomponent reaction (GBBR), **Scheme 1A**, is the most common reaction for this synthetic approach due to its ease of preparation and high yields. The discovery of this synthetic reaction started when Groebke *et al.*, first reported an Ugi-4-component side reaction while investigating the effects of various amines[47]. Groebke and co-workers established that amines with a cyclic structure such as 2-aminoazine, 2-aminopyrimidine and 2-aminopyrazine resulted in the corresponding 3-amino-substituted imidazo[1,2-*a*]pyridines, -pyrimidines and -pyrazines respectively[47] **(Scheme 1B)**. Similarly, Blackburn *et al.* (Millenium Pharmaceuticals) reported similar work around the same time[48] **(Scheme 1C)**. Their work focused on the use of scandium triflate as a catalyst in the reaction for optimal yields. This was, however, consistent with the findings of Groebke *et al.* that a catalytic amount of a Brønsted acid such as acetic acid resulted in improved yields[43]. This approach was based on a proton-assisted activation of the imine intermediate to enable nucleophilic attack by the isocyanide carbon. In the case of a Lewis acid, vacant d-orbitals of the metal salt activate the Schiff base.

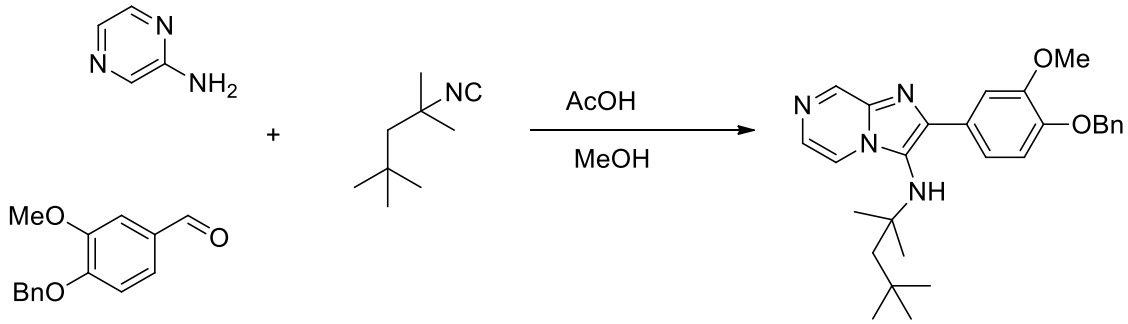
The other inventor of the GBB reaction, Bienaymé *et al.* from Rhône-Poulenc Technologies in France, while investigating new approaches to MCR, reported a 3-component reaction of 2-aminopyrimidine or 2-aminopyridine with isocyanide and an aldehyde in the presence of perchloric acid in methanol[49] **(Scheme 1D)**.

General GBB-3CR Reaction



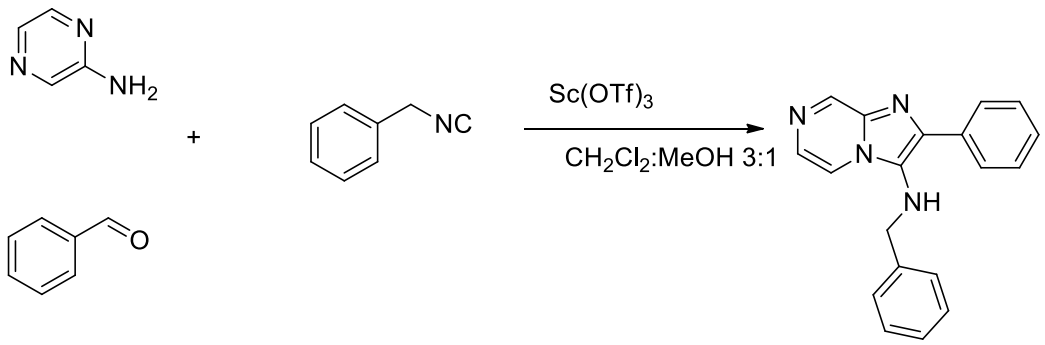
A

Groebke *et al.*

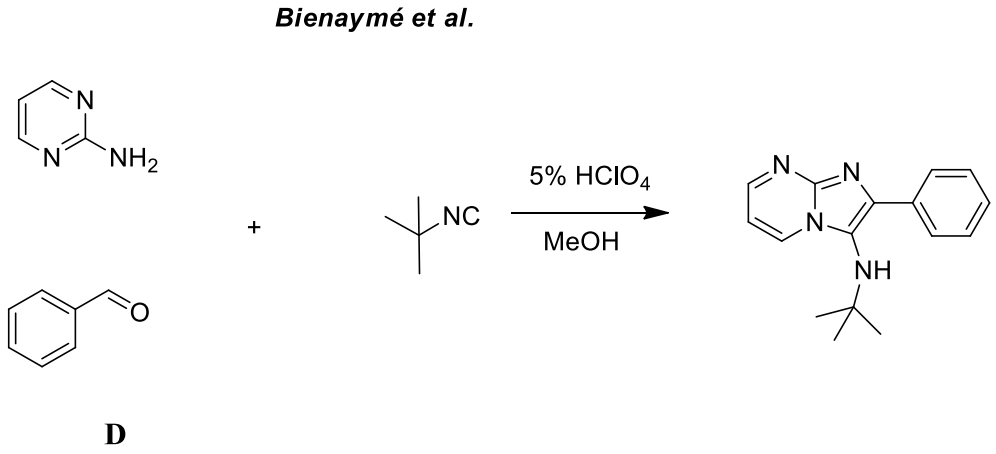


B

Blackburn *et al.*



C



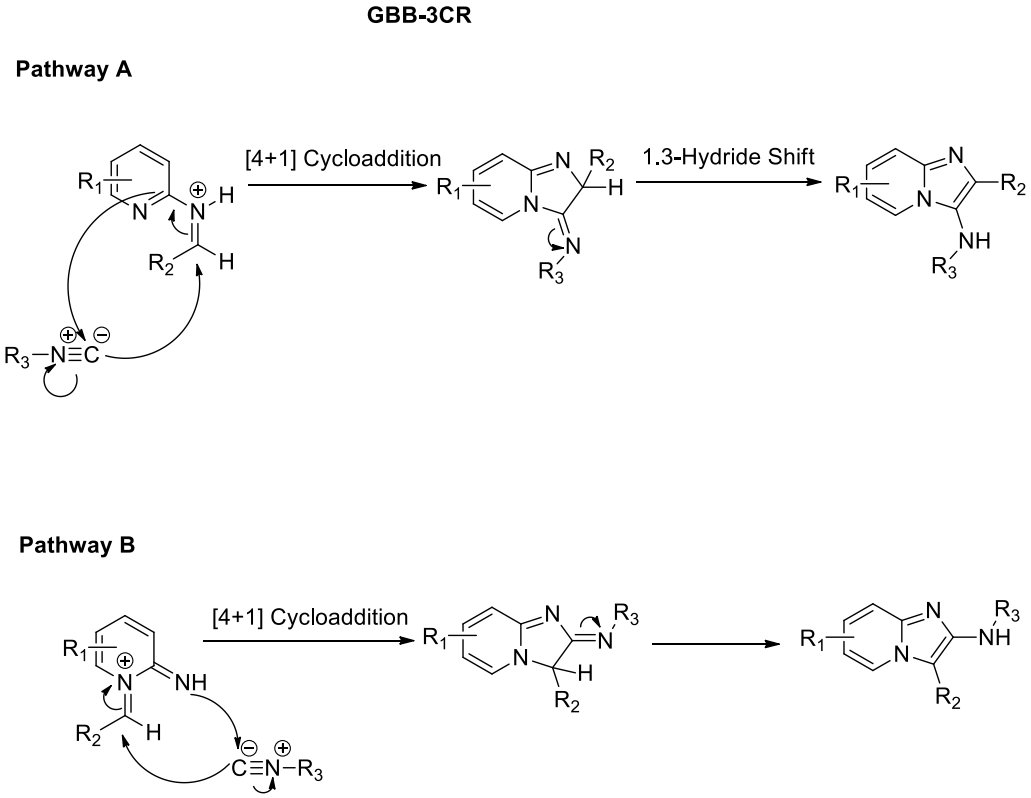
D

Scheme 1: A schematic representation of the GBB multicomponent reaction. **A,** Illustration of the general GBB-3CR. **B,** an example of the Bienaymé reaction using 2-aminopyrimidine, *tert*-butyl isocyanide, benzaldehyde and perchloric acid as a Brønsted catalyst, isolated product was verified by X-ray crystal structure analysis. **C,** Blackburn *et al.* reported scandium triflate as the optimal catalyst. **D,** an example of the Groebke reaction using 2-aminopyrazine and acetic acid as a catalyst.

As a result of the nearly simultaneous discovery of this multicomponent reaction, the reaction would later become known as the Groebke-Blackburn-Bienaymé 3-component reaction or the GBB-3CR in short. To date, more than 200 publications and over 100 patents have been filed, exploiting the GBBR, and interest in the reaction is growing exponentially[43].

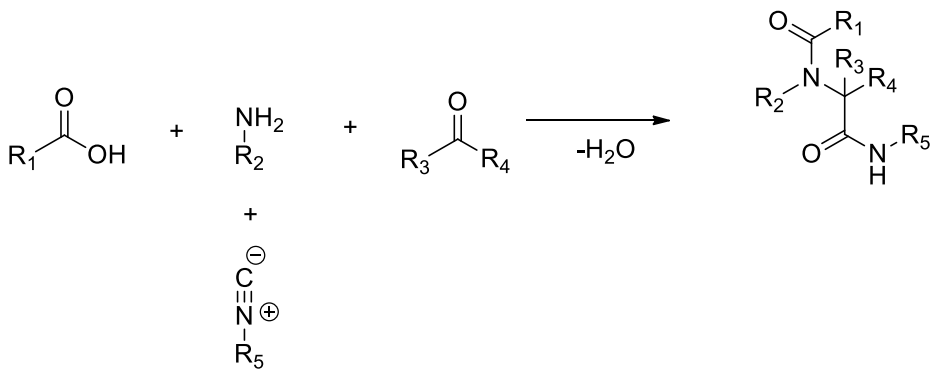
The general reaction proceeds by the condensation of the aldehyde with the basic amine of the 2-aminopyridine, -pyrazine or -pyrimidine. Often the aldehyde is catalytically activated using either a Brønsted-Lowry acid or a Lewis acid. In recent years, Montmorillonite K-10 clay has been found to be an efficient, environmentally friendly, and cost-effective catalyst due to its potential for being both a Lewis acid and a Brønsted-Lowry acid. In the absence of the catalyst, excessive heat is often necessary. Heterocyclization is completed by a [4+1] cycloaddition reaction with the isocyanide nucleophilic carbon attacking the electrophilic Schiff base and subsequent pyridine nitrogen attack on the isocyanide carbon. The GBB-3CR however, has been reported to follow two possible pathways giving rise to two possible regioisomers, as illustrated in **Scheme 2**. Pathway A is more commonly encountered and is often referred to as GBB-3CR whereas pathway B is less commonly encountered and is often referred to as the "Inverse" GBB-3CR. 2-Aminopyrimidines are also reported to form regioisomers, as was first reported by Mandair *et al*., in their attempt to explain the poor

yields of their reactions when the starting material was all but consumed[50]. The second isolated product, with similar TLC-R_f values, identical NMR spectroscopic data as well as mass spectrometric data was revealed by X-ray crystal structure analysis to be an inverse of the conventional imidazo[1,2-*a*]pyridine-3-amine product. Fortunately, the conventional GBB product is the major product in most GBB-3CR reactions and, as reported by Boltjes *et al.*[43], in many cases not even a trace amount of the inverse product is observed.



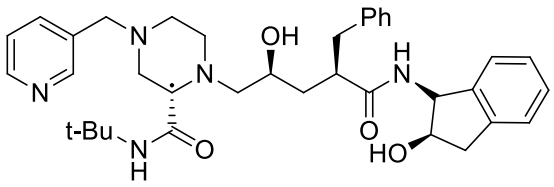
Scheme 2: Mechanistic illustration of the possible pathways of the GBB-multicomponent reaction

The Ugi four component condensation reaction (U-4CR) proceeds by a similar mechanism with the exception that in the U-4CR the acid component is incorporated into the final structure whereas in the GBB-3CR the acid only serves as a catalyst in the reaction. The Ugi reaction also affords an α-acylaminocarboxamide as a product (**Scheme 3**). Other three-component reactions include the Passerini (P-3CR), Biginelli (B-3CR), Gewald (G-3CR), van Leusen (vL-3CR), Hantsch (H-3CR) and many other MCR reactions.

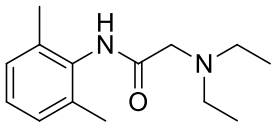


Scheme 3: A schematic representation of the Ugi multicomponent reaction

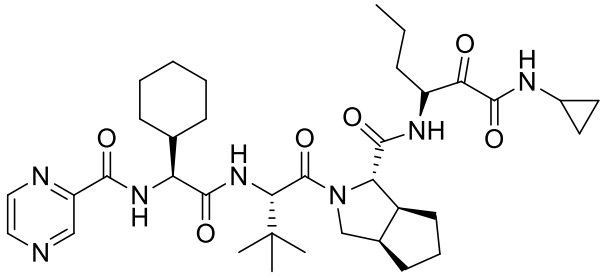
The preparative advantage of the GBBR one-pot synthesis is that it offers remarkably quick access to libraries of compound classes of synthetic targets as well as organic compounds with a wide range of applications. The one-step reaction with only water as a by-product represents a classical green chemistry application. The use of microwave-assisted irradiation in recent times has advanced the potential for multicomponent reactions even further, resulting in quick and simple reactions with a high degree of safety as well as avoiding multiple steps that often lead to lower yields and environmental pollution[51]. The isocyanide-based multicomponent reactions (IMCR) have become an important aspect in drug design and many drugs and pharmacophores have been synthesized using this synthetic protocol. It is estimated that approximately 5 % of current global drug supplies can be assembled by multicomponent reactions[43]. Examples of current marketed drugs and lead compounds that have been assembled by MCR approach are Telaprevir (Passerini-3CR), Xylocaine (Ugi-3CR), Crixivan (Ugi-4CR) and Nifedipine (Hantzsch-3CR) (**Figure 11)**.



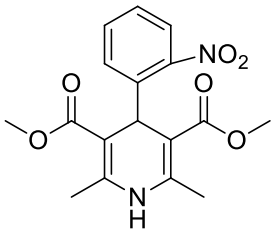
Crixivan® (U-4CR)



Xylocaine (U-3CR)



Telaprevir (P-3CR) and (U-3CR)

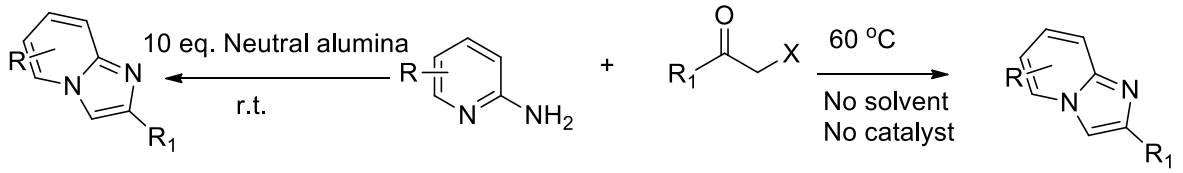


Nifedipine (Hantzsch-3CR)

Figure 11: Commercial drugs synthesized by multicomponent reactions

1.12.1.2 Condensation reactions from α-haloketones

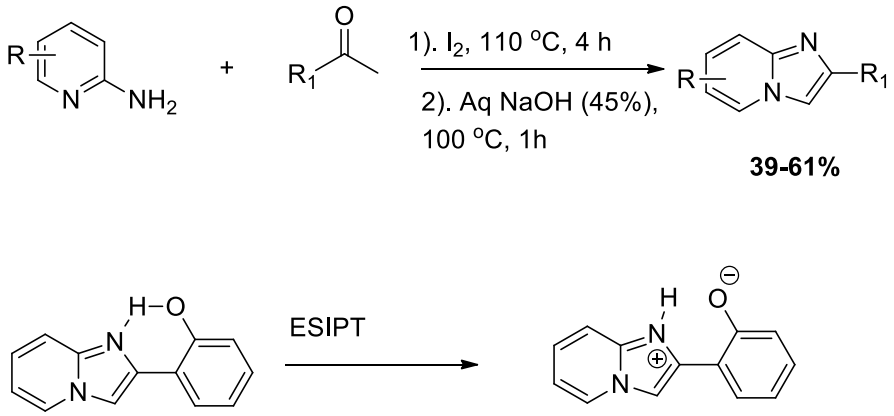
Traditionally considered the only synthetic approach for imidazo[1,2-*a*]pyridine synthesis, the condensation of α-haloketones with 2-aminopyridines has been overshadowed by more recent advances in multicomponent reactions[45]. The reaction proceeds by reductive amination on the keto group of one substrate by the 2-amino group on pyridine, the starting material. This is subsequently followed by the displacement of the halogen that was alpha to the ketone by the pyridine nitrogen, resulting in cyclization of the compound **(Scheme 4).**



Scheme 4: Imidazo[1,2-*a*]pyridine synthesis from α-haloketones

Various attempts have been made to improve the yields using this synthetic approach. For example, Ponnala *et al.*, reportedly made use of neutral alumina as an effective add-on to improve the yield[52]. They were successful in synthesizing various imidazo[1,2-*a*]pyridines using this approach. Chen and Wu reported the synthesis of imidazo[1,2-*a*]pyridines from α-bromo/chloroketones and 2-aminopyridines under solvent- and catalyst-free conditions at 60 °C[52]. Cyrański and co-workers were able to synthesize imidazo[1,2-*a*]pyridine derivatives

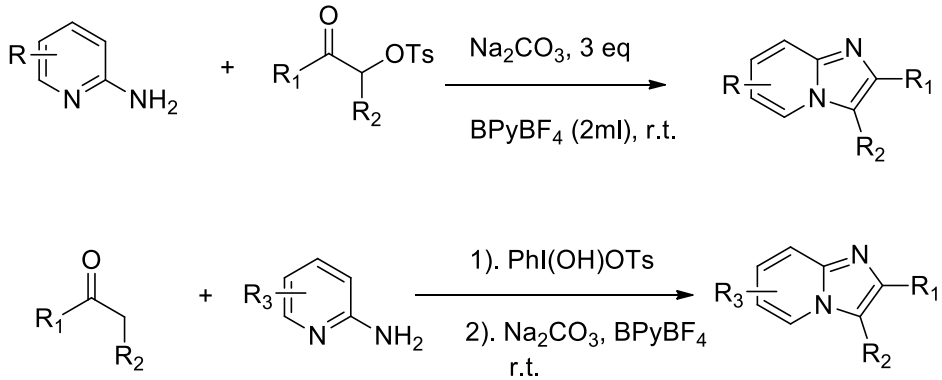
from various ketones by generating α-iodoketones *in situ*[53] **(Scheme 5)**. They studied photochemical properties of the synthesized products and found that imidazo[1,2-*a*]pyridines possessing a 2-hydroxyphenyl attachment exhibit excited state intramolecular proton transfer (ESIPT). They also reported that imidazo[1,2-*a*]pyridines possessing a phenyl substituent at the 2-position showed strong band emission in the blue region.



Scheme 5: Synthesis of imidazo[1,2-*a*]pyridine by *in situ* generation of iodoketones

1.12.1.3 Imidazo[1,2-*a*]pyridine synthesis from α-tosyloxyketone

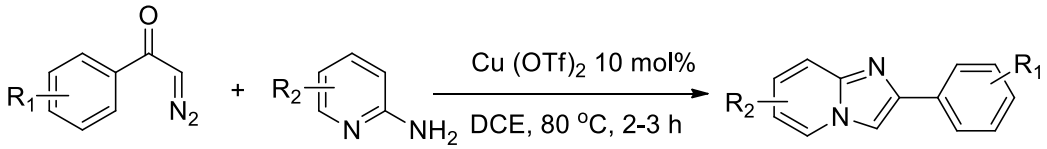
Various attempts have been made to synthesize imidazo[1,2-*a*]pyridines under solvent-free conditions. However, the use of ionic liquids has been shown to improve reaction times and they require little to no heat[54]. The reaction of 2-aminopyridine with α-tosyloxyketones in ionic liquid $BPyBF_4$ was successfully carried out within an hour and gave rise to the desired imidazo[1,2-*a*]pyridines in appreciable yields **(Scheme 6)**. Other reactions were also carried out by direct reaction of the ketone and generating α-tosyloxyketones *in situ* **(Scheme 6).**



Scheme 6: Synthesis of imidazo[1,2-*a*]pyridines from α-tosyloxyketones

1.12.1.4 Imidazo[1,2-*a*]pyridine synthesis from α-diazoketones

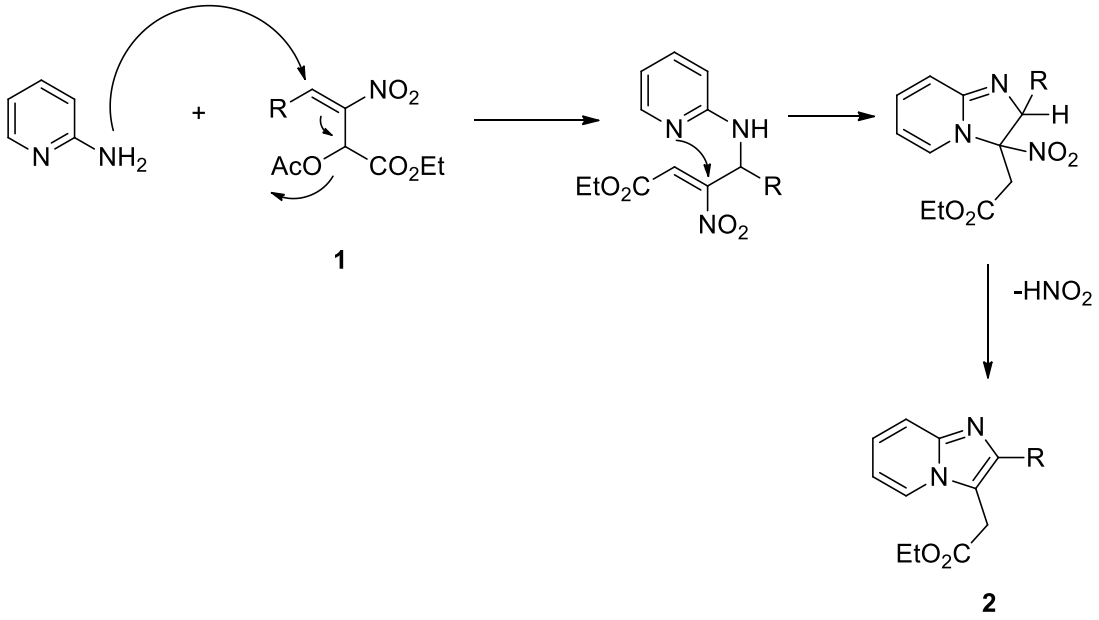
Similarly to α-haloketones, α-diazoketones have been successfully employed in the synthesis of imidazo[1,2-*a*]pyridines[55]. The condensation reaction between 2-aminopyridines and α-diazoketones **(Scheme 7)** is often catalysed by copper salts such as $Cu(OTf)_2$ although other Lewis acids such $In(OTf)_3$, $InCl_3$, $InBr_3$, $Sc(OTf)_3$ and $Bi(OTf)_3$ have been shown to be equally effective. In contrast, Brønsted acids such as Amberlyst-15, heteropoly acid and dodeca-molybdophosphoric acid (PMA) have been proven to be ineffective for this reaction.



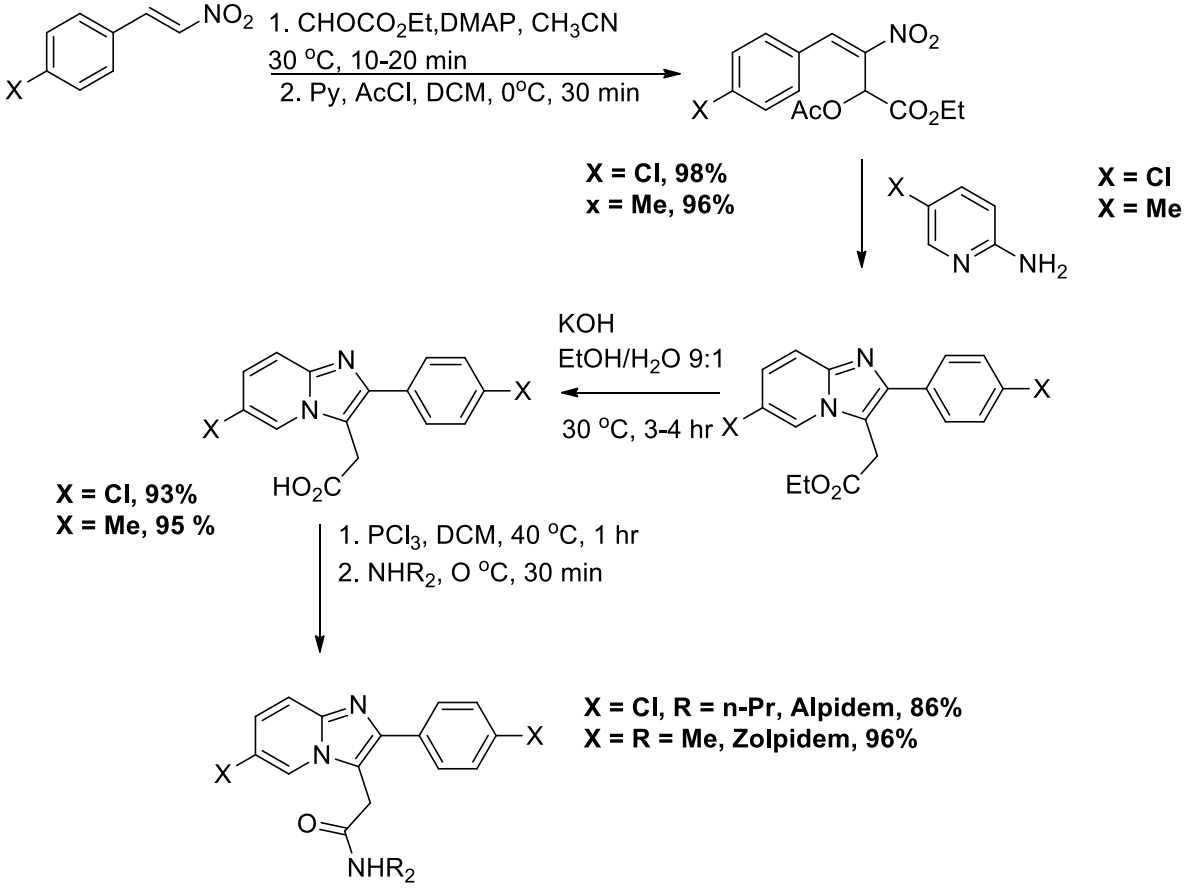
Scheme 7: Synthesis of imidazo[1,2-*a*]pyridine from α-diazoketones

1.12.1.5 Imidazo[1,2-*a*]pyridine synthesis from Morita-Baylis-Hillman (MBH) acetates of nitroalkenes

In agreement with most imidazo[1,2-*a*]pyridine synthesis methods, this one-pot regioselective reaction reported by Namboothiri and co-workers combines 2-aminopyridines with Morita-Baylis-Hillman acetates of nitroalkenes (**1**) at room temperature using MeOH as a solvent **(Scheme 8)**[56]. Namboothiri and co-workers were able to synthesize a small library of imidazo[1,2-*a*]pyridines **(2)** using this strategy within short reaction times, however, the methodology was limited to 2-aminopyridines only. Reactions with 2-aminopyrimidines, -pyrazines and -aminothiazoles were ineffective[45]. Nonetheless, this method was employed in the synthesis of anxiolytic and anti-insomnia drugs alpidem and zolpidem in a six-step process resulting in the overall yield of 72% and 78%, respectively **(Scheme 9)**.



Scheme 8: Synthesis of functionalised imidazo[1,2-*a*]pyridines from Morita-Baylis-Hillman acetate nitroalkenes



Scheme 9: Synthesis of alpidem and zolpidem from Morita-Baylis-Hillman acetates of nitroalkenes (MBH)

1.12.2 Pharmaceutically active imidazo[1,2-*a*]pyridines and drug candidates

Imidazo[1,2-*a*]pyridine heterocycles synthesized by GBB-3CR have given rise to several pharmaceutically active compounds that have made it into the market. Common non-benzodiazepine group of drugs, colloquially referred to as Z-drugs, such as zolpidem **(3)** (Ambien®, Ivedal®, Stilnox®, Sanval®, etc), alpidem **(4)**, saripidem **(5)**, necopidem **(6)** etc (**Figure 12**), are all imidazo[1,2-*a*]pyridine derivatives which act by increasing transmission of the neurotransmitter gamma-aminobutyric acid (GABA) at the $GABA_A$ receptors in the central nervous system[57]. Similar to benzodiazepines, z-drugs are sedative and anxiolytic and as such are used primarily for the treatment and management of insomnia. The main advantage of z-drugs compared to benzodiazepines and barbiturates is that they are much safer, particularly in instances of overdose, and they have less potential for physical dependency and addiction. As such, they are most widely prescribed[58–60].

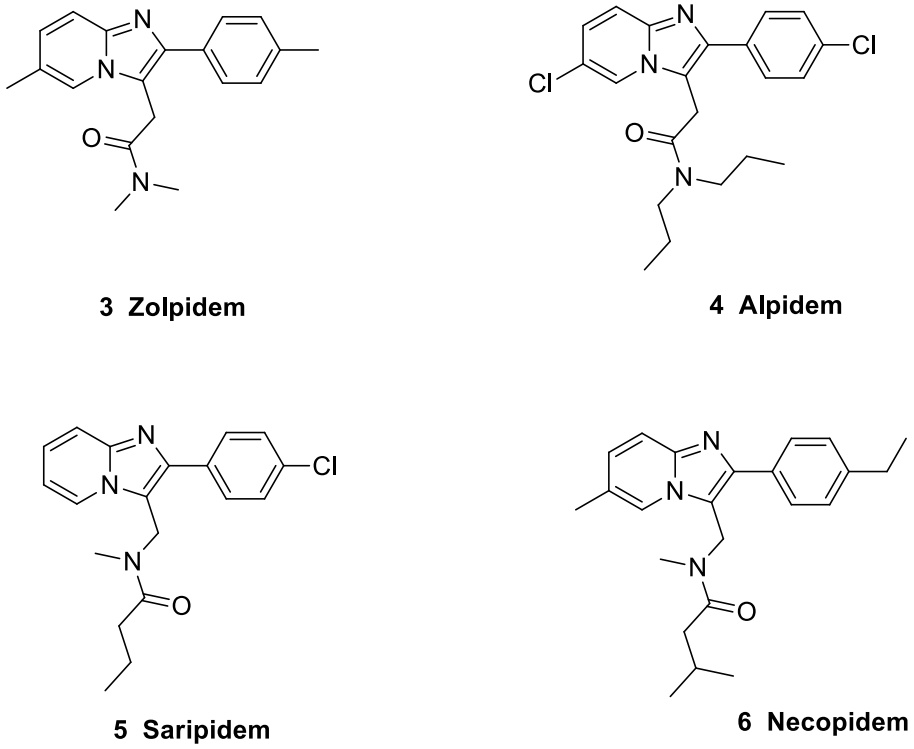
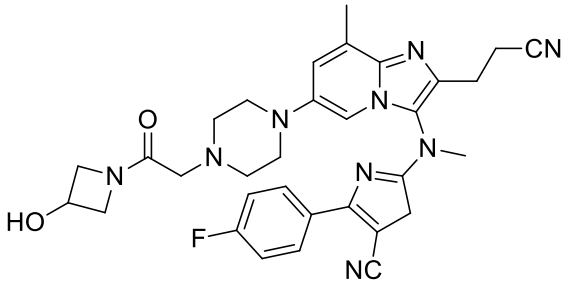


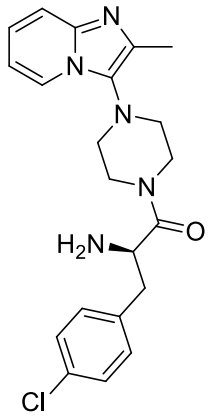
Figure 12: Examples of commercial drugs synthesised using the GBB-3CR reaction and containing the imidazo[1,2-*a*]pyridine fragment.

This, however, is not an indication that the GBB-3CR derived compounds exert their action in a similar biological fashion. The major difference between z-drugs and other pharmaceutically active compounds obtained by GBB-3CR is the exocyclic amine substituent

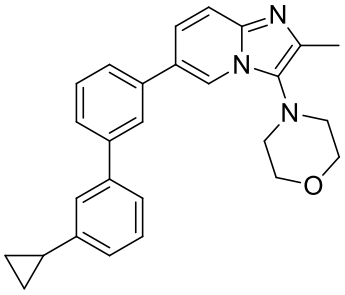
at the 3-position. In addition to various interactions between the imidazopyridine scaffold and proteins surrounding the binding pocket of the target, the exocyclic amine enables hydrogen bonding interactions which are often crucial for conformational stability of the compound at the binding site. Several examples of imidazo[1,2-*a*]pyridine compounds with the pendant amine substituent such as compounds **7-9**, have been reported as bioactive leads **(Figure 13)**. The novel small molecule GLPG1690 **(7)**, an autotaxin-lysophosphatidic acid axis (ATX-LPA) inhibitor, has shown promising therapeutic outcomes against idiopathic pulmonary fibrosis (IPF) and is currently in phase-3 clinical trials[43,61]. It was through high-throughput screening and post-structural modifications that 2,3,6-trisubstituted imidazo[1,2-*a*]pyridines such as GLPG1690 were identified as potent ATX-LPA inhibitors[62]



7 **GLPG-1690**
Galapagos NV, 2013



8 **Array biopharma Inc, 2005**



9 **Rigel Pharmaceuticals, 2014**

Figure 13: Imidazo[1,2-*a*]pyridine compounds with the amine at the 3-position as lead compounds

Ordinarily, it takes on average 15-20 years before a drug candidate can be assembled after the discovery of a new synthetic method[43], however, it was only in 2009, eleven years after the GBB-3CR was first reported, that the first biologically active molecule was identified and reported using the GBB-3CR core as published by Lacerda *et al.*[63]. In their attempt to

perform structural modifications on compound **10**, a selective p38 MAP kinase inhibitor, a GBB-3CR scaffold-hopping method was employed to afford celecoxib **(11)** a non-steroidal anti-inflammatory drug (NSAID) and COX-2 inhibitor and compound **12,** another p38 MAP kinase inhibitor. The aim was to synthesize 3-arylamine-imidazo[1,2-*a*] pyridines with anti-inflammatory and analgesic properties **(Figure 14)**. This approach resulted in the discovery of compound **13**, a prostaglandin-endoperoxide synthase-2 or also known as a COX-2 inhibitor and was identified as acting similarly to SB-203580 **(10)**, altering thermal hyperalgesia induced by capsaicin, a study used to establish analgesic effects. Ultimately, compound **14**, a novel prostaglandin-H synthase-2/COX-2 inhibitor, ten times more potent than celecoxib (Celebrex®), was discovered[43].

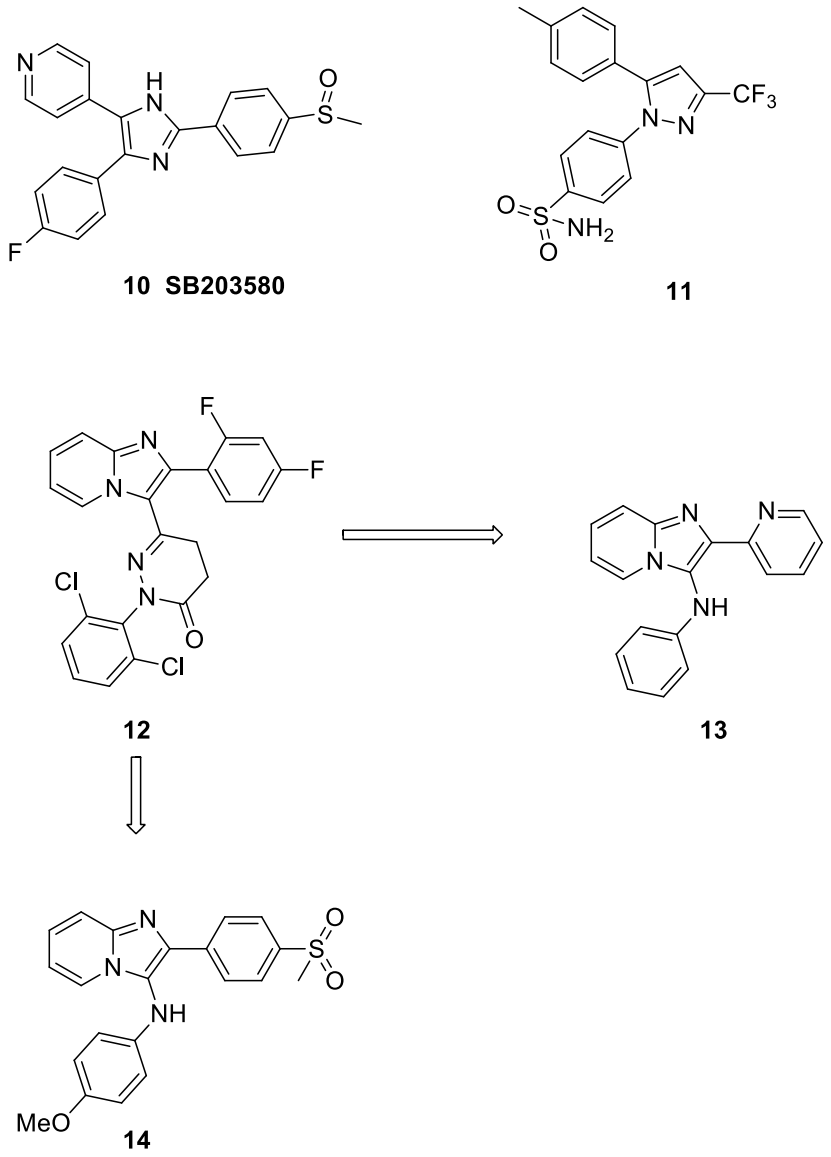
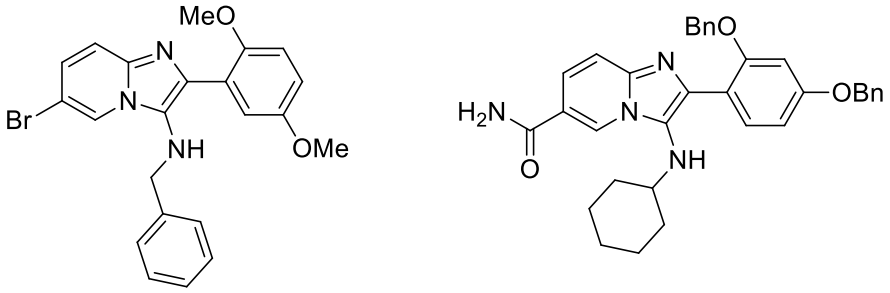


Figure 14: Imidazo[1,2-*a*]pyridine derivatives with anti-inflammatory and analgesic properties

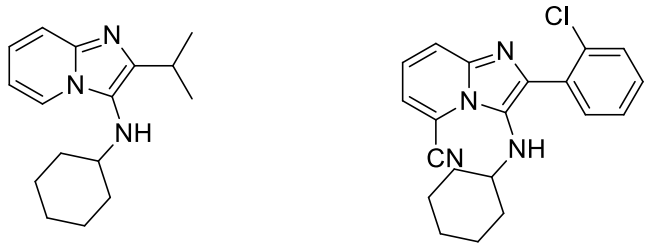
Imidazo[1,2-*a*]pyridines were also examined for effectiveness against various colon cancer cell lines by de Koning and co-workers and showed impressive apoptosis-inducing properties in HT-29 and Caco-2 cancer cell lines when benchmarked against the gold standard camptothecin[64]. A library of 6-substituted-3-amino-imidazo[1,2-*a*]pyridine analogues was developed and their biological activity examined against various colon cancer cell lines. Most compounds showed excellent activity against colon cancer cell lines HT-29 and Caco-2. Compounds **15** and **16** exhibited good cytotoxic effects at µM concentrations with minimal effects on white blood cells[64].



15 **16**

Figure 15: Cytotoxic imidazo[1,2-*a*]pyridine candidates

An in-house library screening by Bode *et al.* identified compound **17** as a potential HIV-1 NNRT inhibitor[46]. Subsequent *in vitro* studies revealed that the compound exhibited appreciable activity against wild-type HIV-1 reverse transcriptase. This prompted the group to prepare a larger library of analogues in an effort to establish their activity against HIV-1 reverse transcriptase. Compound **18 (Figure 16)** showed good enzymatic activity (MAGI whole cell assay IC_{50} = 0.18 µM) and excellent selectivity (SI^e = 868)[46].



17 **18**

Figure 16: Compound **17** led to the discovery of **18** which demonstrated antiviral activity against wild-type HIV-1 reverse transcriptase.

In another study Akritopoulou-Zanze *et al*. reported 5-substituted-imidazo[1,2-*a*]pyridines with an indazole ring as kinase inhibitors by employing GBB-3CR with pyrimidines,

thioamides and van Leusen tosylmethyl isocyanides (TocMICs)[65]. The indazole was successfully added by using indazole-5-carboxaldehyde as one of the reactants in the reaction and this afforded compounds **19-21 (Figure 17)**. Compound **19**, an imidazole[1,2-*a*]pyrimidine, showed maximum inhibitory activity against Gsk3β with K_i = 0.010 µM whereas compound **20** was much less potent with a K_i = 2.611 µM. Changing the isocyanide substituent while maintaining the central imidazole core afforded an analogue **(21)** with improved activity.

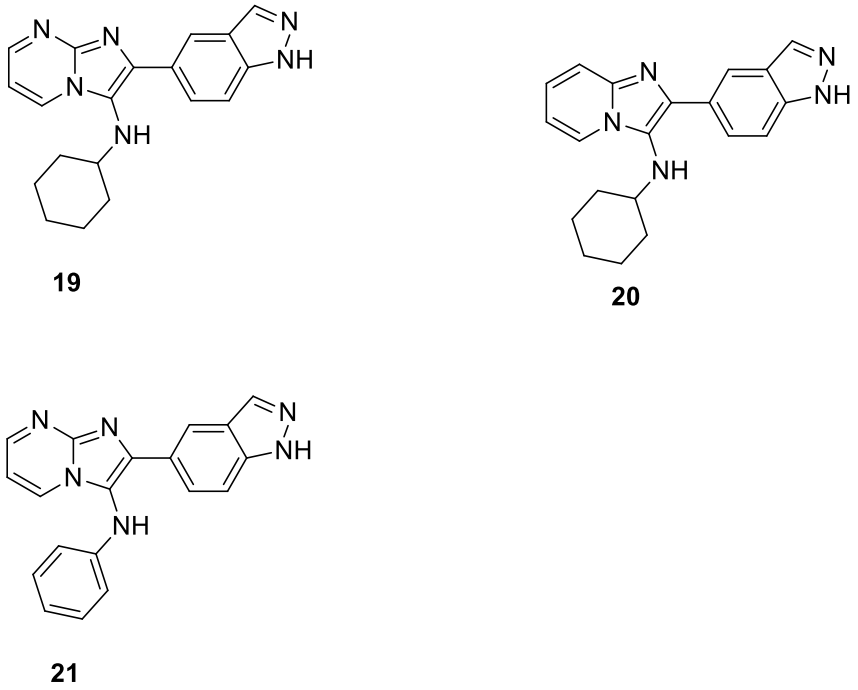
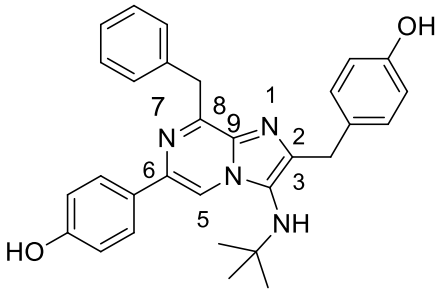
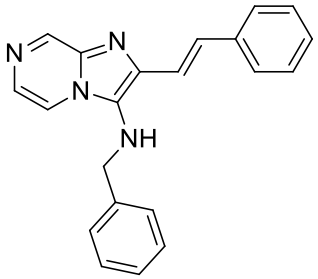


Figure 17: Indazole-substituted imidazo[1,2-*a*]pyridine and imidazo[1,2-*a*]pyrimidines as kinase inhibitors.

The GBB-3CR and many other multicomponent reactions have thus given rise to vast numbers of compounds with a wide range of applications in medicinal chemistry. Generally, the GBB-3CR reaction results in compounds with a phenyl substituent attached to the imidazopyridine ring through a sigma bond. A few exceptions have been observed where the substituent at the C-2 position is linked to the imidazopyridine ring via a -CH or -CH_2 bridge, such as compounds **22** and **23** (**Figure 18**).



22



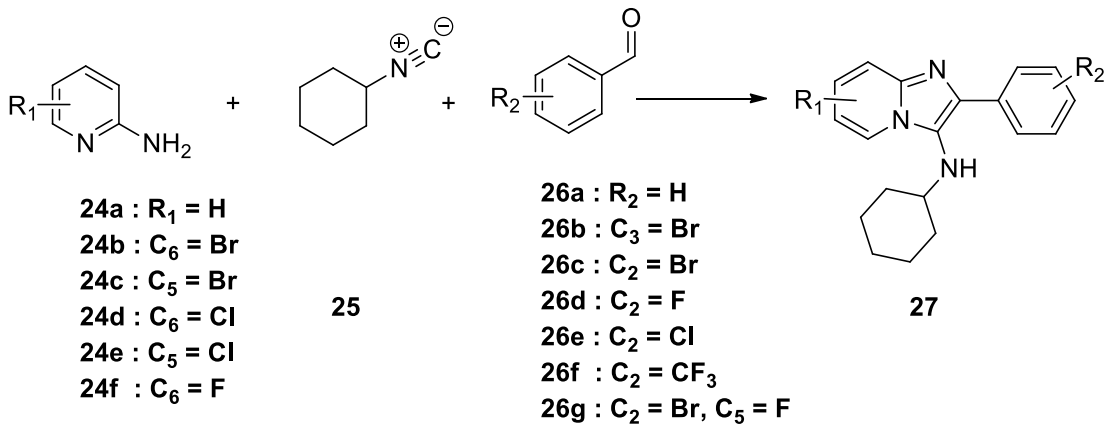
23

Figure 18: Examples of imidazo[1,2-*a*]pyrimidin-3-amines with a -CH/ -CH_2 linker at position C-2.

The presence of a heteroatom bridge would produce compounds with possibly interesting biological activity. However, there are no reported isocyanide-based GBB-3CR compounds with a heteroatom bridge at the C-2 position. This effectively renders these imidazo[1,2-*a*]pyridine derivatives rigid as the sigma bond at C-2 cannot flip up and down, although the rings can be aligned in different ways relative to each other. Essentially, the effectiveness of imidazo[1,2-*a*]pyridine agents against a genetically diverse HIV-1 reverse transcriptase is limited due to various mutations of the enzyme at the allosteric pocket. The amino acid side chains of Y181 and Y188 have been reported to flip either up or down in the presence of a potential inhibitor at the allosteric site[37]. This poses a drug resistance issue with regards to current imidazo[1,2-*a*]pyridines as the rigid conformation of the compounds would not be able to counter conformational variations of the amino acid side chains Y181/Y188 as the enzyme attempts to evade inhibition by the agents.

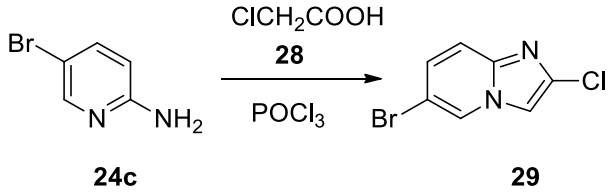
1.13 Study aims and objectives

This study aims to prepare imidazo[1,2-*a*]pyridines that have more structural flexibility. An introduction of a heteroatom and -CH_2 bridge between the imidazopyridine core and the phenyl substituent at the carbon-2 position is envisaged to allow the compounds to adopt different conformations in the allosteric HIV RT binding site resulting in better binding affinity and better tolerance to enzyme mutations. To rationalize this, modelling studies will be conducted to get a better perspective and also to establish what might be a good inhibitor.
Our starting point will be the synthesis of a small library of rigid imidazo[1,2-*a*]pyridine-3-amines **(27)** using cyclohexyl isocyanide **(25)** as the cyanide component in the GBB-3C reaction (**Scheme 10**).



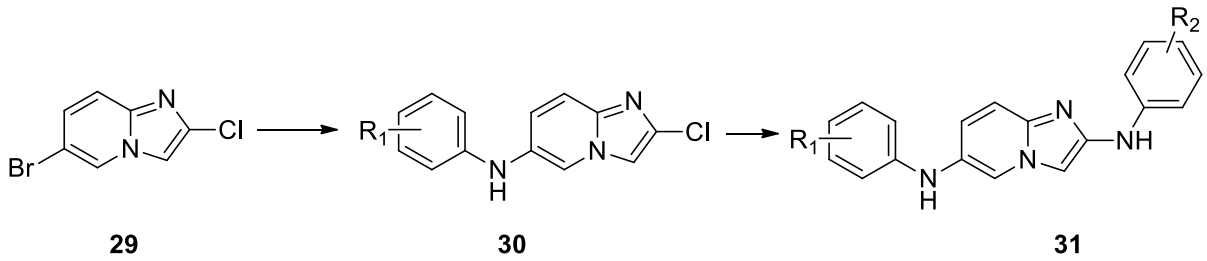
Scheme 10: Schematic outline of the GBB three component coupling reaction to prepare imidazo[1,2-*a*]pyridin-3-amines.

This will be followed by the synthesis of an imidazo[1,2-*a*]pyridine scaffold lacking the position C-3 amino substituent (**29**) from the condensation of 2-amino-5-bromopyridine (**24c**) with chloro acetic acid (**28**) (**Scheme 11**) .



Scheme 11: Condensation of 2-amino-5-bromopyridine with chloroacetic acid.

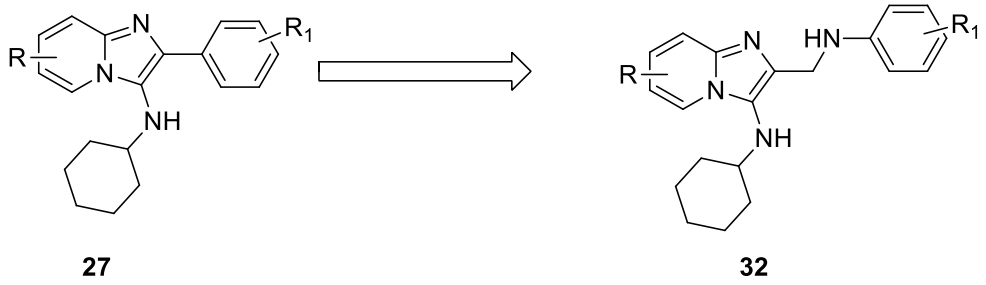
Using a palladium coupling catalyst and a ligand will allow for C-N coupling on the bromo substituted position C-6 of compound **29** followed by another C-N coupling on the chloro-substituted C-2 position of **30** using the BrettPhos ligand to afford the target compounds[66] (**31**) (**Scheme 12**).



29 **30** **31**

Scheme 12: Two-step palladium-catalysed C-N coupling of scaffold **29** to form the target compounds (**31**).

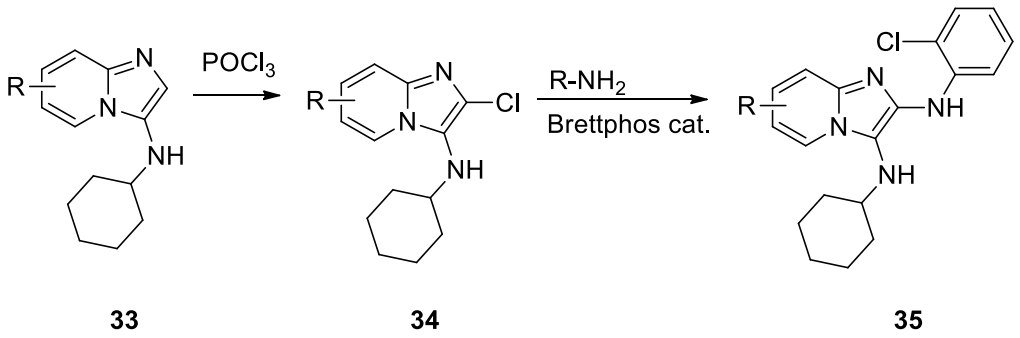
The second part of this study aims to synthesise analogues with a –CH_2-NH- bridge (**32**) which should have more torsional flexibility then the previously synthesised analogues (**27**) (**Scheme 13**).



27 **32**

Scheme 13: Transformation of the sigma bond linking the phenyl substituent at the C-2 position of **27** to a -CH_2-N-H linker (**32**).

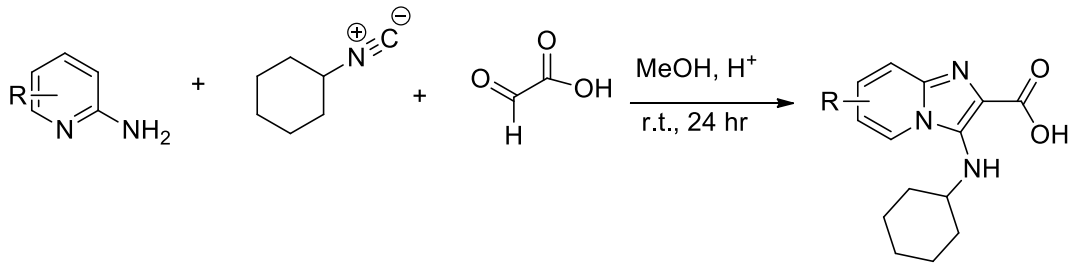
This will be achieved by the synthesis of two types of imidazo[1,2-*a*]pyridine-3-amine compounds. The first of these bears a nitrogen bridge on C-2 of the imidazopyridine core (**35**). Although this will not be a MCR, it will, however, be accessed via imidazopyridines lacking the C-2 substituent (**33**) (**Scheme 14**) which in turn will be assembled by a MCR.



33 **34** **35**

Scheme 14: Palladium-catalysed cross coupling of amine derivatives on the C-2 position to form the target compounds (**35**).

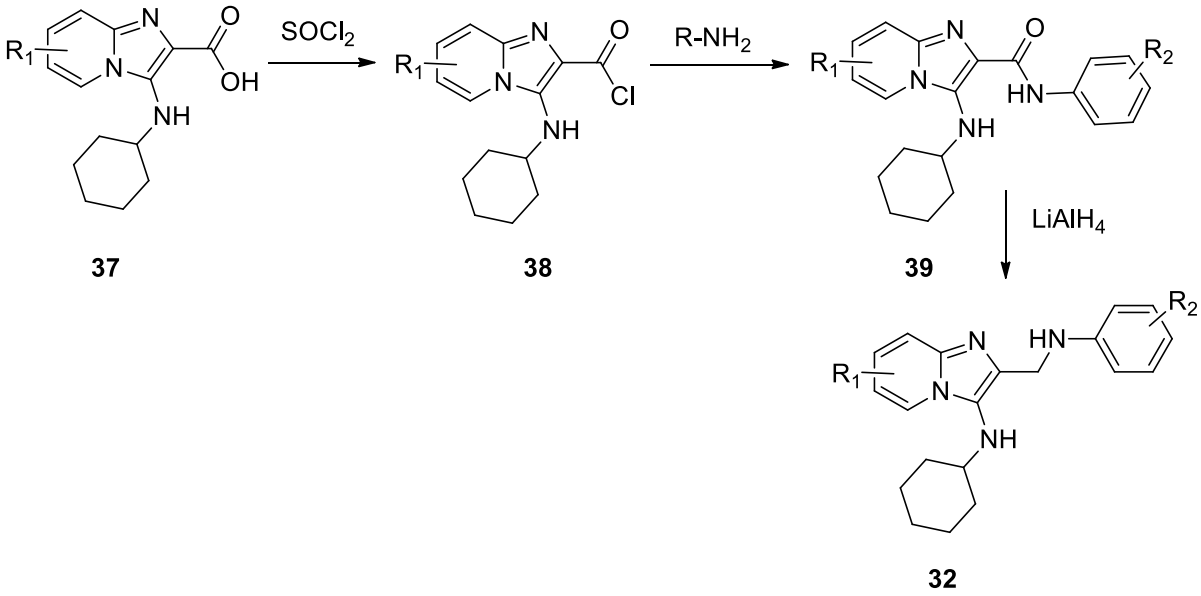
The other types of compounds are those with a -CH_2-NH- bridge (**32**) between the imidazopyridine core and the phenyl substituent at the C-2 position (**Scheme 13**). These will be accessed via exploration of the GBB-3CR synthesis of imidazo[1,2-*a*]pyridine-3-amines with a carboxylic acid attachment at position C-2 (**37**) using glyoxylic acid **(36)** as the aldehyde component (**Scheme 15**). In contrast to the first type of imidazo[1,2-*a*]pyridine-3-amines (**Scheme 14**), these compounds will be assembled using MCR followed by further structural modifications.



24 **25** **36** **37**

Scheme 15: GBB-3CR multicomponent reaction for preparation of imidazo[1,2-*a*]pyridin-3-amine compounds with a carboxylic acid substituent at position C-2.

A carboxylic acid attachment at position C-2 will be transformed to an acyl chloride **(38)** which will in turn be coupled to an amine derivative to form an amide **(39)**. The amide will be reduced to an amine **(32)** to afford the desired product **(Scheme 16).**



Scheme 16: Schematic representation of the synthesis of the target N-H linked imidazo[1,2-*a*]pyridine compound **(32).**

This synthetic approach has not been well covered in literature. However, Warshakoon *et al.* have reported assembly of imidazo[1,2-*a*]pyridine compounds with a carboxylic acid substituent at position C-2 and a further amidation of the acyl chloride that was formed[67]. The difference is that the compounds synthesized by this group lacked the 3-amino-substituent from the isocyanide component. Additionally, Kercher and co-workers as well as Nenajdenko *et al.* have both reported that using glyoxylic acid in the GBB-3CR reaction does not afford the desired carboxylic acid derivatives[68,69]. Our attempt at this reaction is driven by the desire to further explore the different possible products of this reaction and how these can be used as possible HIV RT inhibitors.

Chapter 2: Results and Discussion

Previous work by Bode and co-workers found that compound **18** (see **Figure 15**) demonstrated good antiviral activity against Wild-type (Wt) HIV-1 reverse transcriptase (RT) with minimum inhibitory concentrations comparable to the commercial NNRTI, nevirapine[46]. To rationalize its activity, the compound was docked into the NNRTI allosteric site using CDOCKER (Discovery Studio 2.5.5) modelling interface. Results from the modelling study revealed that the double-fused ring system of the imidazo[1,2-*a*]pyridine core fitted into the hydrophobic region lined by amino acid residues of W229, F227 and Y188. Moreover, the chlorophenyl substituent at position C-2 showed pi-pi stacking interactions with the highly mutative Y188 amino acid. This is undesirable given the high mutative nature of this amino acid residue.

The high degree of mutative amino acids surrounding this inhibitor at the enzyme binding site means that the compound needs to have a certain level of torsional flexibility to tolerate some of the mutations. Given the rigidity of the hit compound as a result of the double fused ring system and the limited conformational variation of the chlorophenyl substituent, the compound is likely to develop intolerance to enzymatic mutations at the binding site.

This study explored the synthetic routes to assemble imidazo[1,2-*a*]pyridine analogues with less rigidity by modifying the structure of the hit compound. To do this, computational modelling studies were first conducted to determine whether structural variation of the hit compound would lead to improved binding. The analogues with the highest docking scores compared to the hit compound were chosen for laboratory synthesis.

2.1 Molecular modelling studies

Modelling was done using Schrodinger Maestro (2019-12.2) modelling interface on a previously reported crystal structure of WT HIV-1 RT/RPV complex, PDB ID: 2ZD1; [2]. Protein preparation for structural refinement was performed using Protein Prep functionality to remove crystallographic artifacts, to rectify missing hydrogen atoms and for pH adjustments. Structure relaxation was performed using restrained minimization with RMSD set at 0.3 Angstroms.

In silico studies of the hit compound simulated on the NNRTI binding pocket of a co-crystallized enzyme, using rilpivirine as a benchmark, showed π-π hydrophobic interactions between the imidazopyridine nucleus and the highly mutative amino acid side chains, Y181 and K103 (**Figure 19**). Furthermore, the chlorophenyl substituent at position C-2 showed π-π stacking interactions with other prevalent NNRTI resistant amino acids, Y188 and W229.

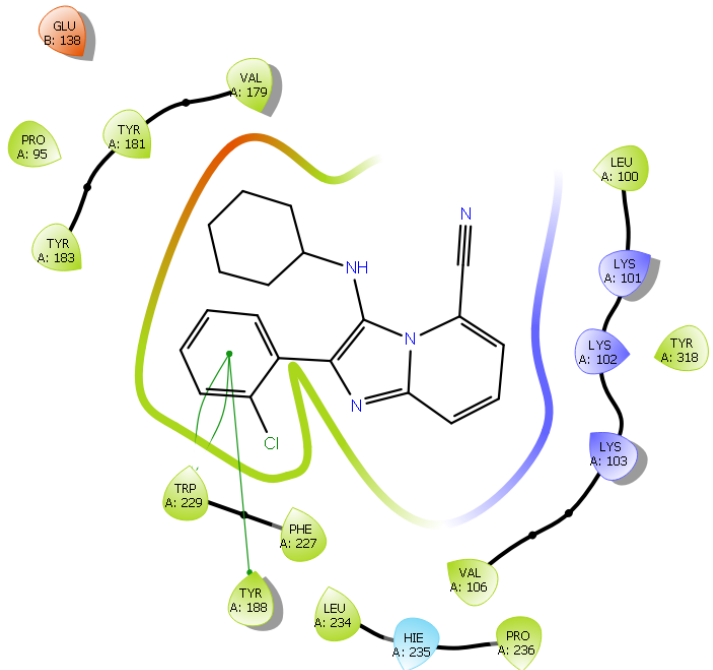


Figure 19: 2D interactions of the docked hit compound within the enzyme binding site. The pear-shaped amino acids show the amino acid residues either facing towards the ligand or away from the ligand.

Previous studies have shown that resistance resulting from Y188 and Y181 is as a result of the amino acid side chains flipping either up or down as the enzyme attempts to evade

inhibition by the ligand[70]. Furthermore, NNRTI-resistance mutations such as Y181C, Y188C, Y188L, Y188, K103N, V179D/E and many others can significantly decrease susceptibility of NNRTIs. Considering the rigidity of the double ring-fused imidazopyridine core as well as the limited ability of the chlorophenyl substituent to adopt various conformations, the hit compound is likely to encounter significant resistance from the highly mutative reverse transcriptase enzyme which would render the agent ineffective. Studies have shown that recent drug design and development efforts against HIV-1 reverse transcriptase have included compounds that avoid interactions with commonly mutated residues such as the amino acid side chains of Y188 and Y181[70]. Nevertheless, newer NNRTIs such as rilpivirine (RPV) and etravirine (ETR) show improved binding affinity for RT as well as tolerance against mutations in amino acid residues such as Y188 and Y181 despite the drug interacting directly with these amino acid side chains **(Figure 20)**.

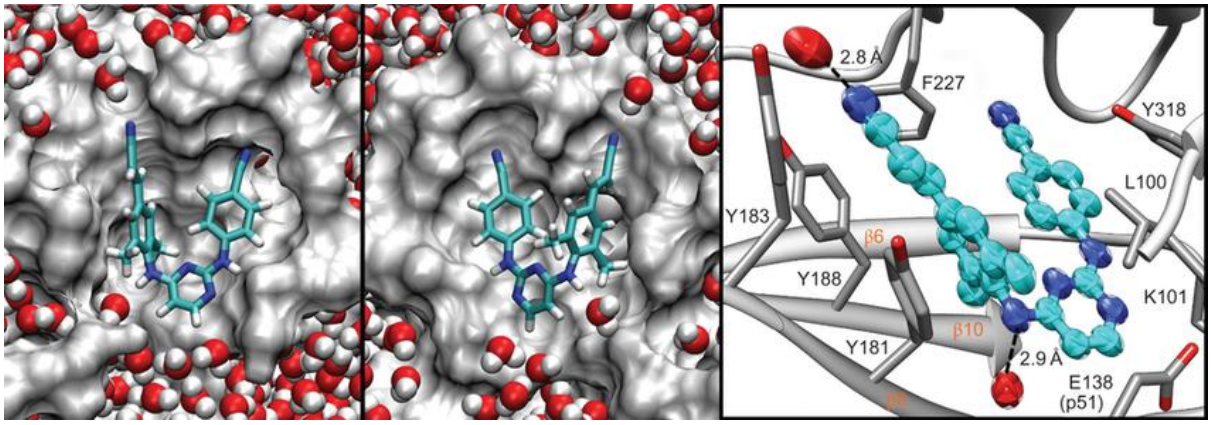


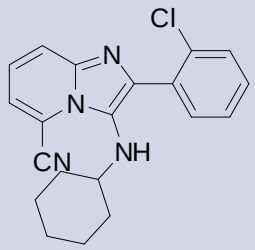
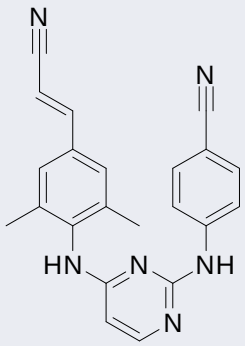
Figure 20: 2D interaction map of rilpivirine at the NNRTI binding site showing different poses of the compound as a result of its structural flexibility.

This could be explained in terms of the compound's structural flexibility and its potential to adopt various conformations at the binding site of the enzyme. Rilpivirine, for example, consists of two aryl substituents linked to the pyrimidine core by nitrogen bridges on either side of the central core making the structure more flexible and adaptable to amino acid mutations at the binding site. Furthermore, the nitrogen atoms have the potential to anchor the compound through hydrogen bonding interactions with amino acid side chains lining the binding pocket.

Thus, to enable our hit compound to withstand enzyme mutations it needs to be more flexible while maintaining current interactions within the binding pocket. This could be achieved by introducing a heteroatom linker between the aryl substituent at position C-2 and the

imidazopyridine core as well as exploring the potential to introduce a substituent at either position C-5 or C-6 on the pyridine ring. Therefore, this study began by conducting a series of molecular modeling studies to examine the binding impact of introducing a heteroatom bridge at position C-2. In addition, simulations were done with various substituents at either position C-5 or position C-6. The docking scores of the analogues were benchmarked against the docking score of the hit compound as well as that of the co-crystallized ligand, rilpivirine (RPV) **(Table 1)**.

Table 1: Docking scores of the hit compound and rilpivirine

Ligand	Docking score
 **Hit compound**	-8,096
 **Rilpivirine**	-10,652

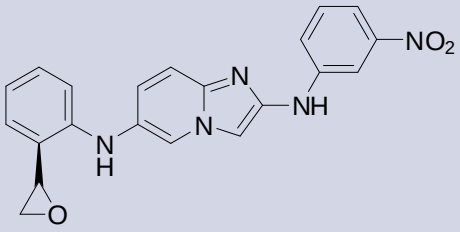
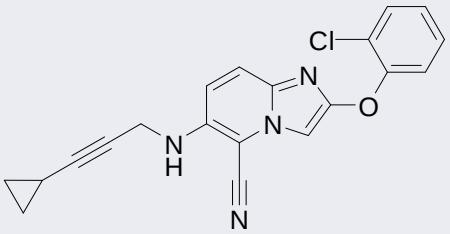
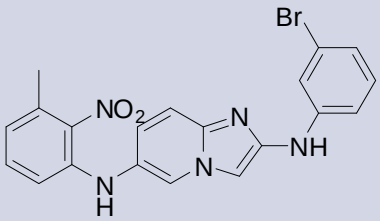
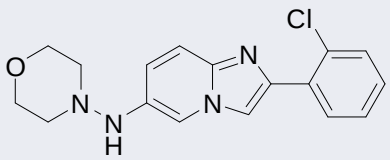
Ligand	Docking Score
 **A**	-8,694
 **B**	-7,859
 **C**	-7,544
 **D**	-7,281

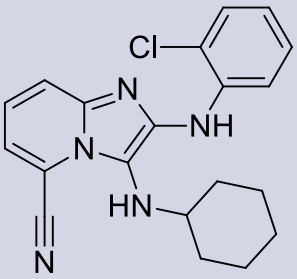
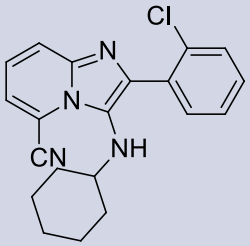
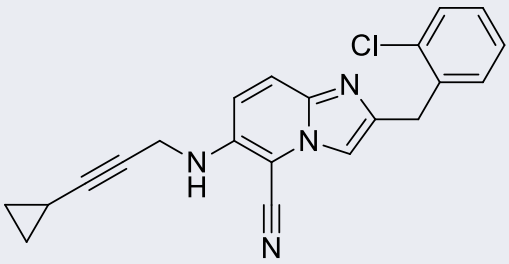
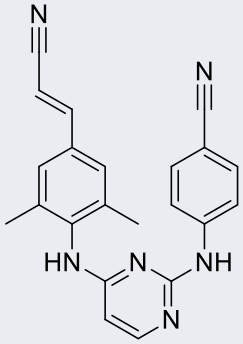
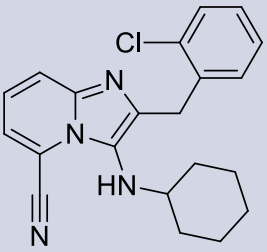
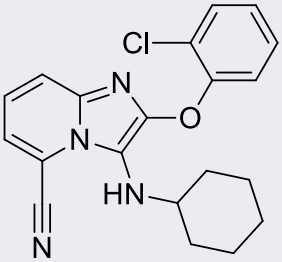
Table 2: Docking scores of the top hits from the first modelling study.

The initial docking study focused on imidazopyridine analogues with bulky substituents at position C-6 yet possessing a nitrogen or oxygen heteroatom bridge at position C-2. Seventy seven analogues in total were first docked into Schrodinger Maestro modelling interface using structure-based virtual screening (SBVS). Of the seventy seven docked compounds, only twenty six were found to be active binders at the HIV-1 RT allosteric site. **Table 2** shows the top binders ranked in order of their docking scores which are based on their binding energies. Analogues with a C-3 amine substituent were found to be inactive while analogue **A (Table 2)** with two phenyl rings linked to the central core by nitrogen atoms was found to have the lowest binding energy and as such, had the highest affinity for the RT binding site. Interesting to note was that the active conformation of this analogue was in the protonated state.

To determine the robustness of the docking model, the top hit compounds in **Table 2** were re-docked into the same RT allosteric site together with known NNRTI decoys (non-binders) obtained from DUD dataset. Early enrichment performance showed a good recovery of known actives with an effective AUC of 0.78 and RMSD <2.5.

Results from this modelling study were, however, not impressive as the docking scores were similar to those of the hit compound. A second modelling study was conducted with a focus to improve interaction of the ligands with the binding site. The second study also benchmarked a series of analogues against the docking score of RPV as well as that of the hit compound (**Table 3**).

Table 3: Results of the second modelling study showing an improvement in docking scores after structural modifications of the first series of docked analogues.

Ligand	Docking score	Ligand	Docking score
 **E**	-9,845	 **Hit compound**	-8,096
 **F**	-9,190	 **Rilpivirine**	-10,652
 **G**	-9,094		
 **H**	-8,387		

The second modelling study shifted focus from using bulky substituents at position C-6 to maintaining the chlorophenyl substituent from the hit compound while varying the linker at position C-2. Results showed that by inserting a nitrogen atom, an oxygen atom or a -CH_2 bridge at position C-2 while maintaining all other structural features of the hit compound, binding of the ligand could be significantly improved. Compound **E** in **Table 3** had the highest docking score and it compared favourably with that of the commercial drug, RPV. Interestingly, analogues that demonstrated improved docking scores against the hit compound retained the cyclohexylamine substituent at position C-3, apart from analogue **F** in **Table 3**, although the cyclohexylamine substituent shows very little interaction with the amino acid residues at the binding site (**Figure 21**). Substituting the cyclohexyl ring with a phenyl ring or an aliphatic substituent alters the binding of the analogue. It appears that the cyclohexyl ring has a stabilizing role whereby it enables the pharmacophore to adopt a favourable conformation that results in maximum interactions between the ligand and the binding site.

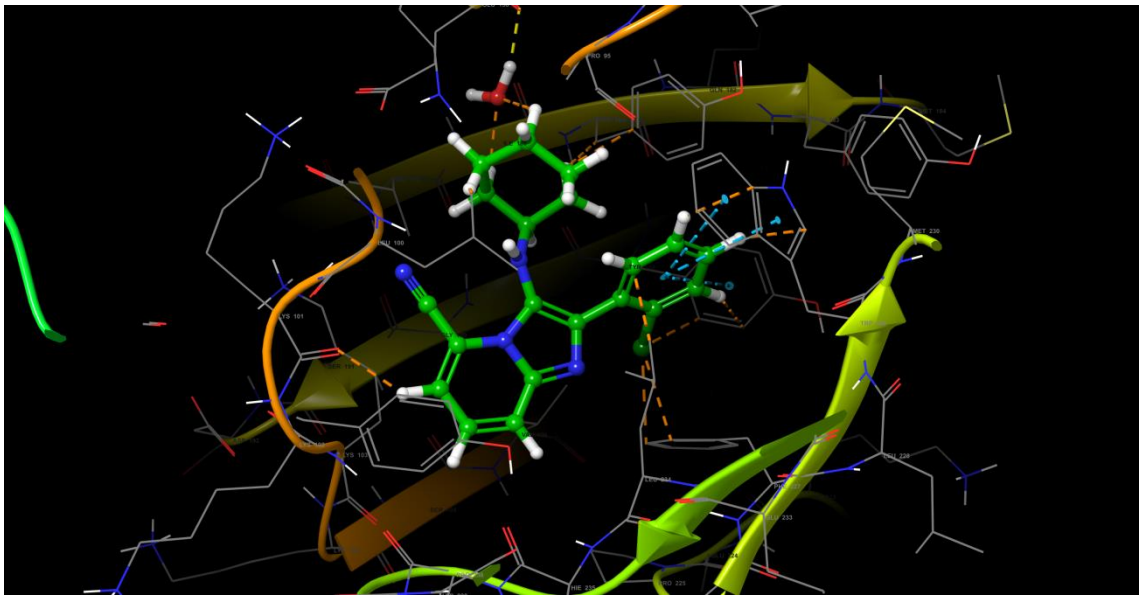


Figure 21: Docked pose of the hit compound at the NNRTI binding pocket showing hydrogen bond interactions between the cyclohexyl substituent hydrogens and the nearby water molecule, pi-pi stacking interactions between the chlorophenyl substituent and the indole ring of Trp229 as well as weak Van der Waals interactions between the chloro substituent and Tyr 188 and Phe 227 residues. The large lime ribbon is the backbone of the p66 subunit whereas the inner orange ribbon shows the backbone of p51 subunit of RT.

Various conformation of the ligands were analysed and the most energy favourable conformation, evidenced by the lowest docking score, was considered. Different dock poses were also studied and showed significant change in interactions between the ligand and amino acid residues lining up the binding site. Introducing an –NH bridge to the hit compound had a significant impact on the binding mode of compound **E**. The chlorophenyl substituent, which proved to be crucial for binding, was observed to have lied flat at the binding site, forming an almost "L" shape in relation to the imidazopyridine ring due to the dihedral angle formed by the –NH linker (**figure 22**). This enabled compound **E** to avoid interaction with Tyr188 in contrast to the hit compound (**figure 21**) without a heteroatom linker. In addition, the chlorophenyl substituent was observed to form hydrogen bonding with carbonyl oxygen atoms of Asp 237, Pro 236 and Lys 101. Further interactions were observed between the cyclohexyl hydrogens and leucine 100 as well as hydrogen bonding between hydrogen of imidazopyridine and the highly conserved Trp 229 amino acid residue. This observation was noteworthy as compound **E** appeared to have avoided interaction with some of the more common mutative amino acid residues such as Y188, Y181 and K103.

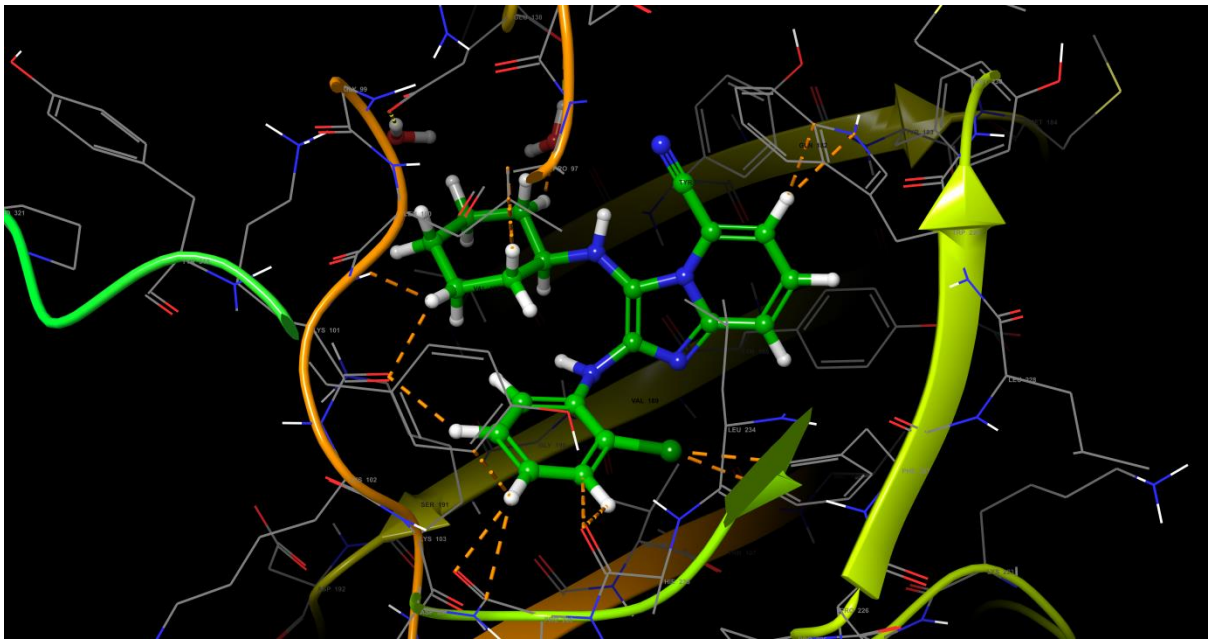


Figure 22: Docked pose of compound **E** at the NNRTI binding site showing the 'L' conformation adopted by the chlorophenyl substituent in relation to the imidazopyridine ring due to the presence of the –NH bridge.

Having determined the feasibility of structural modifications on the hit compound leading to better binding in the binding pocket using computer aided drug design simulation studies, the next step was to explore the synthesis of the analogues. Analogues with the lowest docking

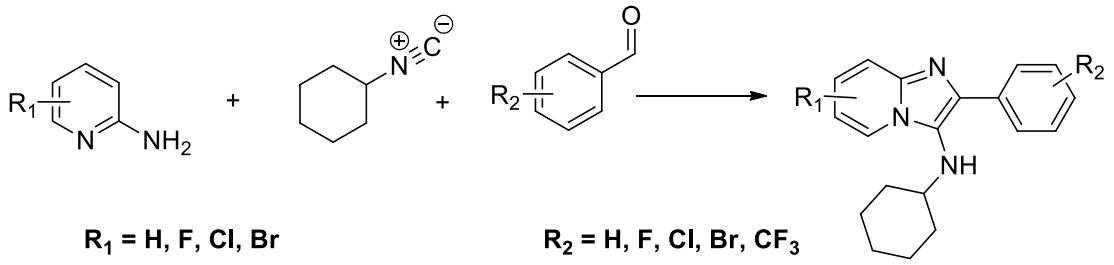
scores **(Table 3)** were chosen for synthesis as they showed promising binding affinity towards the allosteric site of HIV RT. Compound **A** in **table 2** was also chosen for synthesis for comparison purposes.

2.2 Synthesis of imidazo[1,2-*a*]pyridine compounds

2.2.1 Synthesis of rigid imidazo[1,2-*a*]pyridin-3-amine compounds

Using the GBB-3CR multicomponent coupling reaction, a small library of analogues was first synthesized. These compounds were similar in structural properties to the hit compound and were synthesized using the methodology outlined by Bode *et al*[46]. Commercially available cyclohexyl isocyanide and various benzaldehyde derivatives were cyclized with 2-aminopyridine derivatives in the presence of Montmorillonite K-10 clay as a catalyst using either ethanol or methanol as a solvent. **Figure 23** shows a library of compounds synthesised with their respective yields. The yields in this synthesis were low and this could be attributed to the reversibility of the first part of the reaction to form the Schiff base intermediate (**Scheme 2, Introduction**). Moreover, the compounds were purified using both silica gel column chromatography and subsequent recrystallization. Some of the material could have been lost through both purification methods. It is, however, to be noted that studies have reported the unpredictability of the yields arising from these types of reactions[43]. Some of the variables that impact the yield include the type of solvent used, the amount and type of catalyst, the temperature of the reaction and types of substituents on the pyridine ring[43].

Traditionally, the GBB reactions in our laboratory have been conducted using 1,4-dioxane as a solvent. In light of the increasing need to minimize hazardous and toxic solvents and to use greener solvents as outlined by Roger Sheldon[71], methanol and ethanol were used in this study to prepare these compounds. Varying the substituent or position of the substituent on both the pyridine and benzaldehyde ring resulted in diversified compounds with interesting characteristics (**Scheme 17** and **Figure 23**).



Reaction conditions: *2-Aminopyridine (1 e.q), benzaldehyde (1 e.q), cyclohexyl isocyanide (1.1 e.q), montmorillonite k-10 (2 e.q), methanol, 96 ℃, 5-8h*

Scheme 17: GBB reaction used in the synthesis of the rigid imidazo[1,2-*a*]pyridines. R_1 on the pyridine ring (24) was a variation of different halogen substituents and a hydrogen atom and R_2 on the aldehyde was a variation of halogens, hydrogen and trifluoro carbon substituents.

Compounds **41** and **42** are regioisomers and were characterized by the presence of eight aromatic protons and eleven protons upfield corresponding to the cyclohexyl substituent protons on the ^{1}H NMR spectrum. The expected ^{13}C NMR spectroscopic signals were also observed for both compounds. The quaternary carbon carrying the bromine substituent appeared at 122.8ppm for compound **41** while that of compound **42** was observed at 125.9ppm. These were determined using ^{1}H NMR, ^{13}C NMR and HSQC spectroscopic analysis. Interestingly, the N-H proton signal for compound **41** appeared upfield at 3.06 ppm and was partially overlapping the cyclohexyl proton signal on the adjacent carbon attached to the nitrogen which was observed as a multiplet at 3.01-2.95 ppm. This was not observed on the other isomer. In addition to the difference in their ^{1}H NMR spectrum splitting patterns, the physical characteristics of the two compounds were also different. Compound **41** was obtained as an off-white powder with a melting point of 146-148 ℃ whereas compound **42** was obtained as a thick black viscous oil. The –NH stretches were observed at 3710 cm^{-1} for compound **41** while those of compound **42** were observed at 3680 cm^{-1}.

Compound **40** almost mirrored the splitting patterns of the two isomers with the exception that it had one extra proton signal in the aromatic region in the ^{1}H NMR spectrum.

Compounds **43**, **45** and **46** were interesting and noted by their characteristic long range fluorine coupling on the ^{13}C NMR spectrum. The fluorine-carrying carbon on the phenyl substituent on compound **43** was observed as a signal at 155.2 ppm on the ^{13}C NMR

spectrum and was split into a doublet with a coupling constant (*J*) of 249.4 Hz while the other fluorine-carrying carbon on the pyridine ring was observed as a signal at 150.5 ppm and was also split into a doublet with a larger coupling constant of 267.8 Hz. The fluorine-carrying carbon on compound **45** observed at a chemical shift value of 124.1 ppm was split into a quartet with a large coupling constant of 273.8 Hz. Carbon assignment was partly done using *J* values as coupling constants up to ^{4}J splitting were observed.

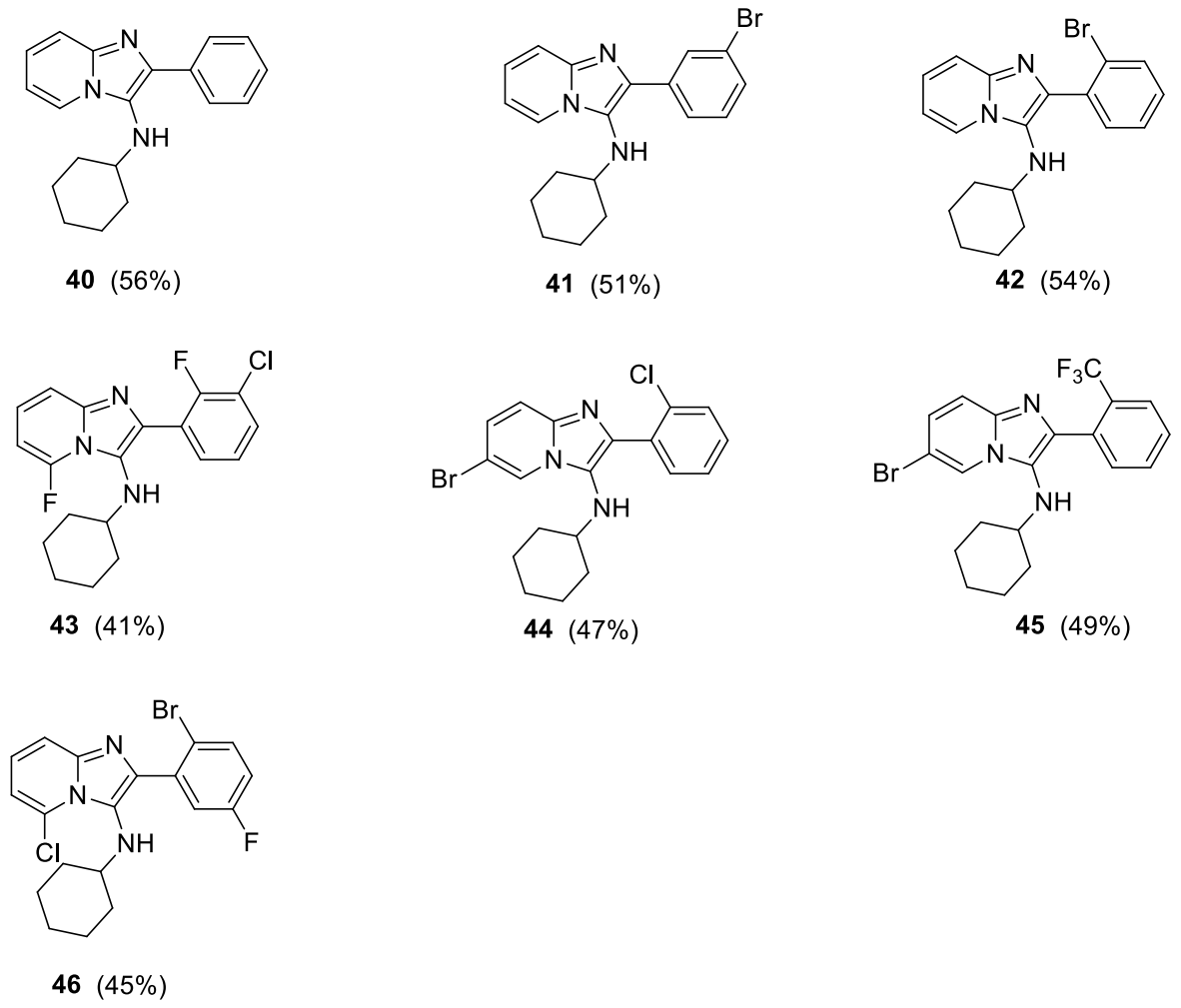


Figure 23: Imidazo[1,2-*a*]pyridin-3-amines initially synthesised to form a small library of compounds.

Interesting to note was that compounds without a substituent on the pyridine ring of the imidazopyridine scaffold gave the highest yields (compounds **40**-**42**) while compound **43** with a difluoro substitution gave the lowest yield.

The ease of preparing imidazopyridines using the classical GBB reaction meant that a large library of compounds could be synthesised in a relatively short period of time using commercially available reagents. A small library of compounds **(40**-**46)** was prepared in this study to test the versatility of this synthetic route. Another advantage of this synthetic method, that has seen exponential growth in popularity in organic synthesis, is its atom efficiency. This was evident during the synthesis of these analogues as there were often no side products observed apart from some 2-aminopyridine derivatives that were not amenable to cyclization such as 2-amino-3,5-dibromopyridine which had several spots on the TLC plate which were difficult to separate. Consistent with previous reports[72], these compounds also showed a high degree of fluorescence when visualized during TLC analysis, particularly at high wavelengths (366 nm). This is a well-documented and studied feature of imidazopyridines. In their study to evaluate the fluorescence emission characteristics of imidazo[1,2-*a*]pyridines, Velázquez-Olvera *et al*. were able to show that compounds with a 3-hydroxymethyl substituent exhibit high fluorescence intensity and that the 3-hydroxymethyl group acts as a fluorescence intensity enhancer[72] (**Figure 24**, compound **47**). As a result, an imidazo[1,2-*a*]pyridine derivative has been used as a biomarker for hypoxic tumour cells[73], a (4-piperidinylfluorophenyl) imidazo[1,2-*a*]pyridine was used in multiple chemosensor fluorescence[72] and an imidazopyrimidine compound was patented for its use as an electron transporter in organic light emitting devices[74]. Photochemical properties of imidazo[1,2-*a*]pyridines have long been a subject of interest for researchers as a result of the their ability to exhibit excited state intramolecular proton transfer (ESIPT), **Figure 24**, compound **48** . Such properties are of great interest in the design of photoluminescence sensors[75], non-invasive optical memory[76], and white-light emitting molecules[77].

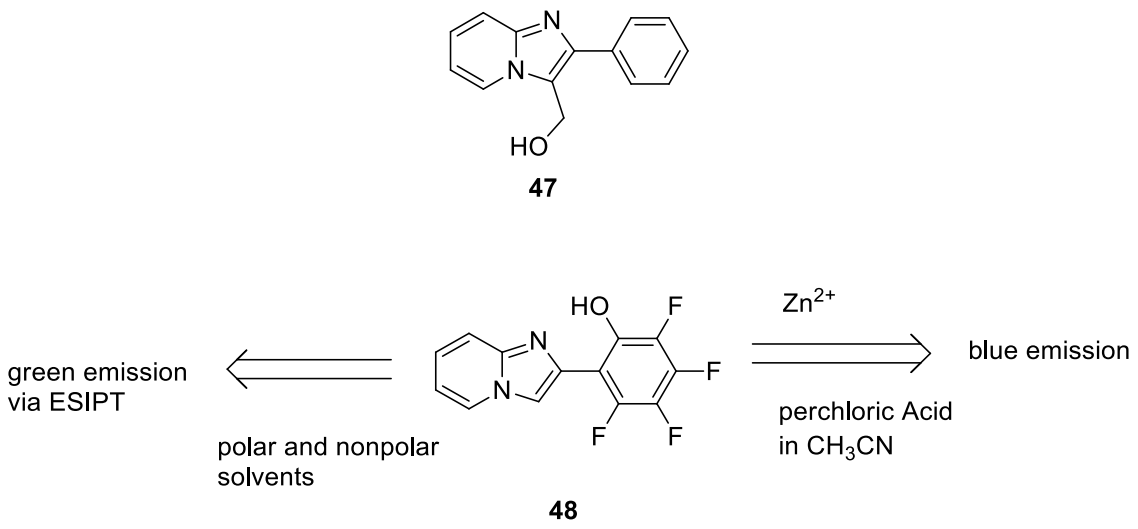
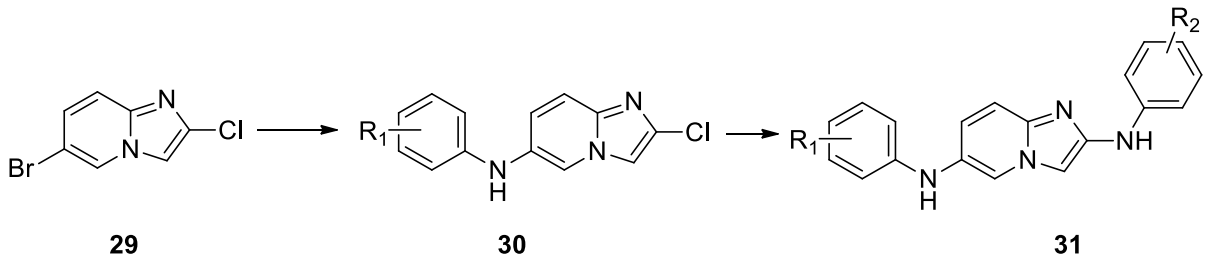


Figure 24: Fluorescent characteristics of tetrafluoro-2-hydroxyphenyl imidazo[1,2-*a*]pyridine under metal complexation and under polar and non-polar solvents.

2.2.2 Towards the synthesis of C-2 and C-6 functionalised imidazopyridines

2.2.2.1 Synthesis of 6-bromo-2-chloroimidazo[1,2-*a*] pyridine

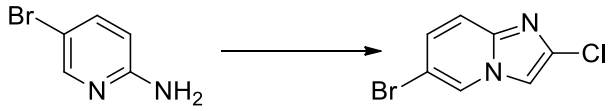
Results from the first part of our modeling studies (**Table 2**) predicts that imidazopyridines lacking the N-H substituent at the 3-position would be active binders at the NNRTI binding site. These compounds also needed to have bulky substituents at position C-2 and position C-6. Apart from compound **D** in **Table 2**, the rest of the compounds had heteroatom linkers at both positions. In order to assemble these compounds, we needed to first synthesize an imidazopyridine core that was structurally diverse enough to allow for substitution at both positions C-2 and position C-6 **(29)**. We envisaged that a halogen substituent on both positions would allow for either a Buchwald-Hartwig cross-coupling reaction[78] or an Ullmann-Goldberg copper-mediated cross coupling reaction[79,80] in a two-step reaction to afford the target compound **(31)** (**Scheme 17**).



Scheme 17: Cross-coupling reaction using aniline derivatives

However, the challenge would be selectivity with regards to which position would be more reactive than the other. To overcome this, a different halogen substituent at the two positions was to be used. Given that the C-Cl bond (ΔH° = 330 KJ/mol) is slightly stronger than the C-Br bond (ΔH° = 275 KJ/mol), effectively making Br a better leaving group than Cl, having Br and Cl substituents would allow the reaction to proceed by first coupling at the Br-substituted position and then followed by cross coupling at the Cl-substituted position.

Several synthetic procedures have been reported in the literature for synthesizing these compounds. For example, Ishida and co-workers reported condensation of 2-amino-5-chloropyridine with chloroacetic acid in CH_3CN in the presence of Et_3N[81]. However, employing this method and using 2-amino-5-bromopyridine **(24c)** only afforded us the product **(29)** in a poor yield of 2% (**Scheme 18**). This result was consistent with that reported by Gudmundsson *et al.*[82]. The group also attempted condensation of 2-aminopyridine derivatives with chloroacetic acid using basic aqueous solutions as well as condensation with chloroacetate in ethanol. However, both procedures were reported to have resulted in very low yields contrary to the previous reported yields by Reindel[83] and Tschitschibabin[84].

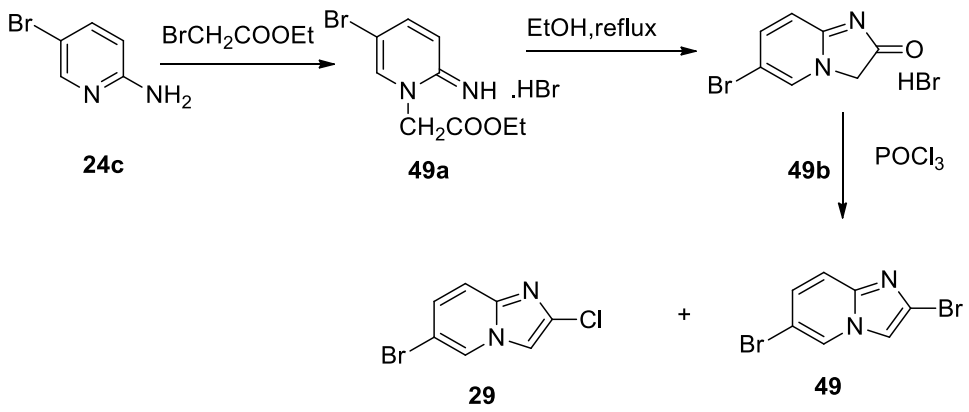


24c **29**

Reaction conditions: *chloroacetic acid (1.5 eq), $POCl_3$, CH_3CN, Et_3N, reflux, 2 h, (2%)*

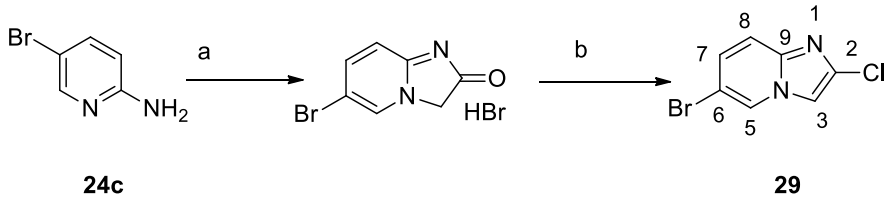
Scheme 18: Preparation of 6-bromo-2-chloroimidazo[1,2-*a*]pyridine by condensation of chloroacetic acid with 2-amino-5-bromopyridine.

Nonetheless, Gudmundsson *et al.* postulated that the low yields resulting from the condensation reaction with chloroacetic acid could be caused by reduced nucleophilicity of the pyridine nitrogen as a result of electron withdrawing properties of the chloro substituent[82]. A more reactive ethyl bromoacetate reagent was suggested as a replacement for chloro-carbonyl compounds. Ethyl bromoacetate was then condensed with 2-amino-5-bromopyridine to afford the iminium (**49a**) which was subsequently refluxed in ethanol to afford the hydrobromide salt of 6-bromoimidazo[1,2-*a*]pyridin-2-one (**49b**). When the pyridinone salt (**49b**) was treated with $POCl_3$, the reaction gave a mixture of 2-chloro and 2-bromo products (**49** & **29**) (**Scheme 19**).



Scheme 19: Schematic representation of the synthesis of 2-chloroimidazopyridine resulting in a mixture of products.

Furthermore, this mixture could not be separated by either column chromatography, HPLC or recrystallization[82]. Gudmundsson and his group suggested the use of an ion exchange resin Amberlyst (Cl^- form) to exchange the hydrobromide salt **(49a and 49b)** for the corresponding hydrochloride salt and this proved to be effective. In our case we had to use a regenerated ion exchange resin (IRA-401(Cl^-)) which might have had a negative impact on the overall yield. Nonetheless, the use of an ion exchange resin proved to be a viable solution in separating the two compounds as compound **29 (Scheme 20)** was successfully obtained and the structure elucidated by NMR spectroscopic analysis and mass spectral analysis. Four proton signals were observed in the aromatic region on the ^{1}HNMR spectrum with two downfield signals at 8.22 ppm and 7.49 ppm corresponding to H-5 and H-3 protons. Two slightly shielded doublets at 7.44 ppm and 7.30 ppm were observed corresponding to H-8 and H-7 protons. Seven signals were observed on the ^{13}CNMR spectrum corresponding to the expected carbon signals. Moreover, the detected mass from mass spectral analysis corresponded with that of compound **29**.

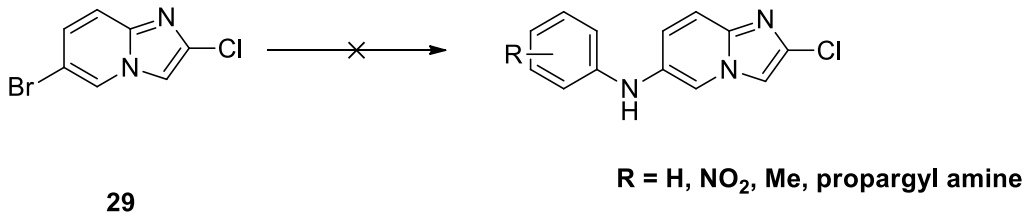


Reaction conditions: *a). ethyl bromoacetate (1.1 eq, Neat), ethanol, reflux, 2h b).phosphorus oxychloride, reflux, 3 h, (59%).*

Scheme 20: An improved synthetic method for preparation of 2-chloroimidazo[1,2-*a*]pyridine

2.2.2.2 Attempted cross coupling reaction on 2-chloro-6-bromoimidazo[1,2-*a*]pyridine

The structure of compound **29** makes it suitable for further modification. As such, our objective was to modify it by attachment of N-H or O- linked substituents at position C-2 and position C-6 to afford our desired flexible compounds. We anticipated challenges with regards to coupling selectivity as both Br and Cl substituents can readily be substituted. However, similar reactions have been reported in literature where the reaction first proceeded by coupling at the Br-substituted position followed by reaction at the Cl-substituted position[85]. We postulated that the coupling reaction would proceed in this same manner where the substrate would first couple at the C-6 position, followed by coupling at the Cl-substituted C-2 position (**Scheme 21**).



29

Reaction conditions: *aniline (1.1 eq), $Pd_2(bda)_3$ (3 mol%), Xantphos (6 mol%), KO^tBu (2.1 eq), dioxane, 120-130 °C, 24 h.*

Scheme 21: Attempted cross coupling reaction

Unfortunately, this reaction did not proceed as planned after several attempts. Initially, a copper-mediated cross-coupling reaction was attempted using a disubstituted aniline (4-fluoro-2-nitroaniline) as a substrate (1.1 eq) in the presence of CuI (5 mol%), $HO(CH_2)_2OH$ (2 eq), K_3PO_4 (2 eq), IPA and toluene[86]. The reaction was allowed to run for 24 h at 80 °C. TLC visualization showed no new spots had formed. We then incrementally increased the amount of the catalyst from 5 mol% to 10 mol% and eventually to 15 mol%. However, the reaction did not take place. We suspected that the electron-withdrawing effects of the aniline substituents could be drawing the electron density away from the aniline nitrogen thus making it less basic and less nucleophilic. We then changed the substrate, and used an unsubstituted aniline instead, but this also did not result in the desired outcome.

We decided to change the reaction conditions and opted for a palladium-catalysed cross-coupling reaction. This was done using unsubstituted aniline in the presence of $Pd_2(dba)_3$ (3 mol%), xantphos (6 mol%) and KO^{t}Bu (2.1 eq) in dioxane[87]. Important to note is that the catalyst [$Pd_2(dba)_3$] was first primed by mixing it with the supporting ligand (xantphos) at 80 °C under nitrogen purge for about 5 minutes prior to adding the rest of the reagents.

The high boiling point of dioxane allowed for an increase in temperature up to 130 °C but this also did not yield the desired outcome. We suspected that the ligand might have accumulated moisture as it had not been stored in a desiccator. It is worth noting that all solvents used in this reaction were distilled prior to use and the reaction vessel was thoroughly degassed and back-filled with nitrogen gas. A ^{31}P NMR spectroscopic experiment was conducted to establish the purity of the ligand. However, the ligand was found to be in good condition as the expected NMR spectroscopic signals were observed and had not shifted since xantphos is a symmetrical compound. We also changed the base from the powdered formulation to the 1.0 M solution in THF, as KO^{t}Bu often accumulates moisture and hydrolyses to KOH which would not be ideal for coupling reactions. However, none of these changes proved to be successful. We envisaged that a bidentate ligand such as *rac*-BINAP which has a narrower bite angle (93˚) compared to that of xantphos (108˚) would be more preferred by the substrate. Unfortunately, we did not have *rac*-BINAP at the time of the reaction, and it needed to be ordered.

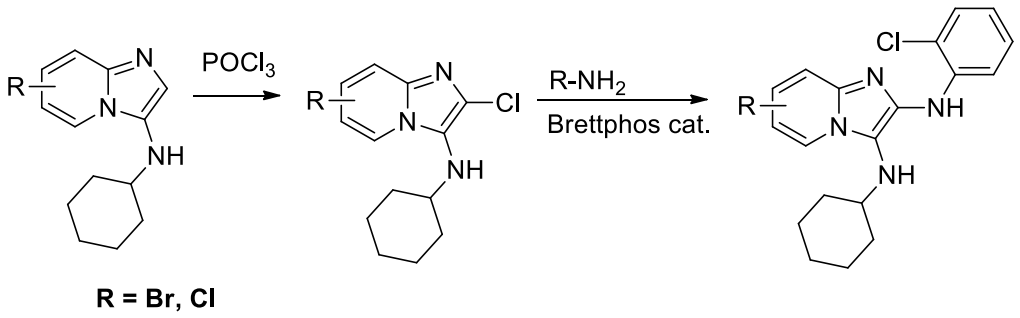
It was evident that optimization studies were needed to determine the suitable reaction conditions. These would have been time consuming and as such, a different approach was adopted. Nonetheless, we managed to explore the possibility of synthesizing imidazo[1,2-*a*] pyridine derivatives lacking the 3-position N-H substituent which has the potential for further structural modifications. Though there are different synthetic routes for synthesizing this scaffold, we believe that the method used in this study, adapted from Gudmundsson *et al*, resulted in better yields and more reliable results.

2.2.3 Synthesis of imidazo[1,2-a]pyridine ester derivatives

-Unexpected twist

We proceeded to attempt to synthesise imidazo[1,2-*a*]pyridine analogues lacking the position C-2 substituent (**33**) in our quest to access compounds from the second modeling study (**Table 3**). These compounds showed better docking scores than compounds in **Table 2**. Of particular interest to this study was compound **E** in **Table 3**. Generally, isocyanide-based imidazo[1,2-*a*]pyridines are synthesized using the GBB-3CR multicomponent coupling reaction, although there are other synthetic pathways that have been reported in literature. The GBB-3CR however, is far more advantageous and has been widely used in various industries for over 20 years due to its capability for diversity oriented synthesis[43]. Equally, the convenience to assemble a versatile scaffold with variations in a single step makes the GBB-3CR less limited compared to other methods of assembling imidazo[1,2-*a*]pyridine scaffolds. However, the general GBB-3CR approach (see **Scheme 2**, Introduction), results in the 2-position being substituted with the aldehyde substituent. Often this substituent is a phenyl ring or a linear chain. This results in a rigid chemical structure and poses a challenge when designing target compounds for highly mutative enzyme species such as RT of HIV-1.

One of the objectives for this study was to design and explore the synthesis of imidazo[1,2-*a*]pyridine compounds that are less rigid than the hit compound previously discovered in our laboratory. To do this, we would have to introduce a heteroatom bridge at the 2-position to be able to assemble compounds similar in structure to compound **E** in **Table 3**. Our first approach was to synthesize 3-substituted imidazo[1,2-*a*]pyridines lacking the 2-position substituent **(33)**. The objective was to then halogenate position-2 to afford compound **34** and subsequently couple this position with an aniline derivative to afford the desired compounds **35** (**Scheme 22**).



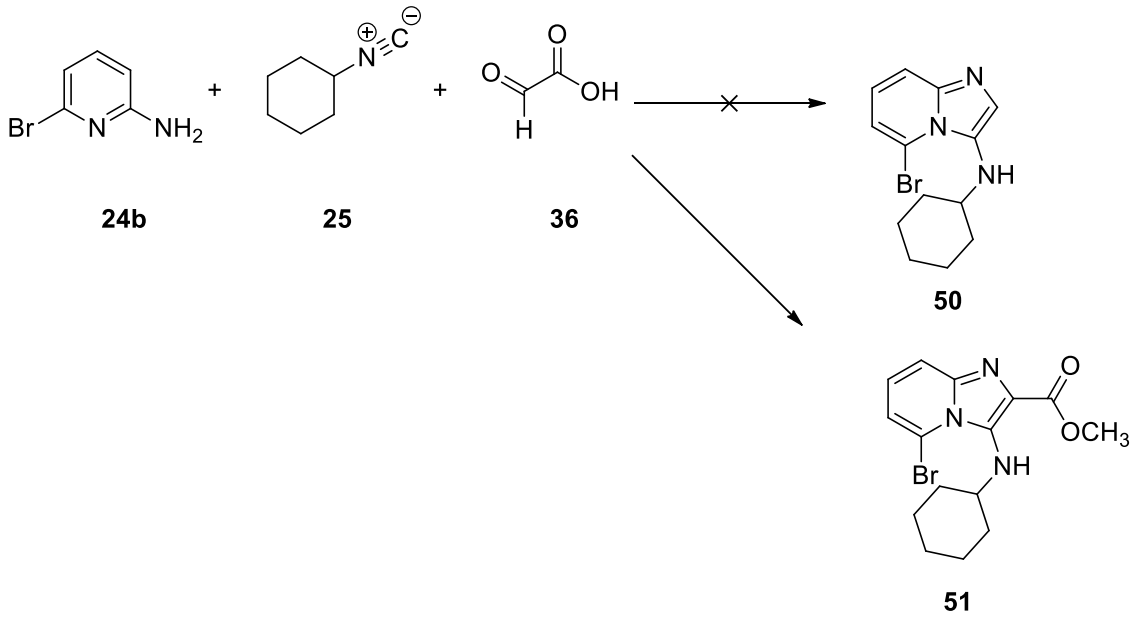
Scheme 22: Initial planned approach to synthesise -NH bridged imidazopyridine compounds.

Following the method by van der Veken *et al.*[88], we embarked on the synthesis of analogues **33**. 2-Aminopyridine derivative **(24b)** was treated with glyoxylic acid mono hydrate and perchloric acid (70%) in methanol at room temperature and the reaction was allowed to stir for 30 minutes. Thereafter, cyclohexyl isocyanide **(25)** was slowly introduced, and the mixture was allowed to stir at room temperature for 24 hours **(Scheme 23)**.

Contrary to reported results by van der Veken and the co-workers, we were unable to obtain position-2 unsubstituted imidazo[1,2-*a*]pyridine compound **50**, instead we obtained compound **51** with an ester substituent at the 2-position (**Scheme 23**). The compound's structure was elucidated by NMR analysis, high resolution mass spectrometry and infrared analysis. Three aromatic proton signals were observed on the ^{1}H NMR spectrum contrary to four signals that would be expected for compound **50**. An intense singlet at 3.98 ppm integrating for three protons was also observed. It was this observation that prompted us to conduct further characterization to determine the structure of the compound. In addition to the expected eleven signals on the ^{13}C NMR, two other signals were observed. One appeared in the aliphatic region at 51.9 ppm and the other appeared heavily deshielded at 165.1 ppm. Infrared spectroscopic analysis revealed the presence of a C=O group in addition to N-H and C-Br stretches. Results from mass spectral analysis showed that the compound possessed a mass of 352.0648 [M+H].

Assembling this data, together with taking the reaction conditions into account led to the conclusion that the singlet peak at 3.98 ppm on the ^{1}H NMR spectrum was the $-OCH_3$ signal and that the ^{13}C NMR signal at 51.9 ppm corresponded to the carbon of this methoxy group. The deshielded signal at 165.1 ppm was the carbonyl carbon signal and the presence of the carbonyl group was further confirmed by infrared spectroscopy.

Furthermore, the mass obtained from mass spectrometry analysis corresponded with the mass of the ester compound **(51)**.



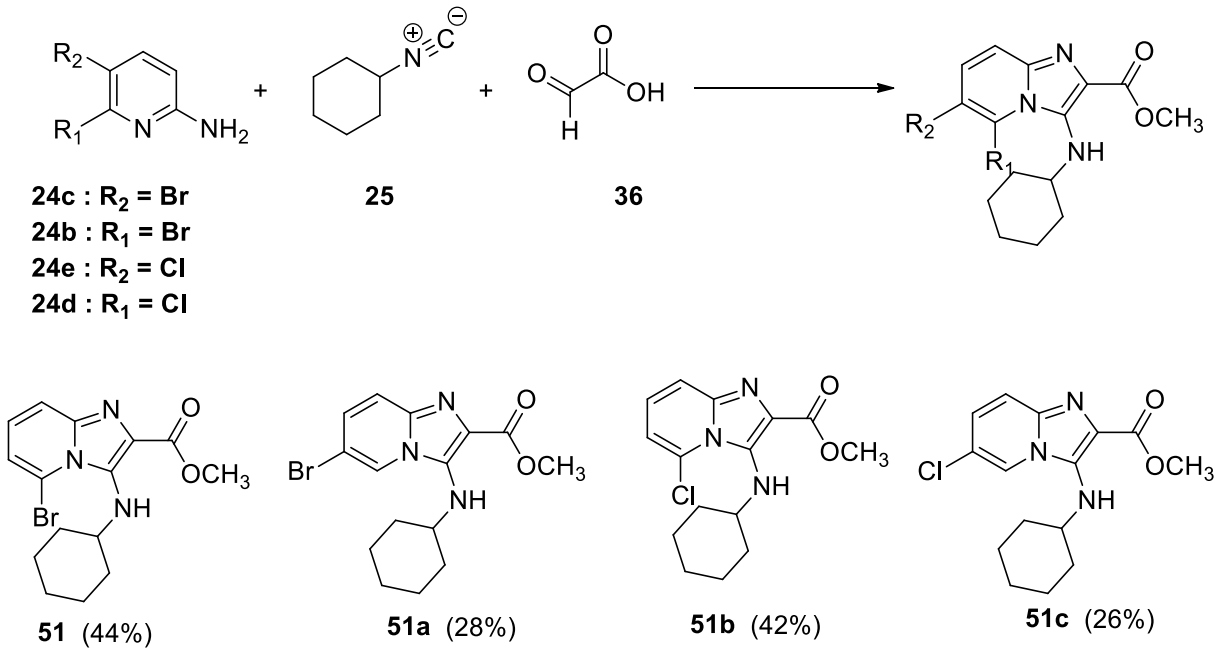
Reaction conditions: *2-Amino-6-bromo-pyridine, cyclohexyl isocyanide (1.1 eq), glyoxylic acid monohydrate (1.5 eq), MeOH, 70% perchloric acid (10 mol%), r.t., 24 h.*

Scheme 23: Schematic representation of the unexpected product obtained during this reaction

The ester compound, however, offered versatility as the ester functional group could be transformed to a carboxylic acid group which would allow for further amidation with an aniline derivative. The amide product could then be reduced to an amine which would give us the final product. This, however, would result in a product with a -CH_2 linker in addition to the N-H linker. This would afford a much more flexible compound than the initial desired compound. Similarly, the ester group could be reduced to an aldehyde followed by reductive amination to afford a -CH_2 and N-H linked product. We could also reduce the ester to an alcohol followed by tosylation of the alcohol. This would enable displacement of the tosyl group by an amine nucleophile to afford the desired product. In brief, the unexpectedly obtained ester product offered space for exploration of different procedures to assemble our desired target compounds.

We decided to explore the versatility of this method by synthesizing compounds with varying substituents on the imidazopyridine ring.

Keeping the structure of the original target compound intact (compound **E**, **Table 3**), the options were to vary substituents at position-5 and position-6 of the imidazopyridine fragment using a small-scale reaction as before **(Scheme 24 and Table 3)**.



Reaction conditions: *cyclohexyl isocyanide (1.1 eq), glyoxylic acid monohydrate (1.5 eq), MeOH, 70% perchloric acid (10 mol %), r.t., 24 h.*

Scheme 24: Schematic outline of the varied positions that were explored

Table 4: Various substituents on the amino pyridine ring and their corresponding yields of the ester product

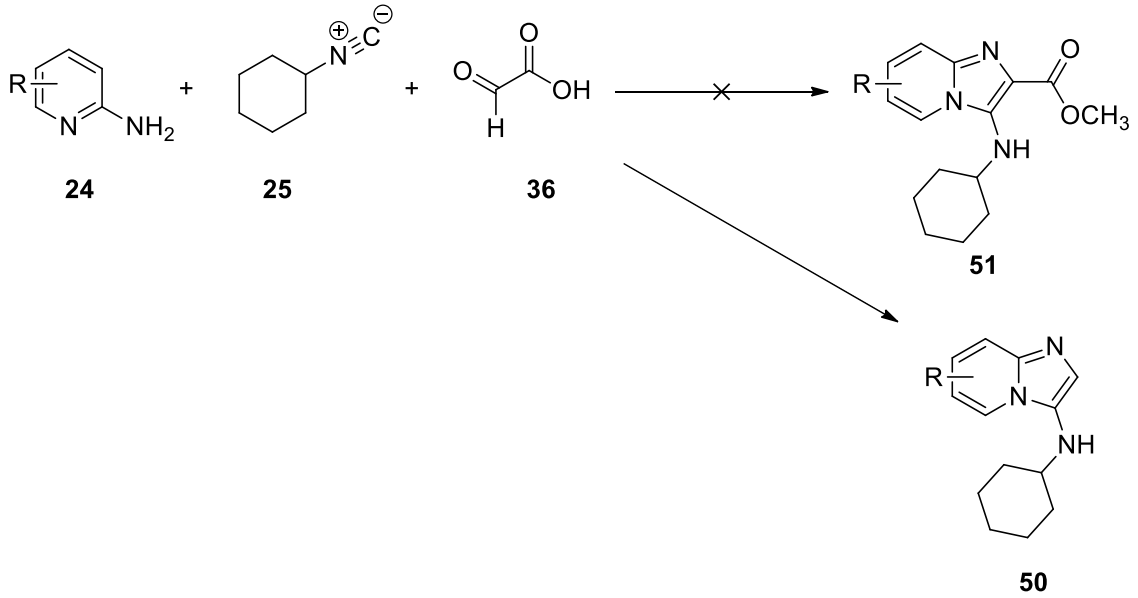
R_1	**R_2**	**Yield**
5-Cl	H	42 %
5-Br	H	44 %
5-Me	H	No reaction
5-CN	H	No reaction
H	6-Br	28 %
H	6-Cl	26 %

It was evident that this reaction was limited in scope as certain substituents were not amenable to cyclization. It is also evident from **Table 4** that larger pyridyl substituents such as a methyl and nitrile group did not favour the reaction whereas smaller substituents such as halogens favoured the reaction. Conclusions could not be drawn on the reason the reaction did not take place with an electron withdrawing CN substituent.

2.2.4 Synthesis of position-2 unsubstituted imidazo[1,2-a]pyridines

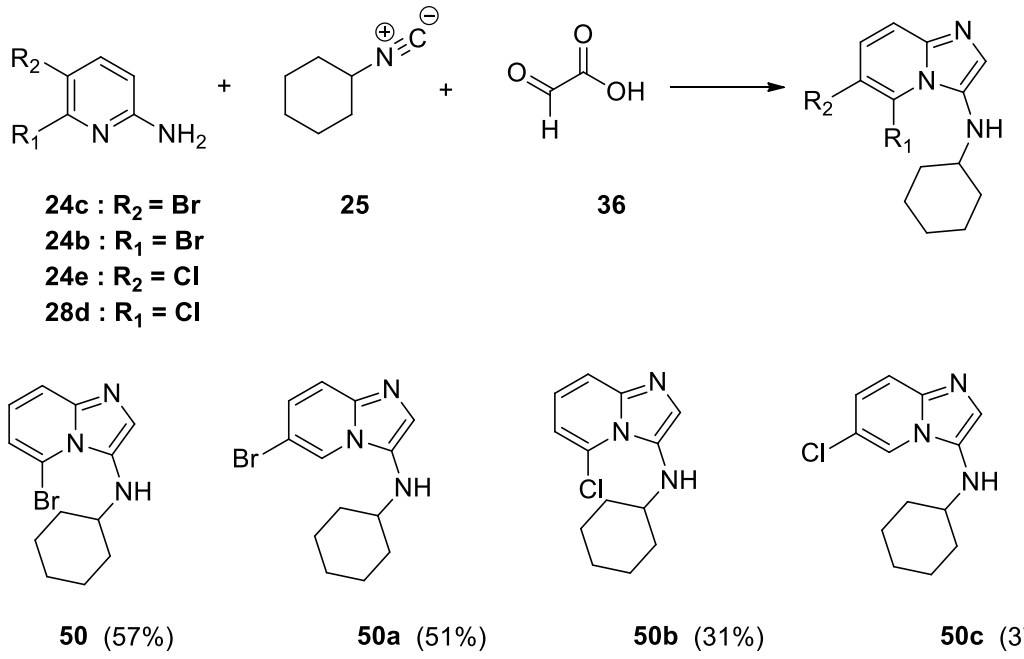
-Unexpected twist

Having unexpectedly obtained imidazo[1,2-*a*]pyridines with an ester substituent at the 2-position and having tested the versatility of the reaction, we decided to scale up the reaction in order to further functionalize the analogues. One-pot multicomponent reactions are a convenient procedure in that a structurally diverse fragment can be synthesized in a single step and further functionalization could be carried out within an appreciable space of time. A one-pot multicomponent reaction was set up using a 2g scale of the 2-aminopyridine derivatives as opposed to the milligram scale initially used, using similar reaction conditions as before. Surprisingly, the expected ester product (**51**) was not obtained. Instead compound **50**, lacking the 2-position substituent was isolated (**Scheme 25**). This is what was reported by van der Veken's group.



Scheme 25: A schematic illustration of the 2-position unsubstituted compound (**50**) obtained unexpectedly from the reaction intended to synthesize the ester compounds (**51**).

We decided to investigate this outcome further by synthesizing a small library of compounds by varying substituents on the pyridine ring. The reaction favoured electron-withdrawing groups similar to the previous ester synthesis reactions. However, these compounds were obtained in poor yields (**Scheme 26**). At a large scale the concentration of the mixture is likely to have influenced the outcome of the reaction that led to the synthesis of **50** as opposed to compounds with an ester group substituent **(51)** that were initially synthesised.



Reaction conditions: *cyclohexyl isocyanide (1.1 eq), glyoxylic acid monohydrate (1.5 eq), MeOH, 70% perchloric acid (10 mol %), r.t., 24 h.*

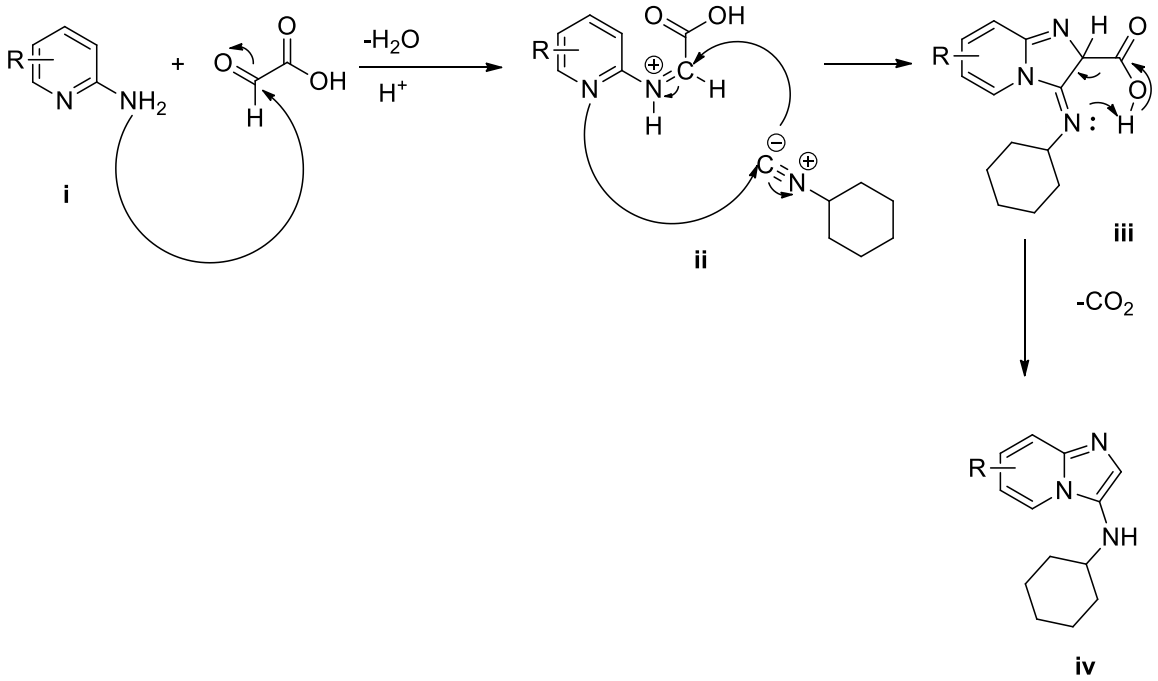
Scheme 26: Illustration of the procedure to synthesize position-2 unsubstituted imidazo[1,2-*a*]pyridines with varying substituents on the pyridine ring.

It was evident from the poor yields that the reaction conditions needed to be optimized to improve the yields.

Interesting to note was that compound **50b** was isolated as an oil whereas its regioisomer (**50c**) was obtained as a solid. Compounds **50** and **50a** could not be distinguished from each another visually as their physical appearance was similar. Their physical properties nonetheless were found to be different as the melting point of compound **50a** (154-155 $^{\circ}$C) was much higher than that of compound **50** (109-111 $^{\circ}$C).

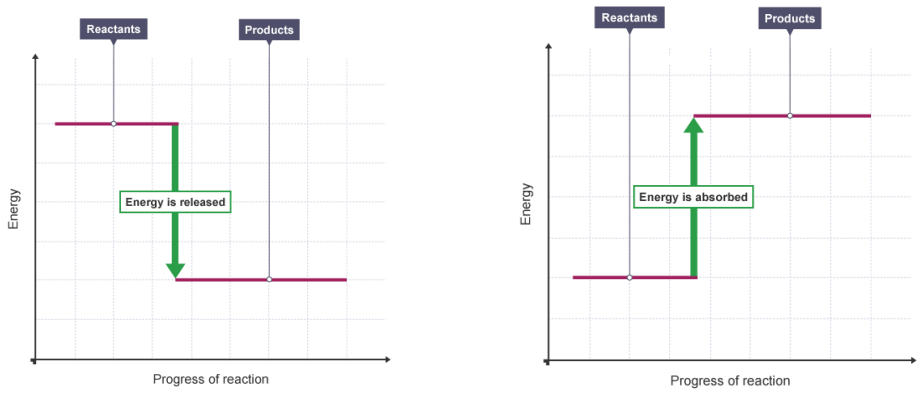
To improve the yield of these compounds we contemplated that a thorough investigation of the exact mechanism of the reaction was needed. It was evident from the molecular structure

of the compounds that a carbon and two oxygen atoms were missing. This is often the case with decarboxylation reactions where CO_2 is liberated from the reaction where carboxylic acids are involved. It was apparent that CO_2 in our reaction came from glyoxylic acid. Thus, we set out to propose a mechanism for the reaction (**Scheme 27**). We speculated that the reaction proceeds via the classical GBB reaction mechanism. However, the 1,2-hydride shift does not take place but instead, the lone pair of electrons on the nitrogen deprotonates the carboxylic acid resulting in the loss of CO_2 (**iii**).



Scheme 27: Proposed mechanism for the decarboxylation reaction.

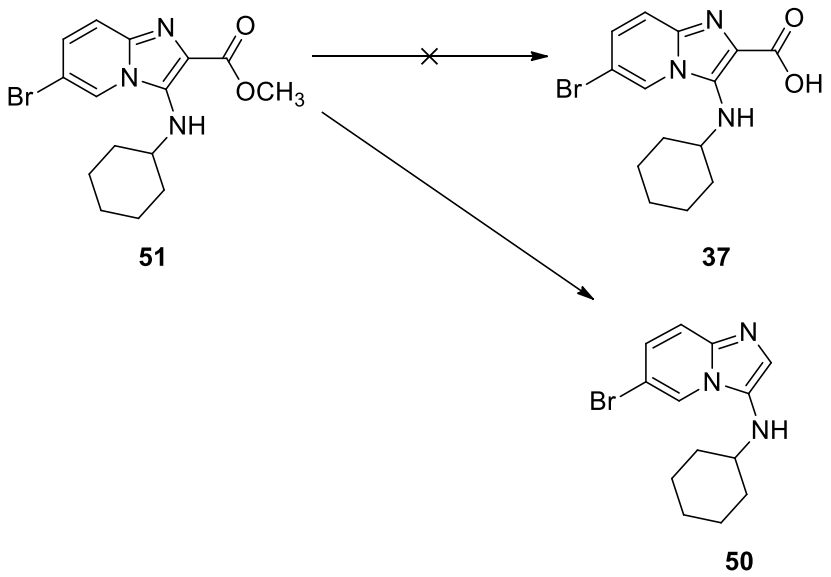
Interesting to note however was that, breaking of chemical bonds often is an endothermic reaction and requires energy or pressure to take place. We conducted these reactions at room temperature and standard atmospheric pressure. It is worth noting as well that heat was liberated during the course of the reaction making the reaction exothermic. Essentially, this meant that the reactants had more energy than the final product, as illustrated in **Figure 25** (**A**). This was, however, theoretical as DFT quantum chemical calculations would be required to examine bond scission enthalpies of these reactions.



A **B**

Figure 25: An energy level diagram (**A**) depicting an exothermic reaction and (**B**) depicting an endothermic reaction.

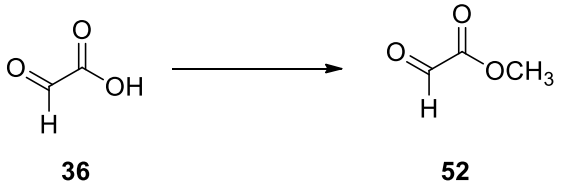
Nevertheless, it was apparent that increasing the scale of the reaction favoured compounds unsubstituted at the 2-position while the opposite favoured ester substitution. This might be as a result of the mixing order of the reactants. It was also evident that imidazo[1,2-*a*]pyridine derivatives with an amine substituted 3-position form unstable compounds where the 2-position substituent is a carboxylic acid (**Scheme 27**). This was contrary to imidazo[1,2-*a*]pyridines lacking the 3-position amine substituent reported by Namal and co-workers[67]. It was, however, consistent with previous work done by Nenajdenko *et al.*[69] as well as Kercher and co-workers[68] who all reported the unstable nature of these carboxylic acids. We further illustrated this by hydrolysing the ester derivative **(51)** with KOH in MeOH. The carboxylic acid product **(37)** that was expected to form was not obtained. Instead, the unsubstituted product **(50)** was obtained (**Scheme 28**).



Reaction conditions: *KOH (2 eq), MeOH, 35-40 °C, 24 h.*

Scheme 28: Ester hydrolysis with KOH in an attempt to synthesize carboxylic acid compound **37**

It was clear that to synthesize carboxylic acid derivatives the carboxylic acid needed to be protected. We therefore esterified glyoxylic acid **(36)** in MeOH using perchloric acid as a catalyst (**Scheme 29**).



Reaction conditions: *Glyoxylic acid monohydrate, MeOH, $HClO_4$ (10 mol%), reflux, 2 h.*

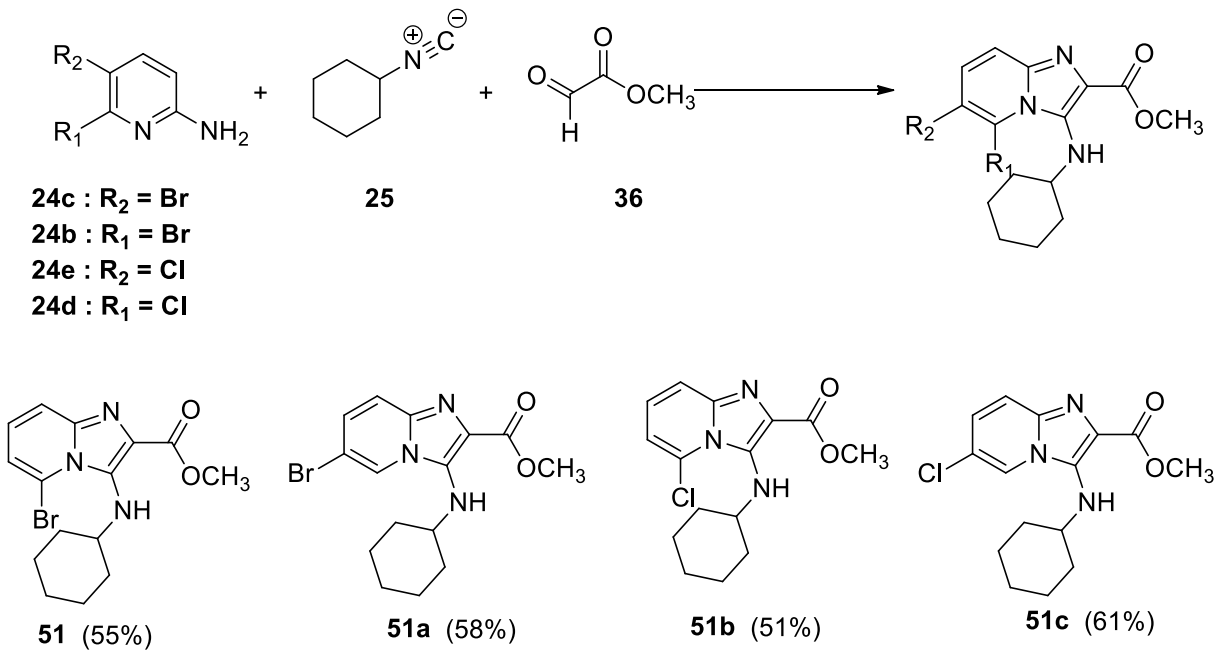
Scheme 29: Esterification of glyoxylic acid

This glyoxylate ester **(52)** was used in the following step without isolation. The mixture was cooled to room temperature prior to proceeding to the next step. 2-Aminopyridine derivative was added, and the reaction was allowed to form the protonated imine at room temperature for 1 hour. This was followed by a slow incremental addition of cyclohexyl isocyanide, over a period of 10-15 minutes. No heat dissipation from the reaction was observed and neither was bubbling, that would indicate evolution of a gas, observed. The reaction was allowed to stir for 24 hours at room temperature. Notably, after 22 hours a yellow precipitate began to

form. Although TLC analysis indicated that the reaction was complete, a further 2 hours was allowed for the reaction to stir. The yellow precipitate was removed by filtration and rinsed several times with 70 % hexane/ethyl acetate. NMR spectroscopic analysis showed that the precipitate was the expected ester product **(51)**. The characteristic $–OCH_3$ intense singlet peak integrating for three protons was observed at 3.97 ppm on the ^1H NMR spectrum. Three aromatic proton signals were also observed, corresponding with the expected protons on the pyridine ring. The N-H proton signal was split into a doublet and appeared at 4.91 ppm. The highly deshielded carbonyl carbon of the ester appeared at 165.1 ppm on the ^{13}C NMR spectrum as expected. The $–OCH_3$ carbon was also observed at 51.8 ppm as confirmation of the ester product.

More product was obtained by purifying the filtrate using silica gel column chromatography. This was by far the most reliable method to synthesize the ester product and it was consistent with the method reported by Nenajdenko *et al*.[69]

We decided to scale up the reaction using different halogen substituents on the pyridine ring as before (**Scheme 30**). The corresponding ester derivatives were obtained; however, the yields were not satisfactory.



Reaction conditions: *Methyl glyoxylate (1.5 eq, in-situ), cyclohexyl isocyanide (1.1 eq), MeOH, $HClO_4$ (10 mol %), r.t., 24 h.*

Scheme 30: Reaction of methyl glyoxylate with different halogen substituents on the pyridine ring.

We decided to optimize the reaction conditions to improve the yield by increasing the amount of the catalyst from 10 % to 20 % and 30 %. Optimal yields were obtained with a 20 % catalytic amount of the acid, whereas a catalytic amount of 30 % did not have any significant impact on the yield (**Table 5**). Other variables were not investigated as an extensive study had already been conducted by van der Veken and co-workers on the effect of changing each variable on the yield, except for the optimal amount of catalyst[89].

Table 5: The effect of changing the amount of the catalyst on the yield.

Compound	**R^1**	**R^2**	**$HClO_4$**		
			10 %	**20 %**	**30 %**
51b	Cl	H	42 %	51 %	48 %
51	Br	H	44 %	55 %	56 %
51a	H	Br	28 %	58 %	56 %
51c	H	Cl	26 %	61 %	63 %

The characteristic singlet peak at 3.98 ppm integrating for three protons in the ^{1}H NMR spectrum, together with the deshielded carbon signal at 165-170 ppm in the ^{13}C NMR spectrum were the defining features of the ester products. The broad N-H signal observed at around 4.85-5 ppm was either a broad singlet peak or a poorly split doublet. The doublet signal was due to N-H coupling with the adjacent CH of the cyclohexyl ring. The splitting pattern of the cyclohexyl protons showed an interesting pattern. The two axial protons (one each on C-12 and C-16) (see **Figure 26**) are equivalent to each other and the two equatorial protons (one on C-12 and C-16) are also equivalent to each other, but the axial and equatorial protons occurred at distinct chemical shift values as expected, since they are not in the same chemical environments due to the non-planar conformation of the cyclohexyl ring. The same was observed for H-13 and H-15 axial and equatorial protons. In the mass spectrum, the splitting of signals into two, separated by 2 mass units, resulting from bromine isotopes (^{81}Br and ^{79}Br) was also noted for compounds containing a bromine substituent. This was a clear indication of the presence of a bromine substituent on the compounds under analysis.

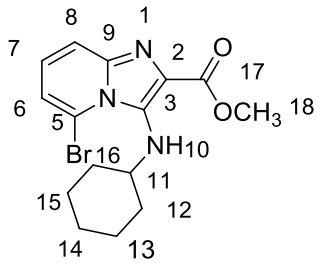
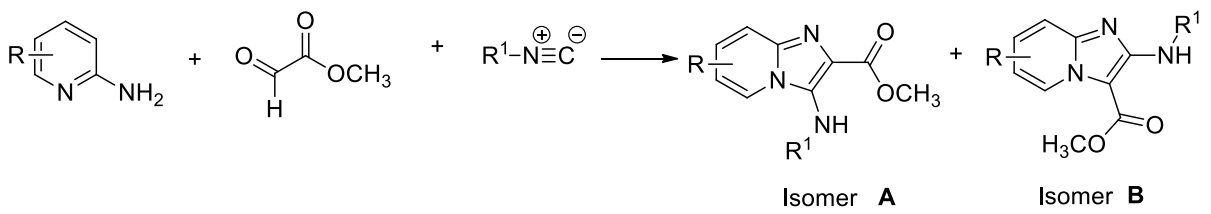


Figure 26: Depiction of the numbering of carbons and protons on the imidazopyridine ester compounds

It is worth noting that using the glyoxylate ester as a carbonyl component for this reaction has been reported to yield, together with the 3-amine heterocycle product, a position-2 substituted amine isomer as a minor by-product[69] (**Scheme 31**).



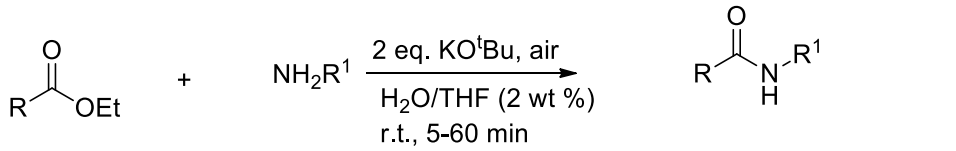
Scheme 31: Two regioisomers that have been observed using glyoxylate ester as a carbonyl component in the GBB reaction.

In this study, however, we exclusively isolated the targeted 3-amine isomer, and no traces of the other isomer were noted. This was based on research work done by Nenajdenko *et al*. which found that isomer **B** is often obtained as a minor by-product and in this particular reaction, no traces of isomer **B** were observed. It is reported in literature, however, that the 3-amine isomer can be exclusively synthesized, in some cases, using non-polar solvents. In this study, in contrast, methanol was used as the solvent, and we were able to isolate the target isomer. Methanol was used as the solvent of choice as it was able to dissolve all the reactants whereas non-polar solvents could not.

2.2.5 Reactions of imidazopyridine ester derivatives

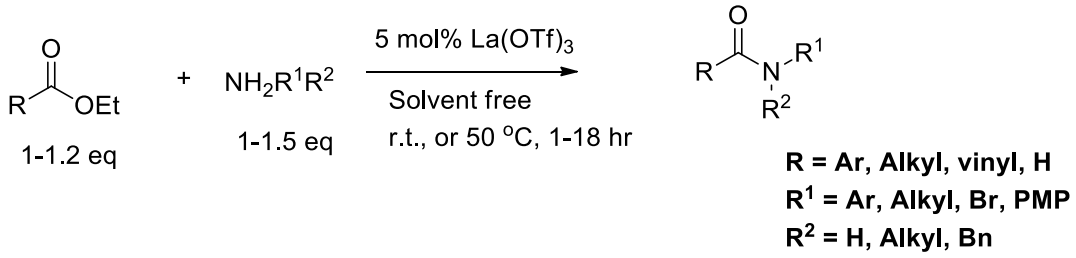
2.2.5.1 Aluminium-catalysed amide synthesis from esters

Having obtained ester derivatives in reasonable yields, we decided to prepare amide compounds by direct displacement of the methoxy group of the ester. In recent years, several methods have been employed in the direct amidation of esters. A method by Kim *et al*, using a primary amine, was used to convert aromatic and aliphatic esters into the corresponding amides using 2 equivalents of KO^tBu as a base and H_2O/THF as a solvent mix[90] (**Scheme 32**). This method is green, economical, and could be used for a wide range of applications from industrial chemistry, organic synthesis, and biochemistry.



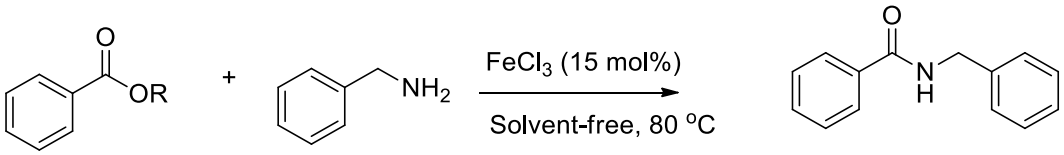
Scheme 32: A versatile, green, and economical method that has been used to convert esters to amides.

Morimoto *et al.* used secondary amines to convert esters to amides at room temperature using 5 mol% $La(OTf)_3$ as a catalyst under solvent-free conditions[91] (**Scheme 33**).



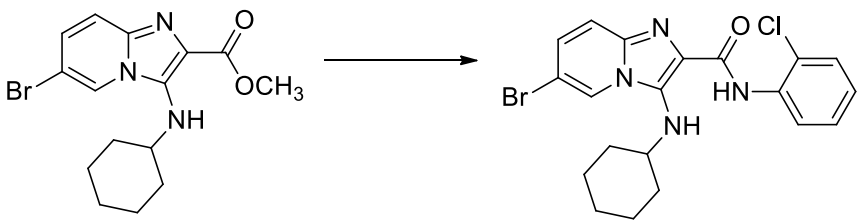
Scheme 33: A solvent-free procedure to convert esters to secondary amides.

More recently, Moshapo and his group successfully converted aliphatic and benzyl esters into amides employing a cost-effective catalyst ($FeCl_3$) under solvent-free conditions[92] (**Scheme 34**).



Scheme 34: Synthesis of primary amides using $FeCl_3$ under solvent-free conditions.

Employing the method by Kim *et al.* (**Scheme 32**) did not yield the desired amide for this study after repeated attempts[90]. We modified reaction conditions by changing the base to K_2CO_3 and *n*-BuLi but none seemed to be effective. We attempted the method by Moshapo's group (**Scheme 34**) using MeOH as a solvent. That also did not produce any tangible results. It is worth noting that in general, aniline, which was a substrate for this study, is not very reactive as a nucleophile. Equally, esters are not very reactive due to resonance stabilization on the carbonyl carbon. Given this information, it was apparent that to force this reaction to happen would require aggressive reaction conditions. A strong base in the form of NaH was then used in the presence of 15 mol% $AlCl_3$ and temperature adjusted to 110 °C. The mixture was allowed to react for a longer duration, 24 hours (**Scheme 35**).



51a **53** (8%)

Reaction conditions: *2-chloroaniline (2 eq), NaH (2 eq), Anhy $AlCl_3$(15 mol%), CH_3CN*

Scheme 35: Direct amidation of the ester using sodium hydride and an aluminium catalyst

This method appeared to have worked and the desired product **(53)** was successfully isolated. However, the yield was a very poor 8% and much of the starting material was retained.

Seven proton signals were observed in the aromatic region on the ^1H NMR spectrum corresponding with the expected number of protons on the product. The N-H signal of the amide was observed downfield as a broad singlet at 9.67 ppm owing to the deshielding

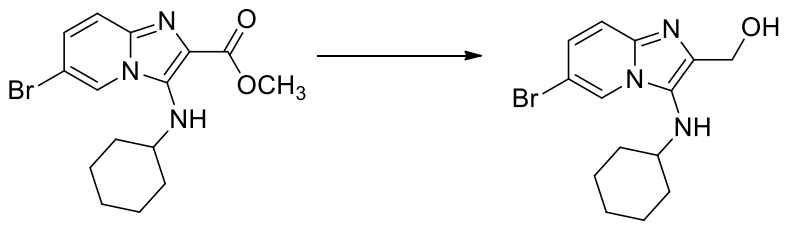
effects of the carbonyl group and the adjacent chloro-substituted phenyl ring. The carbonyl carbon appeared the most deshielded on the ^{13}C NMR spectrum at 162.4 ppm and its presence was further confirmed by IR stretches at 1669 cm^{-1}.

It was clear that direct amidation of the ester using the intended substrate for this study was going to be a challenge. Ester hydrolysis to the carboxylic acid followed by conversion to acid chloride would also not be possible due to decarboxylation that occurs when converting the ester to the carboxylic acid. A revised method for coupling the amine was then formulated.

2.2.5.2 Reduction of ester derivatives to alcohols

Reducing the unreactive ester group to an alcohol would allow for a wide range of options for coupling the aniline substrate. Moreover, the ease of reducing esters fully to alcohols using a strong reducing agent such as $LiAlH_4$ (LAH) is a well-documented procedure. In comparison to $NaBH_4$, which often result in mixtures of compounds, LAH can reduce both ester and the intermediate aldehyde to the alcohol final product. The availability of LAH is an added advantage. However, caution had to be exercised when handling LAH as it ignites upon coming into contact with moisture. Moreover, moisture had to be avoided from getting into the reaction vessel as it would have quenched LAH. As such, pre-distilled solvents were used for this reaction and all reaction vessels were preheated in an oven overnight. The reaction was also performed under inert conditions with a particular emphasis on sealing the joints to prevent any moisture from entering the reaction mixture. LAH also needed to be stored in a desiccator prior and after use, to maintain its integrity.

Using the 6-bromo ester derivative **(51a)** as a test for the reaction, the corresponding alcohol (**54a**) was successfully obtained in an appreciable yield of 99% (**Scheme 36**).

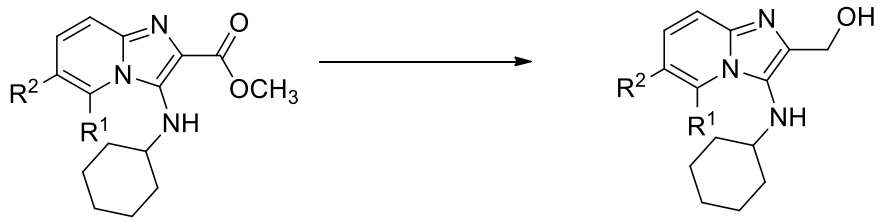


51a **54a** (99%)

Reaction conditions: *$LiAlH_4$ (1,5 eq), THF, 0 °C-r.t., 12-24 h*

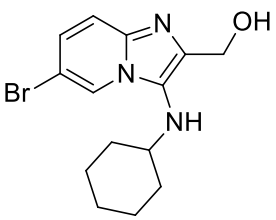
Scheme 36: Reduction of the ester to alcohol using LAH.

We decided to reduce all the ester derivatives applying the same reaction conditions and the corresponding alcohols were successfully obtained in excellent yields (**Scheme 37**).

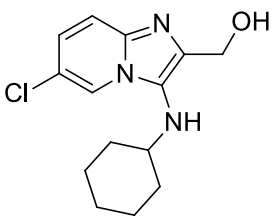


51 : R_1 = Br
51a : R_2 = Br
51c : R_2 = Cl
51d : R_1 = Cl

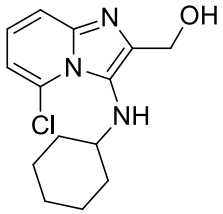
54



54a (99%)



54c (95%)

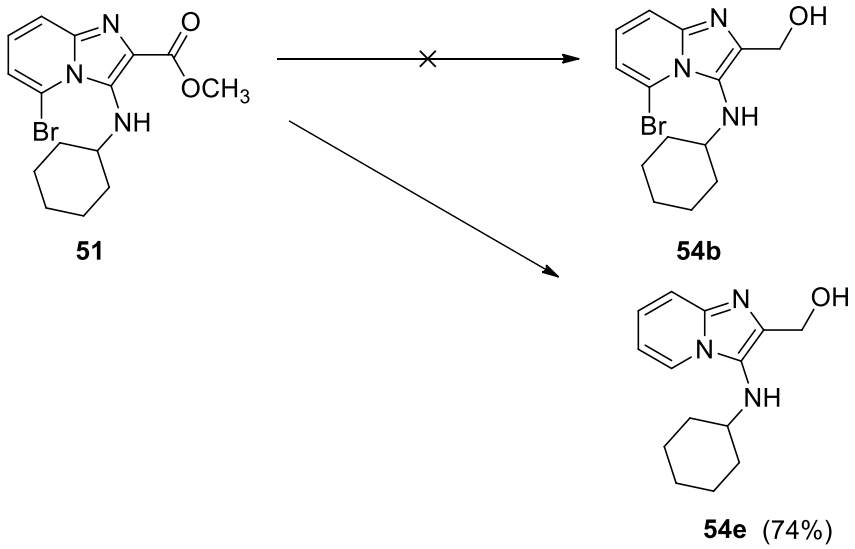


54d (92%)

Reaction conditions: *$LiAlH_4$ (1,5 eq), THF, 0 °C-r.t., 12-24 h*

Scheme 37: Reduction of ester derivatives with LAH to the corresponding alcohols.

Interestingly, however, the reduction of the 5-bromo ester derivative **(51)** resulted in a twist. We did not obtain the intended alcohol product **(54b)**; instead we unexpectedly obtained a debrominated product **(54e)** (**Scheme 38**).



Reaction conditions: *$LiAlH_4$ (1,5 eq), THF, 0 °C-r.t., 12-24 h*

Scheme 38: Unexpected debromination of the 5-bromo ester compound.

This was revealed by ^{1}H NMR spectroscopic analysis as the aromatic region showed an extra proton signal in addition to the expected three proton signals. Moreover, HSQC analysis showed that this deshielded proton (H-5, 8.03 ppm) was coupled to the corresponding C-5 carbon appearing at 123.8 ppm in the ^{13}C NMR spectrum. Equally, mass spectrometry results showed that the mass corresponded with that of the debrominated product and not the expected brominated product.

Examining the structure of the 5-bromo ester compound, it was clear that the C-5 carbon was slightly electrophilic due to the two neighbouring electronegative atoms (N & Br). The two atoms pull the electron density away from the C-5 carbon making it more electron deficient and susceptible to nucleophilic substitution such as H^- from LAH. Interestingly, when the C-5 substituent was a chlorine atom, no substitution was observed. This served to confirm properties of bromine which makes it a good leaving group. Similarly, when bromine was at position 6, no substitution took place. In essence, the strong electronegative properties of the neighbouring nitrogen were a major contributing factor towards the reactivity of the C-5 carbon. Nevertheless, it was later suggested by colleagues that a change in solvent from THF to Et_2O could remedy the situation. However, we did not have the opportunity to explore this possibility.

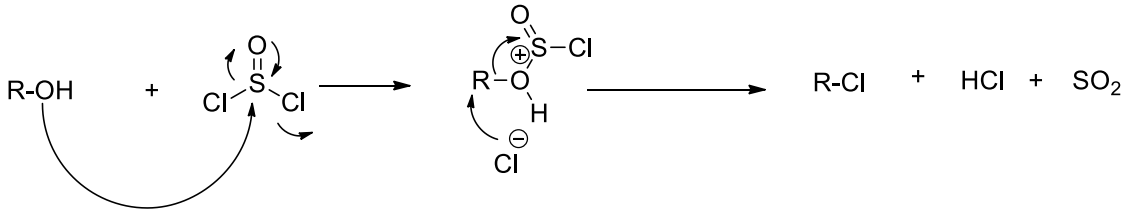
For each of the products, the characteristic $-CH_2$ proton signal appearing in the region of 4.83-5.00 ppm in the ^{1}H NMR spectrum was an indication of the presence of the alcohol product together with the broad -OH singlet at around 3.07-3.49 ppm. The $-CH_2$ carbon was

further confirmed by DEPT-135 NMR spectroscopic experiments. The deshielded carbonyl carbon of the ester that appears at around 168-170 ppm in the ^{13}C NMR spectrum was notably absent, instead, a -CH_2 carbon signal was observed in the aliphatic region, slightly more deshielded than the cyclohexyl carbon attached to N-H, at around 57.1-58.5 ppm in each case.

2.2.5.3 Reactions of the imidazopyridine alcohol

2.2.5.3.1 Attempted chlorination of the alcohol

Having verified the presence of the OH group, we contemplated converting it to an alkyl halide which would be easier to displace with a nucleophile. Chlorination of primary alcohols using thionyl chloride is a procedure that has been reported often in literature. The reaction proceeds by an S_N2 mechanism where the lone pairs of electrons on the OH oxygen attack the electrophilic thionyl group causing delocalization of the pi-bond electrons to the oxygen (**Scheme 39**). Delocalization of electrons from the oxygen anion result in the elimination of a chloride anion which in turn attacks C-O resulting in the elimination of the oxygen-containing group.



Scheme 39: Conversion of a primary alcohol to an alkyl chloride using thionyl chloride.

This reaction was attempted using thionyl chloride based on its wide coverage in literature. However, disappointingly, we were not able to isolate the desired product. The TLC plate upon visualization under UV light showed several spots which were difficult to isolate. Upon a further literature search it was found that Bissinger and Kung did report the limited scope of thionyl chloride with regards to converting primary alcohols to alkyl chlorides[93]. The pair reported at least six different compounds that were isolated from this reaction. We therefore decided not to proceed further with this reaction.

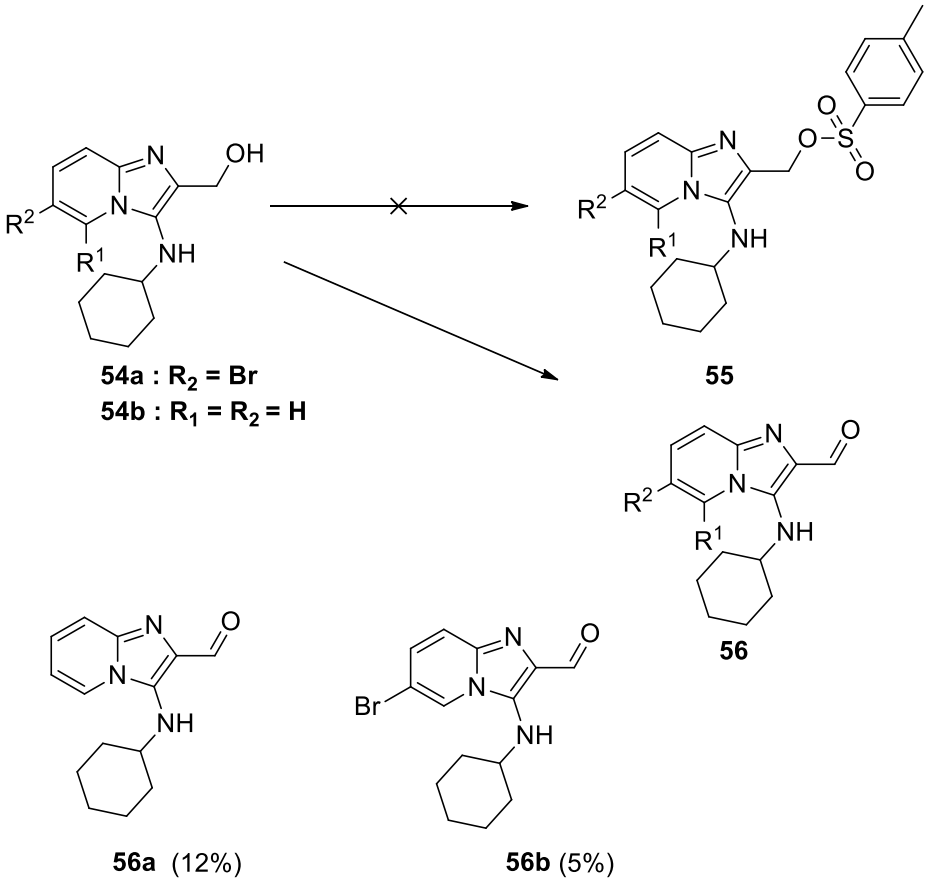
2.2.5.3.2 Tosylation of primary alcohols using p-toluenesulfonyl chloride

An alternative procedure for functional group transformation of alcohols to a better leaving group is the conversion of the OH group to a tosyl group. This procedure has been well documented in literature under various reaction conditions such as the choice of optimal base, catalyst, solvent, and optimal thermodynamics of the reaction. More recently, Jia *et al.* was able to transform derivatives of polyoxometalates to the corresponding tosyl intermediates using DMAP as an activating base and triethylamine as an HCl scavenger[94]. This was consistent with work done in our laboratory by Zimuwandeyi *et al.* in her synthesis of *ent*-pavettamine where she converted aliphatic primary alcohols to tosyl intermediates using DMAP as a base and was able to isolate the target compounds in appreciable yields[95]. However, she reportedly did not use an organic base proton scavenger such as Et_3N. We decided to explore the utility of a proton scavenger in this study by performing the reaction in both a Et_3N-free environment and a Et_3N catalysed environment.

In the first reaction, 6-bromo-substituted imidazo[1,2-*a*]pyridine methanol derivative was dissolved in pre-distilled DCM. DMAP was then subsequently added, and the mixture was stirred at 50 ℃ for 30 minutes to allow the deprotonation of the alcohol. Tosyl chloride (TsCl) was then added, and the mixture was allowed to stir at 50 ℃ for 12 hours. Reaction progress was monitored by TLC, and when no new spot was observed, the temperature was increased to 80 ℃ and the reaction run further for 24 hours. Disappointingly, no new products formed.

We then decided to attempt the second part of the study by adding Et_3N and using a simpler and less substituted alcohol such as the debrominated alcohol obtained from the reduction of the ester reaction (compound **54e**). Applying the same reaction conditions and procedure as before, the reaction was allowed to run for 12 hours at 50 ℃. Upon visualizing the TLC, no new spot was observed. The reaction was allowed to react further for 24 hours at 80 ℃. Again, no new spots on the TLC plate were observed. Et_3N (1.2 eq) was added to the reaction mixture and the reaction was left stirring for a further 12 hours. Surprisingly, a new spot was observed on the TLC plate and was isolated for further characterization. Upon ^1H NMR spectroscopic analysis, it was noted that the reaction did not yield the desired tosyl product.

Instead a 2-position substituted aldehyde **(56a)** (**Scheme 40**) was isolated in a low yield of 12%.

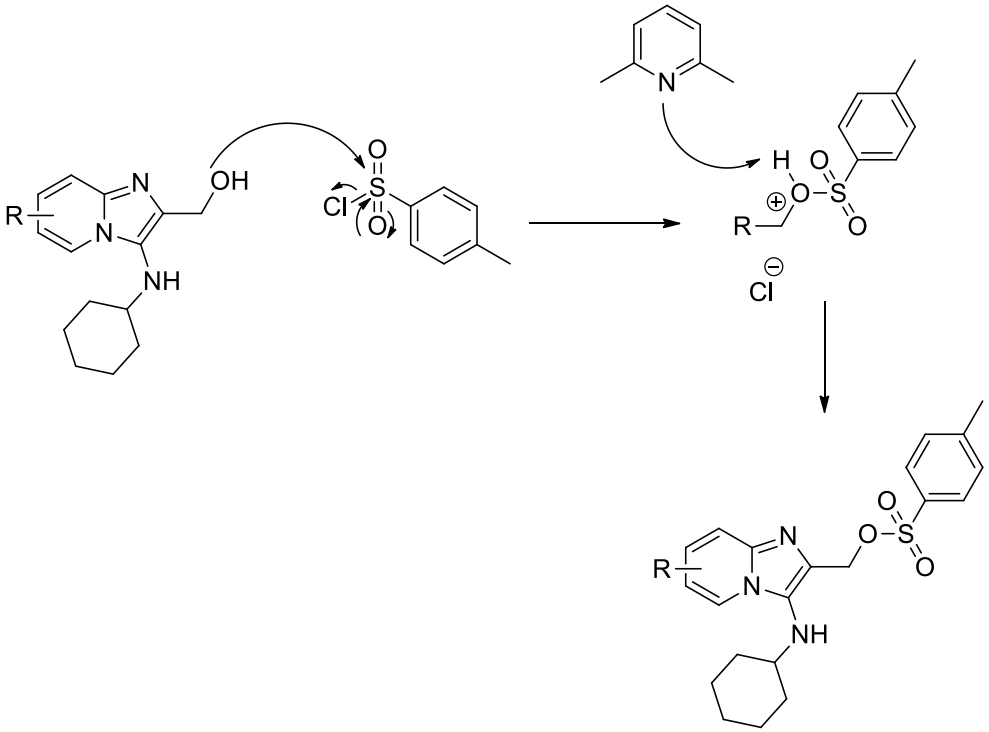


Reaction conditions: *DMAP (2 eq), TsCl (2 eq), Et_3N (1.2 eq), 80 °C, 36 h.*

Scheme 40: Unexpected aldehyde synthesis from the tosylation reaction.

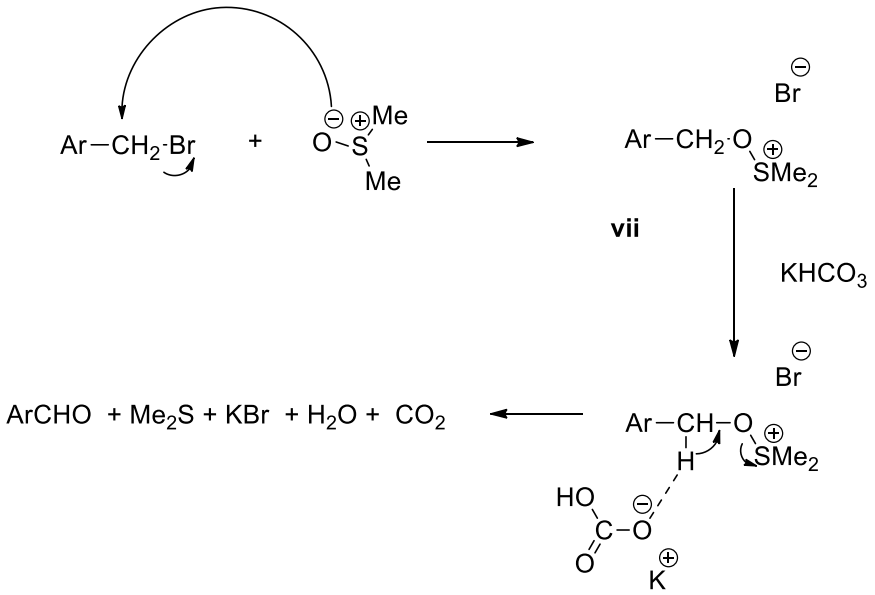
This reaction was explored further using a 6-bromo-substituted alcohol **(54a)** and the target aldehyde **(56b)** was obtained in a very low yield of 5%. It became evident that the reaction did not favour the formation of the expected tosyl product. It is to be noted, however, that tosylation of alcohols with TsCl does not always result in the expected tosylate product[96]. This was noted by Ding *et al.* when they exclusively isolated alkyl chlorides instead of the expected tosyl product.

We considered a possible mechanism for the formation of the aldehyde as there were no literature sources that have reported this observation. The starting point was to understand the mechanism that leads to the formation of the tosyl product from the alcohol (**Scheme 41**).



Scheme 41: Classical tosylation reaction that was expected to take place.

The alcohol group is expected to attack the electrophilic sulfonyl group to give the intermediate cationic species which gets deprotonated by the non-nucleophilic base to afford the product. It was clear that for an aldehyde to form, the oxygen of the alcohol would need to form a pi-bond with the carbon attached to it. It is possible that triethylamine (Et_3N) could have removed one of the acidic protons on the $–CH_2$, in a similar manner to the Kornblum reaction (**Scheme 42**) where potassium bicarbonate removes a proton on the $–CH_2$ group carrying the oxygen resulting in the formation of the aldehyde product. This postulation, however, was not tested and the exact mechanism for the formation of aldehydes from this tosylation reaction remains a mystery.



Scheme 42: Kornblum reaction mechanism for the formation of aldehydes from alkyl halides.

Formation of the aldehydes, nonetheless, offered a reliable option to synthesize the target compounds. Essentially, this meant that position 2-substituted aldehydes were in effect stable as opposed to their carboxylic acid counterparts. High reactivity of aldehydes meant that a reductive amination reaction could be used to obtain the target compounds. Thus, adequate amount of the aldehyde were required since reductive amination is a reversible reaction and is known to result in low yields. Oxidation of alcohols using a strong oxidising agent such as pyridinium chlorochromate (PCC) and Jones reagent have been extensively reported to result in the formation of aldehydes. The toxicity of chromium containing compounds, however, has led to reduced usage of these compounds as oxidising agents. Moreover, the poor selectivity of oxidising agents such as the Jones reagent which is known to over-oxidise alcohols to carboxylic acids, has led to its reduced usage. Other safer, milder and selective reagents have been reported in recent years such as periodinane, 2-iodobenzoic acid (IBX) as well as biological systems such as enzymes. These compounds are gaining attention from researchers due to their availability and safety.

However, unpredictable yields resulting from using biological systems and IBX means that some researchers still rely on agents like PCC. Moreover, biological systems are known to be substrate specific which makes it harder to predict the outcome of the reaction.

2.2.5.3.3 PCC oxidation of alcohols

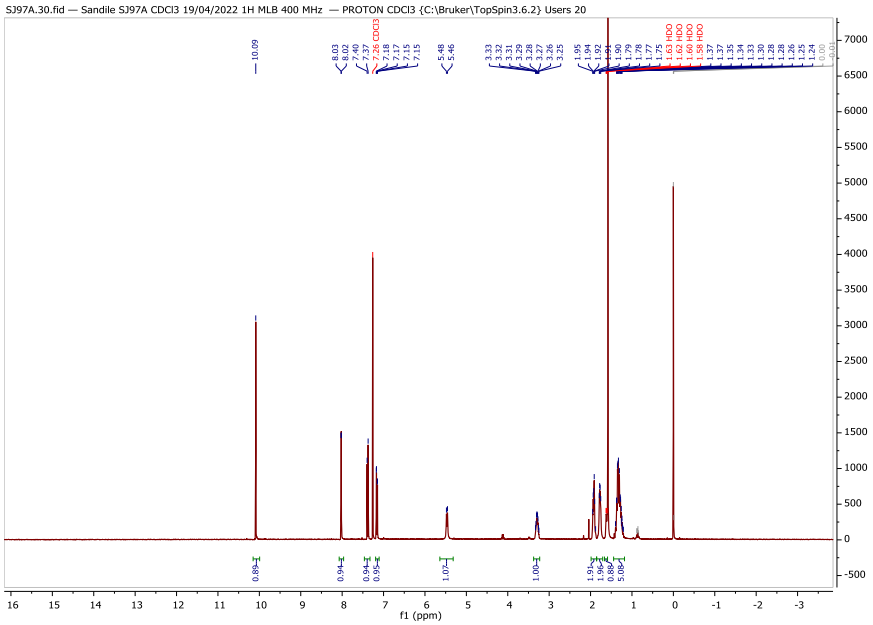
Unexpected twist: Ring-opening

The search for selective, mild, and efficient reagents for simple oxidation of alcohols to carbonyl compounds has been an objective for many researchers[97]. Chromium (VI) containing compounds have been well studied[98], however many of these compounds cannot be conveniently applied in the synthesis of complex and sensitive organic compounds. An example is the Collins reagent, a dipyridine chromium (VI) oxide complex. The red liquid complex must be used in large excess quantities (often five or six equivalents), it is hygroscopic, unstable and it is prepared by unsafe and dangerous procedures which could result in explosions. Moreover, it has poor selectivity with regards to oxidation of alcohols to aldehydes[99]. Studies by Corey *et al.*[100] were as a result of the need to improve efficiency and selectivity of oxidising agents which led to the accidental discovery of pyridinium chlorochromate (PCC). Pyridinium chlorochromate has an advantage over other oxidising agents in that it is easily and conveniently prepared in a safe manner, it is stable, and it is not hygroscopic. Moreover, it is selective and shows high capability of converting primary alcohols exclusively to corresponding aldehydes. Having previously established that carboxylic acid substituents at the 2-position of our compounds were not stable, we decided to employ PCC for oxidation of our alcohol compounds.

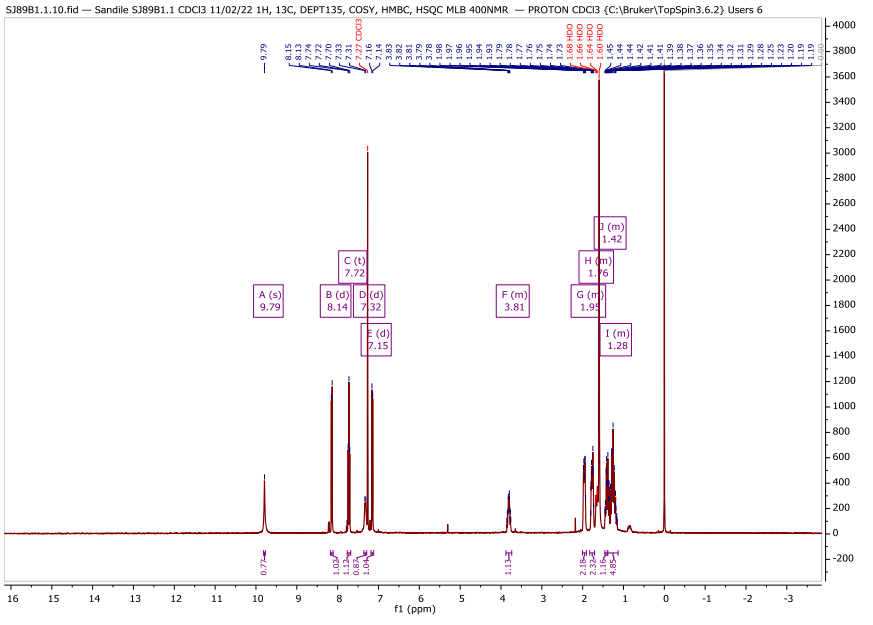
Using a general PCC oxidation procedure, PCC was dissolved in dry DCM and treated with silica gel (mass equivalent of substrate) and the alcohol (**54d**). The reaction flask was evacuated, filled with nitrogen and the reaction was allowed to run at room temperature for 4 hours after TLC analysis confirmed formation of a new product. Unreacted PCC, together with chromium salts, were trapped in the silica and were conveniently removed by filtration using filter paper. Addition of silica or celite to the reaction mixture offers a convenient method for removal of toxic chromium by-products and pyridinium salts prior to further purification of the product. Silica gel column chromatography was used to purify and isolate the product which was highly polar in relation to the starting material. This made it easier and quicker to isolate the product as TLC analysis showed only two spots.

Upon ^{1}H NMR spectroscopic characterization, the expected deshielded aldehyde proton signal was observed at 9.79 ppm. Both the $-CH_2$ and -OH proton signals were absent which confirmed that oxidation had taken place. The expected aliphatic and aromatic protons were all present. However, the N-H signal which often appears around 3.97-5.82 ppm was shifted

into the aromatic region and was overlapping with some of the aromatic signals. The proton signal at 9.79 ppm appeared to be broader and diminished in intensity compared to the aldehyde proton signal from previously synthesised aldehydes (**Figure 27**).



A



B

Figure 27: **A**- A previously synthesised aldehyde with a distinctive intense aldehyde proton at 10 ppm and the expected N-H proton at 5.47 ppm. **B-** product of PCC oxidation of alcohol with a low intensity signal at 9.79 ppm and the N-H signal shifted into the aromatic region at7.32 ppm.

Moreover, the carbonyl carbon signal of a typical aldehyde in the ^{13}C NMR spectrum that appears downfield at around 188-190 ppm was absent. In essence, the compound was missing one carbon atom in its structure. This prompted us to use other characterization techniques to elucidate the structure of the new compound. The crystalline nature of the product coupled with its high solubility in polar solvents meant that we could easily recrystallize the compound and use a Single Crystal X-ray diffractometer (SCXRD) to generate a crystal structure.

Surprisingly, results from the SCXRD analysis revealed that the expected aldehyde was not isolated. Instead, we obtained a ring-opened product with one carbon atom less in its structure compared to the parent alcohol compound (**Figure 28**).

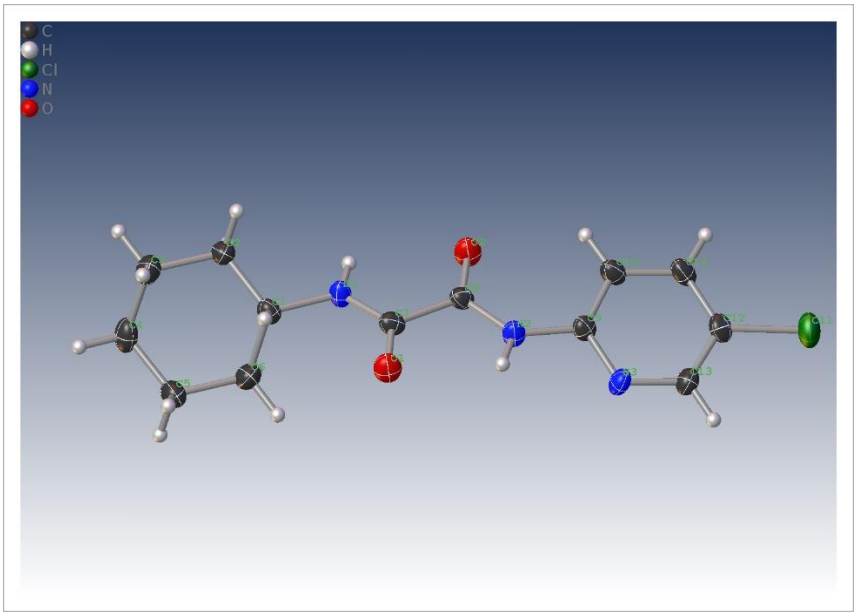
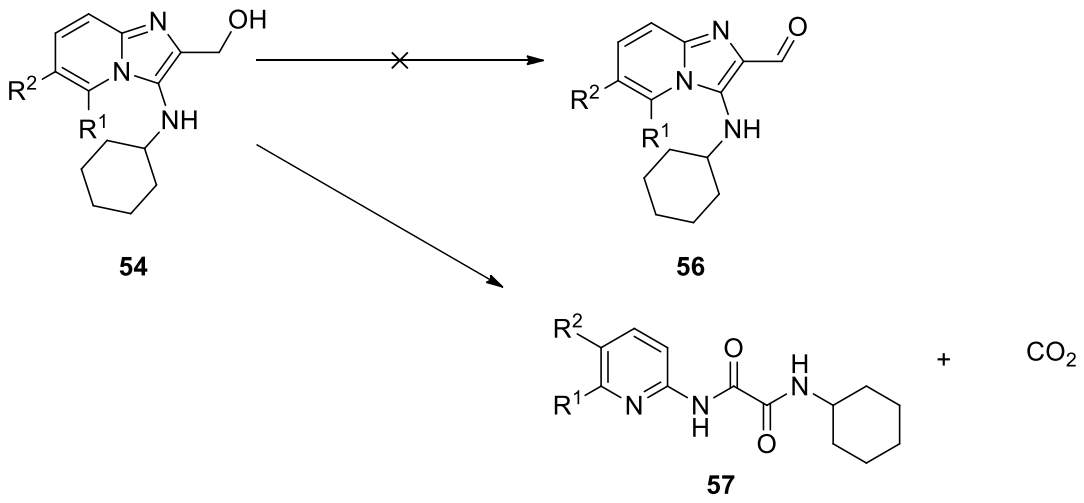


Figure 28: X-ray crystal structure showing a ring-opened product

This data was consistent with NMR spectral analysis. The ^{13}C NMR spectrum showed that the compound was missing a carbon atom and the ^{1}H NMR spectrum showed an unexpected shifting of the N-H proton signal into the aromatic region. It was evident from the SCXRD data that the proton signal at 9.79 ppm was not an aldehyde proton as initially perceived, but it was the amide N-H proton that is closer to the pyridine ring. Equally, the second N-H proton adjacent to the cyclohexyl group corresponded with the N-H proton signal that had shifted into the aromatic region and was appearing at 7.32 ppm. From our experience with the 2-position unsubstituted imidazo[1,2-*a*]pyridines, we speculated that the missing carbon on the open ring product was most likely lost as CO_2.

We decided to further explore this PCC-mediated ring opening reaction by using alcohols with varying substituents on the pyridine ring (**Scheme 43**).



Reaction conditions: *PCC (1.1 eq), SiO_2, DCM, r.t., 4 h*

Scheme 43: Illustration of the ring-opening reaction using PCC.

Compounds **57a-57d** were successfully synthesised despite the poor yields (**Figure 29**).

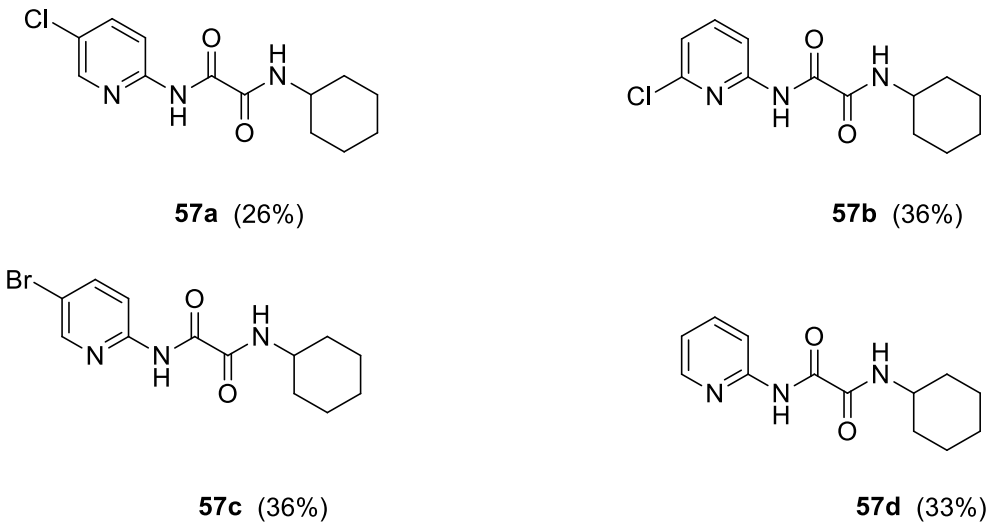


Figure 29: Compounds prepared by PCC-mediated ring-opening of imidazopyridines **54**.

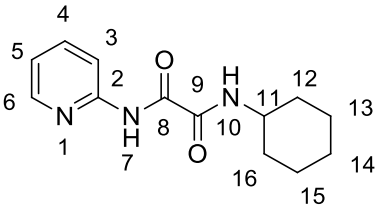
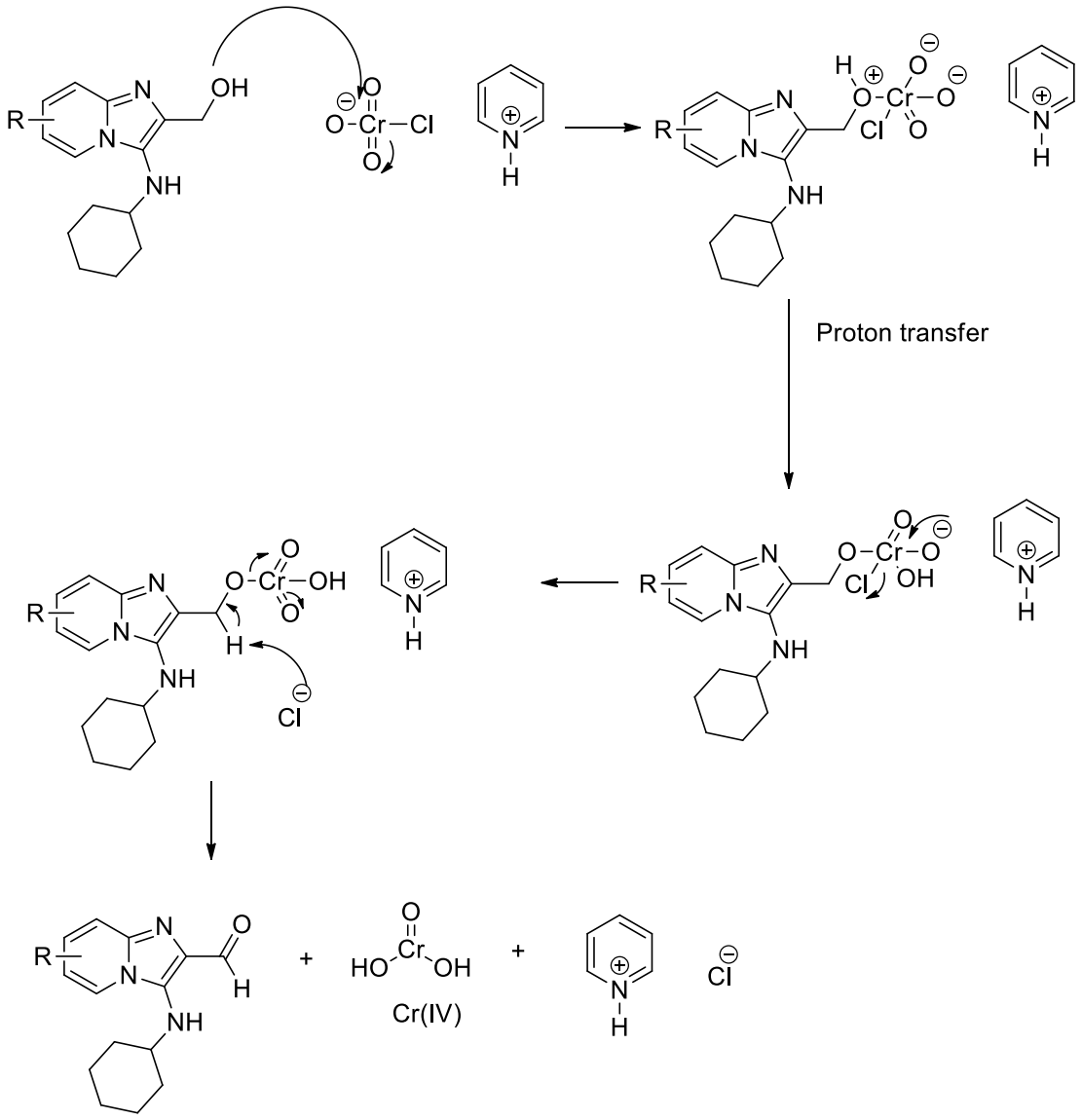


Figure 30: Illustration of the numbering of protons and carbons on the ring-opened product.

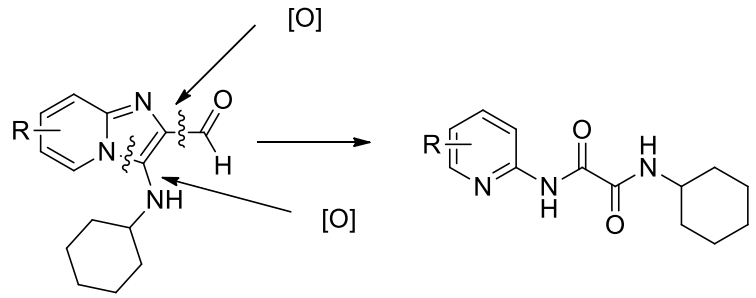
In all the compounds, the characteristic amide N-H (7) proton signal of the amide closest to the pyridine (**Figure 30**) appeared as the most deshielded signal, at 9.77-9.79 ppm, owing to it being attached to the nitrogen with a pyridine and a carbonyl group. The second amide N-H proton signal for compound **57d**, with no substituents on the pyridine ring, appeared slightly downfield at 7.39 ppm compared with that of the other compounds **57a** (7.35 ppm); **57b** (7.32 ppm); **57c** (7.34 ppm)). The two carbonyl carbons were observed downfield in the ^{13}C NMR spectrum for all four compounds, with the carbonyl carbon closest to the pyridine being the most deshielded. Carbonyl stretches on the IR spectra were observed at = 1656 cm^{-1} (**57a**); 1665 cm^{-1}(**57b**); 1657 cm^{-1} (**57c**) and 1658 cm^{-1}(**57d**). Furthermore, high resolution ESI-MS revealed the expected masses corresponding to each compound.

It became clear that oxidation of the alcohols needed to be performed under very mild conditions. **Scheme 44** illustrates the expected pathway for oxidation of the alcohol.



Scheme 44: Schematic representation for oxidation of alcohol with PCC.

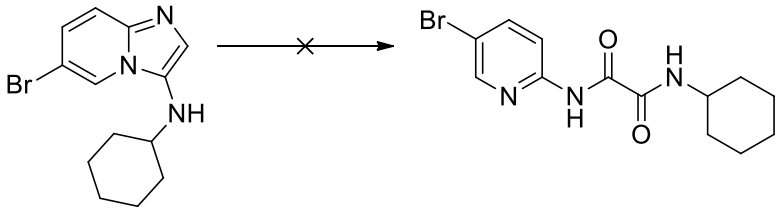
It is possible that in the presence of chromic acid, the aldehyde gets activated by protonation. This enables either chromic acid itself or any excess PCC to further oxidise the aldehyde to a carboxylic acid leading bond cleavage in two positions (**Scheme 45**). This resulted in the loss of CO_2 and could explain the missing carbon in the final product. Interesting to note was that further oxidation took place on carbons at the two cleavage sites (**v**) resulting in the oxalamide product (**vi)**.



v **vi**

Scheme 45: Illustration of bond cleavage sites and subsequent oxidation positions that gave rise to the ring opened compound (**vi**).

We conducted a study on the possible oxidation and ring opening of the 2-position unsubstituted imidazo[1,2-*a*]pyridines **50a** (**Scheme 46**) to evaluate the extent of this ring-opening phenomenon. The results were, however, inconclusive as we did not obtain the product and the starting material was retained after repeated attempts. This makes it unlikely that the mechanism proceeds by oxidation of the alcohol directly to the carboxylic acid followed by decarboxylation and then ring-opening. If this were the case, we would have expected compound **50a** to ring-open under these conditions.



50a **57c**

Reaction conditions: *PCC (1.1 eq), DCM, r.t., 4h*

Scheme 46: Attempted ring opening using position-2 unsubstituted imidazo[1,2-*a*]pyridin-3-amines.

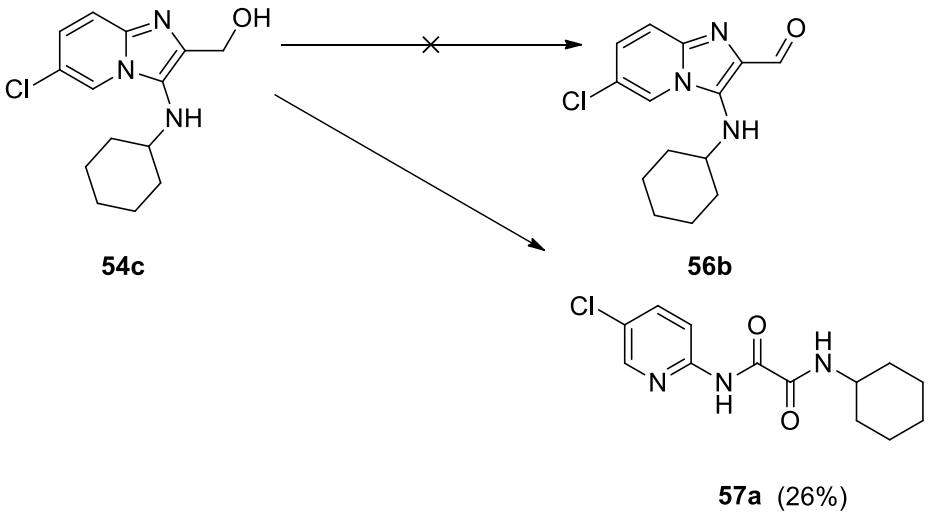
We concluded that the loss of carbon dioxide occurs simultaneously with breaking of the two bonds and in tandem with re-oxidation of the two carbons. We decided henceforth to conduct the reaction under mild conditions using 2-iodoxybenzoic acid as an oxidising agent to examine the possibility of synthesizing the aldehyde.

2.2.5.3.4 Alternative oxidation methods

2.2.5.3.4.1 IBX oxidation of primary alcohols

A gentle and effective alternative reagent for oxidation of primary alcohols to aldehydes is the periodinane, 2-iodoxybenzoic acid. It is advantageous over other oxidation reagents in that it is relatively cheap and easy to prepare from readily available reagents, it is selective and does not over-oxidise alcohols to carboxylic acids. It is easily employed under mild conditions and works within moderate to short duration times. Moreover, it is easy to handle, and it is not moisture sensitive[98]. Its poor solubility in most organic solvents coupled with recent reports of its potential to explode at temperatures over 130 °C pose a serious limitation on its usage[99]. Its simplicity to remove during work up and its low toxicity, however, make it a preferred oxidant in most organic reactions.

We decided to use IBX for oxidation of our alcohol derivatives with the hope that it would be gentle and would result in the desired aldehydes. The challenge with using IBX, as most commonly noted, was finding a solvent that would dissolve both our alcohol and IBX simultaneously. IBX dissolves well in DMSO however; our alcohol substrate disappointingly did not dissolve in DMSO. Several solvents were tested, and it was found that the acetonitrile/chloroform solvent system was ideal to fully dissolve both the alcohol and IBX. After adding 1.2 equivalents of acetic acid to the reaction mixture, the mixture was heated at 80 $^{\circ}$C and allowed to react overnight. After TLC confirmation of the new spot, the mixture was purified by silica gel column chromatography. A white fluffy material was isolated, and this material resembled the previously isolated material from PCC oxidation of alcohols. Characterization of the product by ^{1}H NMR and ^{13}C NMR spectroscopy confirmed our suspicion that instead of the desired aldehyde we had once again obtained a ring-opened product (**57a**) similar to the compounds obtained from PCC reactions (**Scheme 47**).



Reaction conditions: *IBX (1,2 eq), $CHCl_3$/CH_3CN,Acetic acid (1.2 eq), 80 °C, 12 h*

Scheme 47: IBX-mediated ring-opening-oxidation reaction.

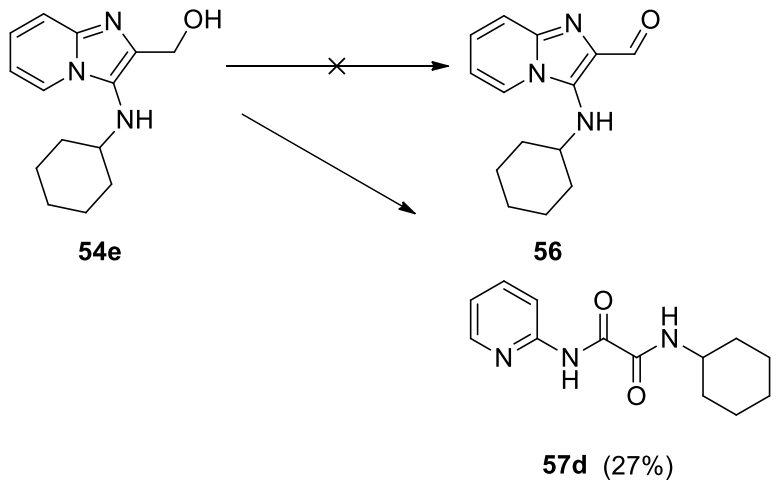
This surprising turn of events led us to believe that perhaps direct oxidation of position-2 methanol substituted imidazo[1,2-*a*] pyridin-3-amines does not afford the desired aldehyde. However, these aldehydes have already been isolated earlier on in this study, and they are stable under standard conditions although the procedure from which they were obtained was not yet clear. Milder approaches were thus attempted.

2.2.5.3.4.2 Biocatalytic oxidation of primary alcohols

A more facile and green method for oxidation of alcohols to aldehydes most commonly employed in our laboratory is enzymatic oxidation. We decided to use enzymes as they have proven effective and efficient in that they are highly selective and therefore the product is easy to isolate as there are no major side products. A series of screening tests were performed to determine which enzyme worked best for the given substrate and under which conditions. Laccase *T. versicolor* in the presence of TEMPO as a mediator worked the quickest and under solvent conditions that were able to solubilize the alcohol substrate. This was in agreement with work done by Heidary *et al.*[101] with the exception that in this study Tris buffer pH 7 was used instead of citrate buffer pH 4.5 that the other group used. The most remarkable feature regarding this reaction was that the product was formed within five minutes and the reaction was run in open air. The reaction was, however, allowed to run for a further 15 minutes to ensure that the substrate was optimally converted to the product.

The effortless work up and purification of the product is a big benefit of using enzymes in organic synthesis. Disappointingly, the isolated product appeared similar to previously

isolated products from previous oxidation reactions. NMR spectroscopic characterization confirmed that the product was indeed the ring-opened compound (**57d**) (**Scheme 48**).



Reaction conditions: *laccase T.versicolor (1 eq), TEMPO (20%), O_2, tris buffer pH 7, THF, 15 minutes*

Scheme 48: Enzyme-mediated ring opening of the alcohol.

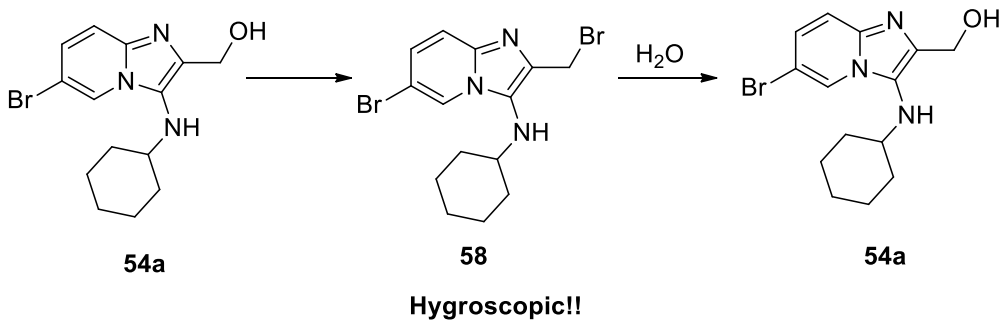
Various oxidation methods were attempted hereafter, but none afforded the target aldehyde. It became evident that oxidising these alcohols to the corresponding aldehydes was a serious challenge that required adequate resources.

2.2.5.3.5 Bromination of alcohols

The methodology for synthesizing the aldehyde was then revised. Instead of directly oxidising the alcohol to form the aldehyde, bromination of the alcohol was to be done followed by conversion of the alkyl bromide to an aldehyde. Kornblum[102] and other investigators have shown that direct displacement of primary halides and tosylates with DMSO in the presence of a base or using high heating conditions, generates aldehydes in moderate yields[99]. In addition, Bratulescu showed that aromatic aldehydes can be synthesised by oxidation of corresponding halides with DMSO and potassium carbonate under microwave irradiation[70].

Motivated by these reports, bromination of the alcohols using phosphorus tribromide in ice cold diethyl ether at room temperature under inert conditions was carried out (**Scheme 49**). Phosphorus tribromide is very corrosive and upon contact with moisture it fumes, forming HBr gas and phosphoric acid. Caution therefore had to be exercised when handling it.

Nevertheless, after reaction completion, confirmed by a new spot on the TLC plate and the starting material being completely used up, a workup was carried out by quenching the mixture with water and extracting the organic layer with dichloromethane. The mixture was purified by silica gel chromatography to afford a light brown solid material (**58**). This was left in the fumehood overnight to dry. Surprisingly, upon attempting to characterize the product the following morning, it was noted that the product had accumulated moisture and liquefied. The product was then dried by slow evaporation using a rotary evaporator followed by drying under high vacuum. However, TLC visualisation showed that the product had hydrolysed back to the alcohol starting material (**54**). It was clear that the brominated compound was highly hygroscopic. Equally, upon contact with moisture it hydrolyses back to the alcohol.



Reaction conditions: *Phosphorus tribromide (1.5 eq), DCM/Et_2O, r.t., 12 h*

Scheme 49: Bromination of the alcohol and subsequent hydrolysis upon contact with moisture.

The plan was to then convert the alkyl bromide product *in situ* to an aldehyde without further isolation. However, the challenge was that to convert the alkyl bromide to an aldehyde, a carbonate salt needed to be dissolved in water and introduced as an aqueous solution into the alkyl bromide mixture. This was going to hydrolyse the alkyl bromide.

When one looks at the mechanism for this reaction, it is clear that the first part of the reaction is the formation of the oxysulfonium salt (**vii**) from the reaction of DMSO and the alkyl bromide (refer to **Scheme 42**). The second part is deprotonation of an acidic -CH_2 proton by the base which give rise to the formation of the aldehyde. From this observation, it meant that we could first react our alkyl bromide with DMSO to form the oxysulfonium salt

intermediate and then add the aqueous base solution. This would prevent the alkyl bromide coming into contact with the aqueous solution.

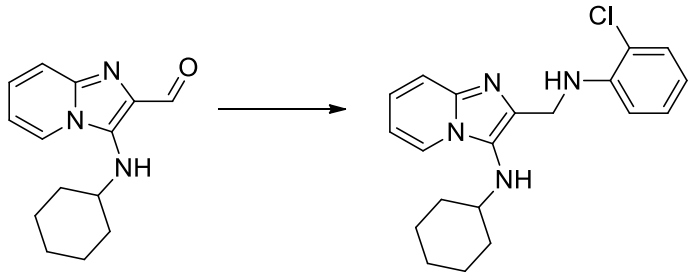
Upon addition of DMSO to the alkyl bromide solution, an immediate red colour started forming. This was an indication of bromide ions being liberated from displacement by oxygen of DMSO. The reaction was allowed to run at room temperature for 30 minutes and thereafter an aqueous solution of sodium bicarbonate was added, and the reaction mixture was heated at 96 °C for 24 hours. Upon TLC visualization, a new spot was observed. A workup of the mixture was performed followed by purification by silica gel chromatography. A dark yellow solid material was isolated and characterized by NMR spectroscopy. It was confirmed from NMR spectral analysis that the isolated product was our target aldehyde. The characteristic intense aldehyde peak observed at 10.09 ppm as a singlet was noted. This signal resembled the signal of the previously synthesised aldehydes, and this was confirmation that indeed the isolated material was the target aldehyde. Moreover, the N-H signal was observed at 5.47 ppm and had not shifted into the aromatic region. This confirmed that the product was not a ring-opened compound. Also, ^{13}C NMR spectroscopic analysis revealed that the product had the expected number of carbons for the aldehyde and the carbonyl carbon of the aldehyde was noted at 189.1 ppm. IR stretches of the carbonyl were also observed at 1734 cm^{-1}. High resolution ESI-MS also revealed the mass corresponded with that of the aldehyde.
This was very exciting to us, and we decided to perform a reductive amination using 2-chloroaniline.

2.2.6 Reductive amination reaction

High reactivity of the carbonyl carbon of aldehydes makes this functional group very versatile and easy to transform into other functional groups. In contrast, aniline is a poor nucleophile due to the lone pair of electrons of nitrogen being resonance stabilized by the aromatic ring. Furthermore, the aniline substrate that we were to use for the reductive amination reaction had an electron withdrawing chloro-substituent in the *ortho* position. This further decreased the nucleophilic character of the nitrogen.

Another challenge for this reaction was that reductive amination reactions are reversible reactions that often require long reaction times and the yields are generally low. To improve the yields, the use of a drying agent such as molecular sieves or the azeotropic removal of

water by a Dean-Stark apparatus is often employed to drive the reaction forward. We decided to explore the reductive amination reaction between the imidazopyridine aldehydes and 2-chloro aniline using molecular sieves as drying agent. Using the aldehyde with no halogen substituents on the pyridine ring (**56**), the reaction was slower but afforded **59** in a low yield of 36% as a brown oil.

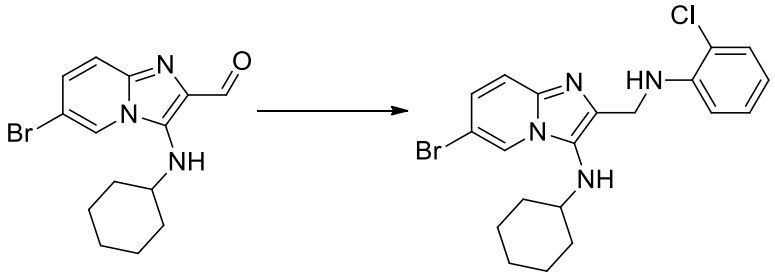


56 **59** (36%)

Reaction conditions: *2-Chloroaniline (1.2 eq), AcOH (pH adjusted to 5), $NaBH_3CN$ (1.2 eq), MS 4Å, MeOH, r.t., 12 h*

Scheme 50: Reductive amination of the unsubstituted aldehyde **56** with 2-chloroaniline to form the target compound **59**

In the second reaction a 6-bromo aldehyde derivative **(56a)** was used, and the target amine compound **(59a)** was obtained as a light brown solid material, in a yield of 56%.



56a **59a** (56%)

Reaction conditions: 2-Chloroaniline *(1.2 eq), AcOH (pH adjusted to 5), $NaBH_3CN$ (1.2 eq), MS 4Å, MeOH, r.t., 12 h*

Scheme 51: Reductive amination of 6-bromo aldehyde **56a**

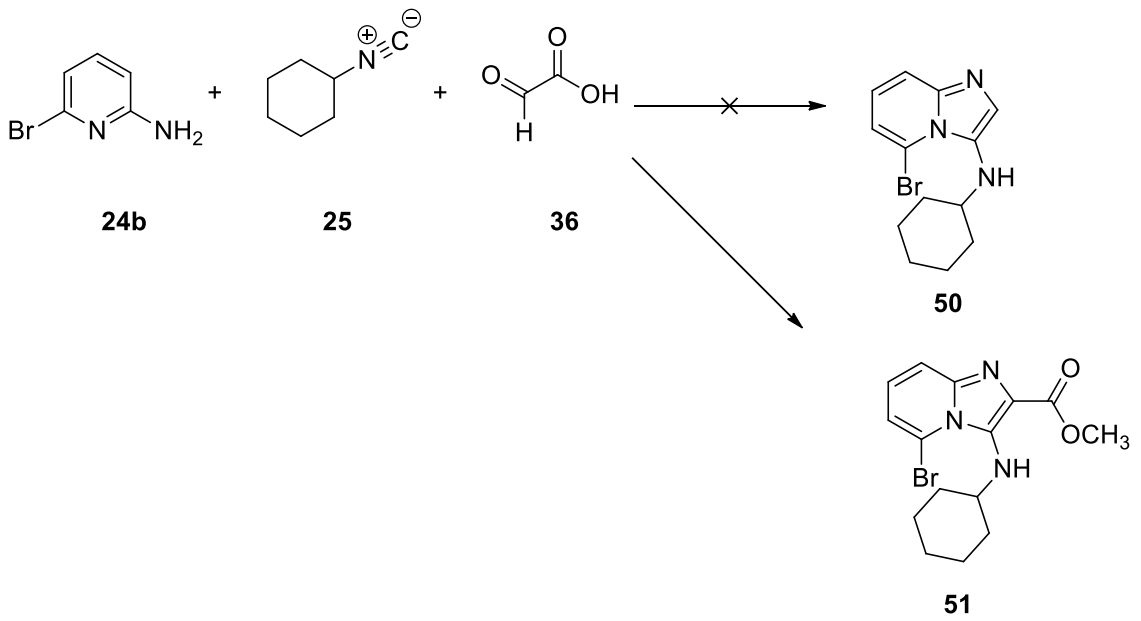
The yield was indeed low as anticipated; however, we believed that it might have been much lower had we not used molecular sieves to remove water from the reaction as well as acetic

acid which served as a catalyst to activate the carbonyl carbon. It would be interesting to examine the yield using unsubstituted aniline as well as aniline with an activating substituent such as a methoxy group.

^{1}H NMR spectroscopic analysis showed the expected -CH_2 proton signal appearing as an intense singlet at 4.50 ppm and integrating for two protons. The two N-H signals were observed as two distinct signals. One was a broad singlet appearing downfield at 4.98 ppm and the other overlapped with the H-11 signal upfield forming a multiplet that integrated for two protons at 2.98-2.86 ppm. The shielded N-H signal at 2.98-2.86 ppm corresponds to the position-3 amine proton and the downfield N-H signal at 4.98 ppm corresponds with the aniline N-H proton due to its direct attachment to the aromatic ring. DEPT-135 NMR spectroscopy was used to confirm the -CH_2 carbon signal and it was found to be a negative signal as anticipated, appearing at 41.8 ppm. IR spectroscopic analysis showed N-H stretches at 3305 cm^{-1} and no carbonyl stretches were observed.

2.3 Conclusion

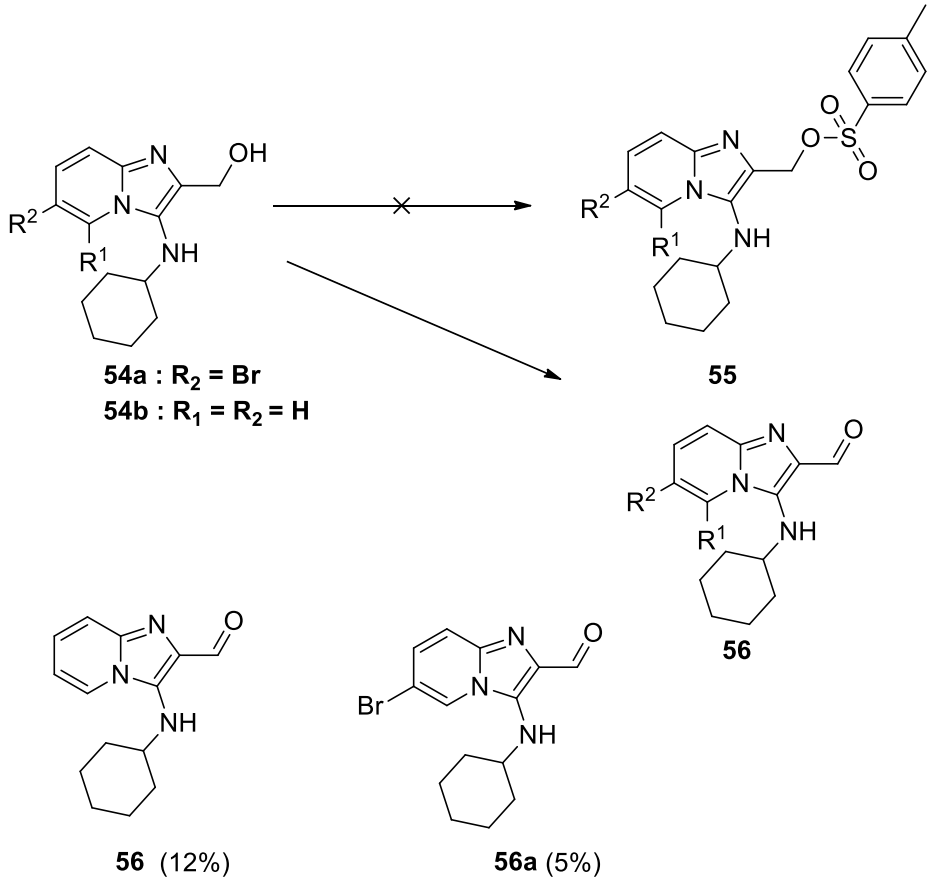
The overall aim and objective of this study was the exploration of the synthesis of imidazo[1,2-*a*]pyridin-3-amines with nitrogen linkers as possible HIV-1 RT inhibitors. Initial modelling studies showed that these compounds have a possibility of better binding at the enzyme binding site. Motivated by these studies we set out to explore the synthesis of these compounds. There were a lot of surprises and unexpected twists. The first one being that ester derivatives were isolated (**51**) instead of the position-2 unsubstituted imidazo[1,2-*a*]pyridin-3-amines (**50**) (**Scheme 52**) in our MCR using glyoxylic acid.



Scheme 52: Schematic representation of the unexpected product obtained during this project.

Following the successful synthesis of a small library of these esters, the reactions were scaled up. Surprisingly, the ester derivatives were not obtained but instead position-2 unsubstituted imidazo[1,2-*a*]pyridin-3-amines were obtained. Motivated by synthesis of the ester compounds and their potential for structural diversity, the possible route for their synthesis was investigated, and it was found that the reaction proceeded by condensation of the glyoxylate ester. Glyoxylic acid was then esterified using methanol and subsequently condensed *in situ* with 2-aminopyridine derivatives and cyclohexyl isocyanide to afford the desired ester imidazo[1,2-*a*]pyridin-3-amines in good yields. The effect of increasing the amount of the acid catalyst was also examined and it was found that optimal yields were obtained at 20 mol% catalytic amounts. The instability of the 2-position carboxylic acids was also noted.

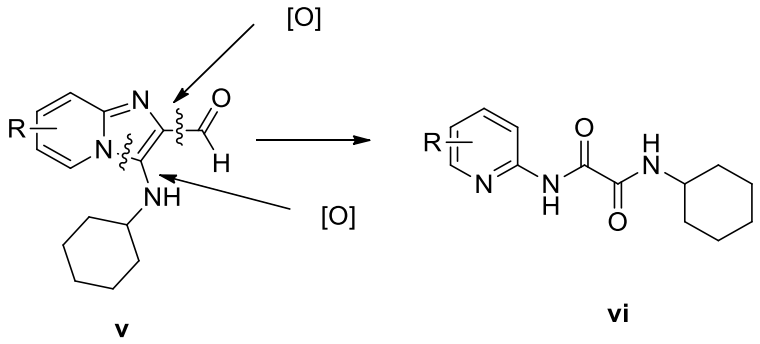
The second twist encountered was the synthesis of aldehydes from a tosylation reaction of imidazopyridine alcohols (**Scheme 53**).



Scheme 53: Synthesis of aldehydes from tosylation reaction

This took us by surprise and we suspected that the reaction mechanism proceeds in a similar manner to the Kornblum oxidation reaction.

The third twist was the ring opening of the imidazopyridine ring during the attempted oxidation of the 2-position alcohol (**scheme 54**).



Scheme 54: Ring opening reaction

It was noted that a mild and gentle oxidant was required to oxidise the alcohol to the target aldehyde. However, after repeated attempts with notable mild reagents it became clear that this oxidation reaction was highly reagent selective and that an indirect oxidation method was preferred to form the aldehyde. The alcohol was then carefully brominated and the Kornblum reaction was carried out to afford the target aldehyde. This was followed by a reductive amination reaction to afford the desired compounds.

Unfortunately, we were unable to assess the potential inhibitory activity of these compounds against HIV-RT due to time constraints. However, there is a potential that these compounds might possess antiviral activity against HIV-RT given the data from our modelling studies.

2.4. Future work

Synthesizing a library of aldehydes using the Kornblum method which we have shown to be effective in converting alkyl bromides to corresponding aldehydes should be undertaken. Subsequent reductive amination will allow for a large library of compounds that could be used in biological screening studies to assess inhibitory activity against HIV-RT. Ring-opening could be extended to other alcohol derivatives and the products could also be biologically tested against a series of viral and bacterial species. Functionalization of position-2 unsubstituted imidazo[1,2-*a*]pyridines should be undertaken. Several biologically active compounds have been reported in literature consisting of this pharmacophore (**Figure 31**).

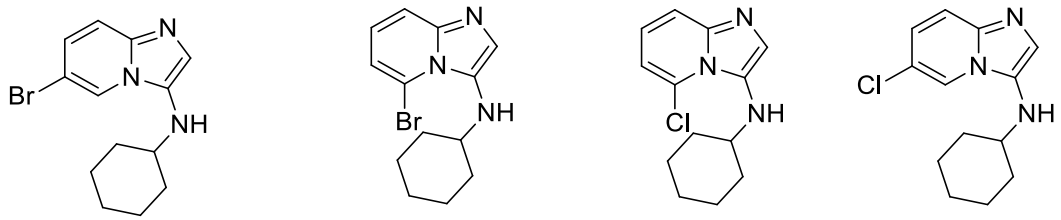


Figure 31*:* C-2 unsubstituted imidazo[1,2-*a*]pyridines that can be functionalized.

This could be done by halogenation of C-2 followed by nucleophilic substitution of the halogen by either an -NH- group or an -OH group to afford compounds with a heteroatom bridge which could also potentially possess antiviral activity against HIV-RT.

CHAPTER 3: EXPERIMENTAL PROCEDURES

3.1 General experimental procedures

The reagents and certain solvents used in this project were purchased from Merck/Sigma-Aldrich without further purification. Solvents that were used in chromatographic separation (hexane and ethyl acetate) were distilled prior to use. Those that were used in chemical reactions were either stored over molecular sieves or potassium hydroxide prior to distillation. Dichloromethane and acetonitrile were distilled from anhydrous calcium hydride whereas tetrahydrofuran and diethyl ether were distilled from a sodium wire using benzophenone as an indicator. HPLC grade commercial solvents were used without further purification. Reactions were monitored by a Thin Layer Chromatography (TLC) using an aluminium backed Macherey-Nagel Alugram Sil G/UV_{254} plates that are coated with 0.25mm silica gel 60. The plates were viewed under UV light using a TLC visualizer operated at either λ=254 nm or λ=366 nm and stained, where necessary, using iodine or DNPH stain (for aldehydes). Column chromatography was performed using Merck or Macherey-Nagel silica gel 60, particle size 0.063-0.200 mm for normal silica or flash column chromatography (silica particle size 0.040-0.063 mm).

^{1}HNMR data was acquired on a Bruker Avance-300 or Bruker Advance-400 spectrometer operating at a frequency of 300 MHz or 400 MHz respectively. Spectra were acquired in deuterated chloroform ($CDCl_3$), deuterated methanol (MeOD- d_4) or deuterated dimethyl sulfoxide (DMSO- d_6). Chemical shift values (δ) are reported in parts per million (ppm) relative to tetramethylsilane (TMS) used as a reference internal standard (δ=0). Coupling constants (*J*) are reported in Hertz (Hz) and spin multiplicities are abbreviated as s (singlet), d (doublet), t (triplet), q (quartert) and m (multiplet).

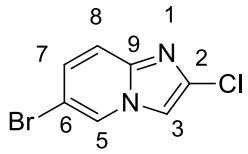
^{13}CNMR spectral data was acquired on a Bruker Avance-300 or Bruker Avance-400 spectrometer at 75.47 MHz and 101 MHz respectively. Spectra were recorded in deuterated chloroform ($CDCl_3$), deuterated methanol (MeOD- d_4) or deuterated dimethyl sulfoxide (DMSO- d_6). All chemical shift values are reported in parts per million (ppm).

High resolution mass spectra were recorded on a Waters SYNAPT G2 mass spectrometer using an electrospray ionization (ESI) technique operating at cone voltage of 15 V.

Infrared (IR) spectra were recorded on a Bruker Tensor 27 Spectrometer. Samples were analyzed by attenuated total reflection (ATR) with a standard KBr beam splitter, resolution = 1 cm^{-1} (apodised) and spectral range of 4000-370 cm^{-1}.

Melting points were recorded on a Stuart SMP 10 melting point apparatus (temp range ≤300 ^{0}C, temp accuracy ± 1.0 ^{0}C at 20 ^{0}C, ± 2.5 ^{0}C at 300 ^{0}C). Recorded melting points are not corrected.

3.2 6-Bromo-2-chloroimidazo[1,2-*a*]pyridine 29



To 2-amino-5-bromopyridine **24c** (1.00 g , 0.0578 mol) was added ethyl bromoacetate (3 ml, 0.271 mol) and the reaction was stirred at room temperature for 8 hours. The resulting heavy white precipitate was removed by filtration and recrystallized from ethanol to yield a red powder. This was refluxed in ethanol for 2 hours to afford a red coloured solution which was concentrated and left in an ice bath to recrystallize. Red crystals were obtained (mass = 1.75g), M.P = 274 $^{\circ}$C (decomposes). These were treated with an ion exchange resin (IRA-401 Cl^-) which was regenerated prior to use, to afford a reddish brown solid. This was treated with $POCl_3$ (7.5 ml) and the mixture heated at reflux under calcium chloride drying tube, for 2 hours. The reaction mixture was cooled to room temperature and excess $POCl_3$ removed under reduced pressure to give a dark brown syrup. Ice water was added to this syrup and ammonium hydroxide (25%) was added slowly to the resulting solution until it remained basic (pH 8-9). The solution was extracted with chloroform (30 ml x 3), the organic phase dried over anhydrous magnesium sulphate, filtered and the filtrate evaporated to dryness to give a solid. This solid was purified by flash column chromatography (EtOAC/ MeOH/ Hex 1:2:2) to give a white to off-white solid that was recrystallized from methanol to give 826 mg (59 %) of compound **29**. **M.p.=** 155-156 ℃. **R_f** =0.42 (EtOAc/ MeOH/ Hex 1:2:2). **^{1}H NMR** (400 MHz, $CDCl_3$): δ_H = 8.22 (d, 1H, *J* = 4 Hz, H-5), 7.49 (s, 1H, H-3), 7.44 (d, 1H, *J* = 9.5 Hz, H-8), 7.30 (d, 1H, *J* = 1.9 Hz, H-7). **^{13}C NMR** (101 MHz, $CDCl_3$): δ_C = 142.2 (C-9), 136.5 (C-2), 128.7 (C-7), 125.1 (C-5), 117.7 (C-8), 108.5 (C-3), 107.8 (C-6). **IR** (ν_m.cm^{-1}) = 1296 (C-N), 741 (C-Cl), 685 (C-Br). **HRMS** (ES^+) calculated for $C_7H_5N_2BrCl$ $[M+H]^+$: 232.9299, found: 232.9298.

3.2.1 Attempted synthesis of 6-bromo-2-chloroimidazo[1,2-*a*]pyridine 29

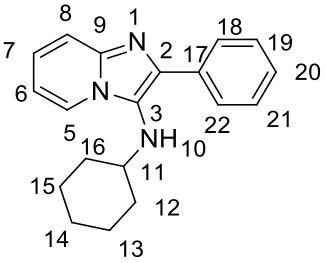
In a 100 ml round-bottom flask containing a solution of chloroacetic acid **(28)** (1.84 g, 19.4 mmol) in water (6 ml), triethylamine (3.06 ml, 22 mmol) was added drop-wise. After stirring for a few minutes, 2-amino-5-bromopyridine **(24c)** (3.98 g, 23 mmol) was added and the mixture was heated to reflux in an oil bath for 5 hours. The reaction mixture was allowed to cool, and ethanol (10 ml) was added and stirred at 5 °C for 2 hours to obtain precipitates which were collected and dissolved in toluene (25 ml) followed by addition of phosphorus oxychloride (9.7 ml, 104 mmol)) and refluxed for 16 hours. The reaction mixture was cooled at room temperature, diluted with cold water (50 ml) and stirred for 15 minutes. The aqueous layer was separated and neutralized with 10% aqueous NaOH. The organic layer was washed with brine, dried over anhydrous $MgSO_4$, and concentrated *in vacuo* to afford a brown powder which was purified by silica gel column chromatography using cyclohexane/ethyl acetate (90/10) as the eluent to yield compound **29** as a light brown powder (129 mg, 2%).

3.3 Synthesis of rigid Imidazo[1,2-*a*]pyridines

General procedure for the Groebke-Blackburn-Bienaymé multicomponent reactions

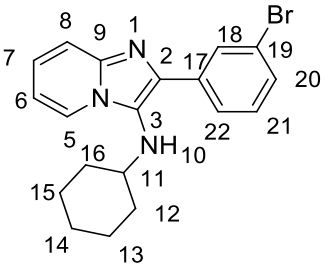
2-Aminopyridine (1eq), aldehyde (1eq) and isocyanide (1eq) were added to a round bottom flask charged with methanol or ethanol. To this mixture was added Montmorillonite K-10 clay (2 eq) or perchloric acid 70% (0.2 eq). The mixture was reacted under conventional heating for 5-8 hours at 95-100 °C or at room temperature where appropriate. After reaction completion, the clay was clay was removed by filtering through celite and the celite was washed several times with methanol. The filtrate was concentrated *in vacuo* and the residue purified by recrystallization or by silica gel column chromatography (elution hexane/ethyl acetate) to afford the compound of interest.

3.3.1 *N*-Cyclohexyl-2-phenylimidazo[1,2-*a*]pyridin-3-amine 40



2-Aminopyridine (**24a)** (125 mg, 1.33 mmol), benzaldehyde (**26a)** (141 mg, 1.33 mmol), cyclohexyl isocyanide **(25)** (148 mg, 1.36 mmol) and Montmorillonite K-10 clay (250 mg) were refluxed for 8 hours. Compound **40** was obtained as a yellow amorphous solid (217 mg, 56 %). $\mathbf{R_f}$ = 0.48 (50% Hex/EtOAc). **M.p.** =142-144 °C. **^{1}H NMR** (400 MHz, $CDCl_3$): δ_H = 8.11 (1H, d, *J* = 6.9 Hz, H-5), 8.04 (2H, d, *J* = 7.7 Hz, H-18 and H-22), 7.55 (1H, d, *J* = 9.1 Hz, H-8), 7.45 (2H, t, *J* = 7.6 Hz, H-19 and H-21), 7.36-7.29 (1H, m, H-20), 7.13 (1H, t, *J* = 7.9 Hz, H-7), 6.78 (1H, t, *J* = 6.9 Hz, H-6), 3.13 (1H, s, H-10), 3.00-2.95 (1H, m, H-11), 1.82 (2H, d, H-12a & H-16a), 1.70-1.68 (2H, m, H-13a and H-15a), 1.60- 1.55(1H, m, H14a), 1.26-1.13 (5H, m, H-16b,H-15b,H-14b, H-13b and H-12b); **^{13}C NMR** (101 MHz, $CDCl_3$): δ_C = 141.6 (C-9), 136.5 (C-3), 134.5 (C-17), 128.5 (C-19 and C-21), 127.3 (C-20), 127.1 (C-22 and C-18), 125.0 (C-2), 123.8 (C-7), 122.7 (C-5), 117.4 (C-8), 111.5 (C-6), 56.9 (C-11), 34.2 (C-12 and C-16), 25.7 (C-14), 24.8 (C-13 and C-15). **IR** (ν_m.cm^{-1}) = 3237 (N-H), 2920 (C-H), 1561 (C=C).

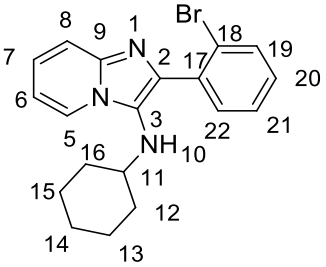
3.3.2 2-(3-Bromophenyl)-*N*-cyclohexyl)imidazo[1,2-*a*]pyridin-3-amine 41



3-Bromobenzaldehyde **(26b)** (738 mg, 3.99 mmol), 2-aminopyridine **(24a)** (376 mg, 3.99 mmol), cyclohexyl isocyanide **(25)** (507µl, 4.08 mmol) and Montmorillonite K-10 clay (752mg) were reacted in methanol (7.5 ml). Compound **41** was obtained as an off-white powder (751 mg, 51 %). $\mathbf{R_f}$ = 0.45 (60% Hex/EtOAc). **M.p**. = 146-148 °C. **^{1}H NMR** (300 MHz, $CDCl_3$): δ_H = 8.34-8.27 (m, 1H, H-5), 8.10 (dt, 1H, *J* = 6.9 Hz, H-22), 8.03 (dt, 1H, *J* = 7.7, 1.3 Hz, H-20), 7.55 (dt, 1H, *J* = 9.0, 1.1 Hz, H-8), 7.45 (dq, 1H, *J* = 8.0, 2.1, 1.1 Hz, H-18), 7.32 (t, 1H, *J* = 7.9 Hz, H-21), 7.22-7.10 (m, 1H, H-7), 6.81 (td, 1H, *J* = 6.8, 1.2 Hz, H-

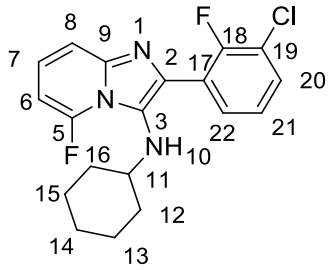
6), 3.06 (s, 1H, N-H (Partially overlapping H-11)), 3.01-2.95 (m, 1H, H-11 (partially overlapping N-H)), 1.91-182 (m, 2H, H-16a & H-12a), 1.77-1.67 (m, 2H, H-13a & H-15a), 1.64-1.60 (m, 1H, H-14a), 1.31-1.16 (m, 5H, H-16b, H-15b , H-14b, H-13b & H-12b); **^{13}C NMR** (75 MHz, $CDCl_3$): δ_C = 141.6 (C-9), 136.5 (C-17), 135.0 (C-3), 130.1 (C-21), 130.0 (C-18), 130.0 (C-20), 125.4 (C-22), 125.3 (C-2), 124.4 (C-5), 122.8 (C-19), 122.7 (C-7), 117.5 (C-8), 111.9 (C-6), 57.0 (C-11), 34.3 (C-12 & C-16), 25.7 (C14), 24.8 (C-13 & C-15). **IR** (ν_m.cm^{-1}) = 3710(N-H), 1632 (C=C), 782 (C-Br).

3.3.32-(2-Bromophenyl)-*N*-cyclohexylimidazo[1,2-*a*]pyridin-3-amine 42



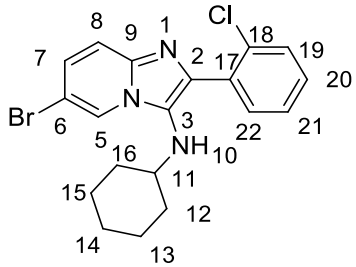
2-Aminopyridine **(24a)** (375.5 mg, 3.99 mmol), 2-bromobenzaldehyde **(26c)** (738 mg, 3.99 mmol), cyclohexyl isocyanide **(25)** (507µl, 408 mmol) and Montmorillonite K-10 clay (751 mg) were reacted to afford **42** as a thick black viscous substance (789 mg, 54 %). $\mathbf{R_f}$ = 0.52 (50% Hex/EtOAc). **^{1}H NMR** (400 MHz, $CDCl_3$): δ_H = 8.16 (d, 1H, *J* = 6.9 Hz, H-5), 7.66 (d, 1H, *J* = 8.0 Hz, H-19), 7.61 (d, 1H, *J* = 7.6 Hz, H-22), 7.55 (d, 1H, *J* = 9.0 Hz, H-8), 7.40 (t, 1H, *J* = 7.5 Hz, H-21), 7.30-7.21 (m, 1H, H-20), 7.16 (t, 1H, *J* = 9.1 Hz, H-7), 6.82 (t, 1H, *J* = 6.8 Hz, H-6), 3.27 (s, 1H, N-H), 2.72-2.61 (m, 1H, H-11), 1.71-1.62 (m, 2H, H-16a & H-12a), 1.62-1.53 (m, 2H, H-15a & H-13a), 1.50-1.41 (m, 1H, H-14a), 1.13-0.94 (m, 5H, H-16b; H-15b; H-14b; H-13b & H-12b); **^{13}C NMR** (101 MHz, $CDCl_3$): δ_C = 141.1 (C-9), 136.6 (C-17), 136.0 (C-3), 132.8 (C-22), 132.6 (C-19), 129.5 (C-20), 127.4 (C-21), 125.9 (C-18), C-2 (could not be detected), 123.9 (C-7), 122.9 (C-5), 117.5 (C-8), 111.7 (C-6), 56.4 (C-11) 33.8 (C-12 & C-16), 25.6 (C-14), 24.6 (C-13 & C-15). **IR** (ν_m.cm^{-1}) = 3680 (N-H), 1647 (C=C), 1020 (C-N), 644 (C-Br).

3.3.4 2-(3-Chloro-2-fluorophenyl)-*N*-cyclohexyl-5-fluoroimidazo[1,2-*a*] pyridin-3-amine 43



2-Amino-6-fluoropyridine **(24f)** (447.3 mg, 3.99 mmol), cyclohexyl isocyanide **(25)** (507 µl, 4.08 mmol), 3-chloro-2-fluorobenzaldehyde **(26d)** (46 9µl, 3.99 mmol) and Montmorillonite K-10 clay (894.6 mg) were refluxed in ethanol (7.5 ml) for 8 hours to afford **43** as light-yellow crystals (591 mg, 41 %). $\mathbf{R_f}$ = 0.38 (70% Hex/EtOAc). **M.p**. = 116-117 °C. **^{1}H NMR** (400 MHz, $CDCl_3$): δ_H = 7.70 (td, 1H, *J* = 8.0, 6.4, 1.7 Hz, H-7), 7.42(td, 1H, *J* = 8.5, 6.9, 1.7 Hz, H-21), 7.34 (d, 1H, *J* = 9.0 Hz, H-7), 7.19 (t, 1H, *J* = 7.9 Hz, H-20), 7.14-7.04 (m, 1H, H-22), 6.36 (t, 1H, *J* = 7.2 Hz, H-6), 3.36-3.29 (m, 1H, N-H), 2.86-2.74 (m, 1H, H-11), 1.78-1.69 (m, 2H, H-16a and H-12a), 1.64-1.53 (m, 2H, H-15a and H-13a), 1.53-1.44 (m, 1H, H-14a), 1.17-0.91 (m, 5H, H-16b, H-15b, H-14b, H-13b, H-12b); **^{13}C NMR** (101 MHz, $CDCl_3$): δ_C =155.2 (d, J_{CF}=249.4 Hz, C-18), 150.5 (d, J_{cf}= 267.8 Hz, C-5), 144.1 (d, J_{CF}=3.2 Hz, C-9), 131.8 (d, J_{CF}=2.7 Hz, C-3), 130.1 (d, J_{CF}=3.2 Hz, C-7),127.3 (d, J_{CF}=3.1 Hz, C-2), 124.7 (d, J_{CF}=4.4 Hz, C-20), 124.5 (d, J_{CF}= 6.6 Hz, C- 22), 123.9 (d, J_{CF}= 14.3 Hz, C-19), 121.5 (d, J_{CF}= 18.8 Hz, C-17), 113.8 (d, J_{CF}= 5.0 Hz, C-8), 93.1 (d, J_{CF}= 17.6 Hz, C-6), 58.3 (C-11), 33.5 (C-12 and C-16), 25.7 (C-14), 24.7 (C-13 and C-15). **IR** (ν_m.cm^{-1}) = 3306 (N-H),1653 (C=C), 1510 (N-H bending), 1093 (C-F), 1310 (C-N), 843 (C-Cl).

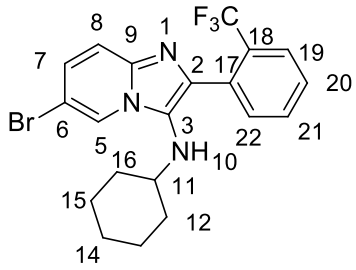
3.3.5 6-Bromo-2-(2-chlorophenyl)-*N*-cyclohexylimidazo[1,2-*a*]pyridin-3-amine 44



2-Amino-5-bromopyridine **(24c)** (690 mg ,3.99 mmol), 2-chlorobenzaldehyde **(26e)** (560 mg, 3.99 mmol), cyclohexyl isocyanide **(25)** (507µl, 408 mmol) and Montmorillonite K-10 clay

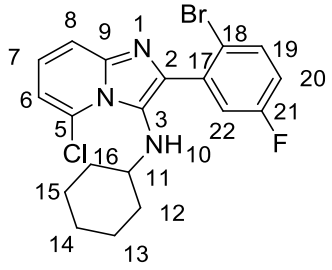
(1g) were reacted to afford **44** as a dark brown powder (850 mg, 47 %). $\mathbf{R_f}$ = 0.41 (70% Hex/EtOAc). **^{1}H NMR** (300 MHz, $CDCl_3$): δ_H = 8.27 (s, 1H, H5), 7.68-7.60 (m, 1H, H-22), 7.50-7.41 (m, 2H, H-8 & H-19), 7.38-7.32 (m, 2H, H-21 & H20), 7.20 (dd, 1H, *J* = 9.5, 2.0 Hz, H-7), 3.26 (s, N-H), 2.73-2.57 (m, 1H, H-11), 1.72-1.61 (m, 2H, H-12a & H-16a), 1.57-1.41 (m, 2H, H-13a & H-15a), 1.29-1.22 (m, 1H, H-14a), 1.14-0.96 (m, 5H, H-16b; H-15b; H-14b; H-13b & H-12b). **^{13}C NMR** (75 MHz, $CDCl_3$): δ_C =140.0 (C-9), 136.2 (C-17), 133.6 (C-3), 132.6 (C-18), 132.5 (C-19), 129.6 (C-20), 129.4 (C-21), 127.2 (C-22), 127.0 (C-7), 126.6 (C-2), 123.0 (C-5), 118.3(C-8), 106.7 (C-6), 56.4 (C-11), 33.8 (C-12 & C-16), 25.6 (C-14), 24.6 (C-13 & C-15). **IR** (ν_m.cm^{-1}) = 3354 (N-H), 1622 (C=C), 1322 (C-N), 848 (C-Cl), 651 (C-Br).

3.3.6 6-Bromo-*N*-cyclohexyl-2-(2-(trifluoromethyl)phenyl)imidazo[1,2-*a*]pyridin-3-amine 45



2-Amino-5-bromopyridine **(24c)** (690 mg, 3.99 mmol), 2-(trifluoromethyl) benzaldehyde **(26f)** (695 mg, 3.99 mmol), cyclohexyl isocyanide **(25)** (507µl , 408 mmol) and Montmorillonite K-10 clay (1.00 g) were reacted to afford **45** a light yellow fluffy solid (1.3 g, 49 %). $\mathbf{R_f}$ = 0.41 (70% Hex/EtOAc). **^{1}H NMR** (300 MHz, $CDCl_3$): δ_H = 8.25 (dd, 1H, *J* = 1.8, 0.7 Hz, H-5), 7.79 (d, 1H, *J* = 7.7 Hz, H-19), 7.66-7.46 (m, 3H, H-8, H-21 & H-22), 7.43 (dd, 1H, *J* = 10.5 Hz, H-7), 7.21 (dd, 1H, *J* = 10.5 Hz, H-20), 3.01 (d, 1H, *J* = 6.0 Hz, N-H), 2.75-2.56 (m, 1H, H-11), 1.69-1.54 (m, 4H, H-12a, H-16a, H-13a & H-15a), 1.50 (d, 1H, *J* = 4.0 Hz, H-14a), 1.16-0.88 (m, 5H, H-12b, H-16b, H-13b, H-15b & H-14b); **^{13}C NMR** (75 MHz, $CDCl_3$): δ_C = 139.5 (C-9), 136.3 (C-3), 133.2 (q, J_{CF}= 2.2 Hz, C-2), 132.7 (C-21), 131.4 (C-22), 129.7 (q, J_{CF}= 30.1 Hz, C-18), 129.2 (C-17), 128.5 (C-8), 127.1 (C-20), 126.3 (q, J_{CF}= 5.2 Hz, C-19), 124.1 (q, J_{CF}= 273.8 Hz, C-23), 123.0 (C-5), 118.4 (C-7), 106.7 (C-6), 56.3 (C-11), 33.8 (C-12 & C-16), 25.6 (C-14), 24.5 (C-13 & C-15). **IR** (ν_m.cm^{-1}) = 3240 (N-H), 1607 (C=C), 1394 (C-F), 690 (C-Br).

3.3.7 2-(2-Bromo-5-fluorophenyl)-5-chloro-*N*-cyclohexylimidazo[1,2-*a*] pyridin-3-amine 46



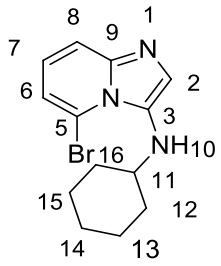
2-Amino-6-chloropyridine **(24d)** (513 mg, 3.99 mmol), 2-bromo-5-fluorobenzaldehyde **(26g)** (810 mg, 3.99 mmol), cyclohexyl isocyanide **(25)** (507µl, 408 mmol) and Montmorillonite K-10 clay (1.00 g) were reacted to afford **46** as creamy lustrous crystals (750 mg, 45 %). $\mathbf{R_f}$ = 0.52 (70% Hex/EtOAc). **M.p.**=144-146 °C. **^{1}H NMR** (400 MHz, $CDCl_3$): δ_H = 7.62 (dd,1H, *J* = 8.9 Hz, 5.3 Hz, H-19), 7.49 (d, 1H, *J* = 9.0, H-8), 7.31 (dd, 1H, *J* = 9.1 Hz, 3.1 Hz, H-7), 7.10-6.93 (m, 2H, H-22 and H-20), 6.78 (d, 1H, *J* = 7.1 Hz, H-6), 3.32 (s, 1H, N-H), 2.92-2.74 (m, 1H, H-11), 1.74-1.61 (m, 2H, H-16a and H-12a), 1.60-1.48 (m, 2H, H-15a and H-13a), 1.49-1.37 (m, 1H, H-14a), 1.17-0.84 (m, 5H, H-16b, H-15b, H-14b, H-13b, H-12b); **^{13}C NMR** (101 MHz, $CDCl_3$): δ_C =162.8 (C-21), 160.4 (C-5), 143.6 (C-9), 138.3 (C-3), 137.8 (C-7), 134.03 (C-17), 128.0 (C-2), 126.1 (C-19), 123.9 (C-6), 119.7 (C-8), 117.8 (C-22), 116.9 (C-20), 114.2 (C-18), 58.5 (C-11), 32.9 (C-12 and C-16), 25.7 (C-14), 24.5 (C-13 and C-15). **IR** (ν_m.cm^{-1}) =3279 (N-H), 1622 (C=C), 1398 (C-F), 866 (C-Cl), 634 (C-Br).

3.4 Synthesis of position-2 unsubstituted imidazo[1,2-*a*]pyridine analogues

General procedure

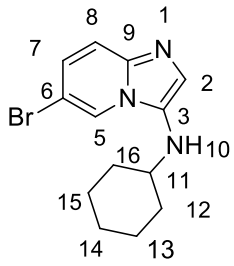
In a 100 ml round bottom flask, an appropriate amount of 2-aminopyridine and glyoxylic acid monohydrate (1.5 eq) were dissolved in methanol (15 ml). Once fully dissolved, perchloric acid 70% (10 mol %) was added and the solution was stirred at room temperature for 45 minutes. Thereafter, cyclohexyl isocyanide (1.1 eq) was slowly added and the reaction was allowed to run at room temperature until completion, usually 12-24 hours. After reaction was completed, any residue formed was filtered using a filter paper. The solvent was removed *in vacuo* and the residue was taken up in 50% ethyl acetate/hexane and purified by silica gel chromatography. Fractions containing the product were pooled together and the solvent was removed under reduced pressure. The product was recrystallized in hot 50% ethyl acetate/hexane to afford the desired product.

3.4.1 5-Bromo-*N*-cyclohexylimidazo[1,2-*a*]pyridin-3-amine 50



2-Amino-6-bromopyridine **(24b)** (2.00 g, 11.6 mmol), glyoxylic acid monohydrate **(36)** (1.32 g, 17.3 mmol), perchloric acid 70% (100 µl, 1.16 mmol) and cyclohexyl isocyanide **(25)** (1.58 ml, 12,7 mmol) were reacted in methanol (15 ml) for 24 hours. Compound **50** was obtained as tan crystals (1.96 g, 57%). **M.p.=** 109-111 °C. **R_f** =0.35 (50% Hex/EtOAC). **^{1}H NMR** (400 MHz, $CDCl_3$): δ_H = 7.45 (dd, 1H, *J* = 8.6, 1.5 Hz, H-6), 7.15 (s, 1H, H-2), 6.89-6.80 (m, 2H, H-8 & H-7), 3.80 (s, 1H, N-H), 3.12-2.93 (m, 1H, H-11), 2.03-1.91 (m, 2H, H-12a & H-16a), 1.82-1.67 (m, 2H, H-13a & H-15a), 1.67-1.54 (m, 1H, H-14a), 1.34-1.22(m, 5H, H-12b, H-13b, H-14b, H-15b & H-16b); **^{13}C NMR** (101 MHz, $CDCl_3$): δ_C =143.9 (C-9), 132.4 (C-5), 124.7 (C-2), 122.5 (C-8), 118.0 (C-7), 117.7 (C-6), 111.3 (C-3), 56.6 (C-11), 33.0 (C-12 & C-16), 26.0 (C-14), 24.6 (C-13 & C-15. **IR** (ν_m.cm^{-1}) = 3354 (N-H), 1620 (C=C), 676 (C-Br). **HRMS** (ES^+) calculated for $C_{13}H_{17}N_3Br$ $[M+H]^+$: 294.0601, found: 294.0593.

3.4.2 6-Bromo-*N*-cyclohexylimidazo[1,2-*a*]pyridin-3-amine 50a

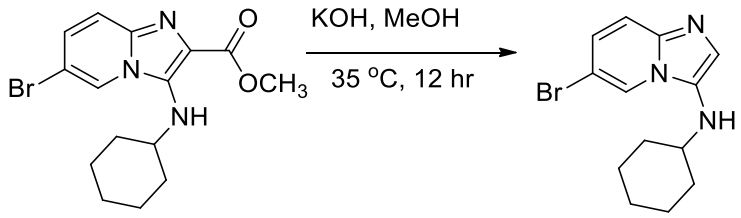


2-amino-5-bromopyridine **(24c)** (2.00 g, 11.6 mmol), glyoxylic acid monohydrate **(36)** (1.32 g, 17.3 mmol), perchloric acid 70% (100 µl, 1.16 mmol) and cyclohexyl isocyanide **(25)** (1.58 ml, 12,7 mmol) were stirred for 24 hours in methanol (15 ml) to afford **50a** as golden-brown crystal (1.7 g, 51%). **M.p.=** 154-155 °C. **R_f** =0.35 (50% Hex/EtOAC). **^{1}H NMR** (400 MHz, $CDCl_3$): δ_H = 8.15 (d, 1H, *J* = 4 Hz, H-5), 7.40 (d, 1H, *J* = 9.4 Hz, H-8), 7.21 (s, 1H, H-2), 7.13 (dd, 1H, *J* = 9.5, 2.0 Hz, H-7), 3.06-2.95 (m, 1H, N-H), 2.94-2.84 (m, 1H, H-11),

2.04-1.93 (m, 2H, H-12a & H-16a), 1.82-1.78 (m, 1H, H-13a), 1.69-1.58 (m, 1H, h-15a), 1.37-1.14 (m, 6H, H-12b, H-13b, H-14a, H-14b, H15b & H-16b); **^{13}C NMR** (101 MHz, $CDCl_3$): δ_C = 140.3 (C-9), 129.7 (C-3), 126.2 (C-7), 124.5 (C-2), 122.4 (C-5), 118.4 (C-8), 106.6 (C-6), 56.3 (C-11), 33.8 (C-12 & C-16), 25.8 (C-14), 24.8 (C13 & C-15). **IR** (ν_m.cm^{-1}) = 3208 (N-H), 1630 (C=C). 588 (C-Br). **HRMS** (ES^+) calculated for $C_{13}H_{17}N_3Br$ $[M+H]^+$: 294.0601, found: 294.0592.

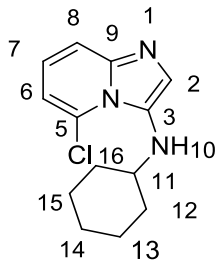
Alternative method:

3.4.2.1 6-Bromo-*N*-cyclohexylimidazo[1,2-*a*] pyridin-3-amine 50a



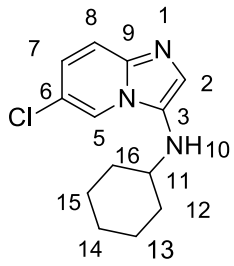
Methyl 6-bromo-3-(cyclohexylamino)imidazo[1,2-*a*]pyridine-2-carboxylate (**51a**) (100 mg, 0.284 mmol) was dissolved in MeOH (2 ml) and 1.4-Dioxane (1 ml) at 35 °C with stirring. KOH (32 mg, 0.568 mmol) was added, and the mixture was allowed to stir. After 2 hours, the mixture was quenched with water (4 ml) and ran for another 10 hours. After the reaction was completed, the solvent was removed *in vacuo* and the mixture was acidified with 4M HCL until the pH was about 1-2. The mixture was extracted with EtOAC, dried over anhydrous $MgSO_4$ and the residue was purified in flash column chromatography using 100 % EtOAC as eluent to afford the product. Compound **50a** was obtained as golden-brown crystal (83 mg 83 %).

3.4.3 5-Chloro-*N*-Cyclohexyl imidazo[1,2-*a*]pyridin-3-amine 50b



2-Amino-6-chloromopyridine **(24d)** (2.00 g, 15.6 mmol), glyoxylic acid monohydrate **(36)** (1.78 g, 23.3 mmol), perchloric acid 70% (134 µl, 1.56 mmol) and cyclohexyl isocyanide **(25)** (2.1 ml, 17.1 mmol) were stirred at room temperature for 24 hours. Compound **50b** was obtained as golden yellow viscous oil (1.2 g, 31%). $\mathbf{R_f}$ =0.32 (60% Hex/EtOAC). **^{1}H NMR** (400 MHz, $CDCl_3$): δ_H = 7.40 (d, 1H, *J* = 9.0 Hz, H-6), 7.10 (s, 1H, H-2), 6.90 (dd, 1H, *J* = 9.0, 7.2 Hz, H-7), 6.66 (d, 1H, *J* = 7.1 Hz, H-8), 3.83 (s, 1H, N-H), 3.09-2.99 (m, 1H, H-11), 2.02-1.94 (m, 2H, H-12a & H-16a), 1.82-1.73 (m, 2H, H-13a & H-15a), 1.67-1.59 (m, 1H, H-14a), 1.32-1.22 (m, 5H, H-12b, H-13b, H-14b, H-15b & H-16b); **^{13}C NMR** (101 MHz, $CDCl_3$): δ_C = 143.8 (C-5), 132.4 (C-9), 125.1 (C-3), 123.7 (C-2), 122.1 (C-7), 117.2 (C-6), 113.4 (C-8), 56.7 (C-11), 33.1 (C-12 & C-16), 25.9 (C-14), 24.6 (C-13 & C-15). **IR** (ν_m.cm^{-1}) = 2960 (N-H), 1626 (C=C), 770 (C-Cl). **HRMS** (ES^+) calculated for $C_{13}H_{17}N_3Cl$ $[M+H]^+$: 250.1106, found: 250.1119.

3.4.4 6-Chloro-*N*-cyclohexylimidazo[1,2-*a*]pyridin-3-amine 50c

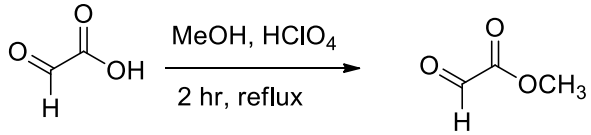


2-Amino-5-chloromopyridine **(24e)** (2.00 g, 15.6 mmol), glyoxylic acid monohydrate **(36)** (1.78 g, 23.3 mmol), perchloric acid 70% (134 µl, 1.56 mmol) and cyclohexyl isocyanide **(25)** (2.1 ml, 17.1 mmol) were reacted in methanol (15 ml) at room temperature to afford the product. The yellow crystals were further recrystallized is hot 50% ethyl acetate/hexane to

afford **50c** as light-yellow crystals (1.5 g, 37%). **M.p.=** 150 °C. $\mathbf{R_f}$ =0.34 (50% Hex/EtOAC). **^{1}H NMR** (400 MHz, $CDCl_3$): δ_H = 8.09 (d, 1H, H-5), 7.47 (d, 1H, *J* = 9.5 Hz, H-8), 7.22 (s, 1H, H-2), 7.06 (dd, 1H, *J* = 9.5, 2.0 Hz, H-7), 3.09 (s, 1H, N-H), 3.03-2.94 (m, 1H, H-11), 2.01-1.92 (m, 2H, H-12a & H-16a), 1.82-1.71 (m, 2H, H-13a & H-14a), 1.68-1.58 (m, 1H, H-14a), 1.31-1.21 (m, 5H, H-12b, H-13b, H-14b, H-15b, H-16b); **^{13}C NMR** (101 MHz, $CDCl_3$): δ_C = 139.9 (C-9), 130.1 (C-3), 124.6 (C-7), 123.6 (C-2), 120.3 (C-6), 120.3 (C-5), 117.8 (C-8), 56.2 (C-11), 33.8 (C-12 & C-16), 25.8 (C-14), 24.8 (C-13 & C-15). **IR** (ν_m.cm^{-1}) = 3312 (N-H), 1551 (C=C), 848 (C-Cl). **HRMS** (ES^+) calculated for $C_{13}H_{17}N_3Cl$ $[M+H]^+$: 250.1106, found: 250.1120.

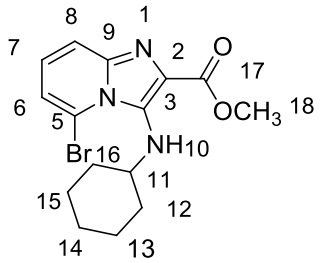
3.5 Synthesis of imidazo[1,2-*a*]pyridin-2-carboxylate derivatives

General procedure for the reaction



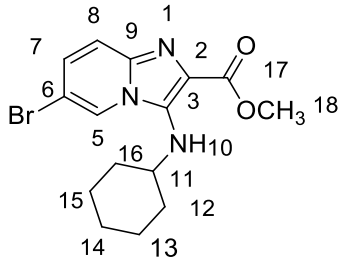
Glyoxylic acid monohydrate (1.5 eq) was reacted with excess methanol under reflux for 2 hours, in the presence of perchloric acid 70% (20 mol %). The reaction was allowed to cool to room temperature and thereafter an appropriate aminopyridine (1.104 mmol) was added to the mixture and the reaction was left stirring at room temperature for 45 minutes under oven dried molecular sieves. The isocyanide component (1.1 eq) was then introduced slowly over a period of 10-15 minutes and the reaction was stirred at ambient temperature until completion, usually 20-24 hours. The solvent was removed under reduced pressure and the concentrate was purified by column chromatography using an appropriate solvent system.

3.5.1 Methyl 5-bromo-3-(cyclohexylamino)imidazo[1,2-*a*]pyridine-2-carboxylate 51



Glyoxylic acid monohydrate **(36)** (660 mg, 8.68 mmol), perchloric acid (1.16 mmol, 100 µl), 2-Amino-6-bromopyridine **(24b)** (1.00 g, 5.78 mmol) and cyclohexyl isocyanide **(25)** (6.54 mmol, 790 µl) were reacted in methanol (12 ml) for 24 hours. Compound **51** was obtained as a dark yellow powder (1.12 g, 55 %). **M.p.=** 133-135 °C. $\mathbf{R_f}$ =0.34 (60% Hex/EtOAC). **^{1}H NMR** (400 MHz, $CDCl_3$): δ_H = 7.51 (d, 1H, *J* = 8.7 Hz, H-8), 7.03-6.92 (m, 2H, H-6 & H-7), 4.84 (d, 1H, *J* = 10.7 Hz, N-H), 3.98 (s, 1H, H-18), 3.17 (d, 1H, *J* = 10.3 Hz, H-11), 1.98 (d, 2H, *J* = 10.3, H-12a & H-16a), 1.75 (s, 2H, H-13a & H15a), 1.32-1.12 (m, 6H, H-12b, H-13b, H-14a, H-14b H15b, H16b; **^{13}C NMR** (101 MHz, $CDCl_3$): δ_C = 165.1 (C-17), 142.6 (C-3), 138.9 (C-9), 125.3 (C-7), 124.6 (C-5), 119.8 (C-6), 118.7 (C-8), 112.6 (C-2), 60.5 (C-11), 51.9 (C-18), 32.9 (C-12 & C-16), 25.7 (C-14), 25.5 (C-13 & C-15).). **IR** (ν_m.cm^{-1}) = 2980 (N-H), 1692 (C=O), 619 (C-Br). **HRMS** (ES^+) calculated for $C_{15}H_{19}N_3BrO_2$ $[M+H]^+$: 352.0656, found: 352.0648.

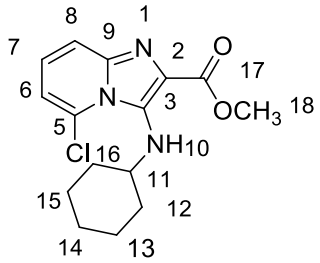
3.5.2 Methyl 6-bromo-3-(cyclohexylamino)imidazo[1,2-*a*]pyridine-2-carboxylate 51a



Glyoxylic acid monohydrate **(36)** (660 mg, 8.68 mmol), perchloric acid (1.16 mmol, 100 µl), 2-Amino-5-bromopyridine **(24c)** (1.00 g, 5.78 mmol) and cyclohexyl isocyanide **(25)** (6.54 mmol, 790 µl) were reacted in methanol (12 ml) for 24 hours to afford **51a** as a dark yellow

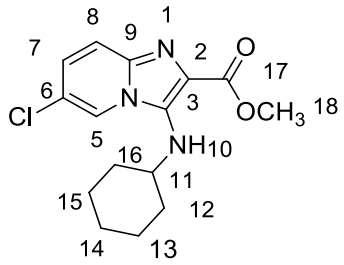
powder (1.18 g, 58 %). **M.p.=** 178-180 °C. **R_f** =0.35 (60% Hex/EtOAC). **^{1}H NMR** (400 MHz, $CDCl_3$): δ_H = 8.04 (s, 1H, H-5), 7.41 (d, 1H, *J* = 9.6 Hz, H-8), 7.18 (dd, 1H, *J* = 9.7, 1.8 Hz, H7), 4.91 (d, 1H, N-H), 3.97 (s, 3H, H-18), 3.17-3.05 (m, 1H, H-11), 1.97-1.88 (m, 2H, H-12a & H-16a), 1.85-1.71 (m, 2H, H-13a & H-15a), 1.65-1.56 (m, 1H, H-14a), 1.40-1.18 (m, 5H, H-12b, H-13b, H-14b, H-15b, H-16b); **^{13}C NMR** (101 MHz, $CDCl_3$): δ_C = 165.0 (C-17), 138.7 (C-3), 136.9 (C-9), 128.5 (C-7), 123.1 (C-5), 122.9 (C-2), 119.9 (C-8), 107.8 (C-6), 55.7 (C-11), 51.8 (C-18), 34.1 (C-12 & C-16), 25.5 (C-14), 24.8 (C-13 & C-15). **IR** (ν_m.cm^{-1}) =3305 (N-H), 1713 (C=O), 666 (C-Br). **HRMS** (ES^+) calculated for $C_{15}H_{19}N_3BrO_2$ $[M+H]^+$: 352.0656, found: 352.0636.

3.5.3 Methyl 5-chloro-3-(cyclohexylamino)imidazo[1,2-*a*]pyridine-2-carboxylate 51b



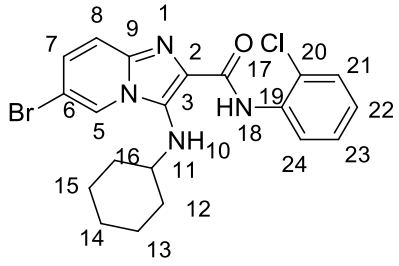
Glyoxylic acid monohydrate **(36)** (594 mg, 7.82 mmol), perchloric acid (1.04 mmol, 90µl), 2-Amino-6-chloropyridine **(24d)** (670 mg, 5.21 mmol) and cyclohexyl isocyanide **(25)** (713 µl, 5.73 mmol) were reacted in methanol (12 ml) to afford compound **51b** as a light-yellow powder (831 mg, 51%). **M.p.=** 127 °C. **R_f** =0.30 (60% Hex/EtOAC). **^{1}H NMR** (400 MHz, $CDCl_3$): δ_H = 7.46 (dd, 1H, *J* = 9.1, 1.1 Hz, H-8), 7.03 (q, 1H, *J* = 9.1, 7.1 Hz, H-7), 6.77 (dd, 1H, *J* = 7.1, 1.1 Hz, H-6), 4.90 (d, 1H, *J* = 10.8 Hz, N-H), 3.98 (s, 3H, H-18), 3.22-3.10 (m, 1H, H-11), 1.97 (d, 2H, H-12a & H-16a), 1.80-1.73 (m, 2H, H-13a & H-15a), 1.62 (s, 1H, H-14a), 1.32-1.12 (m, 5H, H-12b, H-13b, H-14b, H-15b, H-16b); **^{13}C NMR** (101 MHz, $CDCl_3$): δ_C = 165.1 (C-17), 142.5 (C-5), 138.8 (C-3), 126.5 (C-9), 125.0 (C-7), 124.0 (C-2), 118.2 (C-8), 115.0 (C-6), 60.6 (C-11), 51.9 (C-18), 33.1 (C-12 & C-16), 25.7 (C-14), 25.4 (C-15 & C-13). **IR** (ν_m.cm^{-1}) = 3305 (N-H), 1691 (C=O), 788 (C-Cl). **HRMS** (ES^+) calculated for $C_{15}H_{19}N_3ClO_2$ $[M+H]^+$: 308.1161, found: 308.1174.

3.5.4 Methyl 6-chloro-3-(cyclohexylamino)imidazo[1,2-*a*]pyridine-2-carboxylate 51c



Glyoxylic acid monohydrate **(36)** (890 mg, 11.67 mmol), perchloric acid (1.16 mmol, 100µl), 2-Amino-5-chloropyridine **(24e)** (1.00 g, 7.78 mmol) and cyclohexyl isocyanide **(25)** (1.06 ml, 8.56 mmol) were reacted in methanol (12 ml) to afford compound **51c** as a light-yellow powder (983 mg, 61%). %). **M.p.=** 177-179 °C. $\mathbf{R_f}$ =0.30 (60% Hex/EtOAC). **^{1}H NMR** (400 MHz, $CDCl_3$): δ_H = 7.94 (s, 1H, H-5), 7.47 (d, 1H, *J* = 9.7 Hz, H-8), 7.09 (dd, 1H, *J* = 9.7, 1.9 Hz, H-7), 4.91 (d, 1H, *J* = 12 Hz, N-H), 3.97 (s, 3H, H-18), 3.18-2.95 (m, 1H, H-11), 1.98-1.85 (m, 2H, H-12a & H-16a), 1.82-1.70 (m, 2H, H-13a & H-15a), 1.66-1.53 (m, 1H, H-14a), 1.38-1.19 (m, 5H, H-12b, H-13b, H-14b, H-15b & H-16b); **^{13}C NMR** (101 MHz, $CDCl_3$): δ_C = 165.1 (C-17), 138.7 (C-3), 137.1 (C-9), 126.6 (C-7), 123.1 (C-6), 121.2 (C-2), 121.0 (C-5), 119.8 (C-8), 55.7 (C-11), 51.8 (C-18), 34.1 (C-12 & C-16), 25.5 (C-14), 24.8 (C-13 & C-15). **IR** (ν_m.cm^{-1}) = 3312 (N-H), 1714 (C=O), 705 (C-Cl). **HRMS** (ES$^+$) calculated for $C_{15}H_{19}N_3ClO_2$ $[M+H]^+$: 308.1161, found: 308.1176.

3.6 6-Bromo-*N*-(2-chlorophenyl)-3-(cyclohexylamino)imidazo[1,2-*a*]pyridine-2-carboxamide 53



Methyl 6-bromo-3-(cyclohexylamino)imidazo[1,2-*a*]pyridine-2-carboxylate **(51a)** (500 mg, 1.42 mmol) and anhydrous $AlCl_3$ (28 mg, 0.213 mmol) were placed in a two-neck flask fitted with a rubber septum on one end. Acetonitrile (15 ml) was added, and the mixture was stirred for 5 minutes at room temperature. In a separate flask, 2-chloroaniline (724 mg, 568 mmol)

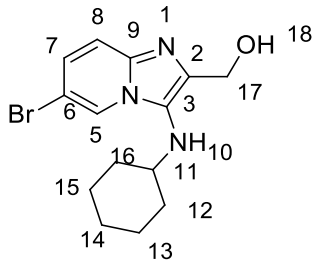
was stirred in NaH (170 mg, 142 mmol) for 5 minutes. The mixture was then transferred into the two-neck flask and the flask completely evacuated and back-filled with nitrogen. The mixture was heated to 110 °C and allowed to run until completion. After reaction was completed, the mixture was filtered through celite, the solvent removed *in vacuo* and the residue was taken up in EtOAC and purified by flash column chromatography using 80% hex/EtOAC as eluent. Compound **53** was obtained as a dark yellow powder (51 mg, 8 %). **M.p.=** 158 °C. $\mathbf{R_f}$ =0.55 (80% Hex/EtOAC). **^{1}H NMR** (400 MHz, $CDCl_3$): δ_H = 9.67 (s, 1H, H-18), 8.53 (d, 1H, *J* = 8.1 Hz, H-24), 8.07 (s, 1H, H-5), 7.41 (d, 2H, *J* = 9.7 Hz, H-21 & H-8), 7.30 (t, 1H, *J* = 7.7 Hz, H-23), 7.21 (dd, 1H, *J* = 9.6, 1.5 Hz, H-7), 7.05 (t, 1H, *J* = 7.7 Hz, H-22), 5.17 (d, 1H, *J* = 10.0 Hz, H-10), 3.22-3.02 (m, 1H, H-11), 1.94 (d, 2H, *J* = 12.6 Hz, H-12a & H-16a), 1.85-1.74 (m, 2H, H-13a & H-15a), 1.67-1.60 (m, 1H, H-14a), 1.44-1.29 (m, 5H, H-16b, H-15b, H-14b, H-13b & H-12b); **^{13}C NMR** (101 MHz, $CDCl_3$): δ_C = 162.4 (C-17), 134.9 (C-3), 134.8 (C-9), 129.2 (C-21), 128.4 (C-7), 128.3 (C-19), 127.6 (C-23), 125.4 (C-20), 124.3 (C-22), 123.4 (C-5), 123.3 (C-2), 121.2 (C-24), 119.4 (C-8), 107.5 (C-6), 55.7 (C-11), 34.1 (C-12 & C-16), 25.5 (C-14), 24.9 (C-13 & C-15). **IR** (ν_m.cm^{-1}) = 3305 (N-H), 1669 (C=O), 1566 (C=C), 569 (C-Br). **HRMS** (ES^+): calculated for $C_{20}H_{21}N_4BrClO$ $[M+H]^+$: 449.0489, found: 449.0527.

3.7 Synthesis of 3-(cyclohexylamino)imidazo[1,2-*a*]pyridin-2-yl-methanol analogues

General procedure

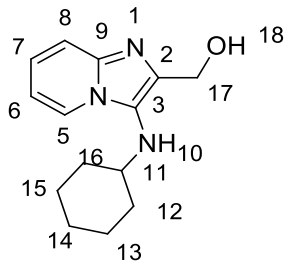
An appropriate amount of the ester was dissolved in dry tetrahydrofuran in an oven dried two-neck flask fitted with a rubber septum. The flask was submerged in an ice bath and allowed to cool to 0 °C. $LiAlH_4$ (1.5 eq) was added portion-wise with stirring. The flask was completely evacuated and backfilled with nitrogen. The reaction was allowed to run at room temperature until completion (8-24 hours). Thereafter, the mixture was quenched with water until there was no visible fizzing. The mixture was allowed to settle for 30 minutes, and the precipitate formed was filtered through a cotton wool plug and the filtrate was extracted with dichloromethane (30 ml x 3). The organic layer was dried over anhydrous $MgSO_4$, and the solvent removed *in vacuo*. The resulting brown solid was recrystallized by boiling in ethyl acetate to give a pure product. More product was obtained by purifying the mother liquor using silica gel column chromatography and chloroform/ethyl acetate/methanol (75:25:5) as eluting solvent.

3.7.1 (6-Bromo-3-(cyclohexylamino)imidazo[1,2-*a*] pyridin-2-yl)methanol 54a



Methyl 6-bromo-3-(cyclohexylamino)imidazo[1,2-*a*]pyridine-2-carboxylate (**51a**) (700 mg, 1.99 mmol) and LAH (113 mg, 2.98 mmol) were reacted in THF (10 ml) for 12 hours. Compound **54a** was obtained as a light brown powder (637.8 mg, 99%). **M.p.=** 143-144 °C. **R_f** =0.46 (75:25:5 $CHCl_3$/EtOAc/MeOH). **^{1}H NMR** (400 MHz, $CDCl_3$): δ_H = 8.16 (dd, 1H, *J* = 1.9, 0.8 Hz, H-5), 7.36 (dd, 1H, *J* = 9.5, 0.9 Hz, H-8), 7.18 (dd, 1H, *J* = 9.4, 1.9 Hz, H-7), 4.81 (s, 2H, H-17), 3.49 (s, 1H, OH), 3.05 (d, 1H, *J* = 6.2 Hz, N-H), 2.87 (s, 1H, H-11), 1.96-1.86 (m, 2H, H-12a & H-16a), 1.78-1.72 (m, 2H, H-13a & H-15a), 1.63 (d, 1H, *J* = 10.7 Hz, H-14a), 1.28-1.21 (m, 5H, H-12b, H-13b, H-14b, H-15b, H-16b); **^{13}C NMR** (101 MHz, $CDCl_3$): δ_C = 139.9 (C-9), 138.5 (C-3), 127.2 (C-7), 125.7 (C-2), 123.0 (C-5), 118.0 (C-8), 106.7 (C-6), 57.8 (C-17), 57.2 (C-11), 34.2 (C-12 & C-16), 25.7 (C-14), 24.9 (C-13 & C-15). **IR** (ν_m.cm^{-1}) = 3305 (N-H), 1566 (C=C), 1408 (OH), 1032 (C-O), 530 (C-BR). **HRMS** (ES^+): calculated for $C_{14}H_{19}N_3OBr$ $[M+H]^+$: 324.0706, found: 324.0694

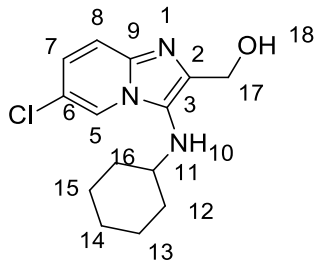
3.7.2 (3-(Cyclohexylamino)imidazo[1,2-*a*] pyridin-2-yl)methanol 54e



Methyl 5-bromo-3-(cyclohexylamino)imidazo[1,2-*a*]pyridine-2-carboxylate **(51)** (700 mg, 1.99 mmol) and LAH (113 mg, 2.98 mmol) were reacted in THF (10 ml) for 12 hours. Compound **54e** was obtained as a brown powder (467.6 mg, 74%). **M.p.=** 142-144 °C. **R_f** =0.36 (75:25:5 $CHCl_3$/EtOAc/MeOH). **^{1}H NMR** (400 MHz, $CDCl_3$): δ_H = 8.03 (dt, 1H, *J* =

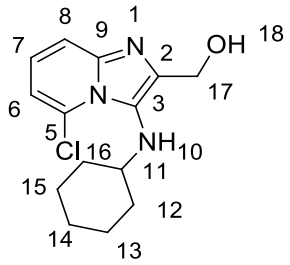
6.8, 1.2 Hz, H-5), 7.47 (dt, 1H, *J* = 9.1, 1.2 Hz, H-8), 7.10 (ddd, 1H, *J* = 9.0, 6.7, 1.3 Hz, H-7), 6.76 (td, 1H, *J* = 6.8, 1.2 Hz, H-6), 5.86 (s, 1H, N-H), 4.83 (s, 2H, H-17), 3.14 (d, 1H, *J* = 6.3 Hz, OH), 2.92-2.80 (m, 1H, H-11), 1.95-1.84 (m, 2H, H-12a & H-16a), 1.77-1.69 (m, 2H, H-13a & H-15a), 1.64-1.56 (m, 1H, H-14a), 1.31-1.12 (m, 5H, H-12b, H-13b, H-14b, H-15b & H-16b).). **^{13}C NMR** (101 MHz, $CDCl_3$): δ_C =141.5 (C-9), 137.9 (C-3), 125.5 (C-2), 123.8 (C-5), 122.8 (C-7), 117.1 (C-8), 111.6 (C-6), 57.2 (C-11), 57.1 (C-17), 34.2 (C-12 & C-16), 25.7 (C-14), 24.9 (C-13 & C-15). **IR** (ν_m.cm^{-1}) = 3247 (N-H), 1345 (OH), 1634 (C=C), 1054 (C-O). **HRMS** (ES^+) calculated for $C_{14}H_{20}N_3O$ $[M+H]^+$: 246.1601, found: 246.1604.

3.7.3 (6-Chloro-3-(cyclohexylamino)imidazo[1,2-*a*] pyridin-2-yl)methanol 54c



Methyl 6-chloro-3-(cyclohexylamino)imidazo[1,2-*a*]pyridine-2-carboxylate (**51c**) (511 mg, 1.66 mmol) and LAH (100 mg, 2.64 mmol) were reacted in THF (10 ml) for 8 hours. Compound **54c** was obtained as a brown powder (405.9 mg, 95 %). **M.p.=** 195-197 °C. **R_f** =0.32 (75:25:5 $CHCl_3$/EtOAc/MeOH). **^{1}H NMR** (400 MHz, $CDCl_3$): δ_H = 8.06 (dd, 1H, *J* = 2.1, 0.9 Hz, H-5), 7.41 (dd, 1H, *J* = 9.4, 0.9 Hz, H-8), 7.08 (dd, 1H, *J* = 9.5, 2.0 Hz, H-7), 4.81 (s, 2H, H-17), 3.97 (s, 1H, N-H), 3.07 (d, 1H, *J* = 6.4 Hz, OH), 2.87 (s, 1H, H-11), 1.93-1.85 (m, 2H, H-12a & H-16a), 1.82-1.75 (m, 2H, H-13a & H-16a), 1.63 (d, 1H, *J* = 10.5 Hz, H-14a), 1.29-1.17 (m, 5H, H-12b, H-13b, H-14b, H-15b & H-16b); **^{13}C NMR** (101 MHz, $CDCl_3$): δ_C = 139.8 (C-9), 138.8 (C-3), 125.9 (C-2), 125.2 (C-7), 120.7 (C-5), 120.2 (C-6), 117.7 (C-8), 57.7 (C-17), 57.2 (C-11), 34.2 (C-12 & C-16), 25.7 (C-14), 24.9 (C-13 & C-15).). **IR** (ν_m.cm^{-1}) = 1567 (C=C), 1321 (OH), 1055 (C-O), 804 (C-Cl). **HRMS** (ES^+) calculated for $C_{14}H_{19}N_3OBCl$ $[M+H]^+$: 280.1212, found: 280.1226.

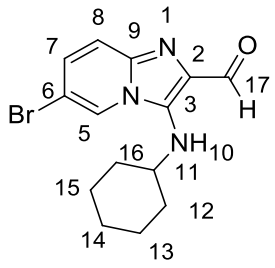
3.7.4 (5-Chloro-3-(cyclohexylamino)imidazo[1,2-*a*] pyridin-2-yl)methanol 54d



Methyl 5-chloro-3-(cyclohexylamino)imidazo[1,2-*a*]pyridine-2-carboxylate (**51b**) (511 mg, 1.66 mmol) and LAH (99.7 mg, 2.64 mmol) were reacted in THF (10 ml) for 8 hours. Compound **54d** was obtained as a brown powder (427.3 mg, 92 %). **M.p.=** 143-144 ℃. $\mathbf{R_f}$ =0.32 (75:25:5 $CHCl_3$/EtOAc/MeOH). **^{1}H NMR** (400 MHz, $CDCl_3$): δ_H = 7.45 (dd, 1H, *J* = 8.9 Hz, H-8), 7.05 (dd, 1H, *J* = 8.9, 7.2 Hz, H-7), 6.75 (dd, 2H, *J* = 7.4, 0.8 Hz, H-6), 4.86 (s, 2H, H-17), 4.27 (s, 1H, N-H), 3.35 (d, 1H, OH), 3.02-2.91 (m,1H, H-11), 1.92-1.79 (M, 3H, H-12 a, H-16a & H-14a), 1.79-1.72 (m, 2H, H-13a & H-15a), 1.30-1.17 (m, 5H, H-12b, H-13b, H-14b, H-15b & H-16b); **^{13}C NMR** (101 MHz, $CDCl_3$): δ_C = 144.3 (C-5), 141.5 (C-9), 125.8 (C-2), 125.7 (C-3), 124.1 (C-7), 116.6 (C-8), 113.8 (C-6), 59.8 (C-17), 58.5 (C-11), 33.0 (C-12 & C-16), 25.8 (C-14), 24.8 (C-13 & C-15). **IR** (ν_m.cm^{-1}) = 1567 (C=C), 1321 (OH), 1055 (C-O), 804 (C-Cl). **HRMS** (ES^+) calculated for $C_{14}H_{19}N_3OBCl$ $[M+H]^+$: 280.1212, found: 280.1197

3.8. Preparation of 3-cyclohexylaminoimidazo[1,2-*a*]pyridine-2-carbaldehyde

3.8.1 6-Bromo-3-(cyclohexylamino)imidazo[1,2-*a*]pyridine-2-carbaldehyde 56b



(6-Bromo-3-(cyclohexylamino)imidazo[1,2-*a*]pyridin-2-yl)methanol (**54a**) (322.6 mg, 0.994 mmol), TsCl (379.4 mg, 1.99 mmol), DMAP (157.9 mg, 1.29 mmol) and DCM (15 ml) were

heated at 50 °C for 24 hours under nitrogen. After reaction was completed, the mixture was purified by flash column chromatography using hexane/ ethyl acetate (70: 30) as eluting solvent to afford **56b** as a dark yellow powder (38 mg, 5%). **M.p.=** 161-163 °C. $\mathbf{R_f}$ =0.52 (70% Hex/EtOAc). **^{1}H NMR** (400 MHz, $CDCl_3$): δ_H = 10.09 (s, 1H, H-17), 8.02 (s, 1H, H-5), 7.38 (d, 1H, *J* = 9.7 Hz, H-8), 7.16 (dd, 1H, *J* = 9.7, 1.7 Hz, H-7), 5.47 (d, 1H, N-H), 3.33-3.25 (m, 1H, H-11), 1.96-1.89 (m, 2H, H-12a & H-16a), 1.80-1.73 (m, 2H, H-13a & H-15a), 1.45-1.17 (m, 6H, H-12b, H-13b, H-14a, H-14b, H-15b & H-16b); **^{13}C NMR** (101 MHz, $CDCl_3$): δ_C = 189.1 (C-17), 139.3 (C-3), 136.5 (C-9), 129.7 (C-2), 128.6 (C-7), 123.6 (C-5), 120.3 (C-8), 108.1 (C-6), 55.1 (C-11), 34.1 (C-12 & C-16), 25.4 (C-14), 24.6 (C-13 & C-15). **IR** (ν_m.cm^{-1}) = 3290 (N-H), 1633(C=C), 1734 (C=O), 517 (C-Br). **HRMS** (ES$^+$) calculated for $C_{14}H_{17}BrN_3O$ $[M+H]^+$: 322.0550, found: 322.0565.

Alternative method:

3.8.1.1 Synthesis of the aldehyde from alkyl bromide imidazopyridines

6-Bromo-2(bromomethyl)-*N*-cyclohexylimidazo[1,2-*a*]pyridin-amine (**58**) (277 mg, 0.716 mmol) was dissolved in 50/50 dioxane-chloroform in a two neck flask. To it was added DMSO (67 mg, 0.859 mmol) and the mixture was stirred at room temperature for 30 minutes. Thereafter, $NaHCO_3$ (72 mg, 0.859 mmol) dissolved in 2ml of water, was added to the mixture. The flask was heated to 96 ℃ and the reaction was allowed to run for 20 hours. Thereafter the reaction was cooled and allowed to stir at room temperature for further 4 hours. The solvent was removed *in vacuo* and the residue was taken up in EtOAC. Water (15 ml) was added, and the mixture was separated using a separatory funnel. Fractions containing the organic layer were combined, dried over $MgSO_4$ and concentrated *in vacuo*. The crude was purified by silica gel column chromatography using $CHCl_3$/EtOAC/MeOH 70:25:5 to afford compound **56b** as a yellow solid (129 mg, 56%).

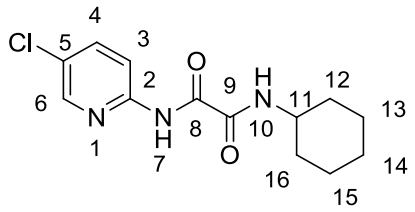
3.9. Oxidative ring-opening of imidazopyridine alcohols

General procedure using PCC

An appropriate amount of the alcohol was dissolved in dry chloroform (12 ml) in an oven dried two neck flask fitted with a rubber septum on one end. To it was added an equivalent amount of flash silica gel, followed by PCC (1.1 eq). The mixture was degassed, flushed with

nitrogen and allowed to run for 4 hours or until a new spot was clearly visible on the TLC. After reaction was completed, the solid was filtered off using a filter paper and rinsed three times with chloroform. The filtrate was then concentrated *in vacuo* and the residue was purified by silica gel column chromatography (70% $CHCl_3$/EtOAc). The colourless fluffy solid material was subsequently recrystallized in hot hexane to afford the pure product.

3.9.1 N^1-(5-Chloropyridin-2-yl)-N^2-cyclohexyloxalamide 57a



(6-Chloro-3-(cyclohexylamino)imidazo[1,2-*a*] pyridin-2-yl)methanol (**54c**) (209 mg, 0.7470 mmol) and PCC (338 mg, 1.57 mmol) were reacted in DCM (10 ml) for 4 hours. Compound **57a** was obtained as a colourless fluffy solid. Upon recrystallization in cyclohexane/ethyl acetate, pure colourless and lustrous crystals were obtained (80 mg, 26%). **M.p.=** 182-184 °C. $\mathbf{R_f}$ =0.59 (70% $CHCl_3$/EtOAc). **^{1}H NMR** (400 MHz, $CDCl_3$): δ_H = 9.79 (s, 1H, H-7), 8.32 (dd, 1H, *J* = 2.5, 0.6 Hz, H-6), 8.19 (dd, 1H, *J* = 8.8, 0.6 Hz, H-3), 7.72 (dd, 1H, *J* = 8.8, 2.6 Hz, H-4), 7.35 (d, 1H, *J* = 8.8 Hz, H-10), 3.88-3.74 (m, 1H, H-11), 2.00-1.91 (m, 2H, H-12a & H-16a), 1.83-1.71 (m, 2H, H-13a & H-15a), 1.70-1.61 (m, 1H, H-14a), 1.43-1.20 (m, 5H, H-12b, H-13b, H-14b, H15b, H16b); **^{13}C NMR** (101 MHz, $CDCl_3$): δ_C = 158.2 (C-8), 157.9 (C-9), 148.2 (C-2), 147.2 (C-6), 138.0 (C-4), 127.9 (C-5), 114.5 (C-3), 49.2 (C-11), 32.6 (C-12 & C-16), 25.3 (C-14), 24.7 (C-13 & C-15). **IR** (ν_m.cm^{-1}) = 3318 (N-H), 1656 (C=O), 743 (C-Cl). **HRMS** (ES^+) calculated for $C_{13}H_{17}N_3O_2Cl$ $[M+H]^+$: 282.1004, found: 282.1002.

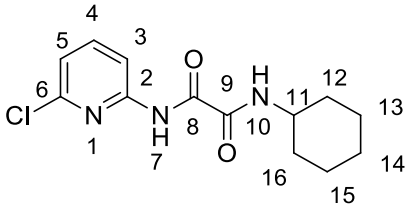
Alternative method:

3.9.1.1 Oxidative ring-opening of imidazopyridine alcohols with IBX

(5-Chloro-3-(cyclohexylamino)imidazo[1,2-*a*] pyridin-2-yl)methanol **(54c)** (1.00g, 3.57 mmol) was dissolved in dry $CHCl_3$ (15 ml) in a two neck flask fitted with a threaded sleeve septum. To it was added glacial acetic acid (0.3 ml, 1.2 eq) and IBX (1.06 g, 1.2 eq), which was dissolved in dry acetonitrile. The mixture was heated at 80 °C and allowed to run overnight. After reaction completion, the solvent was removed *in vacuo* to afford a dark

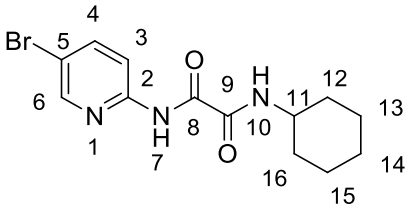
syrup. This was taken up in 70% $CHCl_3$/EtOAc and purified by silica gel column chromatography using 70% $CHCl_3$/EtOAc as eluent. Fractions containing the product were combined and solvent removed *in vacuo* to afford a colourless to yellowish fluffy material (285 mg). This was recrystallized in cyclohexane to afford the product (**57a**) as a clear colourless fluffy solid (260 mg, 26 %).

3.9.2 N^1-(6-Chloropyridin-2-yl)-N^2-cyclohexyloxalamide 57b



(5-Chloro-3-(cyclohexylamino)imidazo[1,2-*a*] pyridin-2-yl)methanol (**54d**) (209 mg, 0.7470 mmol) and PCC (338 mg, 1.57 mmol) were reacted in DCM (10 ml) for 4 hours. Compound **57d** was obtained as a colourless fluffy solid (75.8 mg, 36%). **M.p.=** 157-159 °C. $\mathbf{R_f}$ =0.59 (70% $CHCl_3$/EtOAc). **^{1}H NMR** (400 MHz, $CDCl_3$): δ_H = 9.79 (s, 1H, H-7), 8.14 (d, 1H, *J* = 8.1 Hz, H-3), 7.72 (t, 1H, *J* = 8.0 Hz, H-4), 7.32 (d, 1H, *J* = 8.8 Hz, H-10), 7.15 (d, 1H, *J* =7.7 Hz, H-5), 3.88-3.74 (m, 1H, H-11), 2.00-1.91 (m, 2H, H-12a & H-16a), 1.83-1.71 (m, 2H, H-13a & H-15a), 1.46-1.40 (m, 1H, H-14a), 1.38-1.13 (m, 5H, H-12b, H-13b, H-14b, H-15b & H-16b); **^{13}C NMR** (101 MHz, $CDCl_3$): δ_C = 158.4 (C-8), 157.7 (C-9), 149.8 (C-2), 140.9 (C-4), 120.9 (C-5), 112.0 (C-3), 49.1 (C-11), 32.6 (C-12 & C-16), 25.3 (C-14), 24.7 (C-13 & C-15). **IR** (ν_m.cm^{-1}) = 3261 (N-H), 1665 (C=O), 792 (C-Cl). **HRMS** (ES^+) calculated for $C_{13}H_{17}N_3O_2Cl$ $[M+H]^+$: 282.1004, found: 282.1013.

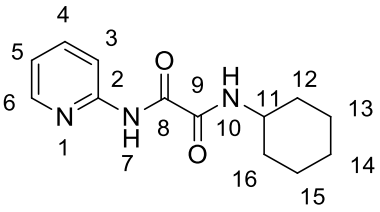
3.9.3 N^1-(5-Bromopyridin-2-yl)-N^2-cyclohexyloxalamide 57c



(6-Bromo-3-(cyclohexylamino)imidazo[1,2-*a*] pyridin-2-yl)methanol (**54a**) (555 mg, 1.58 mmol) and PCC (7.14 mg, 3.31 mmol) were reacted in dry chloroform for 4 hours to afford **57c** as a colourless fluffy solid (186 mg, 36%). **M.p.=** 188-190 °C. $\mathbf{R_f}$ =0.64 (70% $CHCl_3$/EtOAc). **^{1}H NMR** (400 MHz, $CDCl_3$): δ_H = 9.77 (s, 1H, H-7), 8.42 (dd, 1H, H-6), 8.14 (d, 1H, *J* = 8.8 Hz, H-3), 7.86 (dd, 1H, *J* = 8.8, 2.4 Hz, H-4), 7.34 (d, 1H, *J* = 8.7 Hz, H-

10), 3.88-3.73 (m, 1H, H-11), 2.01-1.91 (m, 2H, H-12a & H-16a) 1.83-1.71 (m, 2H, H-13a & H-15a), 1.70-1.61 (m, 1H, H-14a), 1.43-1.19 (m, 5H, H-12b, H-13b, H-14b, H-15b, H-16b); **^{13}C NMR** (101 MHz, $CDCl_3$): δ_C = 158.3 (C-8), 157.9 (C-9), 149.4 (C-6), 148.6 (C-2), 140.8 (C-4), 115.9 (C-5), 115.0 (C-3), 49.2 (C-11), 32.6 (C-12 & C-16), 25.3 (C-14), 24.7 (C-13 & C-15). **IR** (ν_m.cm^{-1}) = 3312 (N-H), 1657 (C=O), 690 (C-Br). **HRMS** (ES^+) calculated for $C_{13}H_{17}N_3O_2Br$ $[M+H]^+$: 326.0499, found: 326.0482.

3.9.4 *N*^{1}-Cyclohexyl-*N*^{2}-(pyridin-2-yl)oxalamide 57d



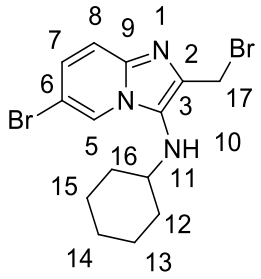
3-(cyclohexylamino)imidazo[1,2-*a*] pyridin-2-yl)methanol (**54b**) (428 mg, 1.74 mmol) and PCC (413 mg, 1.91 mmol) were reacted in chloroform (12 ml) for 5 hours to afford **57d** as a colourless fluffy solid (142 mg, 33%). **M.p.=** 142-144 °C. **R_f** =0.63 (70% $CHCl_3$/EtOAc). **^{1}H NMR** (400 MHz, $CDCl_3$): δ_H = 9.77 (s, 1H, H-7), 8.37 (dd, 1H, *J* = 5.0, 1.8 Hz, H-6), 8.20 (d, 1H, *J* = 8.3 Hz, H-3), 7.76 (td, 1H, *J* = 7.9, 1.9 Hz, H-4), 7.39 (d, 1H, *J* = 8.7 Hz, H-10), 7.12 (qd, 1H, *J* = 7.4, 4.9, 0.9 Hz, H-5), 3.88-3.75 (m, 1H, H11), 2.02-1.91 (m, 2H, H-12a & H-16a), 1.84-1.71 (m, 2H, H-13a & H=15a), 1.48-1.14 (m, 6H, H-12b, H-13b, H-14a, H-14b, H-15b, H-16b); **^{13}C NMR** (101 MHz, $CDCl_3$): δ_C = 158.3 (C-8), 158.2 (C-9), 150.0 (C-2), 148.5 (C-6), 138.4 (C-4), 120.7 (C-5), 113.9 (C-3), 49.1 (C-11), 32.7 (C-12 & C-16), 25.3 (C-14), 24.7 (C-13 & C-15). **IR** (ν_m.cm^{-1}) = 3317 (N-H), 1658 (C=O). **HRMS** (ES^+) calculated for $C_{13}H_{18}N_3O_2$ $[M+H]^+$: 248.1394, found: 248.1425.

Alternative method:

3.9.4.1 Oxidative ring-opening of imidazopyridine alcohols using laccase from T.versicolor

3-(cyclohexylamino)imidazo[1,2-*a*] pyridin-2-yl)methanol **(54b)** (297 mg, 1.21 mmol) was dissolved in THF (7 ml) in a round bottom flask. In a separate flask, Laccase from *T.versicolor* (297 mg, 1 eq), TEMPO (59 mg, 20%) and Tris buffer pH 7.0 were mixed together. The contents of the two flasks were combined and allowed to stir in open air at room temperature. After 10 minutes, water (15 ml) was added, and the mixture was extracted with DCM (15 ml x 3). The organic layer was dried in anhydrous $MgSO_4$, and the solvent was removed *in vacuo*. The residue was taken up in 70% $CHCl_3$/EtOAc and purified by silica gel column chromatography. Fractions containing the product were collected and solvent removed *in vacuo* to afford **57d** as a colourless fluffy solid (80 mg, 27%).

3.10 6-Bromo-2(bromomethyl)-*N*-cyclohexylimidazo[1,2-*a*]pyridin-amine 58



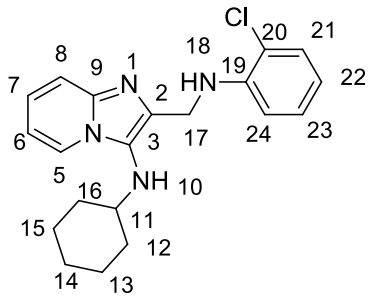
(6-Bromo-3-(cyclohexylamino)imidazo[1,2-*a*] pyridin-2-yl)methanol **(54a)** (232 mg, 0.716 mmol) was dissolved in dry DCM (10 ml) in a two-neck flask fitted with a threaded rubber septum at one end. The flask was evacuated and backfilled with nitrogen. Phosphorus tribromide (113 mg, 0.787 mmol) was introduced dropwise with constant stirring. The reaction was allowed to stir at room temperature for 8 hours. The product was used in the next step without further purification.

3.11 Reductive amination

General procedure

In a 50 ml round bottom flask charged with a magnetic stirrer bar and dried molecular sieves 4Å, was added the aldehyde and MeOH (10 ml). Acetic acid was added to the solution dropwise until the pH was approximately 5. The mixture was subsequently stirred at room temperature for 30 minutes. Thereafter, 2-chloroaniline (1.5 eq) was added and the reaction mixture was stirred further for 45 minutes. Sodium cyanoborohydride (1.5 eq) was introduced and the mixture was allowed to stir for further 12 hours. The thick creamy precipitate together with the molecular sieves were filtered using a filter paper and rinsed several times with MeOH. The filtrate was completely removed *in vacuo* and the residue was taken up in EtOAC. To it was added a saturated solution of $NaHCO_3$ portion-wise until no fizzing was observed. The mixture was extracted with EtOAC (15 ml x 3) and washed with water. The organic layer was dried in $MgSO_4$, concentrated *in vacuo,* and purified by silica gel column chromatography 60% Hex/EtOAC to afford the product.

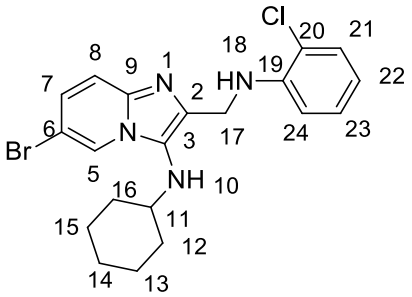
3.11.1 Synthesis of 2-(((2-chlorophenyl)amino)methyl)-*N*-cyclohexylimidazo[1,2-*a*]pyridin-3-amine 59



3-(cyclohexylamino)imidazo[1,2-*a*]pyridine-2-carbaldehyde (129 mg, 0,400 mmol), acetic acid (pH adjusted to 5), 2-chloroaniline (155 mg, 1.22 mmol) and sodium cyanoborohydride (76 mg, 1.21 mmol) were allowed to stir at room temperature for 12 hours to afford compound **59** as a brown oil (71 mg, 36%). $\mathbf{R_f}$ =0.64 (60% EtOAc/Hex). **^{1}H NMR** (400 MHz, $CDCl_3$): δ_H = 8.04 (d, 1H, *J* = 6.9 Hz, H-5), 7.50 (d, 1H, *J* = 9.1 Hz, H-8), 7.25 (s, 1H, H-21), 7.14 (q, 2H, *J* = 7.7 Hz, H-7 & H-23), 6.85-6.74 (m, 2H, H-24 & H-6), 6.65 (t, 1H, *J* = 7.7 Hz, H22), 5.03 (s, 1H, N-H (18)), 4.52 (s, 2H, H-17), 3.06-2.83 (m, 2H, N-H (10) & H-11), 1.90-1.82 (m, 2H, H-12a & H-16a), 1.76-1.70 (m, 2H, H-13a & H-15a), 1.30-1.12 (m, 6H, H-12b, H-13b, H-14a, H-14b, H-15b & H-16b); **^{13}C NMR** (101 MHz, $CDCl_3$): δ_C =144.0 (C-9), 141.6 (C-19), 135.2 (C-3), 129.1 (C-21), 127.8 (C-23), 125.4 (C-2), 123.7 (C-7), 122.6 (C-5), 119.5 (C-20), 117.5 (C-22), 117.3 (C-8), 111.6 (C-6), 111.5 (C-24), 57.2 (C-11), 41.8

(C-17), 34.2 (C-12 & C-16), 24.7 (C-14), 24.9 (C-13 & C-15). **IR** (ν_m.cm^{-1}) = 2929 (N-H), 1598 (C=C), 741 (C-Cl). **HRMS** (ES$^+$) calculated for $C_{20}H_{24}N_4Cl$ [M+H]$^+$: 355.1684, found: 355.1660.

3.11.2 6-Bromo-2-(((2-chlorophenyl)amino)methyl)-*N*-cyclohexylimidazo[1,2-*a*] pyridin-3-amine 59a



6-Bromo-3-(cyclohexylamino)imidazo[1,2-*a*]pyridine-2-carbaldehyde **(56b)** (129 mg, 0,400 mmol) acetic acid (pH adjusted to 5), 2-chloroaniline (77 mg, 0.600 mmol) and sodium cyanoborohydride (34 mg, 0.600 mmol) were allowed to stir at room temperature for 12 hours to afford compound **59a** as a light brown lustrous solid (96 mg, 56%). $\mathbf{R_f}$ =0.64 (60% EtOAc/Hex). **^{1}H NMR** (400 MHz, $CDCl_3$): δ_H = 8.16 (s, 1H, H-5), 7.39 (d, 1H, *J* = 9.4 Hz, H-8), 7.27 (d, 1H, *J* = 6.8 Hz, H-23), 7.20-7.13 (m, 2H, H-7 & H-21), 6.78 (d, 1H, *J* = 8.2 Hz, H-24), 6.66 (t, 1H, *J* = 7.7 Hz, H-22), 4.98 (s, 1H, N-H(18)), 4.50 (s, 2H, H-17), 2.98-2.86 (m, 2H, N-H(10) & H-11), 1.85 (d, 2H, *J* = 4.7 Hz, H-12a & H-16a), 1.73 (s, 2H, H-13a & H-15a), 1.28-1.12 (m, 6H, H-12b, H-13b, H-14a, H-14b, H-15b & H-16b); **^{13}C NMR** (101 MHz, $CDCl_3$): δ_C =143.9 (C-9), 139.9 (C-19), 136.4 (C-3), 129.2 (C-23), 127.8 (C-21), 127.1 (C-7), 125.8 (C-2), 122.8 (C-5), 119.5 (C-20), 118.0 (C-8), 117.7 (C-22), 111.5 (C-4), 106.7 (C-6), 57.3 (C-11), 41.8 (C-17), 34.2 (C-12 & C-16), 25.7 (C-14), 24.8 (C-13 & C-15). **IR** (ν_m.cm^{-1}) = 3305 (N-H), 1599 (C=C), 796 (C-Br). **HRMS** (ES$^+$) calculated for $C_{20}H_{23}{}^{81}BrClN_4$ [M+H]$^+$: 435.0769, found: 435.0748.

Molecular modeling studies

4.1 Docking analysis

Molecular modelling studies were performed using Schrödinger Maestro molecular modeling virtual interfase programme (2019-12.2) under the national academic license by CSIR/CHP. Docking and analysis was conducted using Intel (R) Pentium (R) Gold G5400 CPU @ 3.7GHz and GPU Intel (R) UHD Graphics 610 with GPU RAM of 1.9GB.

4.2 Protein preparation

Protein Data bank (PDB) crystal structure of wild-type RT co-crystallized with an NNRTI ligand (RPV) complex coded WT HIV-1 RT/RPV was obtained from the Brookhaven PDB (www.rcsb.org). Protein preparation wizard incorporated onto the Maestro interphase was employed in preparing the protein structure by removing non-receptor water molecules and other crystallographic artefacts. The prepared protein structure was saved as a project file.

4.3 Ligand preparation

Chemical structures of the 86 ligands were sketched using Maestro's 3D builder and stored as a Maestro file. LigPrep wizard was employed to generate ionization states and tautomers of the ligand using an incorporated tool called Epik. Applyhtreat, the program used by the Hydrogen Treatment panel on maestro was used to add missing hydrogen atoms, consistent with $OPLS_3$ Force field before minimization.

4.4 Docking method validation

To ensure the robustness of the docking model, docking set-up protocols and parameters were validated by performing a redocking study using known decoys. The standard criterion used was the root mean square deviation (RMSD).

4.5 Ligand minimization

The prepared ligands were minimized onto the prepared protein (WT HIV-1 RT) binding site receptor grid and the resultant conformations of the active/probe molecules were generated together with the FEP+ (Free Energy Perturbation) docking results. The ligand poses for these calculations were generated using Glide SP. Of the 86 ligands docked into the binding site, 26 of them were active binders. The 26 active molecules were ranked according to the lowest energy ligand states which corresponded with the most favoured interactions.

4.6 Selection of compounds for synthesis

Compound selection for laboratory synthesis was based on the filter method taking the docking score of the compound and its comparison to the docking score of the previously synthesised hit compound, the docking score of the commercial NNRTI (Rilpivirine) as well the flexibility of the compound and its shape correlation with that of a known NNRTI (Rilpivirine). Using the filter method, 13 compounds were selected for synthesis and four of these compounds (**Table 3**) showed promising docking scores and shape correlation when compared with rilpivirine.

REFERENCES

1. Barré-Sinoussi F, Chermann JC, Rey F, Nugevre MT, Chamaret S, Gruest J, Dauguet C, Axler-Blin C, Vézinet-Brun F, Rouzioux C, *et al*. Isolation of a T-lymphotropic retrovirus from a patient at risk for acquired immune deficiency syndrome (AIDS). *Science*. 1983;**220**:868-871. doi:10.1126/science.6189183
2. Chung-Eun H, Bhagavan NV. *Essentials of Medical Biochemistry With Clinical Cases*. 2nd Edition. Academic Press; 2015.
3. Bailes E, Gao F, Bibollet-Ruche F, Courgnaud V, Peeters M, Marx PA, Hahn BH, Sharp PM. Hybrid origin of SIV in chimpanzees. *Science* . 2003;**300**:1713. doi:10.1126/science.1080657
4. Worobey M, Telfer P, Souquière S, Hunter M, Coleman CA, Metzger MJ, Reed P, Makuwa M, Hearn G, Honarvar S, *et al*. Island biogeography reveals the deep history of SIV. *Science*. 2010;**329**:1487. doi:10.1126/science.1193550
5. Esposito F, Corona A, Tramontano E. HIV-1 Reverse Transcriptase Still Remains a New Drug Target: Structure, Function, Classical Inhibitors, and New Inhibitors with Innovative Mechanisms of Actions. *Mol Biol Int*. 2012;**2012**:1-23. doi:10.1155/2012/586401
6. Gao F, Bailes E, Robertson DL, Chen Y, Rodenburg CM, Michael SF, Cummins LB, Arthur LO, Peeters M, Shaw GM, *et al*. Origin of HIV-1 in the chimpanzee Pan troglodytes troglodytes. *Nature*. 1999;**397**:436-441. doi:10.1038/17130
7. De Witte L, Bobardt M, Chatterji U, Degeest G, David G, Geijtenbeek TBH, Gallay P. Syndecan-3 is a dendritic cell-specific attachment receptor for HIV-1. *Proc Natl Acad Sci U S A*. 2007;**104**:19464-19469. doi:10.1073/pnas.0703747104
8. Sharp PM, Hahn BH. Origins of HIV and the AIDS pandemic. *Cold Spring Harb Perspect Med*. 2011;**1**. doi:10.1101/cshperspect.a006841
9. Esnouf RM, Ren J, Hopkins AL, Ross CK, Jones EY, Stammers DK, Stuart DI. Unique features in the structure of the complex between HIV-1 reverse transcriptase and the bis(heteroaryl)piperazine (BHAP) U-90152 explain resistance mutations for this nonnucleoside inhibitor. *Proc Natl Acad Sci U S A*. 1997;**94**:3984-3989. doi:10.1073/pnas.94.8.3984
10. Esnouf R, Ren J, Ross C, Jones Y, Stammers D, Stuart D. Mechanism of inhibition of HIV-1 reverse transcriptase by non-nucleoside inhibitors. *Nat Struct Biol*. 1995;**2**:303-308. doi:10.1038/nsb0495-303

11. Volberding PA, Sande M, Lange J, Greene W, Gallant J. *Global HIV/AIDS Medicine*. Academic Press; 2008: 846
12. Gallo RC. A reflection on HIV/AIDS research after 25 years. *Retrovirology*. 2006;**3**:1-7. doi:10.1186/1742-4690-3-72
13. Taraphdar P, Guha RT, Haldar D, Chatterjee A, Dasgupta A, Saha B, Mallik S. Socioeconomic consequences of HIV/AIDS in the family system. *Niger Med J*. 2011;**52**:250-253. doi:10.4103/0300-1652.93798
14. Sherr L, Cluver LD, Betancourt TS, Kellerman SE, Richter LM, Desmond C. Evidence of impact: Health, psychological and social effects of adult HIV on children. *Aids*. 2014;**28**:251-259. doi:10.1097/qad.0000000000000327
15. International Labour Office., Delhi Network of Positive People. *Socio-Economic Impact of HIV/AIDS on People Living with HIV/AIDS and Their Families*.; 2003.
16. 11 Top Causes of Global Poverty - World | ReliefWeb. Accessed June 16, 2022. https://reliefweb.int/report/world/11-top-causes-global-poverty
17. Political Declaration on HIV and AIDS: Ending Inequalities and Getting on Track to End AIDS by 2030 | UNAIDS. Accessed June 16, 2022. https://www.unaids.org/en/resources/documents/2021/2021_political-declaration-on-hiv-and-aids
18. WHO releases HIV drug resistance report 2021. Accessed June 16, 2022. https://www.who.int/news/item/24-11-2021-who-releases-hiv-drug-resistance-report-2021
19. Djuric SW, Akritopoulou-Zanze I, Cox PB, Galasinski S. Compound Collection Enhancement and Paradigms for High-Throughput Screening — an Update. *Annu Rep Med Chem*. 2010;**45**:409-428. doi:10.1016/s0065-7743(10)45025-3
20. Grobler JA, Dornadula G, Rice MR, Simcoe AL, Hazuda DJ, Miller MD. HIV-1 reverse transcriptase plus-strand initiation exhibits preferential sensitivity to non-nucleoside reverse transcriptase inhibitors in vitro. *J Biol Chem*. 2007;**282**:8005-8010. doi:10.1074/jbc.m608274200
21. Wu L, Martin TD, Vazeux R, Unutmaz D, KewalRamani VN. Functional Evaluation of DC-SIGN Monoclonal Antibodies Reveals DC-SIGN Interactions with ICAM-3 Do Not Promote Human Immunodeficiency Virus Type 1 Transmission. *J Virol*. 2002;**76**:5905-5914. doi:10.1128/jvi.76.12.5905-5914.2002
22. Hopkins AL, Ren J, Esnouf RM, Willcox BE, Jones EY, Ross C, Miyasaka T, Walker RT, Tanaka H, Stammers DK. Complexes of HIV-1 reverse transcriptase with

inhibitors of the HEPT series reveal conformational changes relevant to the design of potent non-nucleoside inhibitors. *J Med Chem*. 1996;**39**:1589-1600. doi:10.1021/jm960056x

23. Reynolds C, de Koning CB, Pelly SC, van Otterlo WAL, Bode ML. In search of a treatment for HIV – current therapies and the role of non-nucleoside reverse transcriptase inhibitors (NNRTIs). *Chem Soc Rev*. 2012;**41**:4657-4670. doi:10.1039/c2cs35058k
24. Hsiou Y, Ding J, Das K, Clark AD, Hughes SH, Arnold E. Structure of unliganded HIV-1 reverse transcriptase at 2.7 Å resolution: Implications of conformational changes for polymerization and inhibition mechanisms. *Structure*. 1996;**4**:853-860. doi:10.1016/s0969-2126(96)00091-3
25. Zdanowicz MM. The pharmacology of HIV drug resistance. *Am J Pharm Educ*. 2006;**70**. doi:10.5688/aj7005100
26. Idele P, Gillespie A, Porth T, Suzuki C, Mahy M, Kasedde S, Luo C. Epidemiology of HIV and AIDS among adolescents: Current status, inequities, and data gaps. *J Acquir Immune Defic Syndr*. 2014;**66**:144-153. doi:10.1097/qai.0000000000000176
27. Mahy M, Marsh K, Sabin K, Wanyeki I, Daher J, Ghys PD. HIV estimates through 2018: Data for decision-making. *Aids*. 2019;**33**:S203-S211. doi:10.1097/qad.0000000000002321
28. Kakuda TN. Pharmacology of nucleoside and nucleotide reverse transcriptase inhibitor-induced mitochondrial toxicity. *Clin Ther*. 2000;**22**:685-708. doi:10.1016/s0149-2918(00)90004-3
29. Himmel DM, Maegley KA, Pauly TA, Bauman JD, Das K, Dharia C, Clark AD, Ryan K, Hickey MJ, Love RA, *et al*. Structure of HIV-1 Reverse Transcriptase with the Inhibitor β-Thujaplicinol Bound at the RNase H Active Site. *Structure*. 2009;**17**:1625-1635. doi:10.1016/j.str.2009.09.016
30. Mak TW and M. Saunders. *The Immune Response: Basic and Clinical Principles*. Academic Press; 2006. 1-1194
31. Sluis-Cremer N, Tachedjian G. Mechanisms of inhibition of HIV replication by non-nucleoside reverse transcriptase inhibitors. *Virus Res*. 2008;**134**:147-156. doi:10.1016/j.virusres.2008.01.002
32. Rai MA, Pannek S, Fichtenbaum CJ. Emerging reverse transcriptase inhibitors for HIV-1 infection. *Expert Opin Emerg Drugs*. 2018;**23**:149-157. doi:10.1080/14728214.2018.1474202

33. Tabassum T, Azeem SM, Muwonge AN, Frey KM. Application of Structure-based Methods to Analyze Resistance Mutations for Chemically Diverse Non-Nucleoside Reverse Transcriptase Inhibitors. *Curr HIV Res*. 2020;**18**:283-291. doi:10.2174/1570162x18666200603141209
34. Marintcheva B. *Harnessing the Power of Viruses.* Massachesett: Academic Press; 2018: 1-286
35. Kharsany ABM, Karim QA. HIV Infection and AIDS in Sub-Saharan Africa: Current Status, Challenges and Opportunities. *Open AIDS J*. 2016;**10**:34-48. doi:10.2174/1874613601610010034
36. Kohlstaed LA, Wang J, Friedman JM, Rice PA, Steitz TA. Crystal structure at 3.5 Å resolution of HIV -1 reverse transcriptase complexed with an inhibitor. *Struct Insights into Gene Expr Protein Synth*. 2020;**256**:254-261. doi:10.1142/9789811215865_0026
37. Himmel DM, Das K, Clark AD, Hughes SH, Benjahad A, Oumouch S, Guillemont J, Coupa S, Poncelet A, Csoka I, *et al*. Crystal Structures for HIV-1 Reverse Transcriptase in Complexes with Three Pyridinone Derivatives: A New Class of Non-Nucleoside Inhibitors Effective against a Broad Range of Drug-Resistant Strains. *J Med Chem*. 2005;**48**:7582-7591 doi:10.1021/jm0500323
38. Rodgers DW, Gamblin SJ, Harris BA, Ray S, Culp JS, Hellmig B, Woolf DJ, Debouck C, Harrison SC. The structure of unliganded reverse transcriptase from the human immunodeficiency virus type 1. *Proc Natl Acad Sci U S A*. 1995;**92**:1222-1226. doi:10.1073/pnas.92.4.1222
39. Parrish NF, Gao F, Li H, Giorgi EE, Barbian HJ, Parrish EH, Zajic L, Iyer SS, Decker JM, Kumar A, *et al*. Phenotypic properties of transmitted founder HIV-1. *Proc Natl Acad Sci U S A*. 2013;**110**:6626-6633. doi:10.1073/pnas.1304288110
40. Kinch MS, Patridge E. An analysis of FDA-approved drugs for infectious disease: HIV/AIDS drugs. *Drug Discov Today*. 2014;**19**:1510-1513.
41. Vite-Caritino H, Méndez-Lucio O, Reyes H, Cabrera A, Chávez D, Medina-Franco JL. Advances in the development of pyridinone derivatives as non-nucleoside reverse transcriptase inhibitors. *RSC Adv*. 2016;**6**:2119-2130. doi:10.1039/C5RA25722K
42. Cihlar T, Ray AS. Nucleoside and nucleotide HIV reverse transcriptase inhibitors: 25 years after zidovudine. *Antiviral Res*. 2010;**85**:39-58. doi:10.1016/j.antiviral.2009.09.014
43. Boltjes A, Dömling A. The Groebke-Blackburn-Bienaymé Reaction. *European J Org Chem*. 2019;**2019**:7007-7049. doi:10.1002/ejoc.201901124

44. Le Van K, Cauvin C, de Walque S, Georges BB, Boland S, Martinelli V, Demonté D, Durant F, Hevesi L, Van Lint C. New Pyridinone Derivatives as Potent HIV-1 Nonnucleoside Reverse Transcriptase Inhibitors. *J Med Chem*. 2009;**52**:3636-3643 doi:10.1021/jm801438e
45. Bagdi AK, Santra S, Monir K, Hajra A. Synthesis of imidazo[1,2-*a*]pyridines: A decade update. *Chem Commun*. 2015;**51**:1555-1575. doi:10.1039/c4cc08495k
46. Bode ML, Gravestock D, Moleele SS, van der Westhuyzen CW, Pelly SC, Steenkamp PA, Hope HC, Khan T, Nkabinde LA. Imidazo[1,2-*a*]pyridin-3-amines as potential HIV-1 non-nucleoside reverse transcriptase inhibitors. *Bioorg Med Chem*. 2011;**19**:4227-4237. doi:10.1016/j.bmc.2011.05.062
47. Groebke K, Weber L, Mehlin F. Synthesis of imidazo [1, 2-*a*] annulated pyridines, pyrazines and pyrimidines by a novel three-component condensation. *Synlett*. 1998;**1998**:661-663.
48. Blackburn C, Guan B, Fleming P, Shiosaki K, Tsai S. Parallel synthesis of 3-aminoimidazo [1, 2-*a*] pyridines and pyrazines by a new three-component condensation. *Tetrahedron Lett*. 1998;**39**:3635-3638.
49. Bienayme H, Bouzid K. A new heterocyclic multicomponent reaction for the combinatorial synthesis of fused 3-aminoimidazoles. *Angew Chemie Int Ed*. 1998;**37**:2234-2237.
50. Mandair GS, Light M, Russell A, Hursthouse M, Bradley M. Re-evaluation of the outcome of a multiple component reaction—2- and 3-amino-imidazo[1,2-*a*]pyrimidines? *Tetrahedron Lett*. 2002;**43**:4267-4269. doi:https://doi.org/10.1016/s0040-4039(02)00709-8
51. Biggs-Houck JE, Younai A, Shaw JT. Recent advances in multicomponent reactions for diversity-oriented synthesis. *Curr Opin Chem Biol*. 2010;**14**:371-382. doi:10.1016/j.cbpa.2010.03.003
52. Zhu DJ, Chen JX, Liu MC, Ding JC, Wu HY. Catalyst: and solvent-free synthesis of imidazo [1, 2-*a*] pyridines. *J Braz Chem Soc*. 2009;**20**:482-487.
53. Stasyuk AJ, Banasiewicz M, Cyrański MK, Gryko DT. Imidazo[1,2-*a*]pyridines Susceptible to Excited State Intramolecular Proton Transfer: One-Pot Synthesis via an Ortoleva–King Reaction. *J Org Chem*. 2012;**77**:5552-5558. doi:10.1021/jo300643w
54. Xie YY, Chen ZC, Zheng QG. Organic reactions in ionic liquids: Ionic liquid-accelerated cyclocondensation of α-tosyloxyketones with 2-aminopyridine. *Synthesis*. 2002;**2002**:1505-1508.

55. Yadav JS, Reddy BVS, Rao YG, Srinivas M, Narsaiah A V. Cu (OTf) 2-catalyzed synthesis of imidazo [1, 2-*a*] pyridines from α-diazoketones and 2-aminopyridines. *Tetrahedron Lett*. 2007;**48**:7717-7720.
56. Nair DK, Mobin SM, Namboothiri INN. Synthesis of imidazopyridines from the Morita–Baylis–Hillman acetates of nitroalkenes and convenient access to Alpidem and Zolpidem. *Org Lett*. 2012;**14**:4580-4583.
57. Ciraulo DA, Oldham M. Sedative Hypnotics. *Eff Drug Abus Hum Nerv Syst*. 2013:499-532. doi:10.1016/b978-0-12-418679-8.00016-2
58. Lieberman JA. Update on the safety considerations in the management of insomnia with hypnotics: incorporating modified-release formulations into primary care. *Prim Care Companion J Clin Psychiatry*. 2007;**9**:25-31. doi:10.4088/pcc.v09n0105
59. Najib J. Eszopiclone, a Nonbenzodiazepine Sedative-Hypnotic Agent for the Treatment of Transient and Chronic Insomnia. *Clin Ther*. 2006;28(4):491-516. doi:10.1016/j.clinthera.2006.04.014
60. Neubauer DN. New Approaches in Managing Chronic Insomnia. *CNS Spectr*. 2006;**11**:1-16. doi:10.1017/s1092852900026687
61. Zulfikar S, Mulholland S, Adamali H, Barratt SL. Inhibitors of the Autotaxin-Lysophosphatidic Acid Axis and Their Potential in the Treatment of Interstitial Lung Disease: Current Perspectives. *Clin Pharm*. 2020;**12**:97-108. doi:10.2147/cpaa.s228362
62. Kuttruff CA, Ferrara M, Bretschneider T, Hoerer S, Handschuh S, Nosse B, Romig H, Nicklin P, Roth GJ. Discovery of BI-2545: A Novel Autotaxin Inhibitor That Significantly Reduces LPA Levels in Vivo. *ACS Med Chem Lett*. 2017;**8**:1252-1257. doi:10.1021/acsmedchemlett.7b00312
63. Lacerda RB, de Lima CKF, da Silva LL, Romeiro NC, Miranda ALP, Barreiro EJ, Fraga CAM. Discovery of novel analgesic and anti-inflammatory 3-arylamine-imidazo[1,2-*a*]pyridine symbiotic prototypes. *Bioorg Med Chem*. 2009;**17**:74-84. doi:10.1016/j.bmc.2008.11.018
64. Dahan-Farkas N, Langley C, Rousseau AL, Yadav DB, Davids H, De Koning CB. 6-Substituted imidazo[1,2-*a*]pyridines: Synthesis and biological activity against colon cancer cell lines HT-29 and Caco-2. *Eur J Med Chem*. 2011;**46**:4573-4583. doi:10.1016/j.ejmech.2011.07.036
65. Akritopoulou-Zanze I, Wakefield BD, Gasiecki A, Kalvin D, Johnson EF, Kovar P, Djuric SW. Scaffold oriented synthesis. Part 3: design, synthesis and biological

evaluation of novel 5-substituted indazoles as potent and selective kinase inhibitors employing [2+3] cycloadditions. *Bioorganic & Med Chem Lett*. 2011;**21**:1476-1479. doi:10.1016/j.bmcl.2011.01.007

66. Fors BP, Watson DA, Biscoe MR, Buchwald SL. A Highly Active Catalyst for Pd-Catalyzed Amination Reactions: Cross-Coupling Reactions Using Aryl Mesylates and the Highly Selective Monoarylation of Primary Amines Using Aryl Chlorides. *J Am Chem Soc*. 2008;**130**:13552-13554. doi:10.1021/ja8055358
67. Warshakoon NC, Wu S, Boyer A, Kawamoto R, Sheville J, Renock S, Xu K, Pokros M, Evdokimov AG, Walter R, *et al*. A novel series of imidazo[1,2-*a*]pyridine derivatives as HIF-1α prolyl hydroxylase inhibitors. *Bioorg Med Chem Lett*. 2006;**16**:5598-5601. doi:10.1016/j.bmcl.2006.08.089
68. Lyon MA, Kercher TS. Glyoxylic acid and MP-glyoxylate: Efficient formaldehyde equivalents in the 3-CC of 2-aminoazines, aldehydes, and isonitriles. *Org Lett*. 2004;**6**:4989-4992. doi:10.1021/ol0478234
69. Nenajdenko VG, Reznichenko AL, Balenkova ES. The synthesis of aminoimidazo[1,2-*a*]azinecarboxylic acid esters from ethyl glyoxylate. *Russ Chem Bull*. 2007;**56**:560-562. doi:10.1007/s11172-007-0093-1
70. Bratulescu G. Synthesis of aromatic aldehydes by a fast method involving Kornblum's reaction. *Synth Commun*. 2008;**38**:2748-2752. doi:10.1080/00397910802222795
71. Sheldon RA. The greening of solvents: Towards sustainable organic synthesis. *Curr Opin Green Sustain Chem*. 2019;**18**:13-19. doi:10.1016/j.cogsc.2018.11.006
72. Velázquez-Olvera S, Salgado-Zamora H, Velázquez-Ponce M, Campos-Aldrete E, Reyes-Arellano A, Pérez-González C. Fluorescent property of 3-hydroxymethyl imidazo[1,2-*a*]pyridine and pyrimidine derivatives. *Chem Cent J*. 2012;**6**:83. doi:10.1186/1752-153x-6-83
73. Hodgkiss RJ, Middleton RW, Parrick J, Rami HK, Wardman P, Wilson GD. Bioreductive fluorescent markers for hypoxic cells: a study of 2-nitroimidazoles with 1-substituents containing fluorescent, bridgehead-nitrogen, bicyclic systems. *J Med Chem*. 1992;**35**:1920-1926.
74. Kim HY, Yang S gak, Shin JH, Lee CH, Ko HJ. Imidazopyrimidine-based compound and organic light-emitting device employing organic layer including the same. Patent no: CN101265260B. 2010.
75. Chen WH, Xing Y, Pang Y. A highly selective pyrophosphate sensor based on ESIPT turn-on in water. *Org Lett*. 2011;**13**:1362-1365. doi:10.1021/ol200054w

76. Lim SJ, Seo J, Park SY. Photochromic switching of excited-state intramolecular proton-transfer (ESIPT) fluorescence: a unique route to high-contrast memory switching and nondestructive readout. *J Am Chem Soc*. 2006;**128**:14542-14547. doi:10.1021/ja0637604
77. Park S, Kwon JE, Kim SH, Seo J, Chung K, Park SY, Jang DJ, Milián MB, Giershner J, Park SY. A white-light-emitting molecule: frustrated energy transfer between constituent emitting centers. *J Am Chem Soc*. 2009;**131**:14043-14049. doi:10.1021/ja902533f
78. Ruiz-Castillo P, Buchwald SL. Applications of Palladium-Catalyzed C–N Cross-Coupling Reactions. *Chem Rev*. 2016;**116**:12564-12649. doi:10.1021/acs.chemrev.6b00512
79. Ullmann F, Sponagel P. Ueber die phenylirung von phenolen. *Chem Ber*.1905;**38**:2211-2212.
80. Goldberg I. Phenylation with presence of copper as catalyst. *Chem Ber*. 1906;**39**:1691-1692.
81. Ohta K, Itoh S, Kandou Y, Yoshikawa H, Ishida Y. Synthesis and Herbicidal Activity of Sulfonylureas with Fused Heterocyclic Moiety*. *J Pestic Sci*. 1994;**19**:137-141. doi:10.1584/jpestics.19.2_137
82. Gudmundsson KS, Drach JC, Townsend LB. An improved synthesis of 2-chlorinated imidazo[1,2-*a*]pyridines and the application of this procedure for the synthesis of several new polychlorinated imidazo[1,2-*a*]pyridines. *Synth Commun*. 1997;**27**:1763-1775. doi:10.1080/00397919708004089
83. Reindel F. Über eine neue Klasse indigoider Farbstoffe. *Chem Ber*. 1924;**57**:1381-1386.
84. Tschitschibabin AE. über Kondensationen der Aldehyde mit Ammonik zu Pyridinbasen. *J für Prakt Chemie*. 1924;**107**:122-128.
85. Pei M ming, Liu P, Liu Y, Lv X ming, Ma X wei, Dai B. Pd-catalyzed, highly selective C(sp2)-Br bond coupling reactions of o-(or m-, or p-) chloromethyl bromobenzene with arylboronic acids. *Molecules*. 2018;**23**. doi:10.3390/molecules23020433
86. Enguehard C, Allouchi H, Gueiffier A, Buchwald SL. Easy access to novel substituted 6-aminoimidazo[1,2-*a*]pyridines using palladium- and copper-catalyzed aminations. *J Org Chem*. 2003;**68**:4367-4370. doi:10.1021/jo0341463
87. Changunda CRK, Basson AE, van Vuuren SF, Rousseau AL, Bode ML. Palladium-

catalysed cross-coupling as a key step in the synthesis of pyridyl-benzamides,-benzylamines and-sulfonamides. *Tetrahedron*. 2017;**73**:137-147.

88. Gladysz R, Adriaenssens Y, De Winter H, Joossens J, Lambeir AM, Augustyns K, Van der Veken P. Discovery and SAR of Novel and Selective Inhibitors of Urokinase Plasminogen Activator (uPA) with an Imidazo[1,2-a]pyridine Scaffold. *J Med Chem*. 2015;**58**:9238-9257. doi:10.1021/acs.jmedchem.5b01171
89. Christ F, Voet A, Marchand A, Nicolet S, Desimmie BA, Marchand D, Bardiot D, Van der Veken NJ, Van Remoortel B, Strelkov SV, *et al*. Rational design of small-molecule inhibitors of the LEDGF/p75-integrase interaction and HIV replication. *Nat Chem Biol*. 2010;**6**:442-448. doi:10.1038/nchembio.370
90. Kim BR, Lee HG, Kang SB, Sung GH, Kim JJ, Park JK, Lee SG, Yoon YJ. tert-Butoxide-Assisted Amidation of Esters under Green Conditions. *Synthesis.* 2012;**44**:42-50.
91. Morimoto H, Fujiwara R, Shimizu Y, Morisaki K, Ohshima T. Lanthanum(III) Triflate Catalyzed Direct Amidation of Esters. *Organic Lett*. 2014;16:2018-2021 doi:10.1021/ol500593v
92. Mkhonazi BD, Shandu M, Tshinavhe R, Simelane SB, Moshapo PT. Amidation of Esters. *Molecules*. 2020;**25**:1-9.
93. Bissinger WE, Kung FE. A Study of the Reaction of Phenol with Thionyl Chloride. *J Am Chem Soc*. 1948;**70**:2664-2666. doi:10.1021/ja01188a015
94. Jia H, Li Q, Bayaguud A, She S, Huang Y, Chen K, Wei Y. Tosylation of alcohols: an effective strategy for the functional group transformation of organic derivatives of polyoxometalates. *Sci Rep*. 2017;**7**:12523-12633 doi:10.1038/s41598-017-12633-8
95. Zimuwandeyi M, Fernandes MA, Rousseau AL, Bode ML. Total synthesis of ent-pavettamine. *Beilstein J Org Chem*. 2021;**17**:1440-1446. doi:10.3762/bjoc.17.99
96. Ding R, He Y, Wang X, Xu J, Chen Y, Feng M, Qi C. Treatment of alcohols with tosyl chloride does not always lead to the formation of tosylates. *Molecules*. 2011;**16**:5665-5673. doi:10.3390/molecules16075665
97. Piancatelli G, Scettri A, D'Auria M. Pyridinium Chlorochromate: A Versatile Oxidant in Organic Synthesis. *Synthesis*. 1982;**1982**:245-258.
98. Frigerio M, Santagostino M, Sputore S, Palmisano G, Instituto P, Forlanini V, Milanese S, Torino U. Insight Hypervalent. 1995:7272-7276.
99. Boeckman RK, Ganem B. Differentiation of diols; A new synthesis of bromoformates and protected hydroxyaldehydes. *Tetrahedron Lett*. 1974;**15**:913-916.

doi:10.1016/s0040-4039(01)82367-4

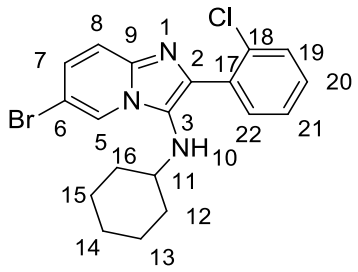
100. Corey EJ, Suggs JW. Pyridinium chlorochromate. An efficient reagent for oxidation of primary and secondary alcohols to carbonyl compounds. *Tetrahedron Lett*. 1975;**16**:2647-2650. doi:10.1016/s0040-4039(00)75204-x

101. Heidary M, Khoobi M, Ghasemi S, Habibi Z, Faramarzi MA. Synthesis of quinazolinones from alcohols via laccase-mediated tandem oxidation. *Adv Synth Catal*. 2014;**356**:1789-1794. doi:10.1002/adsc.201400103

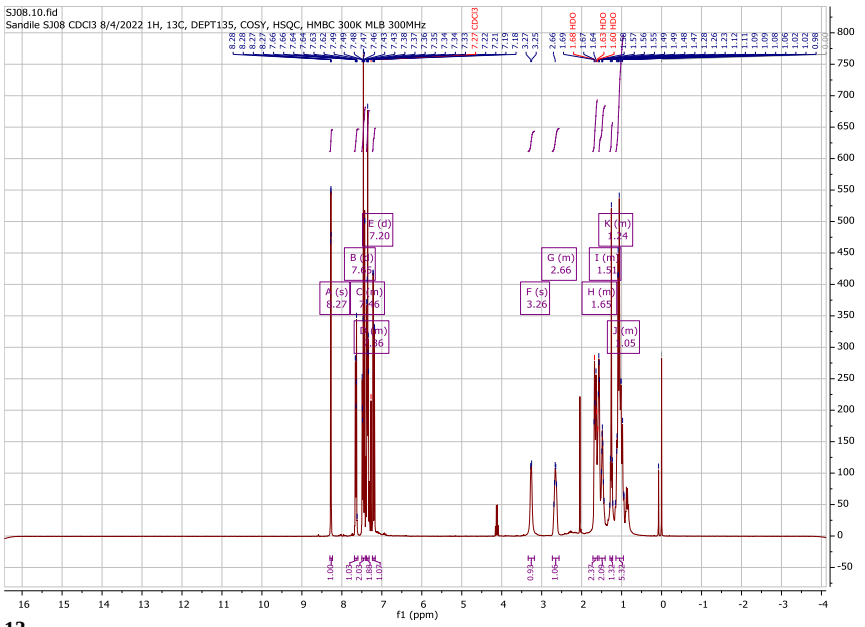
102. Kornblum N, Jones WJ, Anderson GJ. A new and selective method of oxidation. The conversion of alkyl halides and alkyl tosylates to aldehydes. *J Am Chem Soc*. 1959;**81**:4113-4114. doi:10.1021/ja01524a080

Appendix 1: ^{1}H NMR and ^{13}C NMR spectral data for a select number of compounds

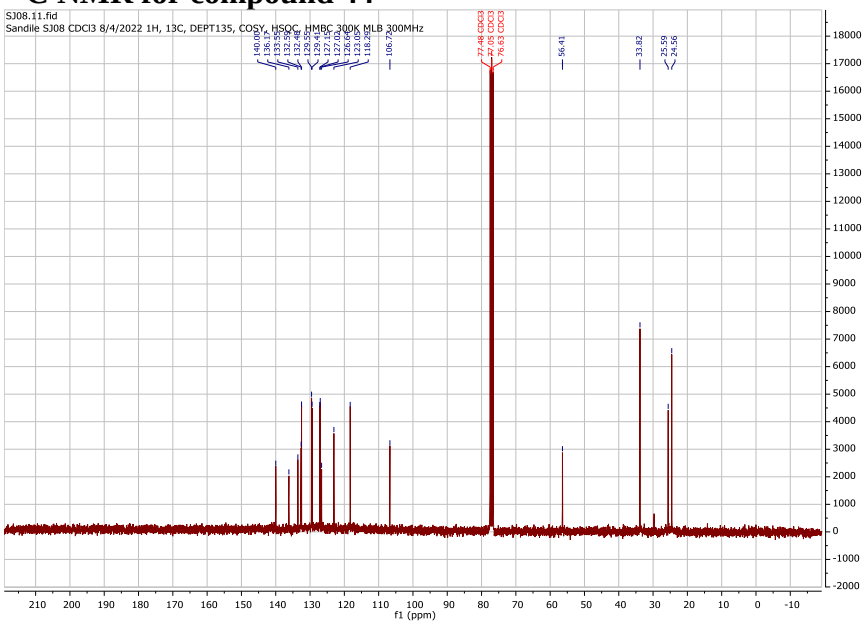
Compound 44



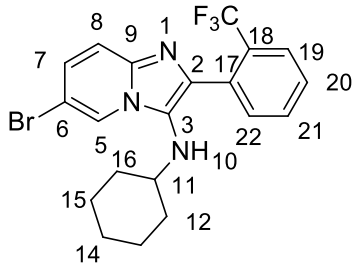
^{1}H NMR at 300MHz



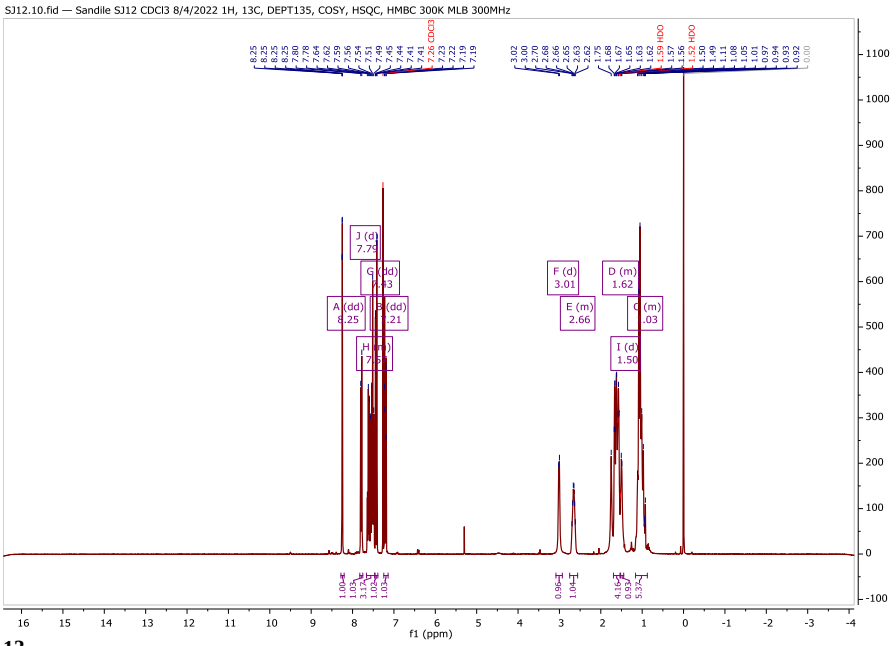
^{13}C NMR for compound 44



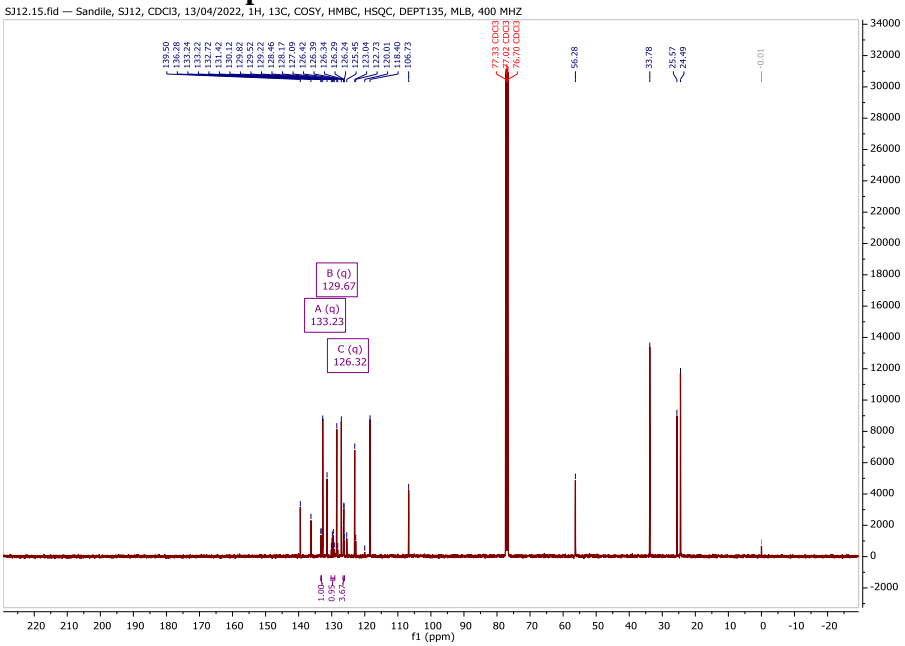
Compound 45



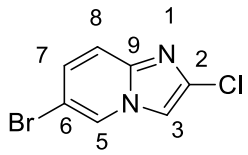
^{1}H NMR at 300MHz



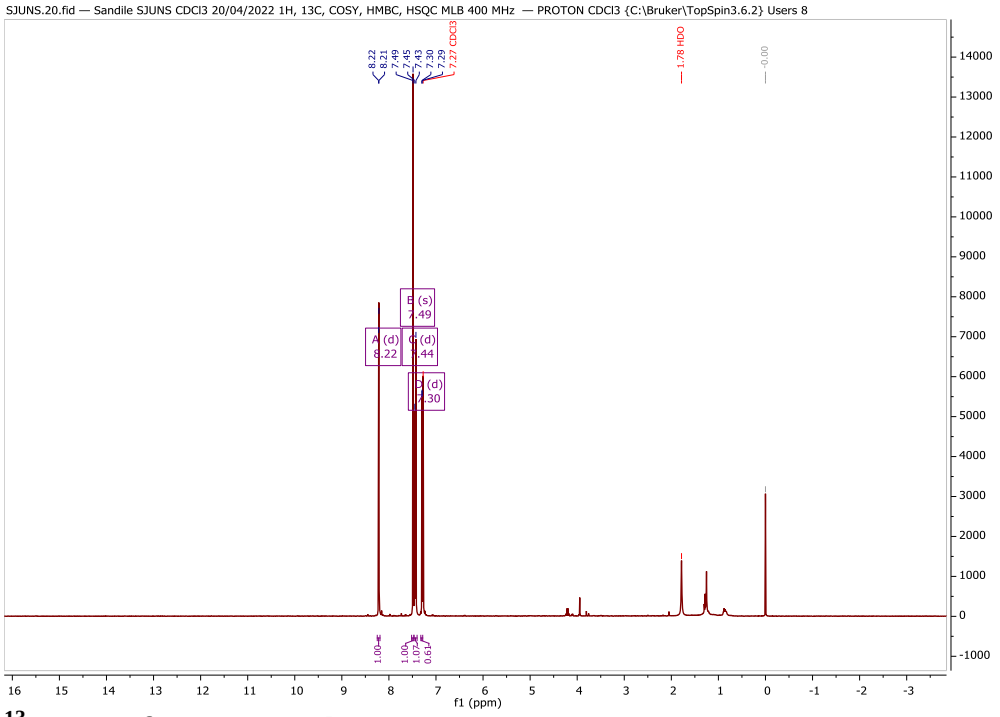
^{13}C NMR for compound 45



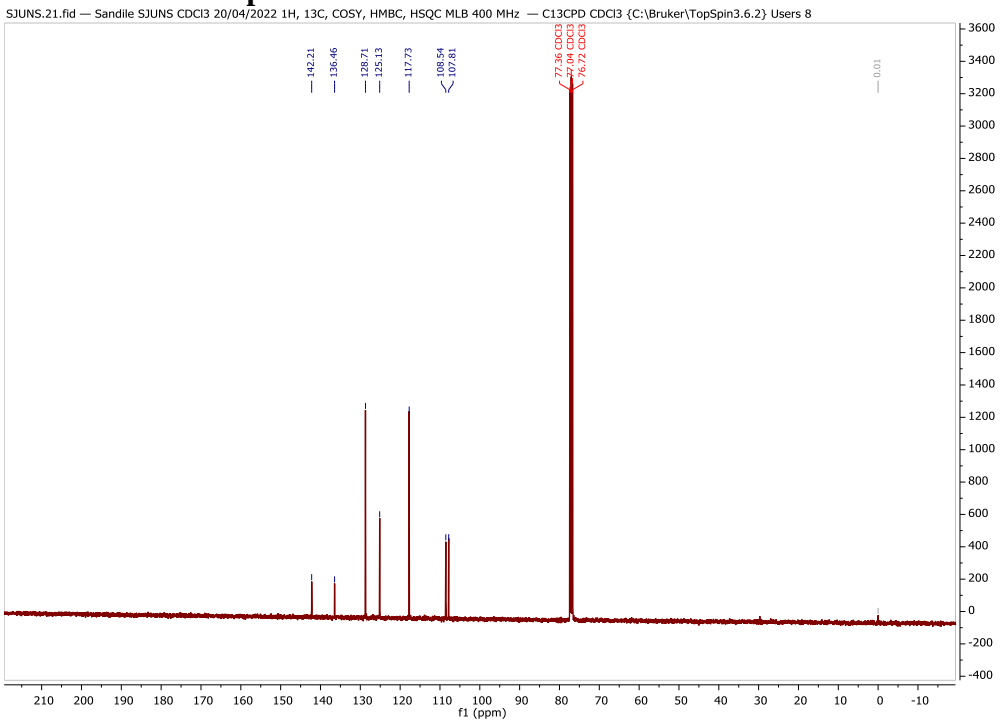
Compound 29



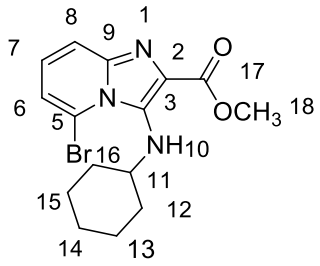
^{1}H NMR for compound 29 at 400MHz



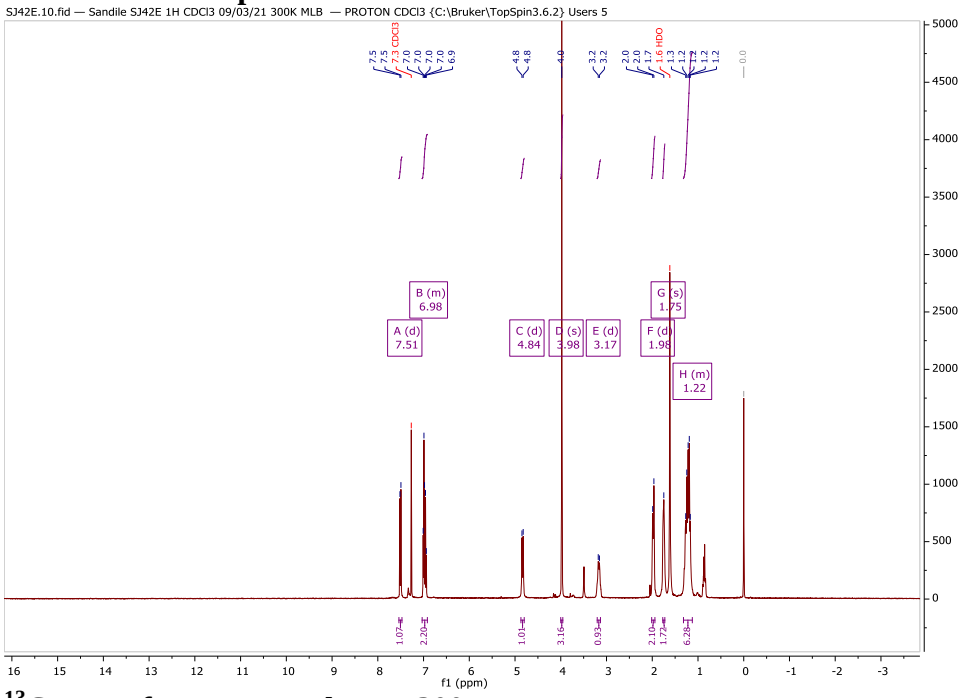
^{13}C NMR for compound 29 at 400MHz



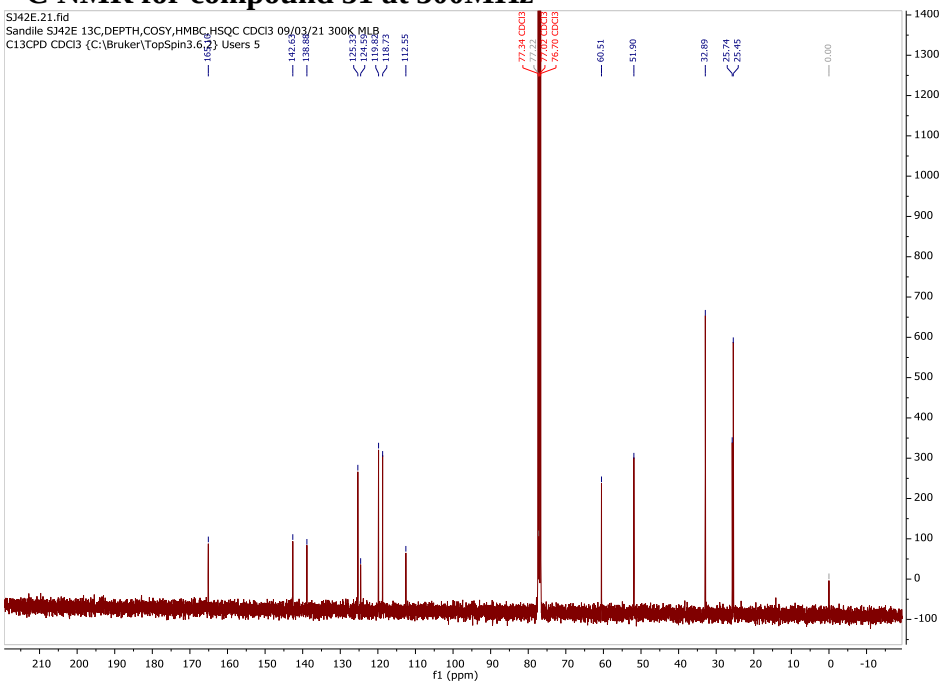
Compound 51



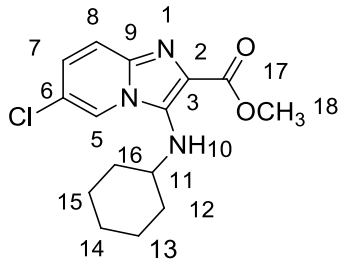
^{1}H NMR for compound 51 at 300MHz



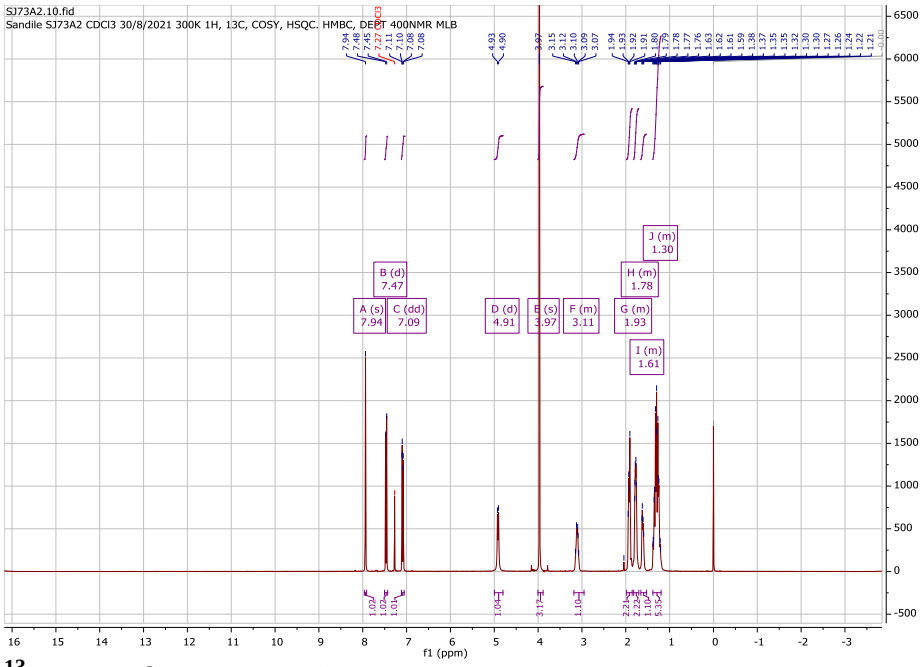
^{13}C NMR for compound 51 at 300MHz



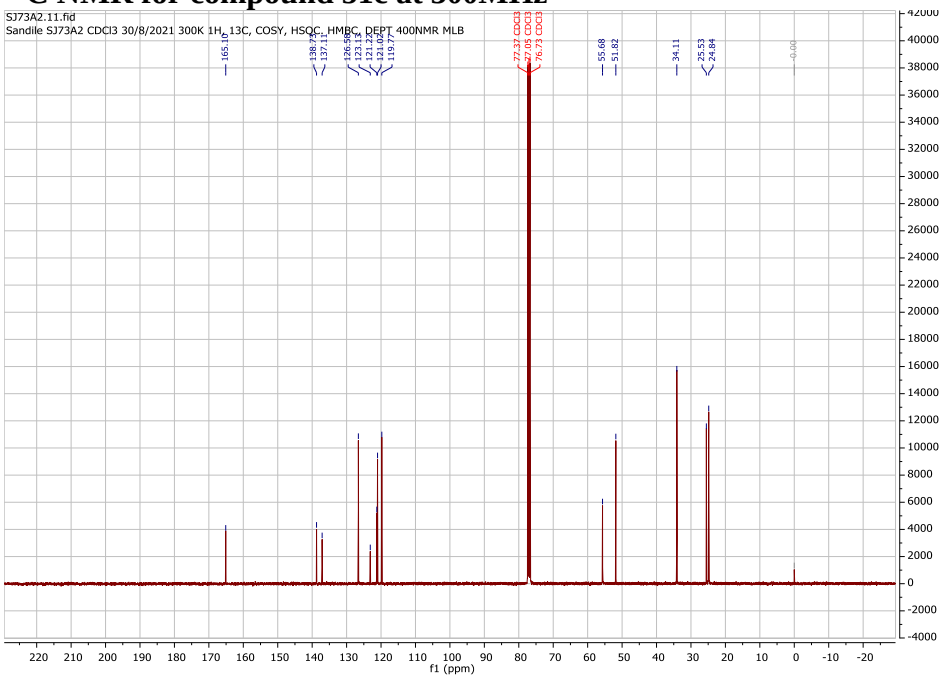
Compound 51c



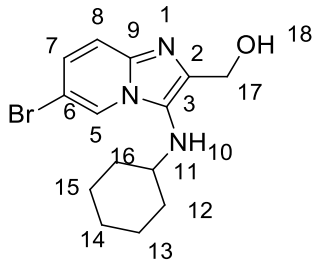
^{1}H NMR for compound 51c at 300MHz



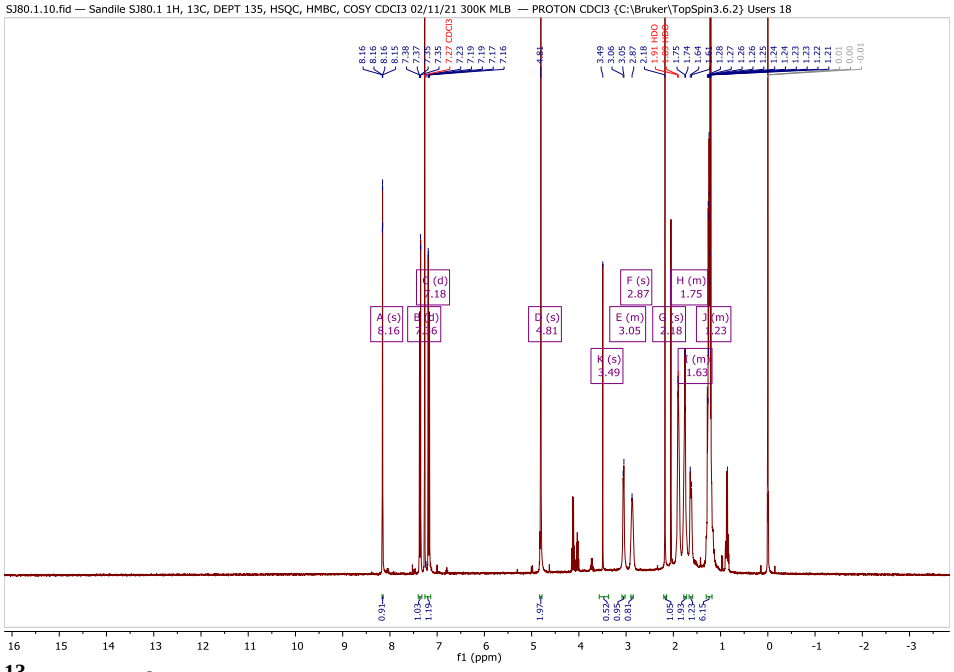
^{13}C NMR for compound 51c at 300MHz



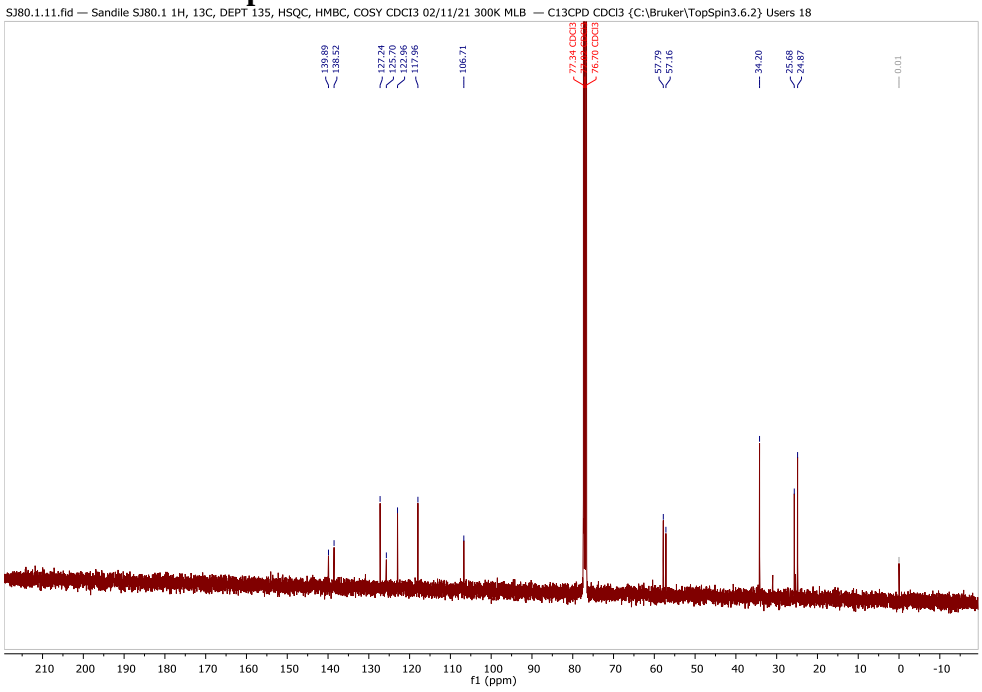
Compound 54a



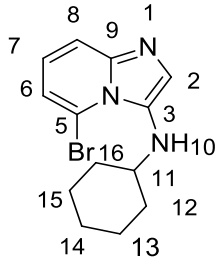
^{1}H NMR for compound 51a at 300MHz



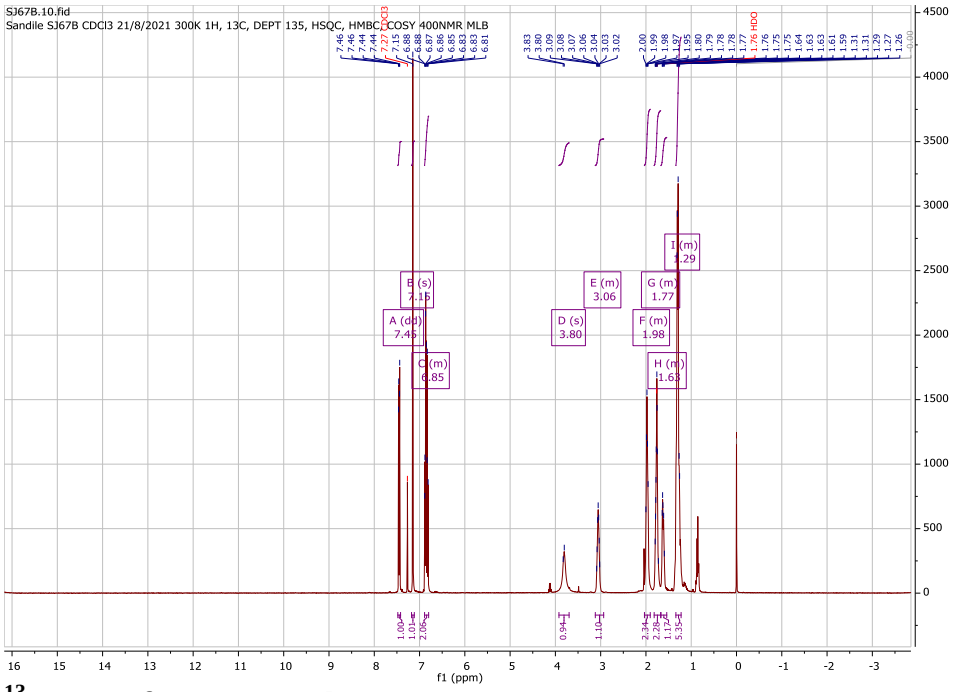
^{13}C NMR for compound 51a at 300MHz



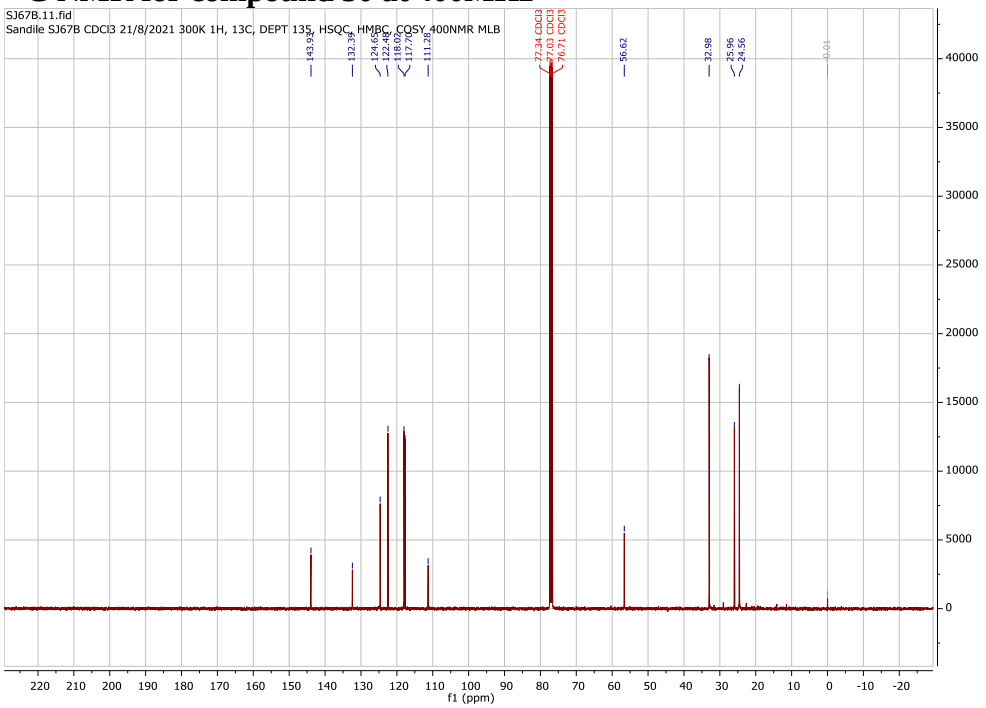
Compound 50



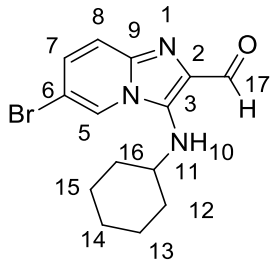
^{1}H NMR for compound 50 at 400MHz



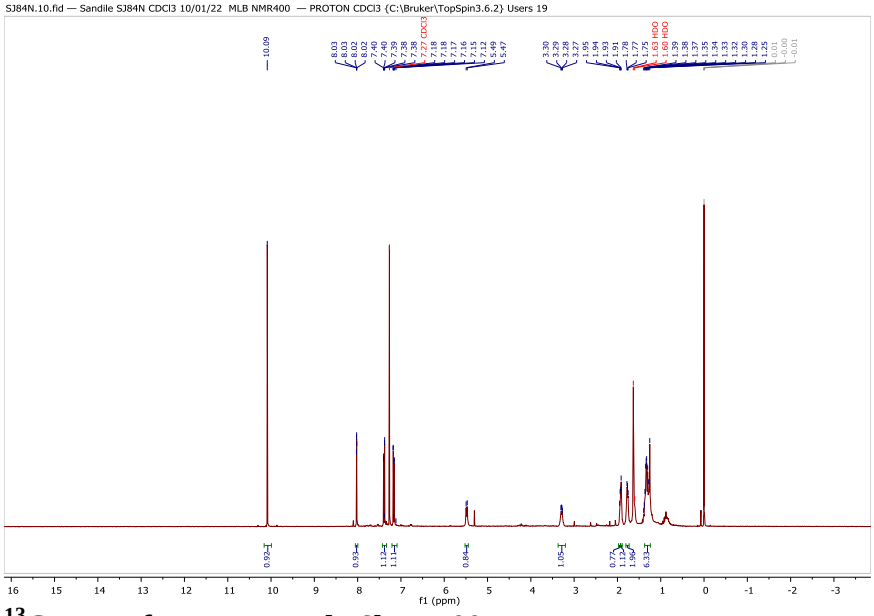
^{13}C NMR for compound 50 at 400MHz



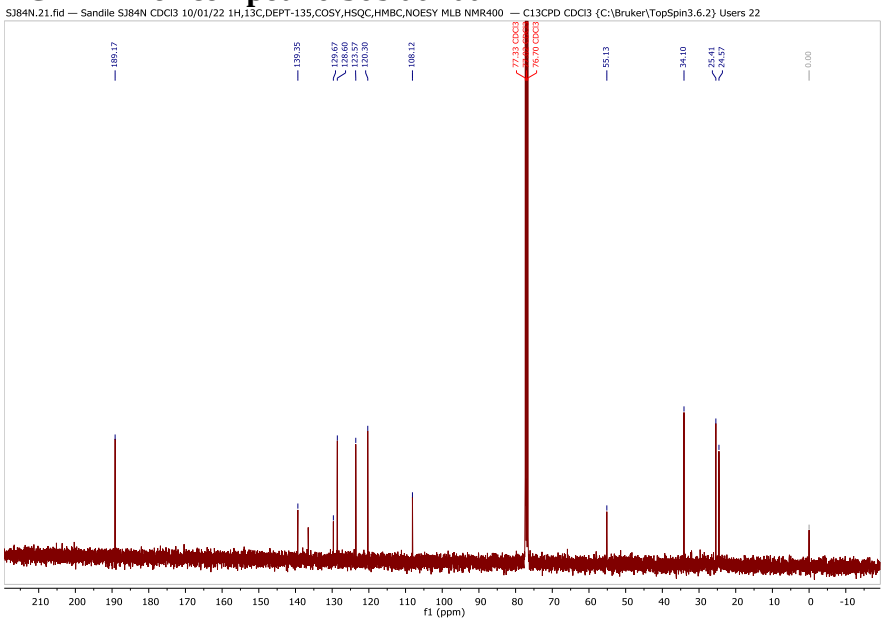
Compound 56b



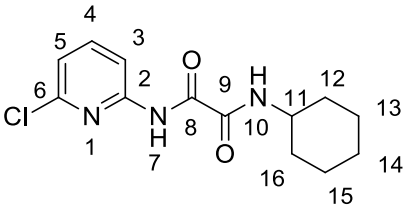
^{1}H NMR for compound 56b at 400MHz



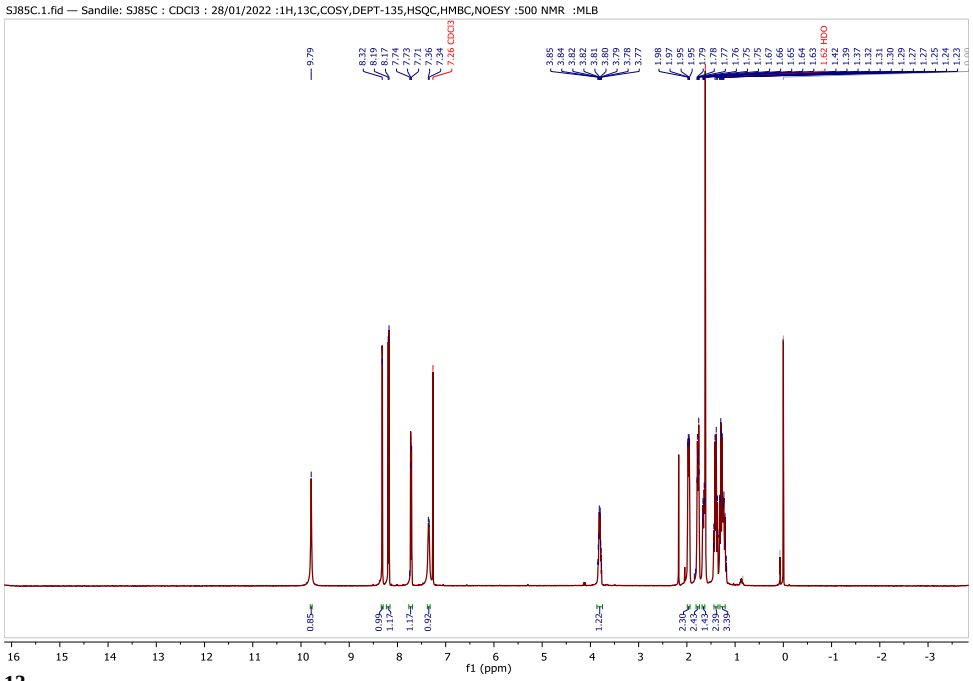
^{13}C NMR for compound 56b at 400MHz



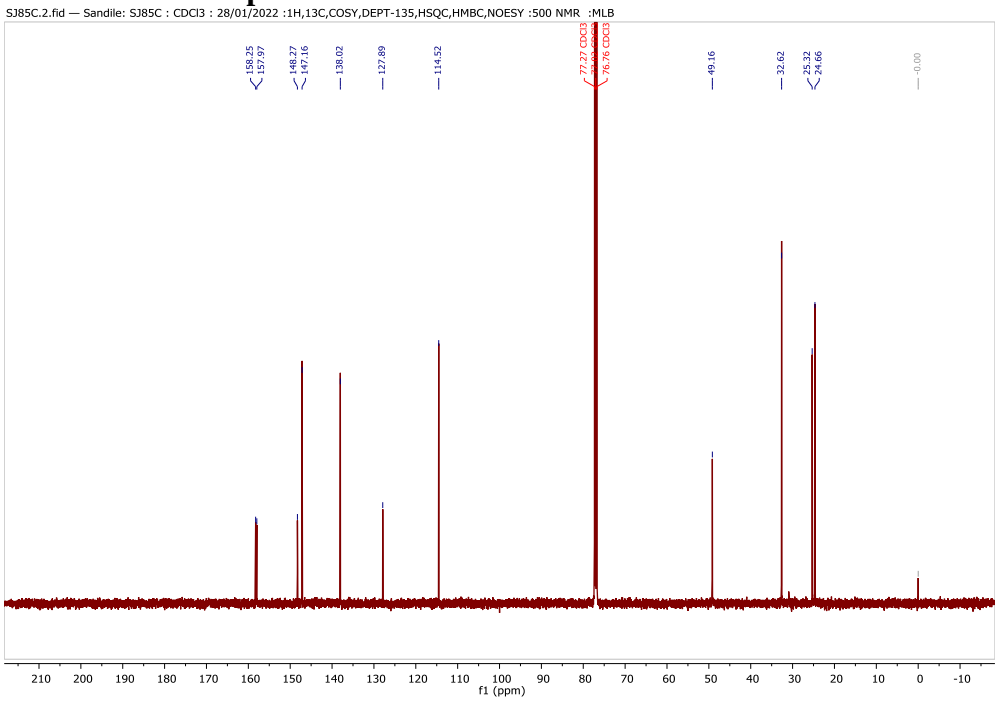
Compound 57b



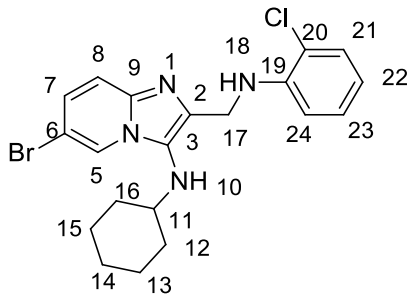
^{1}H NMR for compound 57b at 500MHz



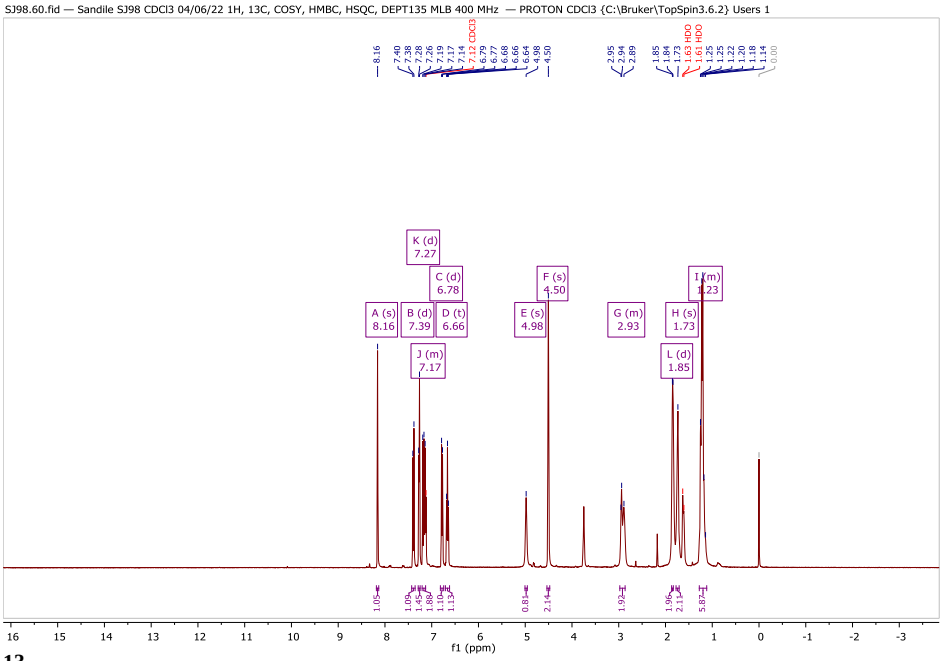
^{13}C NMR for compound 57b at 500MHz



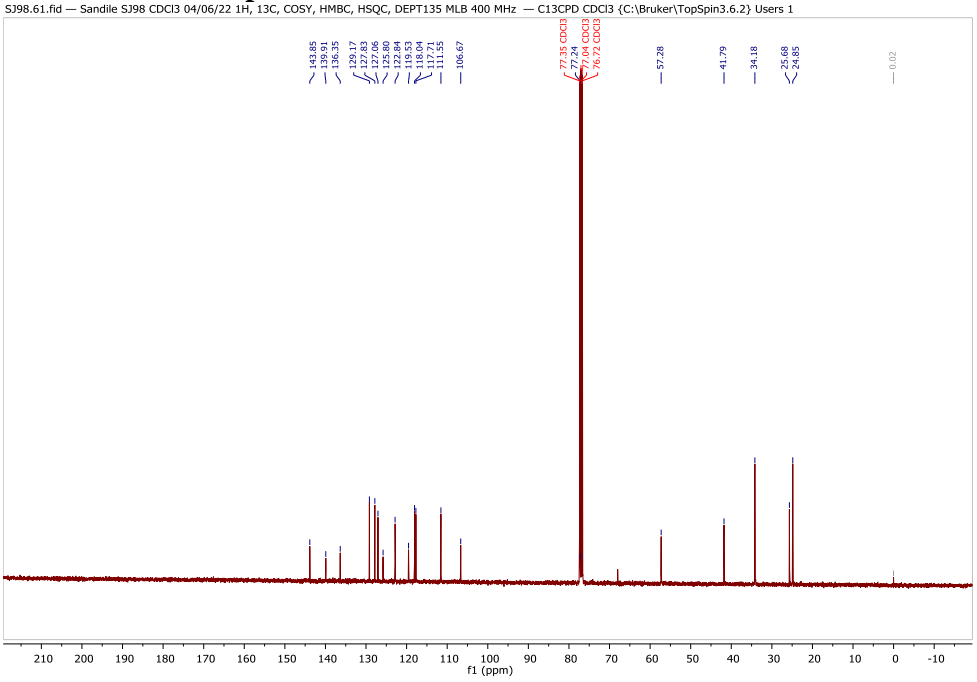
Compound 59a



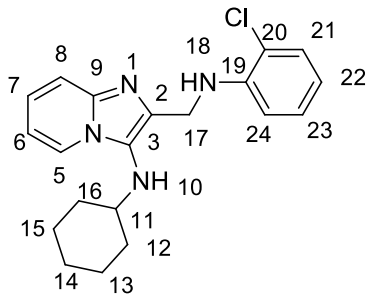
^{1}H NMR for compound 59a at 400MHz



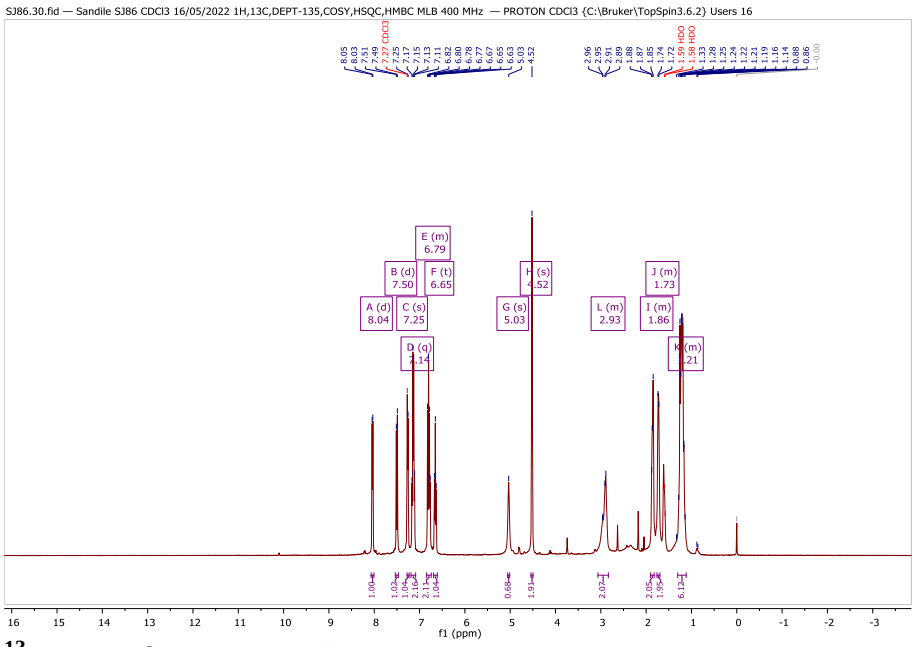
^{13}C NMR for compound 59a at 400MHz



Compound 59



^{1}H NMR for compound 59 at 400MHz



^{13}C NMR for compound 59 at 400MHz

